The most fruitful basis for the discovery of a new drug

is to start with an old drug.

−   Sir James Black

Members of the Jury

Prof. Dr. ir. Nico Boon (Chairman)

Prof. Dr. Nuria Sotomayor

Prof. Dr. Serge Van Calenbergh

Prof. Dr. ir. Marjan De Mey

Prof. Dr. ir. Christian Stevens

Prof. Dr. ir. Matthias D'hooghe (Promoter)

Promoter: Prof. Dr. ir. Matthias D'hooghe

              Department of Sustainable Organic Chemistry and Technology

              Faculty of Bioscience Engineering, Ghent University

Dean: Prof. Dr. ir. Marc Van Meirvenne

Rector: Prof. Dr. Anne De Paepe

FACULTEIT
BIO-INGENIEURSWETENSCHAPPEN

SYNTHESIS OF THIAHETEROCYCLIC BENZOHYDROXAMIC ACIDS AND EVALUATION OF THEIR HDAC6 INHIBITORY ACTIVITY

ir. Rob De Vreese

Thesis submitted in fulfilment of the requirements for the degree of doctor (PhD) in Applied Biological Sciences: Chemistry and Bioprocess Technology

UNIVERSITEIT
GENT

Dutch translation of the title:

Synthese van thiaheterocyclische benzohydroxamzuren en evaluatie van hun HDAC6-inhiberende activiteit

ISBN-number: 978-90-5989-984-1

Gent, January 2017

The author,   The promoter,

ir. Rob De Vreese   Prof. Dr. ir. Matthias D'hooghe

WOORD VOORAF

Vriendschap, collega's, professoren, chemie, veel chemie, nog meer chemie, een leuke tijd, schrijven, veel schrijven, nog meer schrijven, flashen, NMR, MS, klein labo, de keuken, practica, I'm back … HDAC, de conference room, zijn enkele woorden die in me opkomen als ik terugdenk aan de voorbije zes jaar die ik heb doorgebracht in Blok B op het vierde en vijfde verdiep aan de SynBioC groep (Faculteit Bio-ingenieurswetenschappen, Universiteit Gent). Het valt me op dat ik een gelukkig gevoel krijg wanneer ik terugdenk aan deze periode, wat ik te danken heb aan iedereen die mijn pad de voorbije jaren heeft gekruist.

Op de eerste plaats zou ik mijn promotor Prof. Dr. ir. Matthias D'hooghe willen bedanken. Zonder uw advies en steun had ik dit doctoraat niet kunnen aanvatten en zouden de voorbije jaren er anders hebben uitgezien. Tijdens de afgelopen zes jaar stond u altijd klaar om mijn vragen te beantwoorden en hebben we tezamen verschillende publicaties gerealiseerd in internationale toptijdschriften. Bedankt hiervoor!

Furthermore, I would like to take the opportunity to thank the members of the jury. Prof. Sotomayor, Prof. Van Calenbergh, Prof. Boon, Prof. De Mey and Prof. Stevens. Your critical remarks and valuable input lifted this PhD thesis to a higher level for which I would like to thank you very much.

Daarnaast wil ik de veertien thesisstudenten bedanken die ik tijdens mijn doctoraat mocht begeleiden. Jullie inzet heeft geleid tot het behalen van verschillende belangrijke resultaten met tal van publicaties tot gevolg. Deze artikels behandelden voornamelijk de synthese van selectieve HDAC6-inhibitoren, curcumineanalogen en β-lactam/DNA-base-hybriden. Eén topic ontbreekt echter nog, namelijk de aanmaak van bis-8-hydroxychinoline-liganden, wat waarschijnlijk mijn laatste wapenfeit aan de SynBioC groep zal worden.

Ook wil ik alle co-auteurs, Karus Therapeutics, Prof. De Wever en Prof. Bracke bedanken voor hun bijdrage tot verschillende resultaten die geleid hebben tot vijf publicaties, drie patenten en dit doctoraat.

De afgelopen zes jaar hadden niet dezelfde geweest zonder de aanwezigheid van alle SynBioC doctoraatstudenten. Hierbij wil ik enkele personen in het bijzonder bedanken voor de vele leuke momenten die we samen hebben beleefd. Eerst en vooral Yves, mijn partner in crime om alle mysteries te ontrafelen omtrent HDAC6. Jouw inzet, positieve ingesteldheid en de leuke gesprekken die we gehad hebben, zorgden er steeds voor dat ik gemotiveerd bleef om nieuwe resultaten te behalen. Jan en Stéphanie, mijn twee überbureaumies, het was altijd fijn om toe te komen op het werk wanneer jullie aanwezig waren. Jullie stonden altijd klaar

voor een leuke babbel en namen de tijd om mijn vragen te beantwoorden. Daarnaast hebben we tal van culinaire hoogtepunten beleefd samen met Iris, Stijn DB en Wouter en hopelijk kunnen we dit in de toekomst nog meermaals herhalen! Yoshi, Hang, Eli, Stein, Pieter N, Yves en Jan - mijn huidige bureaumies - bedankt om voor een aangename werkomgeving te zorgen. Jullie enthousiasme voor Chemie en uitstekende vorm van humor, zorgden ervoor dat ik met veel plezier kwam werken! Gert, Stijn DK, Koen, Pieter C, Niels, Filip, Cedric, Ewout, Tamara, Sara, Karen, Karel, Elisabeth, Gustavo, Elena, Klicia, Junko, Sonja, Martyna, en de andere ex-collega's bedankt voor de vele toffe momenten op het werk, de Koepuur, de Spa/Blankenberge meetings, de SynBioC activiteiten, … Ook bedankt aan Lena, Marine, Bart, Thomas, Sofie, Arno, Melissa, Nicola, Sari, Tim, Benz, Reinout, Flore, Jonas en Sigrid - de huidige collega's - voor de mooie momenten.

Uiteraard wil ik hier ook de ATP-leden bedanken. Els, Ans en Pieter bedankt om alles in goede banen te leiden aan onze Vakgroep! Bij allerhande problemen kon ik altijd bij jullie terecht en jullie stonden altijd klaar om mij verder te helpen.

Tijdens mijn doctoraat was ik ook fervent lid van twee teams die voor de nodige afwisseling zorgden tijdens mijn lunchpauzes. Eerst en vooral het pingpongteam, of zeg ik beter het tafeltennisteam, die voornamelijk bestond uit Jeroen, Pieter Z, Laurens en mezelf. Het was altijd fijn om een balletje te slaan met jullie. Daarnaast maakte ik ook deel uit van het frietteam, want als Belg mag een frietje op tijd en stond niet ontbreken.

Hierbij wil ik ook mijn familie en vrienden in de spotlights plaatsen. Jullie zorgen en zullen in de toekomst blijven zorgen voor de fantastische momenten naast het werk. Ik hoop dat we een leuke toekomst tegemoet gaan en dat er nog vele leuke gebeurtenissen mogen volgen!

Als laatste wil ik mijn gezinnetje bedanken! Jullie betekenen alles voor mij!

Rob De Vreese

Mei 2017

TABLE OF CONTENT

LIST OF ABBREVIATIONS

AcOH	acetic acid
ADME	absorption, distribution, metabolism, excretion
AIBN	azobisisobutyronitrile
AP-1	activator protein 1
BnBr	benzyl bromide
Boc	*tert*-butyloxycarbonyl
BOP	(benzotriazol-1-yloxy)tris(dimethylamino)phosphonium hexafluoro-phosphate
Bu	butyl
$CDCl_3$	deuterated chloroform
CDI	carbonyldiimidazole
$CHCl_3$	chloroform
CH_2Cl_2	dichloromethane
CH_3CN	acetonitrile
cLogP	calculated partition-coefficient
CNS	central nervous system
CQ	chloroquine
CQR	chloroquine-resistant
CQS	chloroquine-sensitive
CYP	cytochrome P450
DIPEA	*N*-ethyl-*N*,*N*-diisopropylamine
DMF	dimethylformamide
DMSO	dimethylsulfoxide
EDC	1-ethyl-3-(3-dimethylaminopropyl)carbodiimide
Et	ethyl
Et_2NH	diethylamine
Et_2O	diethylether
Et_3N	triethylamine
EtOAc	ethyl acetate
FDA	food and drug administration
GR	glucocorticoid receptor
hERG	human ether-a-go-go-related gene
HAT	histone acetyltransferase

HATU	1-[bis(dimethylamino)methylene]-1*H*-1,2,3-triazolo[4,5-*b*]pyridinium-3-oxide hexafluorophosphate
HBTU	*N,N,N′,N′*-tetramethyl-*O*-(1*H*-benzotriazol-1-yl)uronium hexafluoro-phosphate
HDAC	histone deacetylase
HDLP	histone deacetylase-like protein
HOBt	1-hydroxybenzotriazole
HPLC	high-performance liquid chromatography
HSP90	heat shock protein 90
IC_{50}	half maximal inhibitory concentration
*i*Pr	isopropyl
KO*t*Bu	potassium tertiairy butoxide
LOQ	limit of quantitation
*m*CPBA	*meta*-chloroperbenzoic acid
Me	methyl
MeOH	methanol
MMP	matrix metalloprotease
MTT	3-(4,5-dimethylthiazol-2-yl)-2,5-diphenyltetrazolium bromide
MS	microsomal stability or mass spectrometry
MW	microwave
NAD^+	nicotinamide adenine dinucleotide
NBS	*N*-bromosuccinimide
NF-κB	nuclear factor kappa-light-chain-enhancer of activated B cells
NMP	*N*-methyl-2-pyrrolidone
NMR	nuclear magnetic resonance
OMe	methoxy
PPB	plasma protein binding
PPh_3	triphenylphosphine
Pr	propyl
pTsOH	*para*-toluenesulfonic acid
PyBOP	(benzotriazol-1-yloxy)tripyrrolidinophosphonium hexafluorophosphate
RI	resistance index
rt	room temperature
SAR	structure activity relationship
SI	selectivity index
$SOCl_2$	thionyl chloride

TBDPS	*tert*-butyldiphenylsilyl
TBTA	tris[(1-benzyl-1*H*-1,2,3-triazol-4-yl)methyl]amine
*t*Bu	tertiairy butyl
TFA	trifluoroacetic acid
TFAA	trifluoroacetic anhydride
THF	tetrahydrofuran
THP	tetrahydropyran
WHO	World Health Organisation
Δ	refluxing temperature

PhD ABSTRACT

The hydroxamic acid functionality is an important group in different chemistry disciplines, such as coordination chemistry and medicinal chemistry, due to its excellent metal-chelating properties. In this PhD thesis, the interest in the hydroxamic acid moiety is specifically related to effective and selective histone deacetylase 6 (HDAC6) inhibition. HDAC6 is a member of the broader histone deacetylases enzyme family, which regulate the folding of DNA around histones and thus indirectly influence transcription. A major drawback associated with non-selective HDAC inhibitors concerns their toxic side effects. As HDAC6 recently emerged as a relevant drug target, the aim of this PhD thesis is to move away from classical pan-HDAC inhibitors and thus to synthesize new HDAC6 inhibitors with potential applications in medicine. In particular, three novel classes of thiaheterocyclic benzohydroxamic acids were developed as potent HDAC6 inhibitors displaying excellent selectivity on both an enzymatic and a cellular level. The most promising inhibitors identified in this work can be considered as valuable lead structures for elaborate follow-up studies.

INTRODUCTION AND GOALS

The pharmaceutical industry is continuously searching for new small molecules that could be used as drugs for the treatment of various diseases. Two main approaches 'philosophies' are used to fasten the process of drug discovery; the first one is called 'target-based drug discovery' and the second one 'phenotype-based drug discovery' (Figure 1).[1,2] In target-based drug discovery, an essential protein responsible for the disease state is targeted and molecules are identified to bind to this protein. These identified molecules interrupt the biochemical pathway responsible for the illness. Target-based drug discovery has the advantage that a fast screen of major compound libraries can be accomplished by using a simple binding assay of the molecule to the targeted protein. The downside of this philosophy is that only a binding optimization is pursued, which does not give any information about the impact of the binding on the more complex disease state or, in other words, no information is obtained about the overall effectiveness of the molecule. This problem is more or less avoided when applying phenotype-based drug discovery, which starts with screening the molecules in a more realistic environment and evaluating them for a certain phenotype (an observable characteristic in an organism, tissue or cell). The downside of phenotype-based drug discovery is that the screening of molecules takes a lot longer due to the more complex assays used.
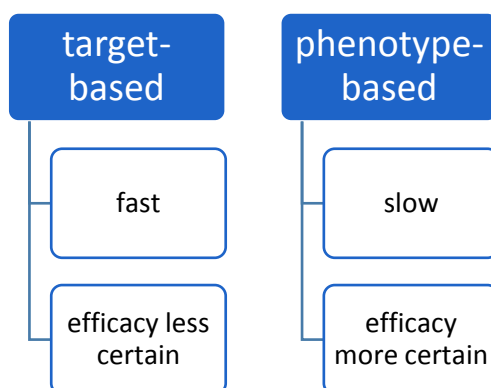
Figure 1. Advantages and disadvantages of target- and phenotype-based screening strategies.

In this PhD thesis, a target-based drug discovery approach will be applied and full attention will be devoted to the selective inhibition of histone deacetylase 6 (HDAC6). HDAC6 belongs to the histone deacetylase (HDAC) family, which controls the deacetylation of histone proteins in the nucleus of cells (Figure 2).[3,4] Simplified, this deacetylation results in a compacted chromatin state which is less accessible for transcription and directs the cell to its basic proliferating functions. Cellular proliferation is a typical phenotype of cancer cells and therefore histone deacetylase inhibitors (HDACi's) play a prominent role as anticancer drugs, as it is believed that these inhibitors redirect cells form a proliferating state to a differentiated state. Now it is known that HDACs have many more functions in cells and also deacetylate non-

histone proteins, and therefore they are more correctly referred to as lysine deacetylases (KDACs).[5]

Figure 2. The removal and addition of acetyl groups from lysine residues of histones by respectively histone deacetylases (HDACs) and histone acetyl transferases (HATs). Histone acetyltransferases (HATs) regulate the reverse biological pathway, forming a relaxed chromatin state more accessible for gene transcription. (Green: histones, Red : DNA)

The HDAC family contains eighteen isoforms, which have been subdivided into four classes based on their homology to yeast HDACs (HDAC classes I-IV). Class I consists of HDAC1, 2, 3 and 8, class IIa comprises HD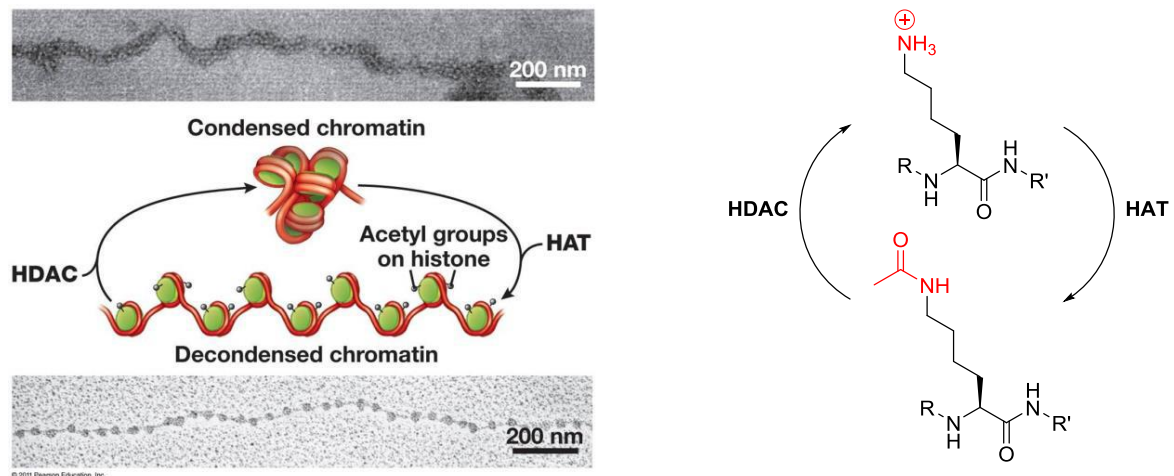AC4, 5, 7 and 9, class IIb contains HDAC6 and 10, class III exists of Sirtuins1-7 and class IV holds only one representative, HDAC11.[6] Class III, the Sirtuins, differ from the zinc-dependent HDACs (class I, II and IV) as they catalyze the removal of acetyl groups from lysine residues via an NAD⁺-dependent (nicotinamide adenine dinucleotide) mechanism. Since the focus of this PhD thesis is directed toward HDAC6, a zinc-containing HDAC, the Sirtuin class will not be discussed here. Phylogenetically speaking, HDAC6 is most closely related to HDAC10, however its resemblance with other HDACs is low, pointing to an early evolutionary separation from the other HDACs. HDAC6 is a unique isoform, being the only representative containing two functional catalytic domains.[7] Unlike its brothers in the HDAC family, HDAC6 is mainly located in the cytoplasm of cells due to the presence of a nuclear export signal motif and a cytoplasmic anchoring motif in its amino acid sequence.[8] Furthermore, the main substrates of HDAC6 comprise non-histone proteins, such as α-tubulin, cortactin and HSP90 (Figure 3). Recently, the crystal structures of the second catalytic domain from *Homo sapiens* HDAC6 and the first and second catalytic domain from *Danio rerio* HDAC6 have been reported, revealing important new insights into the catalytic mechanism and substrate scope of both catalytic domains (Figure 3).[7,9]
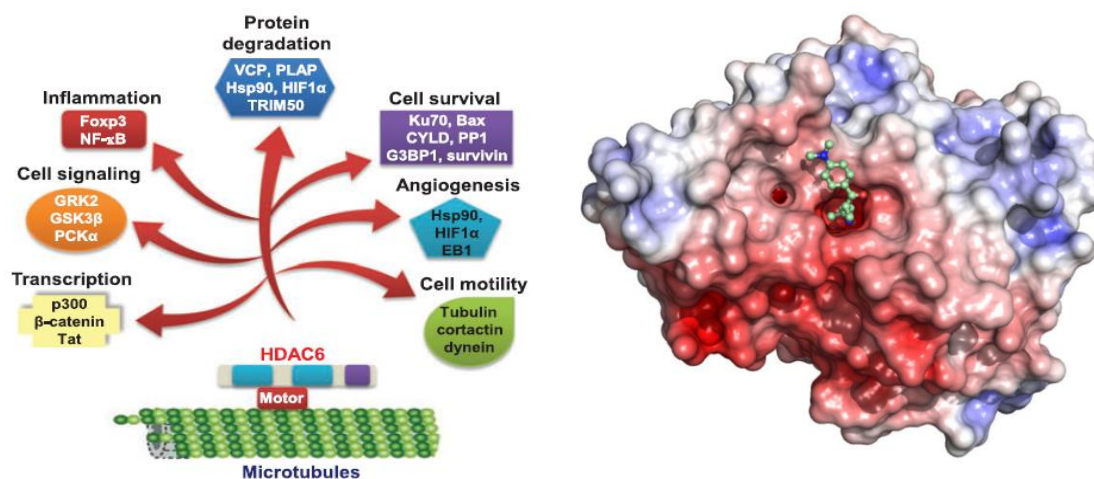
Figure 3. Functions of HDAC6 and the recent published crystal structure of the second catalytic domain of *h*HDAC6 fused to the maltose binding protein, complexed with Trichostatin A (a pan-HDAC inhibitor).[8,9]

At present, four histone deacetylase inhibitors, *i.e.* Vorinostat **1** (SAHA), Belinostat **2** (PXD-101), Romidepsin **3** (FK-228), and Panobinostat **4** (LBH-589), are FDA approved for the treatment of cancer (Figure 4), and several other HDACi's are currently being investigated in clinical trials. The majority of these inhibitors are nonselective and display pronounced toxic side effects due to their broad activity. Therefore, the aim of this PhD thesis is to move away from classical pan-HDAC inhibitors and to synthesize new HDAC6 inhibitors, which may hold superior therapeutic potential over their nonselective counterparts. HDAC6 inhibition represents an enormous therapeutic potential because of the numerous disease states in which this protein is implicated.[10] Especially the therapeutic areas of autoimmune disorders, neurodegenerative diseases and cancer seem to be most prone to changes in HDAC6 activity. Furthermore, as mice lacking HDAC6 have been shown to develop normally, it is believed that no or only minor side effects are expected when HDAC6 is inhibited.[11] HDAC inhibitors all consist of (i) a zinc-binding group complexing the zinc atom in the catalytic pocket of the enzyme (Figure 4, red), (ii) a linker unit filling the tubular space between the catalytic pocket and the outer surface of the enzyme (Figure 4, blue), and (iii) a cap-group for interaction with the outer protein surface (Figure 4, black).

The first selective HDAC6 inhibitor, Tubacin **5** (tubulin acetylation inducer, Figure 4), has been discovered in 2003 through a multidimensional, chemical genetic screen of 7392 small molecules.[12] However, its non-drug-like structure, high lipophilicity and tedious synthesis encouraged other researchers to make easy-to-synthesize, drug-like selective HDAC6 inhibitors. In that regard, Tubastatin A **6** was developed in 2010 via a rational drug design approach through comparing HDAC1 and HDAC6 homology models.[13] This study revealed that the channel toward the catalytic pocket of HDAC6 is wider and shallower, suggesting that

a more space-filling linker and cap-group could enhance the HDAC6 selectivity. Indeed, the aromatic linker in Tubastatin A **6** and the tetrahydro-γ-carboline cap-group significantly increased the potency and selectivity for HDAC6. Ever since, Tubastatin A is considered to be the reference molecule of choice for benchmarking new HDAC6 inhibitors in terms of potency and selectivity.
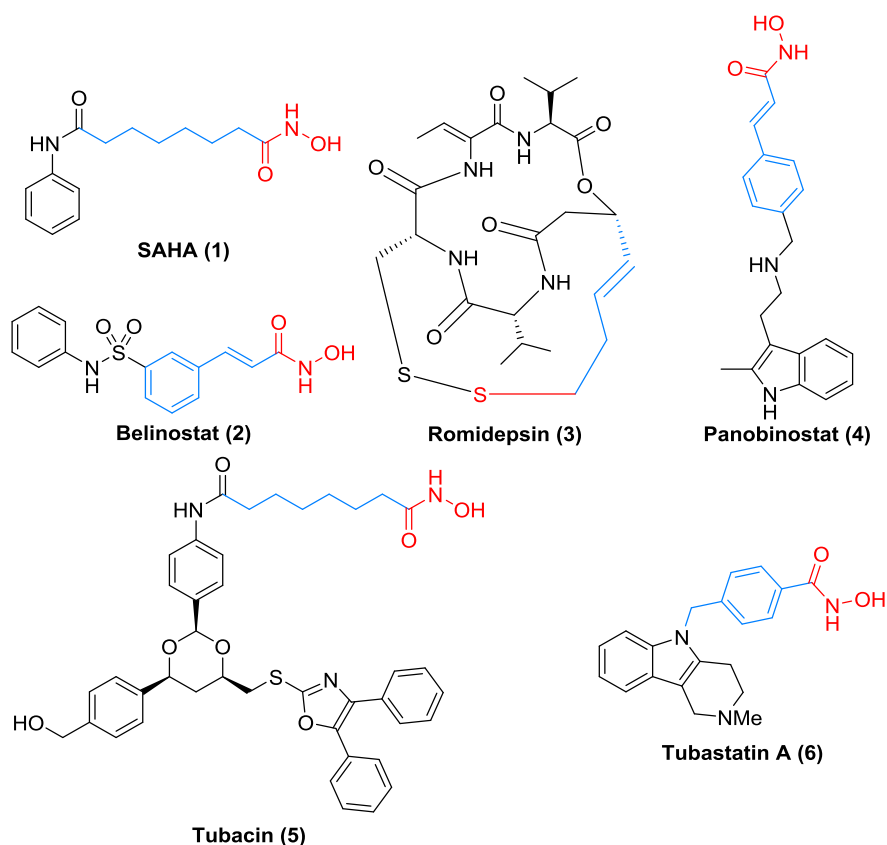
Figure 4. FDA-approved HDAC inhibitors **1-4** and HDAC6 selective inhibitors Tubacin **5** and Tubastatin A **6** (Red: zinc-binding group, Blue: linker, Black: cap-group).

Inspired by the structure of the model HDAC6 inhibitor Tubastatin A, the overall aim of this PhD thesis involved the design, synthesis and evaluation of new HDAC6 inhibitors bearing a benzohydroxamic acid scaffold attached to a large heterocyclic cap-group. In particular, novel benzohydroxamic acids accommodating a thiaheterocyclic cap-group were pursued, as the synthesis of thiaheterocyclic benzohydroxamic acids comprises an unexplored field within HDAC inhibitor design. In collaboration with other groups, the proposed inhibitors were docked in a homology model of HDAC6 to evaluate their *in silico* potency (via computer simulations). When the structures appeared to have a good *in silico* fit, their lab synthesis was attempted, followed by a preliminary assessment of their biological properties. It is essential to note that the main focus of this work was put on the elaboration of new synthetic routes toward novel

thiaheterocyclic benzohydroxamic acids and a preliminary assessment of their biological properties.

The first chapter in this thesis will situate these thiaheterocyclic benzohydroxamic acids in a broader literature context. Therefore, an overview of the synthesis and biological activity of the most representative benzohydroxamic acid-based histone deacetylase inhibitors published to date will be given. In this manner, the reader will get a profound understanding of the state-of-the-art concerning benzohydroxamic acid HDAC inhibitors.

The second and third chapter will be devoted to the design, synthesis and biological evaluation of sulfur analogs **13** of Tubastatin A (Scheme 1). In the first chapter, a select group of compounds will be prepared and evaluated, giving rise to preliminary structure-activity relationships which will be used to design a more potent group of second-generation compounds, discussed in chapter III. For their synthesis, the following synthetic route will be deployed. In a first step, aromatic hydrazines **7** will be converted to thiaheterocyclic cap-groups **9** employing a Fischer-indole synthesis upon treatment with cyclic ketones **8**. The sulfur atom will further be oxidized by means of a *meta*-chloroperbenzoic acid (*m*CPBA) treatment, resulting in oxidized analogs **10**. Both cap-groups **9** and **10** will then be reacted with methyl (bromomethyl)benzoates **11** to furnish esters **12**. In a final step, esters **12** will be transformed to the desired hydroxamic acids **13** using hydroxylamine.
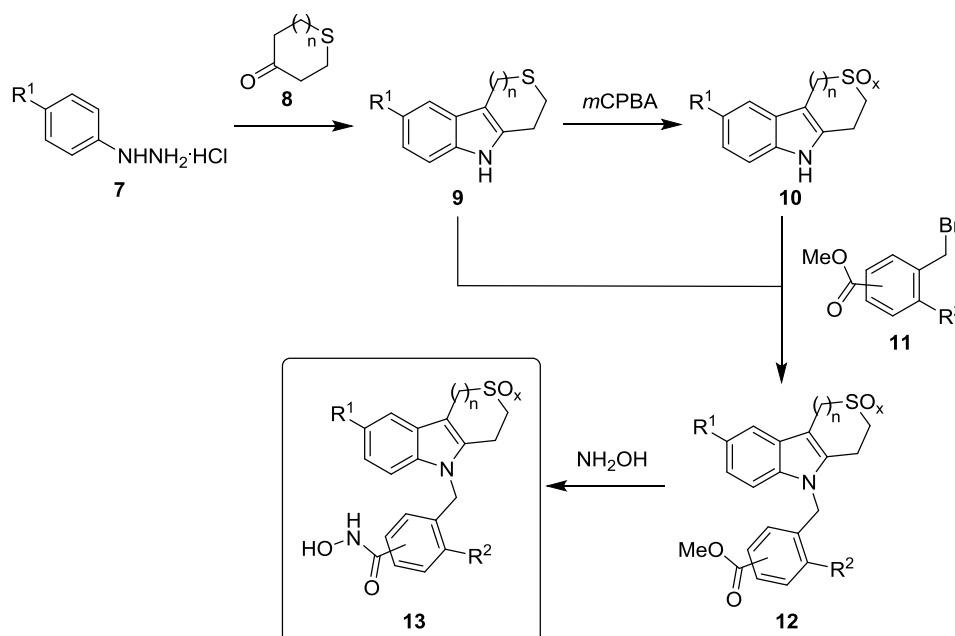
Scheme 1

The fourth and fifth chapter will deal with the design, synthesis and biological evaluation of two other classes of thiaheterocyclic benzohydroxamic acids, more specifically benzothiophene benzohydroxamic acids **18** and annulated benzothiazepine benzohydroxamic acids **23** (Scheme 2 and 3). Benzothiophenes **18** will be prepared via a reductive amination starting from benzothiophene-3-carbaldehydes **14** employing methyl 4-aminobenzoates **15** (Scheme 2). The secondary amino group in esters **16** will be further functionalized through a nucleophilic substitution with an alkyl halide, forming tertiary amines **17**. A final ester to hydroxamic acid interconversion should yield the premised hydroxamic acids **18** from the corresponding substrates **16** and **17**.
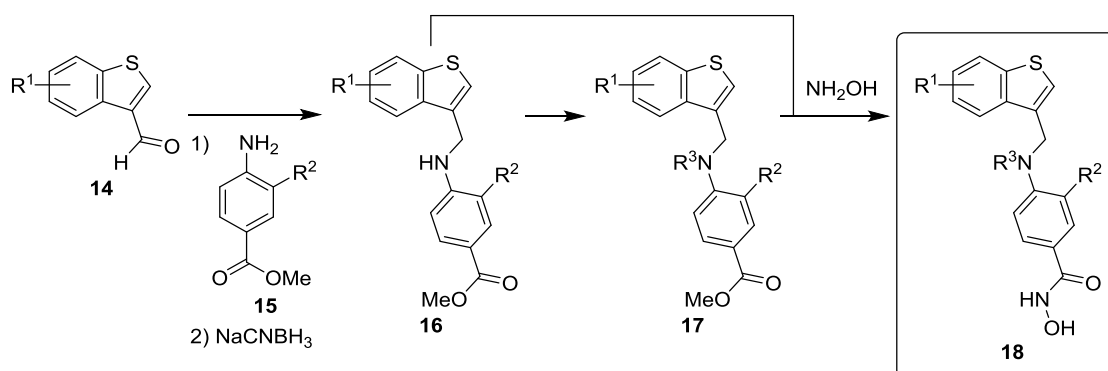
Scheme 2

For the synthesis of benzothiazepine-containing benzohydroxamic acids **23**, cyclic ketones **19** will be transformed into annulated benzothiazepines **20** over several steps (including an aldol condensation with formaldehyde, a tosylation, a reaction with 2-aminothiophenol and a reduction, Scheme 3). A following nucleophilic substitution with methyl 4-(bromomethyl)benzoate **21** will give rise to the formation of esters **22**, which will eventually be converted into hydroxamic acids **23**.
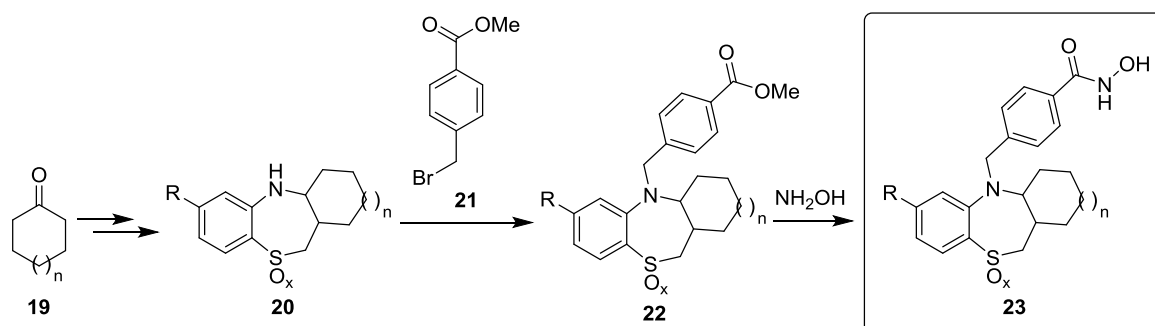
Scheme 3

All synthesized thiaheterocyclic benzohydroxamic acids will be evaluated for their potency to inhibit HDAC6. Therefore, in a first enzyme-substrate assay the percentage inhibition of HDAC6 will be determined using a fixed concentration of 10 µM of inhibitor. Structures demonstrating more than 70% inhibition of substrate conversion with respect to the control will be selected for determination of their IC_{50} value toward HDAC6. The selectivity toward the other zinc-dependent HDACs (HDAC1-11) will only be assessed for representative inhibitors bearing high potency for HDAC6 (having low nanomolar IC_{50} values). This will be accomplished through enzyme assays (by determining the IC_{50} values for HDAC1-11) and cellular assays (by evaluating the acetylation level of a known substrate of HDAC6, α-tubulin, versus the acetylation level of a known substrate of class I HDACs, histones, via Western Blots). The obtained results will be discussed within the respective chapter.

Given the promising antiplasmodial activity of pan-HDAC inhibitors reported in the literature,[14] the final chapter VI will discuss the antimalarial activity of the benzohydroxamic acids synthesized in chapters II-V. These novel selective HDAC6 inhibitors could supersede the therapeutic potential of pan-HDAC inhibitors, because less toxic side effects are expected when isoform-selective inhibitors are administered to the patient. The recurring resistance of the malaria parasite to many antimalarial drugs compels the discovery of new chemical entities, such as the selective HDAC6 inhibitors presented in this thesis.

These six chapters will provide new insights in the evaluation of thiaheterocyclic benzohydroxamic acids as selective HDAC6 inhibitors and give the reader a comprehensive overview of the state-of-the-art of benzohydroxamic acid-based HDAC inhibitors.

LITERATURE REVIEW

1. Synthesis and applications of benzohydroxamic acid-based histone deacetylase inhibitors

Abstract: *This chapter provides an overview of the synthesis and biological activity of the most representative benzohydroxamic acid-based histone deacetylase inhibitors published to date. Benzohydroxamic acids comprise an important class of HDAC inhibitors, and recently several of these structures have been evaluated in clinical trials for the treatment of a variety of cancers. In this overview, benzohydroxamic acids were divided in four different classes based on their reported selectivity toward zinc-dependent HDACs: a first and major class consists of HDAC6 selective inhibitors, a second class deals with pan-HDAC inhibitors, a third class comprises HDAC8 selective inhibitors and a fourth, minor class includes dual HDAC6/8 selective inhibitors. Through this approach, structure-activity relationships were identified for each class, which could help future researchers in the design and development of novel benzohydroxamic acid-based HDAC inhibitors.*

1.1. Introduction

The hydroxamic acid functional group can be considered as a privileged scaffold in several fields of chemistry due to its excellent metal-chelating properties. Metal chelation can occur through a monoanionic hydroxamato form or a dianionic hydroximato form in an *O,O'*-bidentate fashion. As a consequence, hydroxamic acids are ideal ligands for binding the active site of nickel- or zinc-containing metalloproteins (e.g. histone deacetylases, matrix metalloproteases, ureases and carbonic anhydrases), and they form a class of siderophores (iron-sequestering molecules secreted by microorganisms) as well. Hydroxamic acids are also used in heavy metal extraction procedures, nuclear fuel reprocessing and as chiral ligands in asymmetric synthesis.[15]

This review will exclusively focus on the synthesis and biological activity of benzohydroxamic acids as histone deacetylase inhibitors. The development of benzohydroxamic acids indeed involves an important and active field within HDAC inhibitor design, and many research teams from industry and academia are currently participating in this quest.

Histone deacetylases (HDACs) have been discovered as a class of enzymes which regulate the removal of acetyl groups from lysine residues of histones, consequently playing an important regulatory role in epigenetics.[16] In following studies, other proteins have also been identified as HDAC substrates, and therefore these enzymes are more correctly referred to as lysine deacetylases or KDACs.[17] In total, four classes of HDACs can be identified (HDAC I-IV). HDAC classes I, II and IV employ Zn^{2+} as an essential cofactor while HDAC class III, also known as the Sirtuin class, needs NAD^+ to exert activity. Since the focus of this review is directed toward hydroxamic acids targeting zinc-containing HDACs, the Sirtuin class will not be discussed here. In total, eleven zinc-containing isoforms have been discovered, which were subdivided via their homology to yeast HDACs (Class I: HDAC1, 2, 3 and 8, Class IIa: HDAC4, 5, 7 and 9, Class IIb: HDAC6 and 10, Class IV: HDAC11).[6] Due to the involvement of these isoforms in modern-day diseases such as cancer, neurodegenerative diseases and inflammatory disorders, a lot of effort is currently being devoted to the development of safe and efficient histone deacetylase inhibitors (HDACi's).[18,19] In that regard, several HDACi's have reached the patient, with vorinostat, the first clinically approved anti-cancer HDACi for the treatment of cutaneous T cell lymphoma, as a leading example.[20,21] HDAC inhibitors typically consist of (i) a zinc-binding group complexing the zinc atom in the catalytic pocket of the enzyme, (ii) a linker unit filling the tubular space between the catalytic pocket and the outer surface of the enzyme, and (iii) a cap-group for interaction with the outer protein surface. This review is oriented toward the medicinal chemistry of benzohydroxamic acids as privileged structures in HDAC research and will encompass the synthesis and biological activities of the most representative HDACi's bearing a hydroxamic acid zinc-binding group directly connected

to a phenyl ring. This approach will provide insights into the selectivity that can be observed when designing functionalized benzohydroxamic acids and will give an overview of available synthetic routes to obtain this kind of structures.

1.2. Benzohydroxamic acid-based HDAC inhibitors

This overview is based on a classification of benzohydroxamic acids in terms of their reported selectivities. As a result, four groups of inhibitors were identified: a major group of HDAC6 selective inhibitors, a group of non-selective pan-inhibitors, and two smaller groups, one consisting of HDAC8 selective inhibitors and one containing dual HDAC6/8 selective inhibitors. When reading the appropriate literature, one will notice that the term 'selectivity' is interpreted differently by various authors, and therefore the following questions arose when writing this review. Can one claim an inhibitor to be selective for a specific zinc-containing HDAC isoform if not all IC_{50} values for each of the eleven HDAC isoforms have been determined? When is an inhibitor selective over another HDAC isoform, in other words, can a certain threshold value be employed? Is determination of the selectivity based on the purified HDAC isoforms an accurate representation of the selectivity, or should the IC_{50} values be determined based on the selectivity against the in cell existing HDAC complexes?[22] Can conclusions be made by comparing IC_{50} values resulting from different assays (because they depend on the type of substrate and the substrate concentration used), or should dissociation constants (K_i) be used? These important questions should be taken into account when reading the chapters below. In order to avoid any ambiguity concerning the interpretation of the term 'selectivity', an inhibitor will be denoted here as selective toward another isoform if it holds at least a tenfold lower inhibition value (K_i or IC_{50}) over the other isoform. The tenfold cut-off value was determined after evaluating the IC_{50} values (K_i values) of the benzohydroxamic acid HDAC inhibitors present in the literature which gave a general image of the acceptable cut-off value for selectivity used in the literature.

1.2.1. Selective benzohydroxamic acid-based HDAC6 inhibitors

The selective inhibition of HDAC6 is a 'hot topic' in medicinal chemistry, exemplified by the impressive group of benzohydroxamic acids presented in Figure 1. When overviewing compounds **1-17**, it is noticeable that the majority accommodate a rather voluminous cap-group, *para*-substituted with respect to the hydroxamic acid functionality and in close proximity to the phenyl linker. This voluminous cap-group is never directly attached to the phenyl linker, implying that at least one atom (carbon or nitrogen) resides between the cap-group and the phenyl unit. This distance is most likely necessary to avoid a steric clash between the large cap-group and the protein, suggesting that this additional atom is part of the linker unit filling the tubular space to the catalytic pocket. Another feature which emerges when inspecting this group of molecules is that several members share the following common structure: a heterocyclic scaffold linked through a methylene bridge to the benzohydroxamic acid unit.
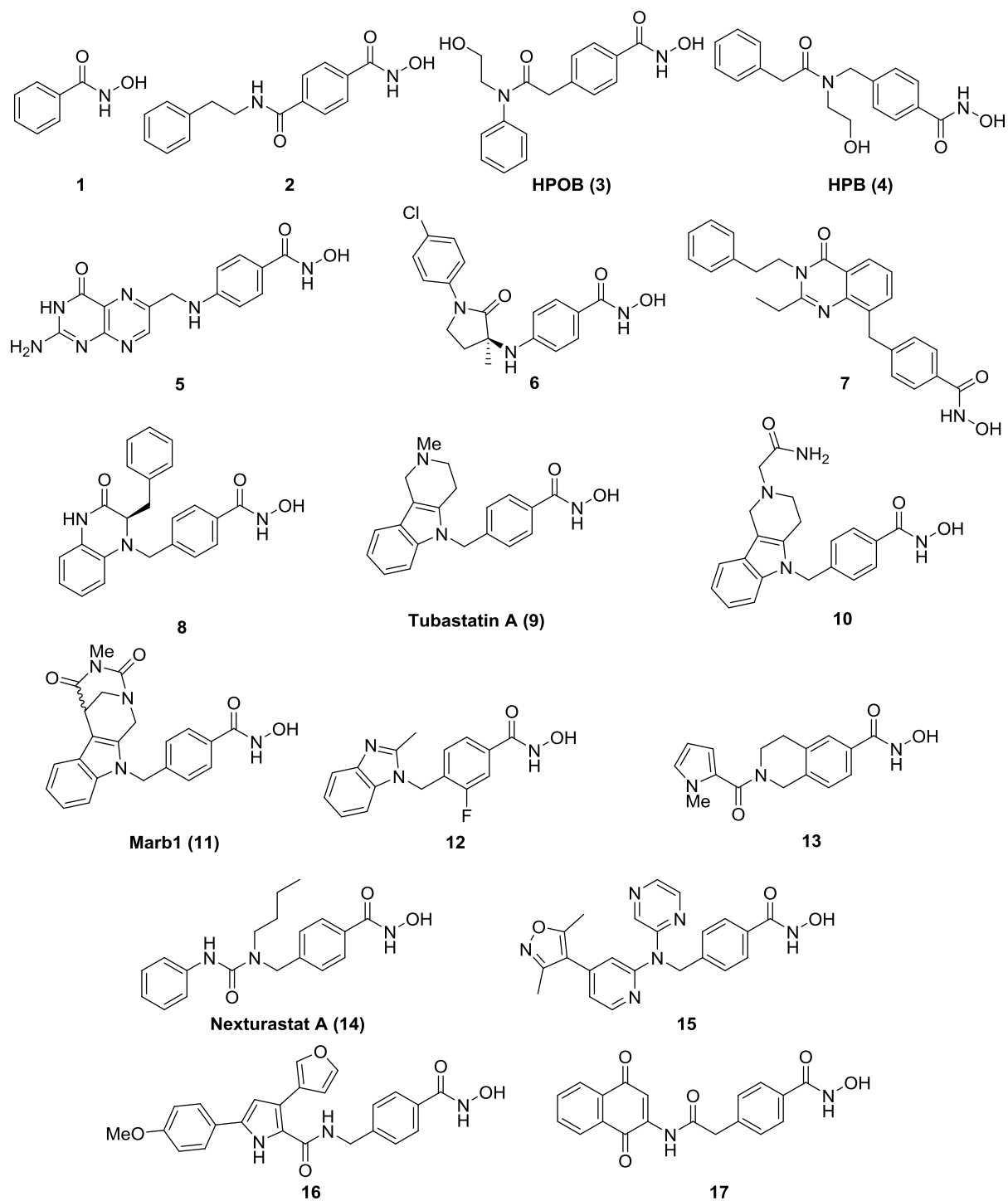
Figure 1. Overview of selective HDAC6 inhibitors bearing the benzohydroxamic acid moiety.

For each inhibitor depicted in Figure 1, the biological activity and synthetic pathway will be discussed below.

When presenting an overview on benzohydroxamic acids as HDAC inhibitors, the simplest representative, *i.e.* benzohydroxamic acid **1** itself, must be included in the discussion as well (Figure 1). The search for selective HDAC6 inhibitors able to penetrate the blood-brain barrier encouraged Wagner and co-workers to design the smallest possible pharmacophore still demonstrating effective HDAC6 selectivity and activity.[23] Therefore, the concept of ligand efficiency was used, defined as the HDAC6 activity over the number of non-hydrogen atoms, which is a known valuable tool in drug design to compare differently sized molecules with similar activity values. Compounds possessing a high ligand efficiency have a higher probability to demonstrate improved pharmacokinetic properties as central nervous system drugs. In that regard, benzohydroxamic acid **1** (a commercially available hydroxamic acid) has been evaluated as HDAC inhibitor and showed good potency and selectivity for HDAC6 (Table 1) and holds a high ligand efficiency, due to the small size of the molecule. The selectivity of this compound was further confirmed in a Western Blot assay in HeLa cells, measuring the acetylation status of α-tubulin (a substrate of HDAC6) and histone H3 (a substrate of class I HDACs).

Table 1. Selective inhibition of HDAC6 by benzohydroxamic acid **1**.

HDAC	1	2	3	4	5	6	7	8	9
IC_{50} (µM)	4.7	7.9	7.8	>33.3	>33.3	0.115	15.6	1.9	>33.3

In the same study several other substituted benzohydroxamic acids were synthesised as well, with compound **2** demonstrating the most pronounced HDAC6 activity (IC_{50} = 0.004 µM, Table 2, Scheme 1).[23]

Table 2. Selective inhibition of HDAC6 by benzohydroxamic acid **2**.

HDAC	2	4	6	8
IC_{50} (µM)	0.607	>33.3	0.004	1.15

All benzohydroxamic acids reported in this article bear a carbamoyl group directly linked to the benzohydroxamic acid scaffold, similar as in structure **2**, and were prepared via the following procedure (no yields reported). Amide **19** was synthesized from acid **18** using peptide coupling chemistry with HATU (1-[bis(dimethylamino)methylene]-1*H*-1,2,3-triazolo[4,5-*b*]pyridinium-3-

oxide hexafluorophosphate) as acid-activating reagent. Subsequently, without purification, ester **19** was treated with an excess of hydroxylamine over twelve hours to yield *N*-hydroxyphtalamide **2** as a white solid.
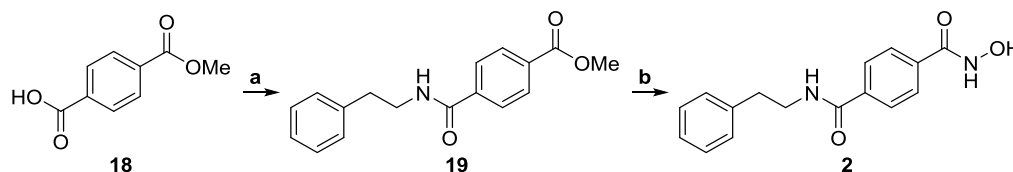
Scheme 1. (a) 2-phenylethylamine (0.84 equiv), HATU (1 equiv), diisopropylethylamine (2.5 equiv), DMF, rt, overnight. (b) NH_2OH (30 equiv, 50% in H_2O), NaOH (10 equiv), CH_2Cl_2/MeOH 1/2, 0°C -> rt, 12h. (no yields reported)

Lee *et al.* have developed HPOB **3** (*N*-hydroxy-4-(2-[(2-hydroxyethyl)(phenyl)amino]-2-oxoethyl)benzamide), a highly selective HDAC6 inhibitor containing a free alcohol and an *N*-phenylamide in the cap-region (Scheme 2).[24] The selective inhibition of HDAC6 is illustrated in Table 3. HPOB demonstrated low nanomolar potency for HDAC6 and micromolar potency for all other zinc-containing HDACs. In a cellular environment, HPOB effectively inhibited HDAC6 by acetylating α-tubulin and peroxiredoxin, two known substrates of HDAC6, and little or no acetylation of histone H3 was observed. The researchers also concluded that HPOB caused growth inhibition of normal and transformed cells, but that no cell death was induced. Besides that, HPOB was evaluated in combination therapies with other anticancer drugs and was shown to enhance the antitumor effects of the chemotherapeutics tested (etoposide, doxorubicin and SAHA).

Table 3. Selective inhibition of HDAC6 by HPOB **3**.

HDAC	1	2	3	4	5	6	7	8	9	10	11
IC_{50} (µM)	2.9	4.4	1.7	>10	>10	0.056	>10	2.8	>10	3.0	>10

The detailed synthesis of HPOB **3** can be found in patent literature published in 2013 (Scheme 2).[25] Reductive amination of glycolaldehyde with aniline **20** in dichloromethane, using sodium triacetoxyborohydride as reductant, resulted in the formation of β-aminoalcohol **21**. A following protection of the alcohol with a *tert*-butyldimethylsilyl group gave silyl ether **22** in an excellent yield. The secondary amine in silyl ether **22** was then coupled to 2-[4-(methoxycarbonyl)phenyl]acetic acid, using EDC (1-ethyl-3-(3-dimethylaminopropyl)-carbodiimide) as a coupling reagent, and produced amide **23**. The ester functionality present in this structure **23** was finally converted to hydroxamic acid **24** and the alcohol protecting

group was removed using trifluoroacetic acid. This approach resulted in the synthesis of HPOB **3** in five steps in an overall yield of 36%.
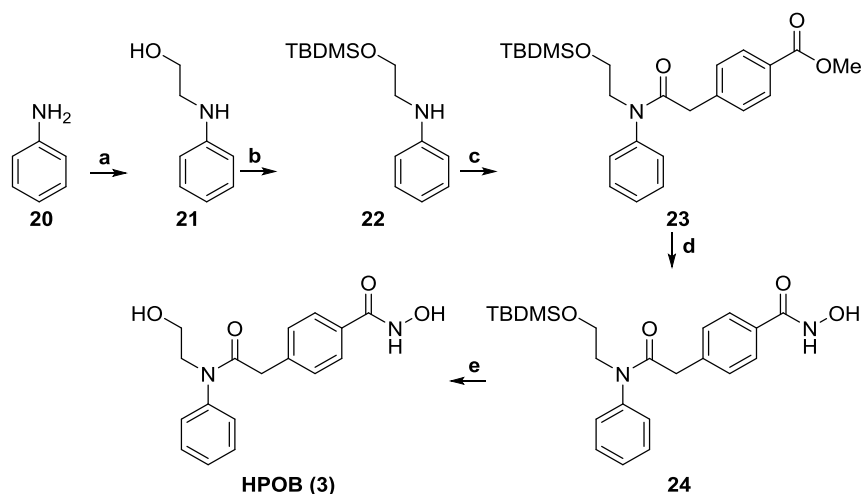

Scheme 2. (a) glycolaldehyde (1 equiv), dichloroethane, rt, 0.5h, Ar(g) -> sodium triacetoxyborohydride (1.15 equiv), rt, 4h. 72%. (b) TBDMS-Cl (1.1 equiv), imidazole (3 equiv), CH_2Cl_2, rt, 3h, Ar(g). 92%. (c) 2-[4-(methoxycarbonyl)phenyl]acetic acid (1.5 equiv), EDC (1.5 equiv), CH_2Cl_2, rt, overnight, Ar(g). 90%. (d) NH_2OH (58 equiv, 50% in H_2O), KCN (cat.), THF/MeOH (1/1), rt, 16h, Ar(g). 66%. (e) TFA (5% in CH_2Cl_2), rt, 5 min. 68%.

After the discovery of HPOB **3**, the same research group developed a similar selective HDAC6 inhibitor named HPB **4** (*N*-hydroxy-4-([*N*-(2-hydroxyethyl)-2-phenylacetamido]methyl)-benzamide, Scheme 3).[26] This molecule has been reported to be as effective as paclitaxel in anticancer activity in tumor-bearing mice and to block the growth of normal and transformed cells, but not to induce cell death of normal cells. Moreover, no toxic side effects were observed when this inhibitor was used. A full HDAC1-11 selectivity screen was performed, and HPB **4** revealed to be 15- to almost 400-fold selective for HDAC6 over the other HDACs (Table 4).

Table 4. Selective inhibition of HDAC6 by HPB **4**.

HDAC	1	2	3	4	5	6	7	8	9	10	11
IC$_{50}$ (µM)	0.8	2.2	2.1	2.2	9.5	0.025	1.1	0.4	5.3	0.7	3.7

The detailed synthesis of this inhibitor can again be found in the patent literature (Scheme 3).[27] First a mesylation on alcohol **25** was performed to create an appropriate leaving group. The resulting mesylate **26** was then treated with *tert*-butyldimethylsilyl-protected 2-aminoethanol to synthesize secondary amine **27**. This amine **27** could be converted into amide **28** using 2-phenylacetyl chloride. In a final step, amide **28** was transformed into hydroxamic acid **4** using a similar approach as for the synthesis of HPOB **3** (step d, Scheme 2). Overall, this selective HDAC6 inhibitor **4** was obtained in four steps in a combined yield of 17%.
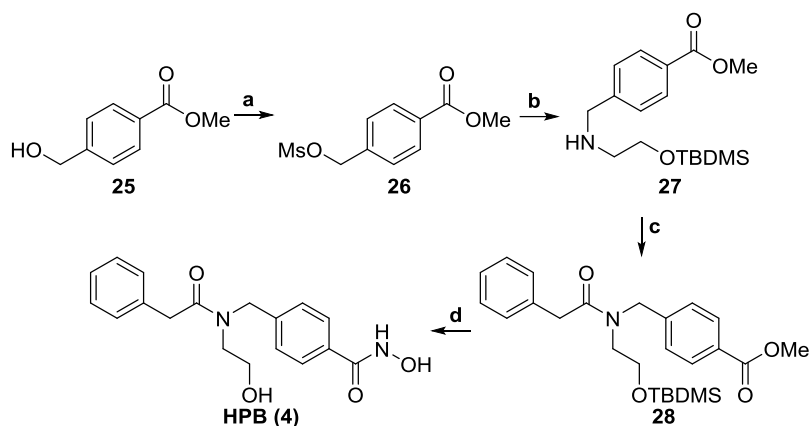
Scheme 3. (a) mesyl chloride (1.2 equiv), triethylamine (TEA, 1.5 equiv), CH_2Cl_2, 0°C-rt 1h. (b) 2-TBDMS-ethanamine (1.2 equiv), TEA (1 equiv), DMF, rt, 2h. (c) 2-phenylacetyl chloride (1.2 equiv), TEA (1.8 equiv), CH_2Cl_2, 0°C-rt, 4h. (d) NH_2OH (7.2 equiv, 50% in H_2O), KCN (cat.), MeOH, rt, 16h, Ar(g). No individual yields reported, overall yield 17%.

The hydroxamic acid of pteroic acid, structure **5**, has been designed to improve the delivery of HDACi's to solid tumors by targeting the folate receptor, a protein overexpressed in several cancer cells (Scheme 4).[28] This strategy should augment the delivery of the drug to cancer cells while minimizing its effect on healthy cells. Pteroic hydroxamic acid **5** was shown to be HDAC6 selective (Table 5) but did not demonstrate any cytotoxic activity on KB and HeLa cells up to 100 µM. The authors further established a positive correlation between potency of HDAC1 inhibition and cytotoxicity, pointing to HDAC1 inhibition as the responsible factor for cytotoxic effects in KB and HeLa cells.

Table 5. Selective inhibition of HDAC6 by pteroic hydroxamic acid **5**.

HDAC	1	6	8
IC$_{50}$ (µM)	2.39	0.018	0.58

Pteroic hydroxamic acid **5** has been prepared from folic acid **29** in three steps, but no detailed reaction conditions have been reported in the article for the first two steps (Scheme 4). In the first step, the glutamic acid side chain in folic acid **29** was cyclized to imide **30** using trifluoroacetic anhydride (TFAA). During this reaction, the amino functionalities and the free acid were reacted with TFAA forming two amides and an anhydride, respectively. After the addition of ice, one of the amides was retransformed into the free amine, and the free carboxylic acid was regenerated. This resulted in the formation of structure **31**, which could be converted to hydroxamic acid **5** after the addition of five equiv of hydroxylamine. Also, note that during this final step the secondary amine presented in structure **5** was regenerated.
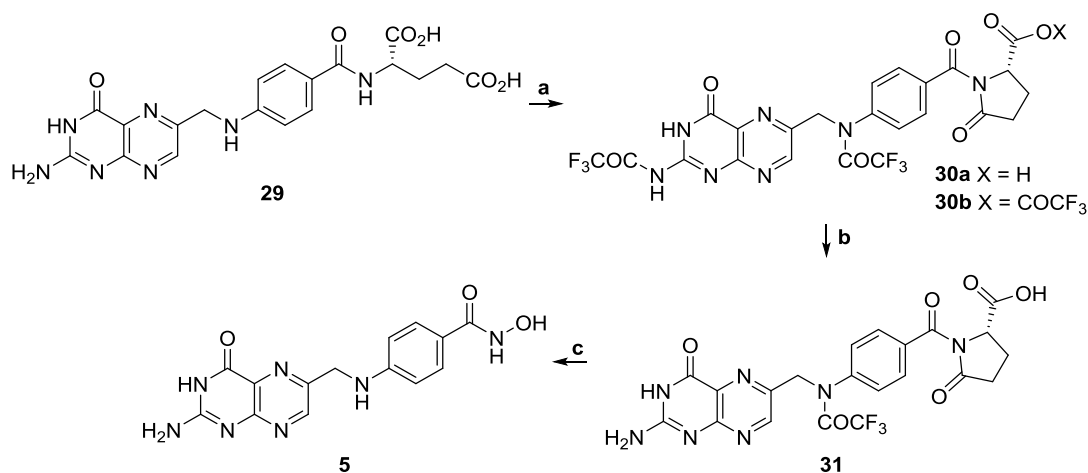
Scheme 4. (a)* TFAA, THF, rt. (b)* THF, ice. (c) NH_2OH (5 equiv, 50% in H_2O), DMSO, rt, 5h. 32%. *No detailed reaction conditions are reported.

3-Aminopyrrolidinone-based hydroxamic acids, such as structure **6**, have been prepared as a new class of selective HDAC6 inhibitors via scaffold hopping starting from an earlier discovered dual HDAC6/8 selective inhibitor (Scheme 5).[29,30] Thorough structure-activity relationship, drug metabolism and pharmacokinetic studies were performed on this class of compounds and revealed enantiomer **6** to display the best properties in that regard (Table 6). Molecular docking of the compounds revealed that the *para*-substituted amino group (with respect to the hydroxamic acid functionality) could be involved in hydrogen bonding with HDAC6, rationalizing the excellent potency for this HDAC isoform.

Table 6. Selective inhibition of HDAC6 by 3-aminopyrrolidinone-based hydroxamic acid **6**.

HDAC	1	6	8
IC_{50} (µM)	74.1	0.017	0.18

The chiral synthesis of compound **6** started by a copper-catalyzed coupling between (*S*)-methionine **32** and methyl 4-iodobenzoate (Scheme 5). The resulting acid **33** was then further transformed to amide **34** using a coupling reagent and 4-chloroaniline. Ring closure was realized by adding methyl iodide to sulfide **34**, furnishing a dimethylsulfonium salt which was intramolecularly displaced by the amide functional group. In a final step, hydroxamic acid **6** was formed from ester **35** using a hydroxylamine solution in water.
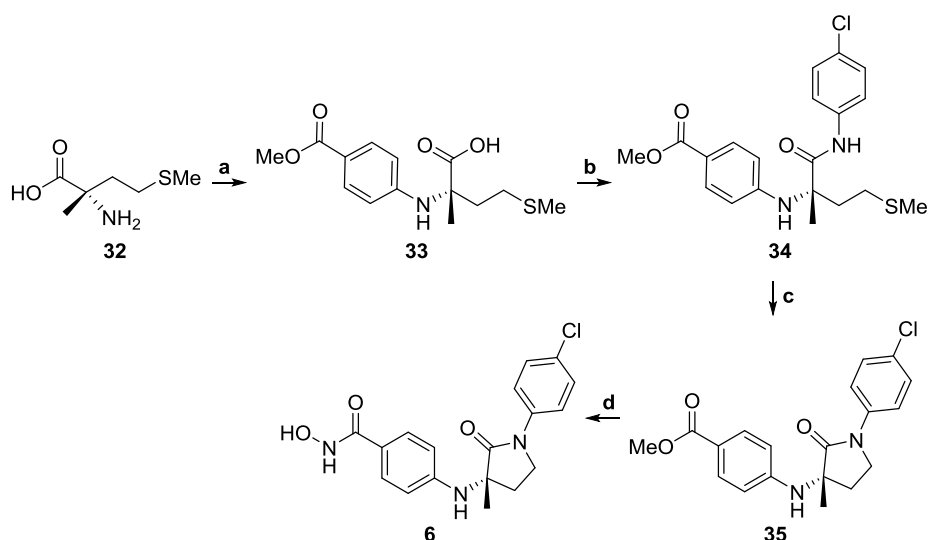
Scheme 5. (a) methyl 4-iodobenzoate (0.66 equiv), CuI (3.3 mol%), K$_2$CO$_3$ (1 equiv), DMSO, 150°C, 10 min, MW. 90%. (b) 4-chloroaniline (1.2 equiv), HATU (1.2 equiv), TEA (2.5 equiv), DMF, rt, 6h. 60%. (c) MeI (4 equiv), CH$_3$CN, rt, overnight -> NaH (1.2 equiv), DMF, rt, 6h. 70%. (d) NH$_2$OH (12 equiv, 50% in H$_2$O), KOH (cat.), MeOH, 60°C, rt. 70%.

Quinazolin-4-one-based HDAC6 inhibitors have been designed and synthesized as novel drug candidates for the treatment of Alzheimer's disease (Scheme 6).[31] It is known that HDAC6 levels significantly increase in the hippocampi of Alzheimer patients and correlate with decreased neuronal survival. Therefore, the quinazolin-4-one moiety was introduced in the structure of these inhibitors, because this moiety is known to exert neuroprotective activity. In this series, the compounds bearing an *N*-hydroxyacrylamide functionality possessed the best HDAC6 activity and ADME/Tox properties, but also the benzohydroxamic acids demonstrated potent activity and selectivity for HDAC6. From all benzohydroxamic acids tested, compound **7** was judged to be the most selective over the other HDACs, except for HDAC8 (Table 7). The safety of this drug was tested by determining inhibition values for cytochrome P450 (CYP) and the human ether-a-go-go-related (hERG) channel, but similar as for the HDAC6 activity the *N*-hydroxyacrylamide-substituted compound showed to have a superior and safer profile than benzohydroxamic acid **7**. Note that compound **7** does not comply with the tenfold selectivity rule described in the introduction, and should therefore perhaps be better classified as a dual selective HDAC6/8 inhibitor.

Table 7. Selective inhibition of HDAC6 by quinazolin-4-one **7**.

HDAC	1	2	6	8	11
IC$_{50}$ (µM)	>50	>10	0.079	0.282	37.1

The synthesis of hydroxamic acid **7** started with the formation of the quinazolin-4-one moiety by reacting aromatic amino acid **36** with propionyl chloride and subsequently with an appropriate amine under microwave irradiation. Next, chlorinated quinazolin-4-one **37** was subjected to a Negishi coupling using ethyl 4-(bromomethyl)benzoate and zinc, which resulted in the formation of ester **38**. After ester hydrolysis, *O*-benzylhydroxamate formation and hydrogenation, benzohydroxamic acid **7** was obtained in pure form as white needles.
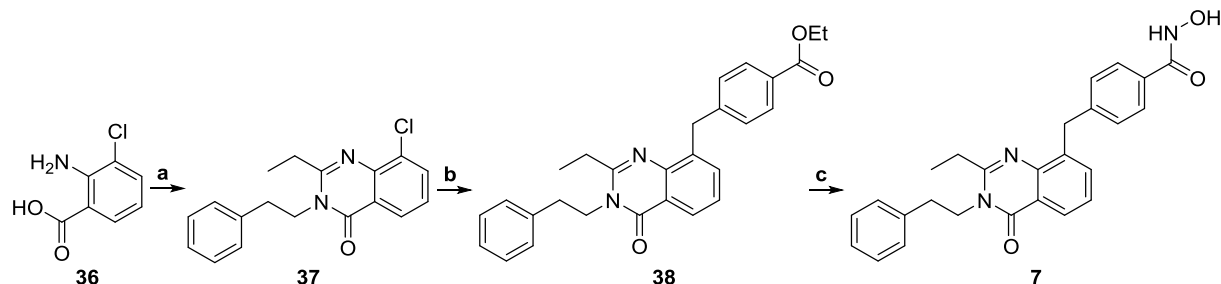
Scheme 6. (a) i) P(OPh)$_3$ (1.2 equiv), EtCOCl (1.5 equiv), pyridine, 250W, 15 min, MW. ii) Ph(CH$_2$)$_2$NH$_2$ (1.5 equiv), 250 W, 10 min, MW. 47%. (b) *p*-EtO$_2$CC$_6$H$_4$CH$_2$Br (1 equiv), Zn (1.1 equiv), THF, rt, 7h -> Pd$_2$(dba)$_3$ (2 mol%), [(*t*Bu)$_3$PH]BF$_4$ (8 mol%), NMP, 200W, 15 min, MW. No yield reported. (c) i) LiOH (2.5 M), MeOH/THF 1/5, rt, 4 h. ii) NH$_2$OBn.HCl (1.1 equiv), EDC (1.1 equiv), HOBt (1.1 equiv), TEA (1.1 equiv), CH$_2$Cl$_2$, rt, 20h. iii) Pd (10% on carbon), H$_2$, THF/MeOH 1/4, rt, 5h. 49% in last step.

In 2009, the first selective HDAC6 inhibitor containing a 4-(aminomethyl)benzohydroxamic acid moiety has been reported.[32] As can be seen in Figure 1**,** later on many other selective HDAC6 inhibitors **8-16** containing this moiety have been synthesized and biologically evaluated. To gain HDAC6 selectivity, a chiral capping moiety was introduced in the structure of this inhibitor **8**. The authors envisaged that this was most rapidly and efficiently accomplished through the use of commercially available chiral starting materials, such as *R*- and *S*-amino acids. As such, *R*-enantiomer **8** was synthesized and exhibited a 26- and 53-fold selectivity for HDAC6 over HDAC2 and 8, respectively (Table 8, Scheme 7). In contrast, the *S*-enantiomer of compound **8** showed only moderate activity for HDAC6 (IC$_{50}$ HDAC6 = 0.22 μM) and no HDAC6 over HDAC8 selectivity. Therefore, introducing chirality in the capping region could be an efficient approach to obtain selective HDAC6 inhibitors.

Table 8. Selective inhibition of HDAC6 by *R*-enantiomer **8**.

HDAC	2	6	8
IC$_{50}$ (μM)	0.26	0.01	0.53

For the synthesis, first an aromatic nucleophilic substitution of *R*-phenylalanine across 1-fluoro-2-nitrobenzene **39** was performed.[33] Esterification of the resulting acid **40** with iodomethane and potassium carbonate gave methylester **41** in quantitative yield. Hydrogenation of this

nitrobenzene **41** and *in situ* cyclisation afforded 3,4-dihydroquinoxalin-2(1*H*)-one **42**. Functionalisation of the cyclic amino moiety in this structure was achieved via a reductive amination employing 4-formylbenzoic acid, catalytic dibutyltin dichloride, and phenylsilane as reductant. In a final step, acid **43** was converted to hydroxamic acid **8** using hydroxylamine hydrochloride and (benzotriazol-1-yloxy)tris(dimethylamino)phosphonium hexafluoro-phosphate (BOP reagent) as a coupling reagent.
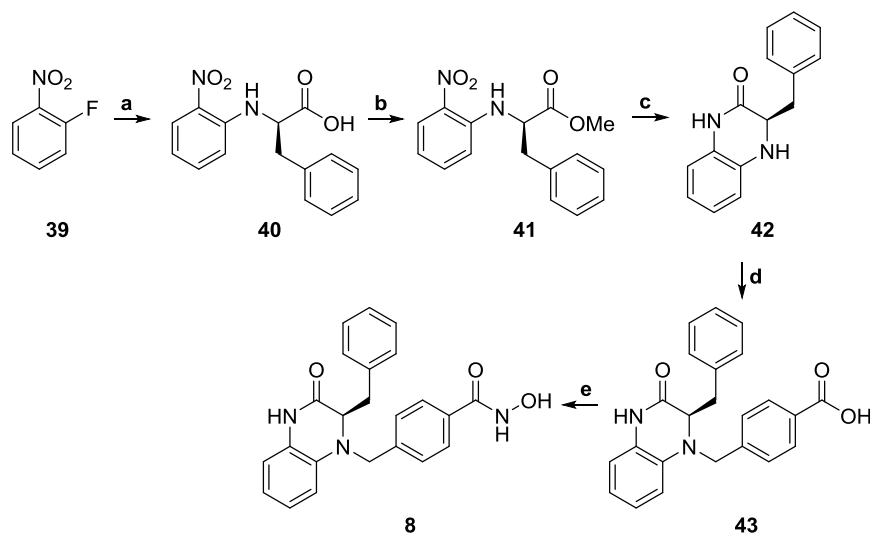

Scheme 7. (a) *R*-phenylalanine (1 equiv), K$_2$CO$_3$ (0.77 equiv), EtOH/H$_2$O 5/1, 100 °C, 16h, sealed tube. >95%. (b) MeI (3 equiv), K$_2$CO$_3$ (4 equiv), DMF, rt, 16h. >95% (c) Pd (10% on carbon), H$_2$, MeOH/EtOAc 2/1, rt, 16h. >80%. (d) 4-formylbenzoic acid (1 equiv), PhSiH$_3$ (1.1 equiv), Bu$_2$SnCl$_2$ (0.1 equiv), THF, rt, 16h. >80%. (e) NH$_2$OH.HCl (1.2 equiv), BOP (1.2 equiv), TEA (4 equiv), pyridine, rt, 8h. >50%.

Tubastatin A **9** is one of the most intensively discussed selective HDAC6 inhibitors to date and is frequently used as a positive control for the evaluation of other selective HDAC6 inhibitors. This molecule has been discovered in 2010 via structure-based drug design combined with homology modelling.[13] Comparison of two homology models of HDAC1 and HDAC6 revealed that the catalytic channel rim differ greatly between both isoforms and suggested that this channel is wider and shallower for HDAC6 than for HDAC1. Therefore, a bulky and shorter aromatic moiety was proposed to fit this channel to possibly enhance the selectivity of the inhibitor for HDAC6. Indeed, when comparing IC$_{50}$ values for HDAC1 and 6 of inhibitors bearing an alkyl versus an aromatic linker, the aromatic ones demonstrated the best potency and selectivity. The outstanding selectivity profile of Tubastatin A was further established by determining the IC$_{50}$ values for HDAC1-11 (Table 9). Furthermore, Tubastatin A **9** conferred dose-dependent protection in primary cortical neuron cultures against glutathione depletion-induced oxidative stress and did not show neuronal toxicity, pointing to the potential use of selective HDAC6 inhibitors as drugs for the treatment of neurodegenerative diseases.

Table 9. Selective inhibition of HDAC6 by Tubastatin A **9**.

HDAC	1	2	3	4	5	6	7	8	9	10	11
IC$_{50}$ (µM)	16.4	>30	>30	>30	>30	0.015	>30	0.85	>30	>30	>30

For the preparation, the cap-group was made via a Fisher indole synthesis employing 1-methyl-piperidin-4-one **44** and phenylhydrazine (Scheme 8), and the corresponding tetrahydro-γ-carboline **45** was obtained as a beige solid in an excellent yield. Next, a nucleophilic substitution with methyl 4-(bromomethyl)benzoate yielded ester **46**, which was converted to Tubastatin A **9** using hydroxylamine hydrochloride and sodium methoxide as a base. Final purification was done using preparative HPLC and afforded pure Tubastatin A **9** as its trifluoroacetic acid salt.
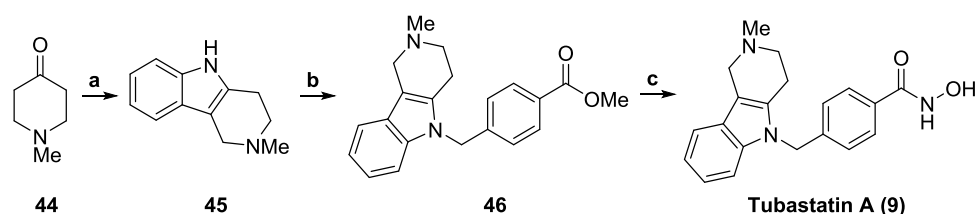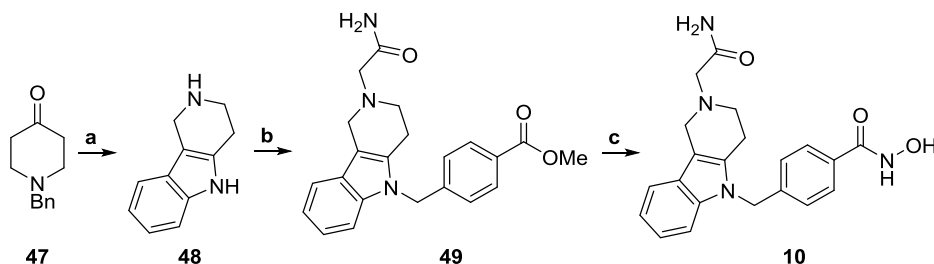

Scheme 8. (a) phenylhydrazine (1 equiv), H$_2$SO$_4$ (conc.), 1,4-dioxane, 0°C to 60°C, 2h. 93%. (b) methyl 4-(bromomethyl)benzoate (1 equiv), KOtBu (1.05 equiv), KI (cat.), DMF, 80°C, 2h, Ar(g). 61%. (c) NH$_2$OH.HCl (6 equiv), NaOMe (25% in MeOH, 8 equiv), MeOH, 0°C to rt, 24h. 31%.

In the following years after the discovery of Tubastatin A, several selective HDAC6 inhibitors have been prepared bearing a very similar structure, with only the heterocycle in the cap-region slightly adapted (Figure 1, structures **10-12**). The same research group of Kozikowski developed second generation Tubastatin A analogs, optimizing the activity, selectivity and physiochemical properties by fine-tuning the tetrahydrocarboline cap-group.[34] They discovered that substitution at the 2-position of the γ-carboline group was beneficial to obtain more active and selective compounds. This resulted in the design of compound **10** (Scheme 9), having an HDAC6 IC$_{50}$ value of 0.8 nM and a 5000-fold selectivity over HDAC1. In this second paper, also the ability of these compounds to enhance Treg suppression of Teff proliferation, both *in vitro* and *in vivo*, was established and warranted the further investigation of selective HDAC6 inhibitors as immunosuppressors.

The preparation of this compound followed a similar approach as for the synthesis of Tubastatin A. First, a Fisher indole synthesis with phenylhydrazine and piperidinone **47** resulted in the formation of the γ-carboline structure, in which the benzyl group was removed by hydrogenation. The obtained product **48** was then alkylated twice, first on the secondary

amino group with 2-bromoacetamide and then on the indole nitrogen atom with methyl 4-(bromomethyl)benzoate. A final conversion of this ester **49**, similar as with Tubastatin A, yielded the final inhibitor **10** as its trifluoroacetic acid salt after preparatory HPLC.


Scheme 9. (a) i) phenylhydrazine (1 equiv), H_2SO_4 (conc.), 1,4-dioxane, 0°C to 60°C, 2h. 93%. ii) Pd (10% on carbon), H_2, EtOH/H_2O 7/3, 70°C, 24h. 93%. (b) i) 2-bromoacetamide (1 equiv), TEA (2 equiv), MeCN, 60°C, 2h, Ar(g). ii) methyl 4-(bromomethyl)benzoate (1 equiv), KOtBu (1 equiv), DMF, 80°C, 2h, Ar(g). 50%. (c) $NH_2OH.HCl$ (6 equiv), NaOMe (25% in MeOH, 8 equiv), MeOH, 0°C to rt, 16h. 15%.

Another compound structurally related to Tubastatin A is the patented molecule Marb1 **11** (Scheme 10).[35] In a large series of analogs, Marb1 **11** showed to have improved anti-proliferative effects on 42 solid tumor cell lines over the other compounds tested. The selectivity was assayed by determining the IC_{50} values against a panel of HDACs and showed that Marb1 is a potent and selective HDAC6 inhibitor (Table 10).

Table 10. Selective inhibition of HDAC6 by Marb1 **11**.

HDAC	1	2	4	5	6	8	11
IC_{50} (µM)	3.62	7.45	3.82	1.57	0.004	0.25	10.5

For the synthesis, first the nitro group in compound **50** was reduced to the amine using an acidic hydrochloric acid solution and zinc dust (Scheme 10). This was followed by a Pictet-Spengler reaction on indole **51**, resulting in tetrahydro-β-carboline **52**. Urea **53** was then made using *N*-succinimidyl *N*-methylcarbamate and could be cyclised employing cesium carbonate in dioxane under reflux. As such, cap-group **54** was obtained and then *N*-alkylated with *tert*-butyl 4-(bromomethyl)benzoate. Subsequent deprotection of the *tert*-butyl group produced the free carboxylic acid **55**. Coupling of this carboxylic acid **55** with *O*-(tetrahydro-2*H*-pyran-2-yl)hydroxylamine and THP deprotection resulted in the formation of hydroxamic acid **11** in 46% yield.
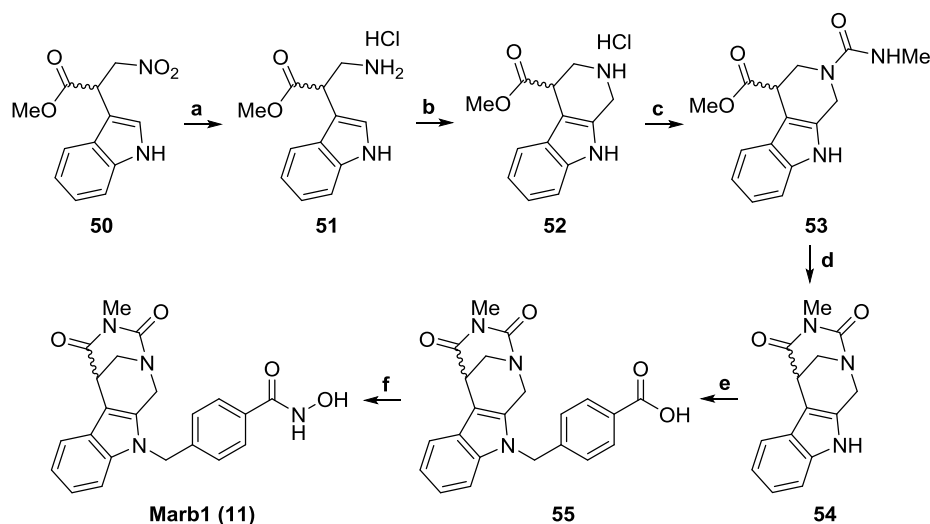
Scheme 10. (a) Zn, CuSO$_4$, HCl (3N), THF/MeOH 1/1, Δ, 2h. 83%. (b) formaldehyde (35% in H$_2$O, 1.2 equiv), MeOH, 60°C, 1h. 86%. (c) *N*-succinimidyl *N*-methylcarbamate (1.2 equiv), DIPEA, CH$_3$CN, rt, 16h. 92%. (d) Cs$_2$CO$_3$ (1.2 equiv), dioxane, Δ, 4h, N$_2$(g). 72%. (e) i) *tert*-butyl 4-(bromomethyl)benzoate (1.1 equiv), NaH (1.1 equiv), DMF, 0°C to rt, till completion, N$_2$(g). 73%. ii) TFA, rt, 15 min. 99%. (f) i) *O*-(tetrahydro-2*H*-pyran-2yl)hydroxylamine (4 equiv), BOP (1 equiv), TEA (3 equiv), rt, till completion. 65%. ii) HCl (0.6M in H$_2$O), MeOH, rt, till precipitation. 46%.

Bicyclic-capped HDAC6 inhibitor **12** substituted with a fluorine atom in the linker has been developed as novel drug for the treatment of the Charcot-Marie-Tooth disease (Scheme 11).[36] The rationale behind using selective HDAC6 inhibitors was the recent discovery that HDAC6 can serve as a druggable target for the treatment of this neurological disorder.[37] Several classes of bicyclic-capped benzohydroxamic acids were evaluated, whereof benzimidazole **12** showed best-in-class activity. Not only the potency and selectivity was assessed (Table 11), but also the ADME/Tox and pharmacokinetic properties were determined and compared with those of Tubastatin A. From the obtained data it was concluded that the studied compound showed an improved profile over Tubastatin A for certain parameters.

Table 11. Selective inhibition of HDAC6 by benzimidazole **12**.

HDAC	1	2	3	4	5	6	7	8	9	10	11
IC$_{50}$ (μM)	9.0	20.3	12.5	0.5	0.2	0.0008	0.03	0.2	0.07	20.4	12.9

Benzimidazole **12** has efficiently been synthesized in two steps from 2-methylbenzimidazole **56** (Scheme 11). First, a nucleophilic substitution was performed at nitrogen with methyl 4-(bromomethyl)-3-fluorobenzoate, and secondly, ester **57** to hydroxamic acid **12** conversion was achieved through the use of an excess of hydroxylamine.
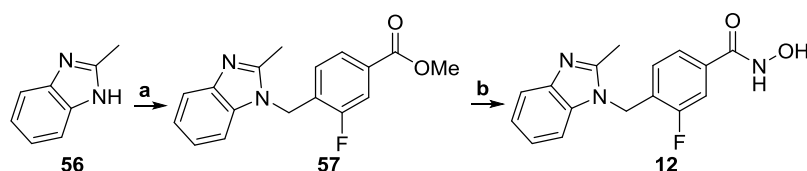
Scheme 11. (a) methyl 4-(bromomethyl)-3-fluorobenzoate (1 equiv), K_2CO_3 (2 equiv), DMF, 80°C, 2h. 71%. (b) NH_2OH (50% in H_2O, 50 equiv), NaOH (4 equiv), THF/MeOH 1/1, 0°C to rt, 30 min. 50%.

A screen of different hydroxamic acid structures revealed tetrahydroisoquinoline **13** to have unexpected selectivity for HDAC6 over the other HDAC isoforms (Scheme 12).[38] The selectivity was attributed to the aromatic linker which more effectively accesses the broad tubular channel to the catalytic pocket, as explained previously for Tubastatin A. Furthermore, the hydrophobic capping group can also interact with the protein surface, further improving the potency and selectivity. Tetrahydroisoquinoline **13** showed to have an excellent selectivity profile (Table 12) and displayed negligible inhibition of matrix metalloproteases (MMP2, 4 and 9 IC_{50} > 100 µM). Also the aqueous solubility was assessed and shown to be high (2 mM at pH 7.5), and the compound demonstrated a high Caco-2 permeability and a low efflux ratio (A-B = 22 x 10^{-6} cm s^{-1} B-A = 1.5 x 10^{-6} cm s^{-1}).

Table 12. Selective inhibition of HDAC6 by tetrahydroisoquinoline **13**.

HDAC	1	2	3	4	5	6	7	8	10	11
IC_{50} (µM)	45.0	>50	46.0	>50	>50	0.036	>50	2.1	>50	>50

The synthesis of compound **13** has been performed in a polypropylene deep-well plate without purification of the intermediate ester **59** (Scheme 12). Tetrahydroisoquinoline **58** was used as starting material and connected to *N*-methylpyrrole-2-carboxylic acid employing *N,N,N',N'*-tetramethyl-*O*-(1*H*-benzotriazol-1-yl)uronium hexafluorophosphate (HBTU) as a coupling agent. The resulting ester **59** was used for hydroxamic acid formation by means of hydroxylamine hydrochloride and potassium hydroxide treatment. Purification of hydroxamic acid **13** was accomplished by preparative HPLC and yielded 32% of compound **13** over the two steps.
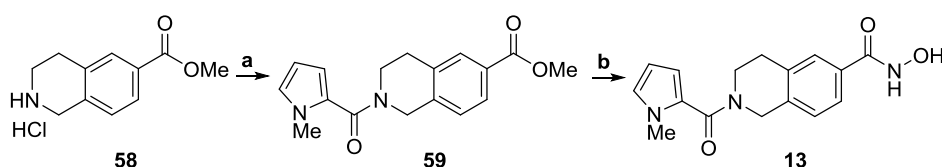

Scheme 12. (a) *N*-methylpyrrole-2-carboxylic acid (1.15 equiv), HBTU (1.4 equiv), *N*-methylmorpholine (1.5 equiv), 1,2-dichloroethane, rt, 16h. (b) $NH_2OH.HCl$ (2.2 equiv), KOH (4.35 equiv), MeOH, 70°C, 4h. 32% over step a and b.

Another selective HDAC6 inhibitor which has been developed by the group of Kozikowski, besides Tubastatin A and analogs, is Nexturastat A **14** (Scheme 13).[39] The design of this inhibitor was based on the knowledge that the same structure without a butyl substituent on the urea moiety is a modest inhibitor of HDAC6 that has no selectivity relative to HDAC1 (IC_{50} HDAC1 = 265 nM, IC_{50} HDAC6 = 139 nM). The fact that HDAC6 accommodates a broader tubular channel with respect to other HDACs stimulated the researchers to add substituents on both nitrogen atoms of the urea functionality. After evaluation of this class of substituted ureas, it became clear that the presence of a butyl substituent on the nitrogen atom proximal to the hydroxamic acid moiety afforded the compound with the best properties, and as such Nexturastat A **14** was discovered. This molecule displayed high selectivity toward HDAC6 (Table 13) and demonstrated potent inhibition of melanoma cell growth.

Table 13. Selective inhibition of HDAC6 by Nexturastat A **14**.

HDAC	1	2	3	4	5	6	7	8	9	10	11
IC_{50} (µM)	3.02	6.92	6.68	9.39	11.7	0.005	4.46	0.95	6.72	7.57	5.14

Nexturastat A **14** has been prepared in three steps from methyl 4-formylbenzoate **60** (Scheme 13). The first step comprised a reductive amination employing methyl 4-formylbenzoate **60,** *n*-butylamine and sodium cyanoborohydride mixed in a 5% solution of acetic acid in dichloromethane. In the second step, secondary amine **61** was treated with phenylisocyanate to obtain urea **62**. The third and final step consisted of an hydroxamic acid synthesis by adding an excess of hydroxylamine to ester **62** in a basic environment. Nexturastat A **14** was finally obtained via preparative HPLC purification in 68% yield.
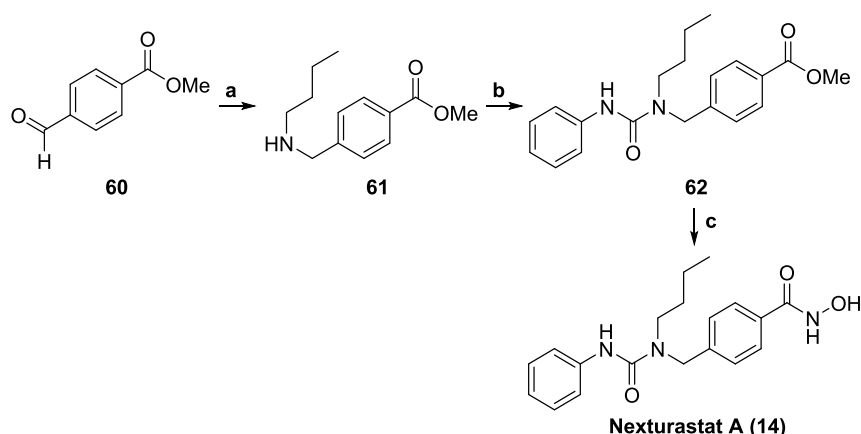
Scheme 13. (a) *n*-butylamine (1 equiv), AcOH (5% in CH_2Cl_2), $NaCNBH_3$ (1 equiv), rt, overnight, Ar(g). 68%. (b) phenylisocyanate (1 equiv), CH_2Cl_2, rt, overnight, Ar(g). 98%. (c) NH_2OH (50% in H_2O, 42 equiv), NaOH (8 equiv), THF/MeOH 1/1.6, 0°C to rt, 30 min. 68%.

In a recent publication, benzohydroxamic acids having a structure similar to compound **15** have been patented as selective HDAC6 inhibitors (Scheme 14).[40] Structure **15** is one of the compounds which showed a promising activity and selectivity for HDAC6 as compared to HDAC1 (IC_{50} values ≤ 500 nM and ≥ 10 µM, respectively).

The synthesis started with a regioselective Buchwald-Hartwig amination of 2,4-dibromopyridine **63** with pyrazine-2-amine, resulting in the formation of structure **64**. Then a straightforward nucleophilic substitution of secondary amine **64** with methyl 4-(bromomethyl)benzoate in the presence of sodium hydride gave ester **65**. The 4-bromosubstituent in structure **65** was replaced by a 1,2-oxazole moiety through a Suzuki-Miyaura reaction using an organoboron species and tetrakis(triphenylphosphine)palladium as the catalyst. A final conversion of ester **66** to hydroxamic acid **15** was established by the addition of an excess of hydroxylamine and two equiv of sodium hydroxide.
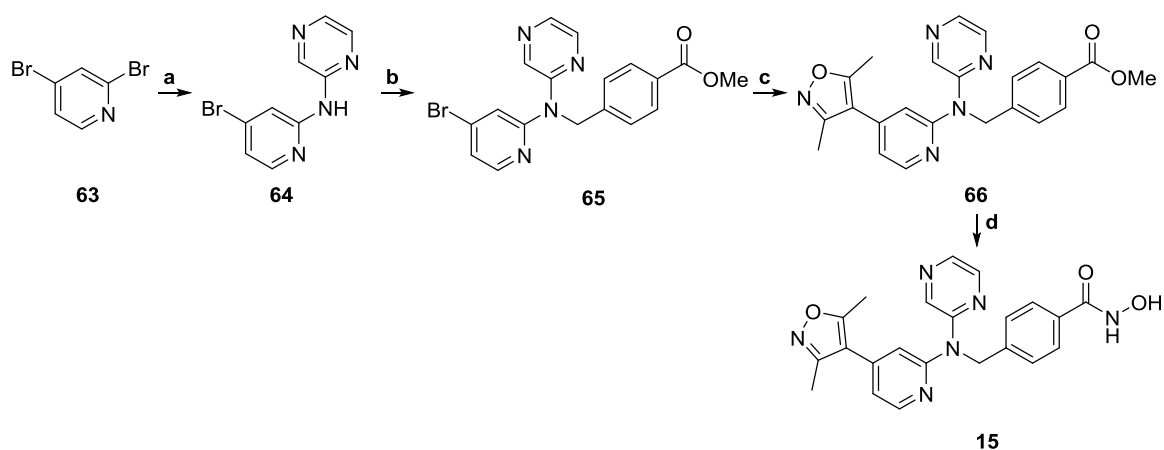
Scheme 14. (a) pyrazine-2-amine (1.1 equiv), Cs_2CO_3 (2.2 equiv), xantphos (5 mol%), $Pd_2(dba)_3$ (2 mol%), dioxane, 90°C, overnight, N_2(g). 49%. (b) i) NaH (1.2 equiv), DMF, 0°C, 30 min, N_2(g) ii) methyl 4-(bromomethyl)benzoate (1.1 equiv), DMF, 50°C, 1.5h, N_2(g). 53%. (c) 3,5-dimethyl-4-(tetramethyl-1,3,2-dioxaborolan-2-yl)-1,2-oxazole (1 equiv), $Pd(PPh_3)_4$ (10 mol%), Cs_2CO_3 (2 equiv), DMF/H_2O 4/1, 90°C, 2h, N_2(g). 18%. (d) NH_2OH (50% in H_2O, 20 equiv), NaOH (6N, 2 equiv), rt, 1h. 16%.

In another patent, trisubstituted pyrroles such as compound **16** (Figure 1) have been described as HDAC inhibitors with preferential inhibition of HDAC6 (Table 14).[41] This compound showed superior anticancer activity across a panel of 42 different cancer cell lines. No detailed synthesis of this structure was disclosed.

Table 14. Selective inhibition of HDAC6 by trisubstituted pyrrole **16**.

HDAC	1	2	3	4	5	6	7	8	9	10	11
IC_{50} (nM)	71	157	75	1083	222	2	290	148	163	294	341

Inspired by the novel HDAC6 selective inhibitor 2-phenylamidonaphthoquinone (NQN-1), benzohydroxamic acid **17** was designed, also bearing the amidoquinone functionality.[42] This inhibitor proved to be a strong HDAC6 inhibitor (IC_{50} = 6 nM) and showed promising toxicity toward acute myeloid leukemia cells, but unfortunately no selectivity data have been reported. Nonetheless, this compound is mentioned here, as the only reported HDAC inhibition value is the one for HDAC6.

The synthesis of amidoquinone **17** started with the selective esterification of one of the carboxylic acid functionalities in bis-acid **67** by using a catalytic amount of thionyl chloride in methanol (Scheme 15). In this manner, mono-ester **68** was obtained, in which the remaining carboxylic acid group was converted to a tetrahydropyranyl-protected hydroxamate in structure **69**. Then, hydroxamic acid **70** was formed from ester **69** employing an excess of hydroxylamine. The next step (step d) comprised the key step of this synthetic pathway, producing amidonaphthoquinone **71** from hydroxamic acid **70** and 1,4-naphthoquinone. The final step encompassed the deprotection of the tetrahydropyranyl-protected hydroxamate moiety with a catalytic amount of *para*-toluenesulfonic acid, and delivered the pure hydroxamic acid **17** in 31% yield after preparative reversed-phase HPLC.
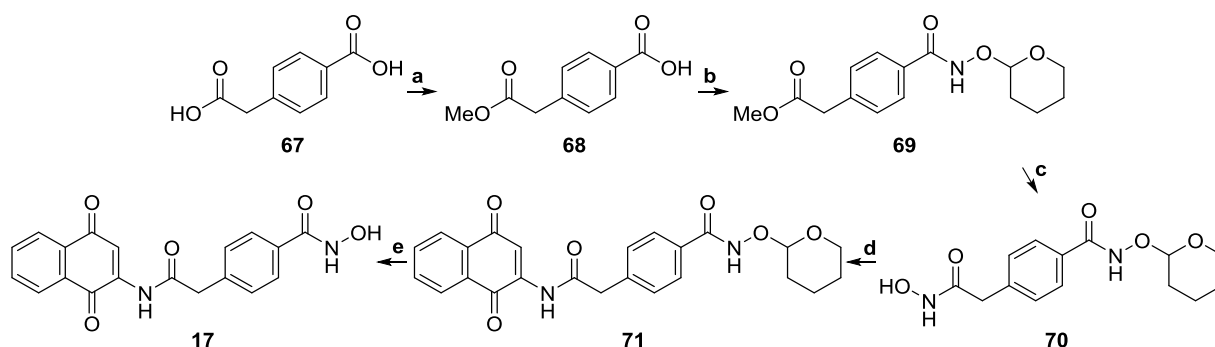
Scheme 15. (a) $SOCl_2$ (cat.), MeOH, rt, 5h. No purification. (b) i) $SOCl_2$ (1.45 equiv), DMF (cat.), CH_2Cl_2, rt, overnight. ii) NH_2OTHP (1 equiv), TEA (1.1 equiv), CH_2Cl_2, rt, 2h. No yield reported. (c) NH_2OH (50% in H_2O, 30 equiv), KOH (10 equiv), CH_2Cl_2/MeOH 1/2, 0°C to rt, overnight. No purification. (d) 1,4-naphthoquinone (1.1 equiv), DIPEA (2 equiv), CH_3CN, 70°C, overnight. 35%. (e) $TsOH.H_2O$ (0.2 equiv), MeOH, rt, overnight. 31%.

1.2.2. Benzohydroxamic acid-based pan-HDAC inhibitors

A second important group of benzohydroxamic acids **72-78** is presented in Figure 2. All these structures inhibit multiple zinc-dependent HDAC isozymes simultaneously and display potent anti-cancer activity. Several of them are currently studied in clinical trials as anticancer drugs. In contrast to HDAC6 selective benzohydroxamic acids, these compounds mostly contain a heterocyclic group in the cap-region which is located further away from the benzohydroxamic acid scaffold and which is less space filling then the heterocyclic cap-groups present in HDAC6 selective inhibitors. For each inhibitor presented in Figure 2 the biological activity and synthetic pathway will be discussed.
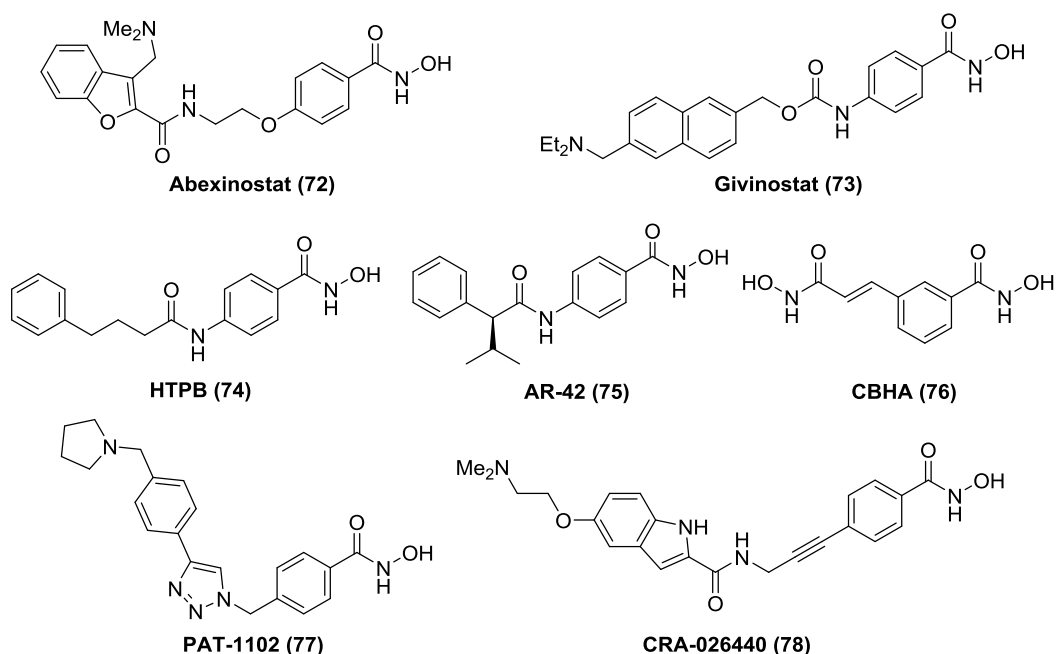
Figure 2. Overview of pan-HDAC inhibitors bearing the benzohydroxamic acid moiety.

Abexinostat **72** is one of the benzohydroxamic acids which is currently in phase 2 clinical trials as an anticancer agent and which demonstrated nanomolar dissociation constants for HDAC1, 2, 3, 6, 8 and 10 (K_i = 7 - 280 nM, Table 15), explaining its classification as a pan-HDAC inhibitor. During the design of this molecule, careful optimization of the cap-group appeared to be essential to obtain a drug with excellent *in vivo* efficacy and pharmacokinetics.[43]

Table 15. Pan-inhibition of several HDACs by Abexinostat **72**.

HDAC	1	2	3	6	8	10
K_i (µM)	0.007	0.019	0.008	0.017	0.28	0.024

The synthesis of Abexinostat **72** has been disclosed in a patent published in 2004 and started with the formation of the 3-substituted (dimethylaminomethyl)benzofuran cap-group **83** (Scheme 16).[44] In a first step carboxylic acid **79** was converted to methyl ester **80** using oxalyl chloride and several drops of DMF to form the corresponding acid chloride via the *in situ* generated Vilsmeier reagent. Subsequently, triethylamine and methanol were used to convert the acid chloride into methyl ester **80**. A radical bromination at the benzylic position generated alkylbromide **81**, which was transformed to tertiairy amine **82** using dimethylamine. Finally, saponification and acidification generated benzofuran-2-carboxylic acid **83**, which was coupled to methyl 4-(2-aminoethoxy)benzoate using the coupling reagents 1-ethyl-(3-dimethylaminopropyl)carbodiimide hydrochloride (EDC.HCl) and 1-hydroxybenzotriazole hydrate (HOBt.H$_2$O) to obtain methyl ester **84**. In a final stage, this methyl ester **84** was treated with an excess of hydroxylamine to generate Abexinostat **72**.
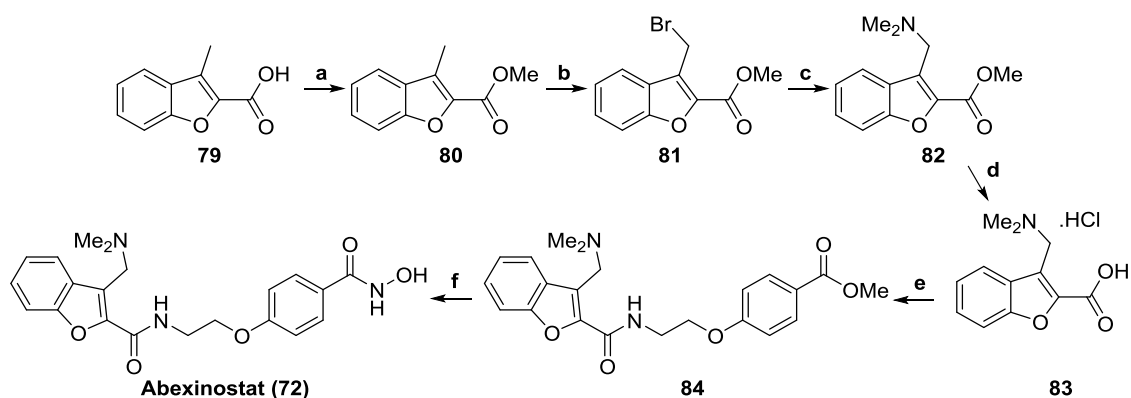

Scheme 16. (a) oxalyl chloride (1.1 equiv), DMF (5 drops), THF, rt, 1h -> MeOH, TEA (9 equiv), rt, overnight. 94%. (b) NBS (1 equiv), AIBN (0.1 equiv), CCl$_4$, Δ, 3h. 99%. (c) dimethylamine (3 equiv in THF, 2M), DMF, rt, 1-2h. 56%. (d) NaOH (1N till pH 13), MeOH, rt, 1-1.5h -> HCl (aq. till pH 3). 99%. (e) EDC.HCl (1.4 equiv), HOBt.H$_2$O (1.5 equiv), DMF, rt, 0.5-1h -> methyl 4-(2-aminoethoxy)benzoate hydrochloride (1 equiv), TEA (1.2 equiv), DMF, rt, overnight. (f) NH$_2$OH (excess), NaOH (aq. till pH 10-11), rt, overnight -> HCl (aq. till pH 7-8). 48% over two steps.

Givinostat **73** (also known as ITF2357) represents another benzohydroxamic acid which is currently in phase 2 clinical trials as an anticancer agent. This molecule reduces the production of pro-inflammatory cytokines *in vitro* (TNFα, IL-1α, IL-1β and IFNγ) and has anti-inflammatory effects *in vivo*.[45] Several studies confirmed the anticancer activity of this molecule in multiple tumor cell lines and in patients with hematologic cancers.[46] Data of *h*HDAC inhibition could not be found in the literature, but the compound has been tested against three maize HDACs (HD2, HD-1B and HD-1A) and exhibited low nanomolar potency (IC$_{50}$'s = 7.5-16 nM) against these isoforms.

The synthesis of Givinostat **73** started with the amidification of 2,6-naphthalenedicarboxylic acid **85** utilising 1-ethyl-3-(3-dimethylaminopropyl)carbodiimide (EDC) and hydroxybenzotriazole (HOBt, Scheme 17).[47] Lithium aluminium hydride reduction of acid **86**

was performed to give access to amino alcohol **87** in an excellent yield of 79%. Nucleophilic addition of the alcohol group of molecule **87** across *N,N*-disuccinimidyl carbonate and consecutive addition of 4-aminobenzoic acid resulted in the formation of carbamate **88** in 64% yield. Final conversion of acid **88** to hydroxamic acid **73** was accomplished through acid chloride formation with thionyl chloride and subsequent hydroxylamine addition in a basic environment (NaHCO$_3$, NaOH).
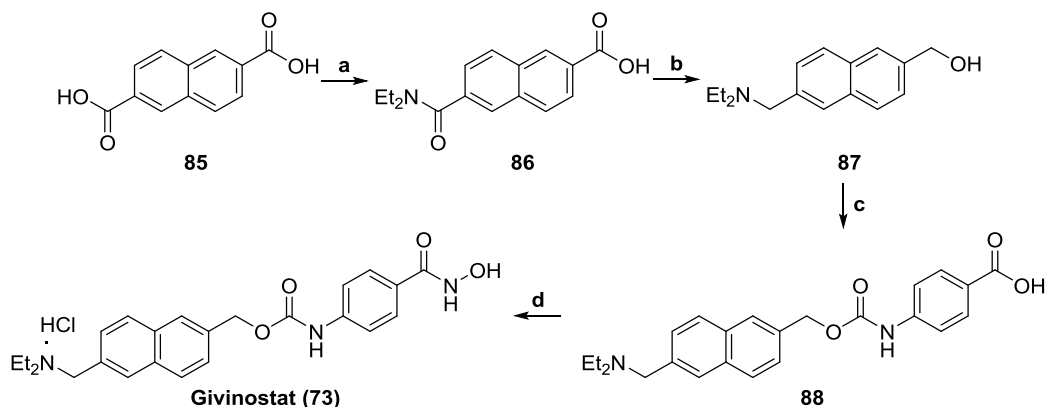

Scheme 17. (a) EDC.HCl (1 equiv), HOBt (1 equiv), DMF, rt, 2h -> diethylamine (3 equiv), rt, overnight. 60%. (b) LiAlH$_4$ (3 equiv), THF, Δ, 1h 79%. (c) *N,N*-disuccinimidyl carbonate (1 equiv), CH$_3$CN, rt, 3h -> 4-aminobenzoic acid (1 equiv), Na$_2$CO$_3$ (1 equiv), H$_2$O/THF (2/1), rt, overnight. 64%. (d) thionyl chloride (3 equiv), CHCl$_3$, Δ, 4h -> NH$_2$OH.HCl (1.2 equiv), NaHCO$_3$ (2 equiv), NaOH (1.2 equiv 1N, H$_2$O), H$_2$O/THF (3/1), rt, overnight -> HCl (1.5 N, ether), THF. 41%.

Starting from short chain fatty acids, Lu *et al.* have synthesized a group of hydroxamic acids, of which the benzohydroxamic acids showed the most pronounced HDAC inhibition.[48] Aromatic linkers were chosen to increase the structural rigidity and to increase van der Waals contacts with the tube-like hydrophobic region of HDACs. Hydroxamate-tethered phenylbutyrate **74** (HTPB, Scheme 18) was identified as the most promising HDAC inhibitor, exhibiting an IC$_{50}$ of 44 nM in a HDAC assay using a nuclear extract (derived from DU-145 prostate cancer cells) rich in histone deacetylases. The pan-inhibitory effect of this inhibitor was further proven through Western Blot analysis of acetylated histones H3 and H4 (substrates of class I HDACs), showing a pronounced effect at 1 µM of HTPB. HTPB also reduced cell proliferation of several cancer cell lines (DU-145, AN3CA, SW-48 and HCT-15) at submicromolar concentrations.

The first step toward the synthesis of HTPB **74** enclosed a carbodiimide coupling of methyl 4-aminobenzoate to 4-phenylbutyric acid **89**, yielding ester **90** (Scheme 18). Saponification of this ester employing potassium hydroxide afforded acid **91**, which was converted to *O*-benzylhydroxamate **92** by means of bis(2-oxo-3-oxazolidinyl)phosphordiamidic chloride as coupling reagent and *O*-benzylhydroxylamine hydrochloride as nucleophile. In a final step,

hydroxamate **92** was *O*-deprotected using hydrogen gas and palladium on carbon, which resulted in the formation of HTPB **74**.
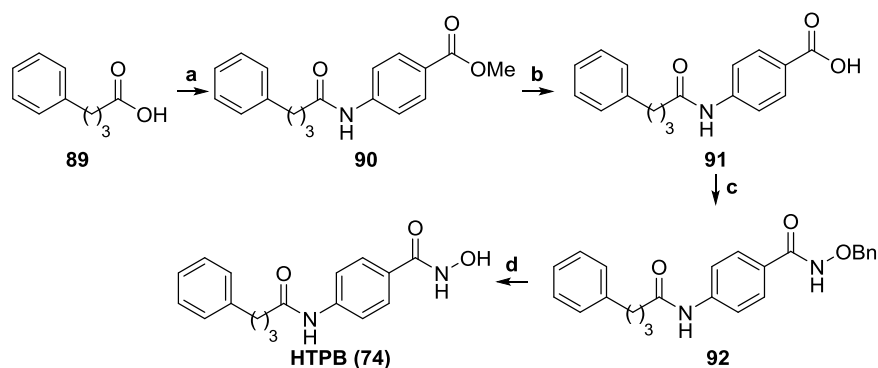
Scheme 18. (a) methyl 4-aminobenzoate (1 equiv), EDC (1.3 equiv), THF, rt, overnight, N_2. (b) KOH/MeOH (2M), 80°C, 1h -> HCl (2N to pH 3), 0°C. (c) TEA (1 equiv), THF, rt, 10 min, N_2 -> *O*-benzylhydroxylamine hydrochloride (1 equiv), bis(2-oxo-3-oxazolidinyl)phosphordiamidic chloride (1.1 equiv), TEA (3 equiv), THF, rt, overnight, N_2. (d) Pd (10% on carbon), H_2 (1 atm), MeOH/THF (1/1), rt, 2h. No yields reported.

In a consecutive study, Lu *et al.* have further optimized the structure of HTPB **74** by conducting docking studies on the crystal structure of histone deacetylase-like protein (HDLP).[49] They observed that HDLP contains a hydrophobic microdomain nearby amino acids Phe-198 and Phe-200 that could be exploited by introducing an extra alkyl group in α-position with respect to the amide present in HTPB **74**. As a result, they developed AR-42 **75** as another promising pan-HDAC inhibitor (currently in phase 1 and 2 clinical trials) against several cancer cell lines.[50-55] In this study, also the *R*-enantiomer of AR-42 was made and showed considerably less HDAC inhibition than AR-42 itself (AR-42 IC_{50} HDAC nuclear extract = 16 nM, *R*-enantiomer IC_{50} HDAC nuclear extract = 84 nM).

Although HTPB **74** and AR-42 **75** show a lot of structural similarities, AR-42 was made through a different synthetic pathway (Scheme 19). First, 4-aminobenzoic acid **93** was Boc-protected to give molecule **94**, which was subsequently coupled with *O*-benzylhydroxylamine using the same procedure as for the synthesis of HTPB **74** (Scheme 18, step c). Deprotection of compound **95** lead to the free amine **96**, which was treated with (*S*)-3-methyl-2-phenylbutanoic acid (obtained through chiral resolution). Final deprotection of benzyl-protected hydroxamate **97** formed AR-42 **75**.
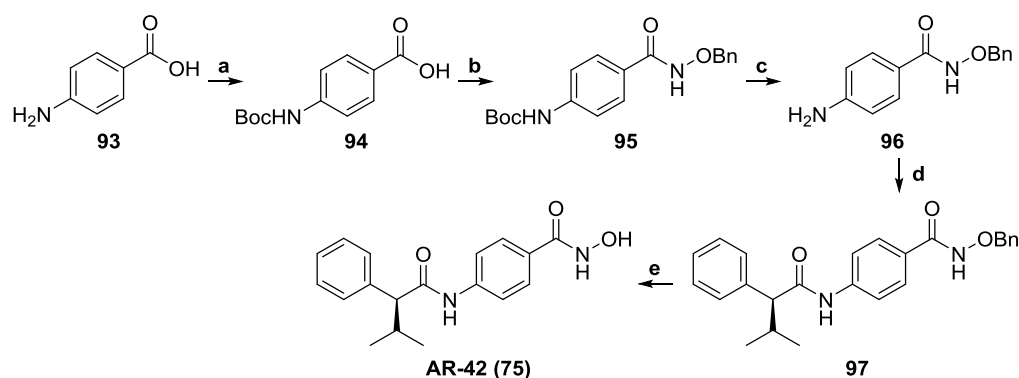
Scheme 19. (a) Boc$_2$O (1.5 equiv), TEA (1.5 equiv), dioxane/H$_2$O (1/1), rt, overnight. (b) TEA (1 equiv), THF, rt, 10 min, N$_2$ -> *O*-benzylhydroxylamine hydrochloride (1 equiv), bis(2-oxo-3-oxazolidinyl)phosphordiamidic chloride (1.1 equiv), TEA (3 equiv), THF, rt, overnight, N$_2$. (c) CH$_2$Cl$_2$/TFA (6/1), rt, 2h. (d) (*S*)-3-methyl-2-phenylbutanoic acid (1 equiv), EDC (1.3 equiv), THF, rt, overnight, N$_2$. (e) Pd (10% on carbon), H$_2$ (1 atm), MeOH/THF (1/1), rt, 2h. No yields reported.

Meta-carboxycinnamic acid bishydroxamide **76** (CBHA, Scheme 20) has a quite peculiar structure as it contains both a benzohydroxamic acid and a cinnamoylhydroxamic acid group, two prevalent scaffolds in HDAC inhibitor design.[56] CBHA is denoted as a polar hybrid compound, typically consisting of two polar groups separated by an organic spacer. This polar hybrid structure inhibited HDAC1 and 3 with submicromolar potency and increased the acetylation status of histone H4, which points to the pan-inhibitory activity of this molecule.

The synthesis of CBHA **76** has been described in a patent, utilizing bis-acid chloride **98** as a starting point (Scheme 20).[57] Four equiv of *O*-trimethylsilyl hydroxylamine, one equiv of acid chloride **98**, methanol, and an acid workup were necessary to obtain CBHA **76** in 91% yield.
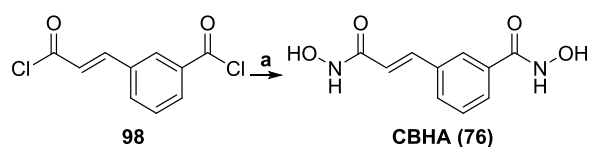
Scheme 20. (a) Me$_3$SiONH$_2$ (4 equiv), CH$_2$Cl$_2$, -78°C, Ar(g) -> 2h, rt -> 0.5h, Δ -> MeOH, -78°C -> MeOH, Δ, 0.5h -> HCl (0.2 N), 2h, rt. 91%.

PAT-1102 **77** is a recently discovered orally active pan-HDAC inhibitor with encouraging antitumor activity in mice (Scheme 21).[58] The inhibitory activity of this hydroxamic acid has been tested against HDAC1, 2, 3, 6, 8 and a HeLa nuclear extract (Table 16). PAT-1102 was shown to be active in the low nanomolar range against all enzymes (IC$_{50}$ = 2-29 nM), only against HDAC8 a higher inhibition value was observed (IC$_{50}$ = 280 nM). Clear dose-dependent acetylation of histones H3 and H4 was detected, comparable with vorinostat, proving the pan-HDAC activity of the inhibitor. The compound was active at low micromolar concentrations against 26 different cancer cell lines, and showed comparable activity in human tumor

xenograft models with other inhibitors such as vorinostat and pracinostat (a promising HDAC inhibitor in clinical trials).

Table 16. Pan-inhibition of several HDACs by PAT-1102 **77**.

HDAC	1	2	3	6	8	nuclear extract
IC$_{50}$ (µM)	0.025	0.029	0.002	0.011	0.28	0.003

PAT-1102 **77** has been prepared in seven steps from 4-bromobenzaldehyde **99** (Scheme 21). First, a Sonogashira coupling produced alkyn **100** in 80% yield. Removal of the trimethylsilyl group resulted in the synthesis of aldehyde **101** (61%), which was reduced to alcohol **102** using sodium borohydride. Alcohol **102** was subsequently converted into a good leaving group by mesylation (91%). Nucleophilic substitution of mesylate **103** with pyrrolidine gave structure **104**, but no yields of this reaction were documented in the literature. A yield of 91% was reported for a structurally related compound bearing a dimethylamino group instead of a pyrrolidinyl group. Triazole **105** was then formed using 'click chemistry' between methyl 4-(azidomethyl)benzoate and alkyne **104**. For the synthesis of the hydroxamic acid functional group an excess of hydroxylamine hydrochloride and sodium methoxide was used and generated PAT-1102 **77** (25% yield for the synthesis of a structurally related compound).
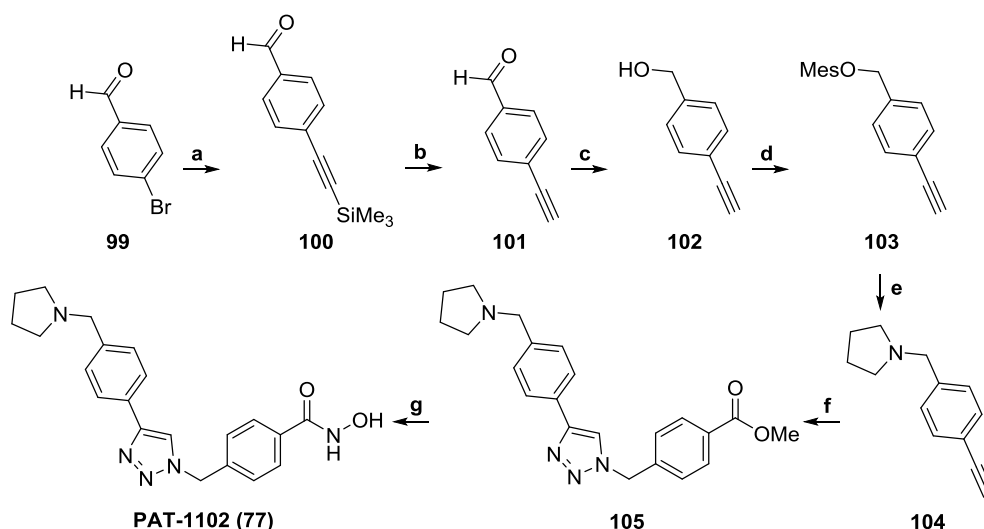
Scheme 21. (a) trimethylsilylacetylene (1.5 equiv), bis(triphenylphosphine)palladium(II)dichloride (1 mol%), CuI (2 mol%), diisopropylamine (solvent), 0°C, 0.5h -> Δ, 3h. 80%. (b) K$_2$CO$_3$ (0.1 equiv), MeOH, rt, 1h. 72%. (c) NaBH$_4$ (2 equiv), MeOH, 0°C, 5 min -> rt, 1h. 61%. (d) mesyl chloride (no equiv reported), TEA (3 equiv), CH$_2$Cl$_2$, 0°C -> rt, 12h. 91%. (e) pyrrolidine (2.5 equiv), TEA (2 equiv), 0°C -> rt, 12h. 91%*. (f) methyl 4-(azidomethyl)benzoate (0.9 equiv), CuI (0.45 equiv), sodium ascorbate (cat.), N-ethyldiisopropylamine (1.85 equiv), DMF, rt, 12h. 92%*. (g) NH$_2$OH.HCl (100 equiv), NaOMe (150 equiv), MeOH, 0°C, 0.5h -> rt, 3h. 25%*. *yields reported for closely related derivatives.

Another pan-HDAC inhibitor with a benzohydroxamic acid moiety, which has been evaluated as an anticancer agent, is CRA-026440 **78** (Figure 2).[59] Determination of the dissociation

constants against HDAC1, 2, 3, 6, 8 and 10 revealed CRA-026440 **78** to be a pan-HDAC inhibitor (Table 17). Moreover, CRA-026440 **78** inhibited *ex vivo* angiogenesis and reduced the tumor growth in HCT116 or U937 tumor xenograft mice significantly. The synthesis of CRA-026440 **78** was described in a patent (compound 29 in the patent), but no exact details were given.[60]

Table 17. Pan-inhibition profile of CRA-026440 **78**.

HDAC	1	2	3	6	8	10
K_i (μM)	0.004	0.014	0.011	0.015	0.007	0.020

1.2.3. Selective benzohydroxamic acid-based HDAC8 inhibitors

Looking at the HDAC8 selective benzohydroxamic acids **106-112** presented in Figure 3, the *meta*-substitution pattern of the cap-group with respect to the hydroxamic acid functionality in four out of seven compounds (**106**, **107**, **111** and **112**) is remarkable. Also in PCI-34051 **108**, a similar *meta*-substitution-like arrangement can be perceived. Only compounds **109** and **110** do not comply with this *meta*-orientation condition. Besides that, none of the HDAC6 selective or pan-HDAC inhibitors described above (Figures 1 and 2) contain such a *meta*-substituted structure (except for the peculiar hybrid polar inhibitor CBHA **76**, Figure 2). From each inhibitor presented in Figure 3, the biological activity and synthetic pathway will be discussed.
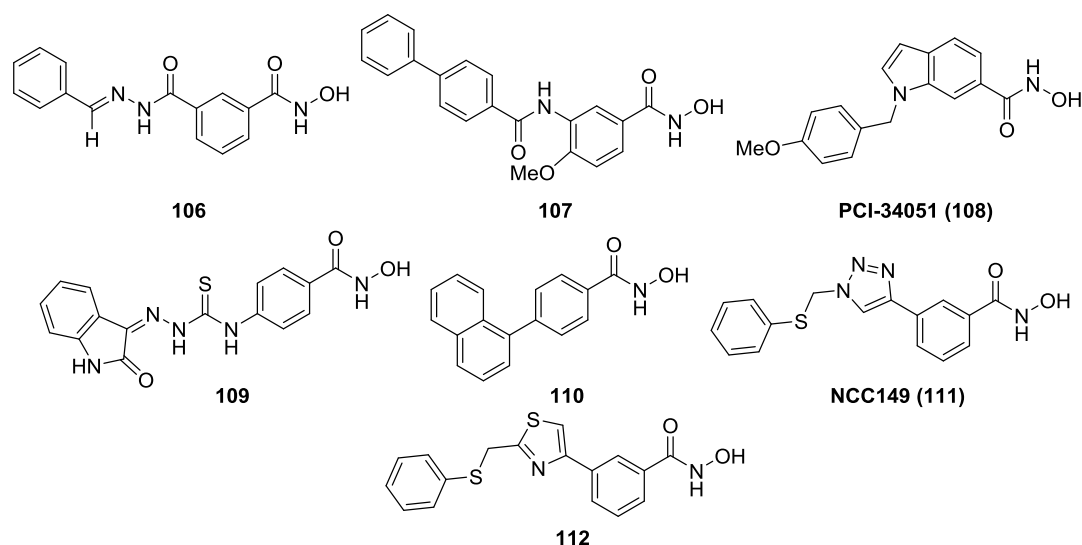
Figure 3. Overview of selective HDAC8 inhibitors bearing the benzohydroxamic acid moiety.

Miniaturized high-throughput synthesis and screening has been performed in 96-well plates to discover new selective histone deacetylase 8 inhibitors, such as representative example **106** (Figure 3).[61] This high-throughput screening revealed that the hydrazones *meta*-substituted with respect to the hydroxamic acid functionality showed the best selectivity for HDAC8. As a representative example, compound **106** is highlighted, which demonstrated micromolar inhibition of HDAC2 and 3, and nanomolar inhibition of HDAC8 (Table 18). However, it should be noted that no HDAC6 inhibition data were provided, making this HDAC8 selectivity claim rather premature.

Table 18. Selective inhibition of HDAC8 by hydrazone **106**.

HDAC	2	3	8
IC$_{50}$ (µM)	20	18	0.052

A two-step high-throughput synthesis process has been developed converting a first pool of primary alcohols into aldehydes (aldehyde **113** as an example, Scheme 22), which were further condensed with a second pool of hydrazides (hydrazide **114** as an example) to the corresponding hydrazones (hydrazone **106** as an example). All compounds, hydrazone **106** inclusive, were formed from 18 hydrazides and 15 aldehydes and obtained in a purity of 90%.
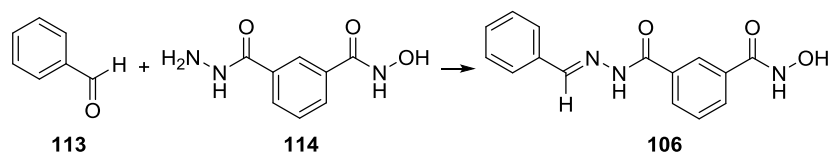
Scheme 22. High-throughput synthesis of representative example **120**.

Another class of novel benzohydroxamic acids has been developed to obtain a drug with a new mode of action against schistosomiasis.[62] This is a major neglected parasitic disease affecting more than 265 million people worldwide. The main goal was to obtain inhibitors for the HDAC8 isoform of *Schistosoma mansoni*, but from the results it appeared that these inhibitors also potently and selectively inhibited human HDAC8. The most potent inhibitor was structure **107** (Scheme 23, Table 19), having low nanomolar IC_{50} values for *sm*HDAC8 and *h*HDAC8 (75 nM and 26 nM, respectively) and low micromolar IC_{50} values for *h*HDAC1 and *h*HDAC6 (6.3 µM and 0.4 µM, respectively). This compound was effective in killing schistosomula *in vitro*, clearly demonstrating the potential of *sm*HDAC8 inhibitors to address this parasitic infection.

Table 19. Selective inhibition of HDAC8 by compound **107**.

HDAC	*h*1	*h*6	*h*8	*sm*8
IC_{50} (µM)	6.3	0.4	0.026	0.075

The synthesis of inhibitor **107** started with an esterification of acid **115**. The resulting methyl ester **116** was then treated with an acid chloride to give amide **117**. Hydrolysis of the ester group in compound **117** and subsequent treatment of the obtained acid **118** with *O*-(tetrahydro-2*H*-pyran-2-yl)hydroxylamine and the coupling reagent benzotriazol-1-yl-oxytripyrrolidinophosphonium hexafluorophosphate (PyBOP) resulted in the protected hydroxamate, which was liberated using a catalytic amount of hydrogen chloride. This approach produced the target structure **107** in 3.5% overall yield.
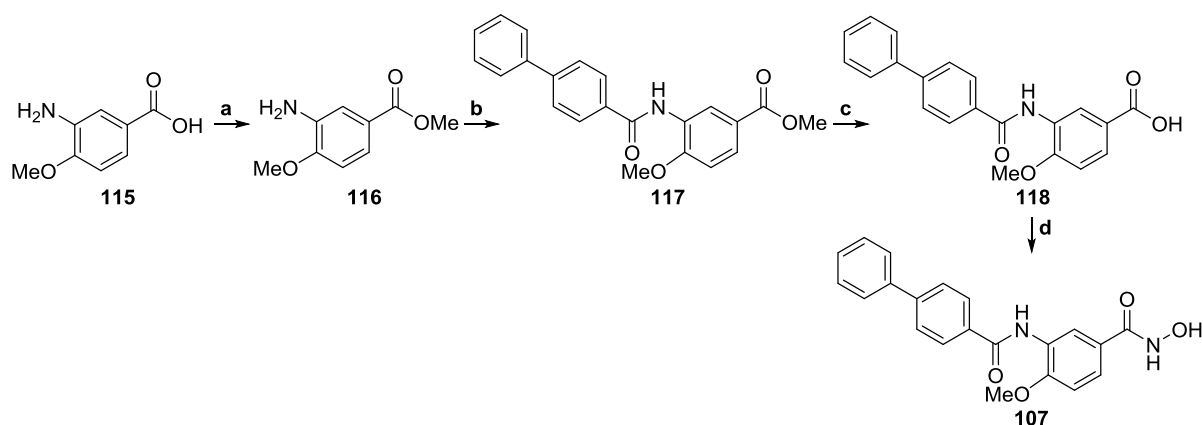
Scheme 23. (a) SOCl$_2$ (3 equiv), MeOH, 0°C to Δ, 1h (b) 4-phenylbenzoyl chloride, DIPEA, THF, rt, till completion. (c) NaOH (1M aq.), MeOH, 50°C, 2h. (d) i) NH$_2$OTHP (1.5 equiv), PyBOP (1.2 equiv), DIPEA (2.5 equiv), THF, rt, overnight. ii) HCl (cat.), THF, rt, till completion. 3.5% for last step, no other yields reported. For step b, no equiv reported.

From a patented series of indole hydroxamic acids, PCI-34051 **108** (Scheme 24) demonstrated potent inhibition of HDAC8 and showed to be more than 200 fold selective over five other HDAC isoforms (Table 20).[63,64] This inhibitor was tested against an array of tumor cell lines and induced caspase-dependent apoptosis in T-cell lymphomas or leukaemia's, but not in other hematopoietic or solid tumors. Further prove for the HDAC8 selectivity was provided by determining histone and tubulin acetylation via Western Blots. Detectable increases of acetylation of histones and tubulin will appear when a broad-spectrum HDAC inhibitor is administered to a cell. In contrast to this, PCI-34051 did not increase the acetylation level of histones and tubulin up to a concentration of 25 μM in Jurkat cells. Due to this HDAC8 selectivity and the discovered selectivity for T-cell-derived tumors, it could be expected that PCI-34051 **108** will be much less toxic than pan-HDAC inhibitors and should thus be further explored in this context.

Table 20. Selective inhibition of HDAC8 by PCI-34051 **108**.

HDAC	1	2	3	6	8	10
IC$_{50}$ (μM)	4	>50	>50	2.9	0.01	13

The synthesis of PCI-34051 **108** has been realized in only two steps (Scheme 24). First, a nucleophilic substitution was performed on 4-(methoxybenzyl)bromide by deprotonating methyl 1*H*-indole-6-carboxylate **119**. In this way, *N*-substituted indole derivative **120** was obtained in 54% yield after column chromatography. The second step comprised an ester to hydroxamic acid interconversion by adding an excess of hydroxylamine and five equiv of sodium hydroxide to ester **120**. Hydroxamic acid **108** was thus obtained in an excellent yield (84%) as a white powder.
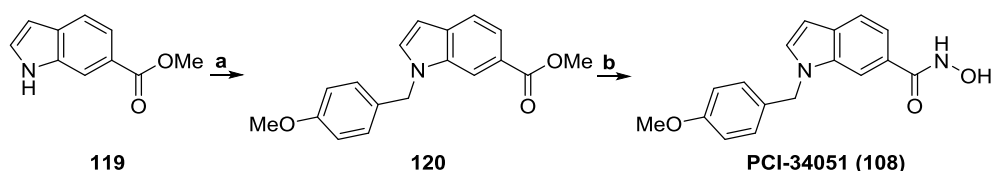
Scheme 24. (a) 4-(methoxybenzyl)bromide (1.1 equiv), NaH (1.15 equiv), DMF, rt, 3.5h. 54%. (b) NH$_2$OH (50% in H$_2$O, 33 equiv), NaOH (5 equiv), THF/MeOH 1/1, rt, 1h. 84%.

Compound **109** has been reported as a selective HDAC8 inhibitor with a rather low potency (Scheme 25).[65] This *para*-aminobenzoic acid derivative was the most potent HDAC8 inhibitor described in a series of twelve similar compounds and holds an IC$_{50}$ value of 15.7 µM for HDAC8. The percentage inhibition at 100 µM for two other isoforms, HDAC1 and 6, was also determined to evaluate the selectivity. Less than 10% of HDAC1 was inhibited at this high concentration, and HDAC6 was inhibited for 41%, demonstrating the HDAC8 selectivity. The HDAC8 selectivity and moderate potency could potentially be improved by synthesizing the *meta*-substituted analogs in future follow-up studies.

Hydrazine **121** was treated with ice cold carbon disulfide in the presence of potassium hydroxide and subsequently with methyl iodide to generate methyl hydrazinecarbodithioate **122**. After heating carbodithioate **122** under reflux together with isatin and a drop of concentrated sulfuric acid, structure **123** was generated. In the following step, compound **123** was treated for 3-4 days with one equiv of 4-aminobenzoic acid, which yielded thiosemicarbazone **124**. Final conversion to hydroxamic acid **109** was achieved through the formation of an intermediate anhydride by treatment of carboxylic acid **124** with phenyl chloroformate in the presence of a base. This intermediate anhydride was then added to a solution of hydroxylamine, producing inhibitor **109**.
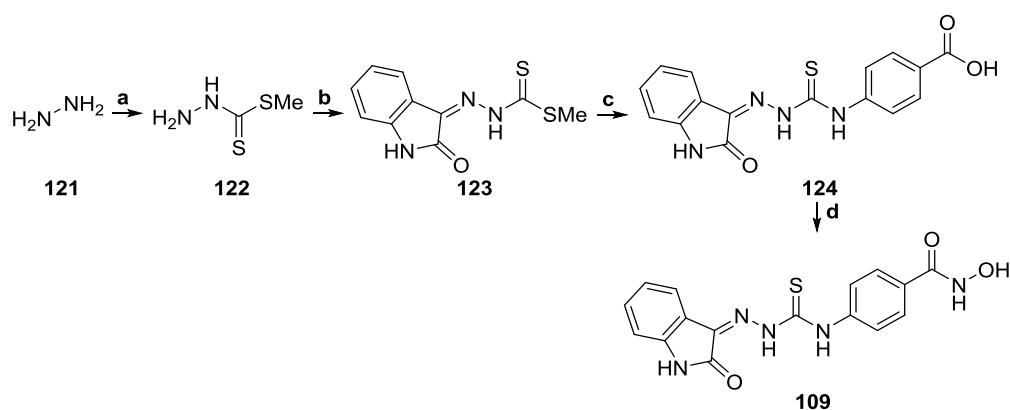
Scheme 25. (a) i) CS$_2$ (1 equiv), KOH (1 equiv), *i*PrOH, <10°C, 2.5h. ii) MeI (1 equiv), <10°C, 3.5h. (b) isatin (1.2 equiv), MeOH, H$_2$SO$_4$ (cat.), Δ, 6-7h; (c) 4-aminobenzoic acid (1 equiv), EtOH, Δ, 3-4 days. (d) i) phenyl chloroformate (1 equiv), TEA (1 equiv), THF, rt, 1h. ii) NH$_2$OH, rt, 3h. No yields reported.

By means of careful inspection of HDAC8 crystal structures bound to several types of HDAC inhibitors, a unique sub-pocket has been discovered in the HDAC8 active site.[66] This sub-pocket could be exploited for the design of isoform selective HDAC8 inhibitors. In this work, six hydroxamic acids were designed which specifically target this sub-pocket. From these six new hydroxamic acids, naphthalene-containing derivative **110** showed the highest potency and selectivity for HDAC8 (Table 21, Scheme 26).

Table 21. Selective inhibition of HDAC8 by hydroxamic acid **110**.

HDAC	1	6	8
IC$_{50}$ (µM)	>100	55	0.3

Deployment of a Suzuki coupling between 4-bromobenzoic acid **125** and naphthalen-1-ylboronic acid provided structure **126** (Scheme 26). In a following step, this acid **126** was converted to acid chloride **127** using thionyl chloride and a catalytic amount of DMF. Without purification, the crude acid chloride was treated with hydroxylamine in water/THF and yielded hydroxamic acid **110** in more than 80% yield over steps b and c.
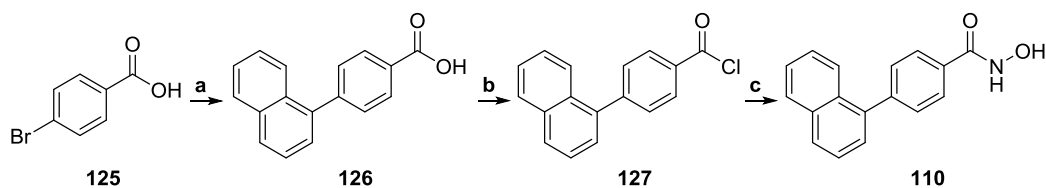

Scheme 26. (a) No reaction details given. (b) SOCl$_2$, DMF (cat.). (c) NH$_2$OH (in H$_2$O/THF), TEA, H$_2$O. Yield >80% for steps b and c. No detailed reaction conditions given.

In another study, a library of potential HDAC8-selective inhibitors has been prepared by using 'click chemistry'.[67] To that end, eight alkynes and fifteen azides were made and reacted with each other to give a collection of 120 triazoles. These structures were then evaluated for their HDAC8 inhibitory properties and their inhibition of HeLa nuclear extract rich in HDAC1 and 2. This assay revealed two *meta*-substituted benzohydroxamic acids as lead structures for further optimization. Therefore, a second library was designed containing 31 new triazoles bearing this *meta*-substituted benzohydroxamic acid structure and revealed NCC149 **111** as the most potent and selective HDAC8 inhibitor (Table 22, Scheme 27). Molecular docking further revealed that the orientation of the phenylthiomethyl group in structure **111** is important to fit the unique hydrophobic sub-pocket of HDAC8 to confer selectivity. This is the same sub-pocket also observed by Krennhrubec *et al.*, who designed hydroxamic acid **110** (Scheme 26).[66]

Table 22. Selective inhibition of HDAC8 by NCC149 **111**.

HDAC	1	2	4	6	8	nuclear extract
IC$_{50}$ (µM)	38	>100	44	2.4	0.07	54

Esterification of acid **128** employing concentrated sulfuric acid and methanol yielded methyl ester **129**. A subsequent Sonogashira coupling with trimethylsilylacetylene gave compound **130**, which was hydrolysed to afford acid **131**. Next, an EDC/HOBt-mediated coupling was performed with *O*-(tetrahydro-2*H*-pyran-2-yl)hydroxylamine, resulting in hydroxamate **132**. The tetrahydropyranyl group was removed employing *para*-toluenesulfonic acid, and the free hydroxamic acid **133** was thus obtained. In a final step through 'click chemistry', selective HDAC8 inhibitor **111** was obtained via a cupper-catalyzed coupling between alkyne **133** and azidomethyl phenyl sulfide.
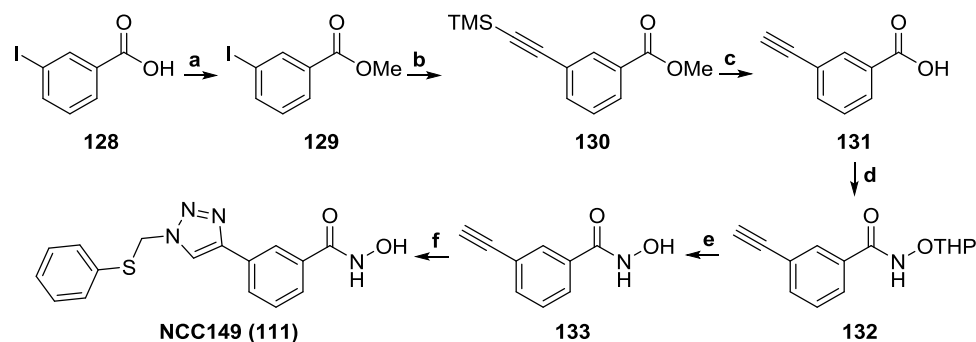
Scheme 27. (a) H$_2$SO$_4$ (conc.), MeOH, Δ, 30h. (b) trimethylsilylacetylene (1.5 equiv), PdCl$_2$(PPh$_3$)$_2$ (1 mol%), CuI (1.5 mol%), rt, 18h. (c) NaOH (2N, 2 equiv), MeOH, rt, 5h. (d) NH$_2$OTHP (1.5 equiv), EDC (1.2 equiv), HOBt.H$_2$O (1.2 equiv), rt, 24h. (e) TsOH.H$_2$O (0.1 equiv), MeOH, rt, 12h. 68%. (f) azidomethyl phenyl sulfide (1.2 equiv), TBTA (0.1 equiv), CuSO$_4$.5H$_2$O (0.1 equiv), sodium ascorbate (0.5 equiv), DMSO, rt, 1-3 days. 92%.

In an attempt to improve the HDAC8 potency and selectivity of NCC149 **111**, derivatives in which the triazole moiety is replaced by another aromatic ring (benzene, thiazole, oxadiazole, reversed triazole, thiophene), have been made.[68] Evaluation of the potency and selectivity for HDAC8 with enzyme and cellular assays revealed that thiazole **112** (Scheme 28) displayed an improved profile over NCC149 **111** (Table 23).

Table 23. Selective inhibition of HDAC8 by thiazole **112**.

HDAC	1	2	3	4	6	8	nuclear extract
IC$_{50}$ (µM)	>100	>100	12	>100	14	0.15	>100

For the synthesis of thiazole **112**, α-bromoketone **136** and thioamide **139** were made as precursors (Scheme 28). α-Bromoketone **136** was formed from acid **134** by an esterification toward methyl ester **135** and a subsequent α-bromination. For the thioamide synthesis, acid

137 was converted to amide **138** by means of oxalyl chloride, dimethylformamide and ammonia, and further into thioamide **139** using Lawesson's reagent. Cyclisation was performed via a Hantzsch thiazole synthesis and gave thiazole **140** in 78% yield. Final conversion toward hydroxamic acid **112** was accomplished in three steps from ester **140** in 48% overall yield. The three steps involved hydrolysis, *O*-(tetrahydro-2*H*-pyran-2-yl)hydroxylamine coupling and tetrahydropyranyl deprotection.
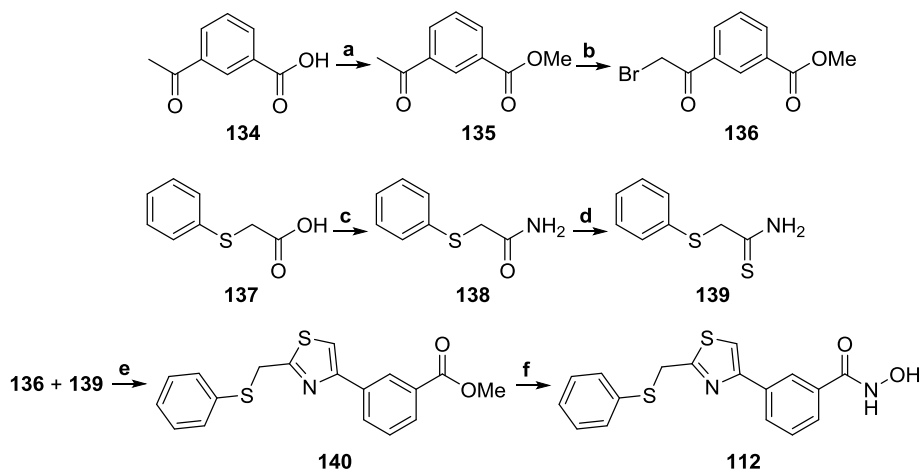
Scheme 28. (a) H_2SO_4 (conc.), MeOH, Δ, 26.5h. 97%. (b) Br_2 (0.93 equiv), 25% HBr-AcOH (cat.), $CHCl_3$, 0°C to rt, 2h. quant. (c) i) $(COCl)_2$ (2.6 equiv), DMF (cat.), THF, 0°C, 0.5h. ii) NH_3 (aq. 25%), THF, 0°C, 1.5h. 83%. (d) Lawesson's reagent (0.47 equiv), toluene, 80°C, 3.5h. 21%. (e) MS (3Å), EtOH/$CHCl_3$ 1/1, 70°C, 3h, N_2(g). 78%. (f) i) NaOH (2N aq., 4 equiv), MeOH/THF/$CHCl_3$ 2/1/1, rt, 5h. 68%. ii) NH_2OTHP (2.85 equiv), EDC.HCl (2.95 equiv), HOBt.H_2O (3.04 equiv), DMF, rt, 30h. 96%. iii) TsOH.H_2O (0.1 equiv), MeOH, rt, 5.5h. 73%.

1.2.4. Dual selective benzohydroxamic acid-based HDAC6/8 inhibitors

The last group of benzohydroxamic acid-based HDAC inhibitors comprises three structures **141**, **142** and **143**, all of them being nanomolar inhibitors of HDAC6 and 8 (Figure 4). Structures **141** and **143** are *meta*-(like) substituted compounds typically resulting in excellent HDAC8 inhibitory activity. In contrast to what can be expected, *para*-substituted compound **142** also demonstrated potent activity toward HDAC8. This proves that *para* versus *meta* substitution is not an absolute requirement to deliver HDAC6 or HDAC8 selective inhibitors, respectively. For each inhibitor presented in Figure 4, the biological activity and synthetic pathway will be discussed.
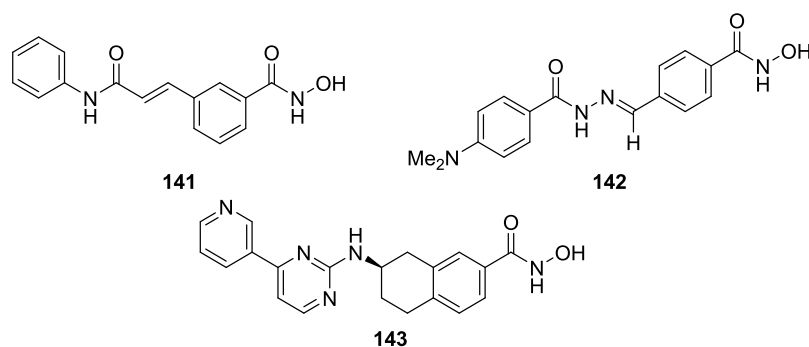

Figure 4. Overview of dual selective HDAC6/8 inhibitors bearing the benzohydroxamic acid moiety.

Benzohydroxamic acid **141** (Scheme 29) represents the first discovered, potent and selective dual HDAC6/8 inhibitor.[69] Selective inhibition of these two isoforms is expected to improve the therapeutic window by increasing the biological activity through beneficial additive or synergistic effects, while still keeping possible side effects to a minimum. As can be seen from Table 24, dual selective inhibitor **141** has low nanomolar potency for HDAC6 and 8, and low micromolar potency for the other HDACs tested (HDAC1-5, 7 and 9), clearly demonstrating its dual selectivity and potency. *Meta*-substitution with a hydrophobic cap-group again proved to be a necessary requirement in this case to obtain potent HDAC8 inhibition. This assumption was also supported by docking studies with HDAC8, were these structures filled the secondary hydrophobic pocket of HDAC8 with their cap-group.

Table 24. Selective dual inhibition of HDAC6 and 8 by compound **141**.

HDAC	1	2	3	4	5	6	7	8	9
IC_{50} (µM)	6.1	4.8	18	14	26	0.021	8.4	0.037	12

The synthesis of inhibitor **141** has been realized in two steps (Scheme 29). First, the acid functionality in structure **144** was converted to an amide by using 1-[bis(dimethylamino)-

methylene]-1*H*-1,2,3-triazolo[4,5-*b*]pyridinium-3-oxide hexa-fluorophosphate (HATU) as a coupling reagent. Secondly, hydroxamic acid **141** was formed from ester **145** by employing an excess of hydroxylamine and sodium hydroxide.
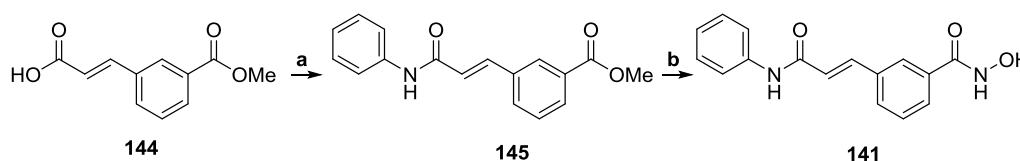

Scheme 29. (a) aniline (0.91 equiv), HATU (1.4 equiv), DIPEA (2.7 equiv), DMF, rt, till completion. (b) NH$_2$OH (50% in H$_2$O, 30 equiv), NaOH (1M, 10 equiv), CH$_2$Cl$_2$/MeOH 1/2, 0°C to rt, till completion. No yields reported.

From the structure of trichostatin A, a new class of *N*-acylhydrazones has been designed (e.g. structure **142**, (Scheme 30) with pronounced HDAC6/8 inhibitory activity.[70] As it is known from the literature that *meta*-substitution within benzohydroxamic acids is usually favourable with respect to HDAC8 inhibition, it was surprising to see that the *para*-substituted benzohydroxamic acids in this case showed more potent dual HDAC6/8 inhibition. From the derivatives tested, *N*-acylhydrazone **142** is a representative example demonstrating potent and selective inhibition of both HDAC6 and 8 (Table 25). It was also shown that this class of compounds exhibited pronounced antitumor activity against melanoma and hepatocellular carcinoma cells.

Table 25. Selective dual inhibition of HDAC6 and 8 by *N*-acylhydrazone **142**.

HDAC	1	2	6	8
IC$_{50}$ (µM)	>3	>3	0.015	0.23

A convergent synthetic approach has been applied for the synthesis of *N*-acylhydrazone **142** (Scheme 30). To that end, ester **147** was prepared by oxidizing aldehyde **146** using iodine and potassium hydroxide in methanol. This ester **147** was further converted to the proposed hydrazide **148** by means of hydrazine. In a second parallel pathway, aldehyde **149** was protected using 2,2-dimethoxypropane in an acidic environment. After treatment of the formed acetal-ester **150** with hydroxylamine, hydroxamic acid **151** was obtained in 90% yield. Hydrolysis of the acetal group in structure **151** with aqueous sulfuric acid resulted in the formation of aldehyde **152**. In the final step, condensation of aldehyde **152** with hydrazide **148** took place under acidic catalysis and yielded 84% of *N*-acylhydrazone **142.**
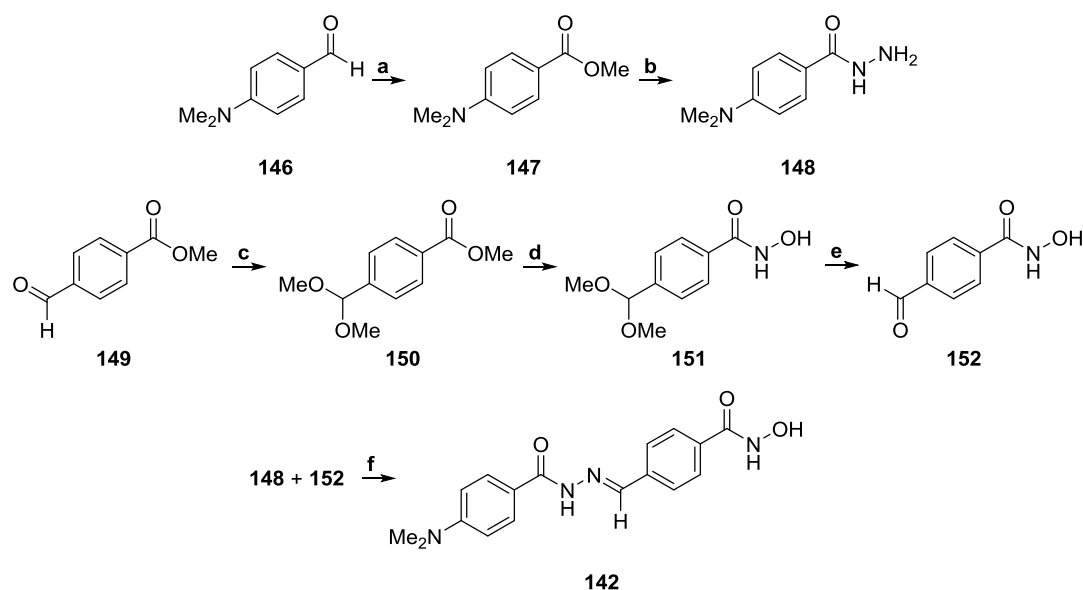
Scheme 30. (a) I_2 (3 equiv), KOH (6 equiv), MeOH, 0°C, 10h. 57%. (b) $NH_2NH_2.H_2O$ (10 equiv), MeOH, 70°C, 18h. 95%. (c) 2,2-dimethoxypropane (1.5 equiv), TsOH (0.1 equiv), MeOH, rt, 2h. 82%. (d) $NH_2OH.HCl$ (8 equiv), KOH (12 equiv), MeOH, rt, 4h. 90%. (e) H_2SO_4 (15% w/v aq.), acetone, rt, 2h. 91%. (f) HCl (cat.), EtOH, rt, 2h. 84%.

R-Aminotetralin **143** has been discovered through the generation of a focused library containing hydroxamic acids directly attached to fused bicyclic linkers and various capping groups.[29] In this way, a tetrahydroisoquinoline was identified as a novel lead compound. However, metabolic instability issues of the tetrahydroisoquinoline group urged the researchers to replace this system by an aminotetralin scaffold. As such, a second library was designed and *R*-aminotetralin **143** was discovered as the most potent and selective inhibitor of HDAC6 and 8 (Table 26). The selectivity was further proven by cellular assays determining the acetylation status of α-tubulin and the induction of p21.

Table 26. Selective dual inhibition of HDAC6 and 8 by *R*-aminotetralin **143**.

HDAC	1	2	3	4	5	6	7	8	9	10	11
IC_{50} (µM)	6.31	>100	>100	>100	>100	0.05	30.8	0.08	35.0	>100	>100

The synthesis of *R*-aminotetralin **143** started with the separation of racemate **153** through chiral supercritical fluid chromatography (Scheme 31). This generated *R*-enantiomer **154**, which was converted to amino ester **155** through a palladium-catalyzed carboxylation and Boc-deprotection. Nucleophilic aromatic substitution gained access toward 2-aminopyrimidin **156**, which was converted to hydroxamic acid **143** in a final step employing hydroxylamine.
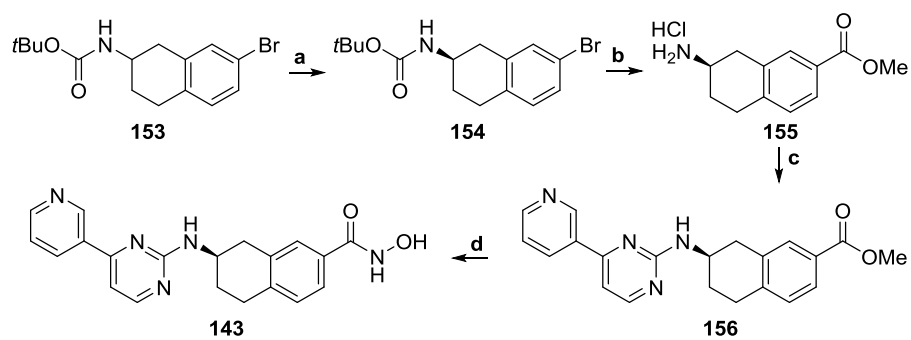
Scheme 31. (a) chiral supercritical fluid chromatography. (b) i) Pd(OAc)$_2$ (cat.), 1,3-bis(diphenylphosphino)propane (cat.), TEA (4 equiv), DMF/MeOH 3/10, CO (g), 80°C, 12h. ii) HCl/MeOH (1M), rt, 2h. (c) aryl chloride, DIPEA, DMF, 150°C, 1h, MW. (d) NH$_2$OH (50% in H$_2$O), NaOH, MeOH, rt, 1h. No reaction details reported.

1.3. Conclusions

Benzohydroxamic acids have been amply shown to be privileged building blocks in medicinal chemistry, especially when introduced as a zinc-binding moiety in the chemical architecture of HDAC inhibitors. This literature review shows that careful optimization of the part following the benzohydroxamic acid, *i.e.*, the linker region and the cap-group, can give rise to HDAC6 selective, non-selective, HDAC8 selective or dual HDAC6/8 selective inhibitors. When overviewing these four classes, general structure-activity relationships can be proposed for each class, although exceptions are present. The HDAC6 selective class mainly consists of inhibitors having a bulky cap-group in close proximity to the benzohydroxamic acid moiety. The non-selective pan-inhibitors have a rather elongated shape, and the HDAC8 selective inhibitors are mainly *meta*-(like) substituted with respect to the hydroxamic acid moiety. The last group of selective benzohydroxamic acid-based dual HDAC6/8 inhibitors is small and no class-specific structural properties can be defined at this point. The fact that exceptions on these structure-activity relationships can occur, and the fact that the selectivity data obtained through enzymatic screens (HDAC1-11) always confirmed the selectivity data obtained through more complex cellular screens (histone and α-tubulin acetylation, p21 induction), prove the importance of a HDAC1-11 screen as a preliminary tool for lead molecule selection. Finally, the synthetic pathways presented here could inspire future medicinal chemists to develop new syntheses to obtain an effective HDAC inhibitor eventually reaching the patient.

52

RESULTS AND DISCUSSION

Chapters II to VI are based on the following papers:

- **De Vreese, R.**; Verhaeghe, T.; Desmet, T.; D'hooghe, M. "Potent and selective HDAC6 inhibitory activity of *N*-(4-hydroxycarbamoylbenzyl)-1,2,4,9-tetrahydro-3-thia-9-azafluorenes as novel sulfur analogs of Tubastatin A" *Chem. Commun.* **2013**, 49, 3775-3777. (I.F. 6.72)

- **De Vreese, R.**; Depetter, Y.; Verhaeghe, T.; Desmet, T.; Benoy, V.; Haeck, W.; Van Den Bosch, L.; D'hooghe, M. "Synthesis and SAR assessment of novel Tubathian analogs in the pursuit of potent and selective HDAC6 inhibitors" *Org. Biomol. Chem.* **2016**, 14, 2537-2549. (I.F. 3.56)

- **De Vreese, R.**; Van Steen, N.; Verhaeghe, T.; Desmet, T.; Bougarne, N.; De Bosscher, K.; Benoy, V.; Haeck, W.; Van Den Bosch, L.; D'hooghe, M. "Synthesis of benzothiophene-based hydroxamic acids as potent and selective HDAC6 inhibitors." *Chem. Commun.* **2015**, 51, 9868-9871. (I.F. 6.57)

- **De Vreese, R.**; Galle, L.; Depetter, Y.; Franceus, J.; Desmet, T.; Van Hecke, K.; Benoy, V.; Van Den Bosch, L.; D'hooghe, M. "Synthesis of potent and selective HDAC6 inhibitors bearing a cyclohexane- or cycloheptane-annulated 1,5-benzothiazepine scaffold" *Chem. Eur. J.* **2017**, 23, 128-136. (I.F. 5.77)

- **De Vreese, R.**; de Kock, C.; Smith, P. J.; Chibale, K.; D'hooghe, M. "Exploration of thiaheterocyclic *h*HDAC6 inhibitors as potential antiplasmodial agents" *Future Med. Chem.* **2017**, 9, 357-364. (I.F. 3.35)

2. Potent and selective HDAC6 inhibitory activity of *N*-(4-hydroxycarbamoylbenzyl)-1,2,4,9-tetrahydro-3-thia-9-azafluorenes as novel sulfur analogs of Tubastatin A

Abstract: Eight N-(4-hydroxycarbamoylbenzyl)-1,2,4,9-tetrahydro-3-thia-9-azafluorenes were efficiently prepared as sulfur analogs of Tubastatin A and thus evaluated as new HDAC6 inhibitors. All compounds exhibited potency against HDAC6, and four of them were active in the nanomolar range (IC_{50} = 1.9-22 nM). Further analysis revealed that the sulfone derivatives (designated as Tubathians) are superior to their non-oxidized sulfide analogs, and the two most active sulfones showed good to excellent HDAC6 selectivity compared to all other HDAC isoform classes.

2.1. Introduction

The enzymatic addition and removal of acetyl groups at specific lysine residues comprise important biochemical reactions with a significant impact on many cellular processes.[3,71] The addition of acetyl groups within histone proteins, the chief protein components of chromatin, is catalyzed by histone acetyltransferases (HAT), and histone deacetylases (HDAC) mediate the corresponding deacetylation reactions. The inhibition of the latter group of deacetylases has become a hot topic in medicinal chemistry, and the use of HDAC inhibitors (HDACi's) has found many applications with regard to cancer and CNS disorder therapies (central nervous system).[19,72-74] In general, HDACi's act on 11 zinc-dependent HDAC isozymes, which are divided into four groups: class I (HDACs 1, 2, 3, 8), class IIa (HDACs 4, 5, 7, 9), class IIb (HDACs 6, 10), and class IV (HDAC11).[6] The majority of known HDACi's primarily inhibit the class I enzymes, making them excellent candidates for cancer therapy applications, but other than class I HDACi's are normally required for the pursuit of non-oncological applications.[75] Another important issue relates to the potential toxicity of compounds inhibiting multiple isozymes, as acetylation is involved in the control of many cellular processes and inhibition of some isozymes may cause undesirable side effects. Thus, the design and development of isozyme-selective inhibitors has emerged as an important challenge within the search for novel HDACi's.[76] In recent years, HDAC6 has been acknowledged as an attractive target for drug development,[77-81] and an increasing number of research teams are currently involved in the quest for new compounds endowed with HDAC6 inhibitory activity.[32,82-88] In addition to the potential of HDAC6-selective inhibitors for applications in the treatment of CNS disorders and neurodegenerative diseases, these compounds seem to provoke fewer side effects, hence the growing interest in their preparation.[89] An important milestone in that respect concerns the identification of Tubacin as a selective HDAC6 inhibitor, although the application of this compound is hampered by its poor druglikeness and cumbrous synthesis.[90] Since then, considerable advances have been made with regard to the preparation of new HDAC6 inhibitors, leading to an array of different molecular entities with improved chemical and pharmacological properties. From a chemical viewpoint, many of these molecules comprise the typical HDACi basic structure accommodating an aromatic cap group (surface recognition domain), a linker and a zinc-binding hydroxamic acid unit. A major breakthrough was accomplished recently, involving the rational design and synthesis of Tubastatin A as a novel and selective HDAC6 inhibitor.[13] Elaborate studies in this direction showed that the HDAC6 isozyme tolerates modifications of the Tubastatin A chemical structure at the level of the cap group and, more specifically, that the introduction of structural diversity at the 2- and 8-position of the tetrahydropyrido[4,3-*b*]indole scaffold can be beneficial with regard to the overall bioactivity.[34]

Inspired by these recent SAR findings, and intrigued by the fact that several new HDAC6 inhibitors contain a sulfur atom in their molecular structure,[32,84,85] efforts were made toward the preparation of a number of sulfur analogs (sulfides and sulfones) of Tubastatin A in the present study, supported by HDAC6 ligand docking. Furthermore, the replacement of a methylene group with a sulfone moiety in medicinally relevant compounds has been shown to induce a significant beneficial increase in stability,[91] suggesting this modification as a preferred change during compound optimization and thus providing an additional rationale for the work undertaken in this study. The results obtained point to the potential of sulfur analogs of Tubastatin A as new HDAC6 inhibitors, especially those containing a sulfone moiety in their structure.

2.2. Synthesis and biological evaluation of *N*-(4-hydroxy-carbamoylbenzyl)-1,2,4,9-tetrahydro-3-thia-9-azafluorenes

The 1,2,4,9-tetrahydro-3-thia-9-azafluorene scaffold was prepared via a bismuth nitrate-promoted Fisher indole synthesis employing a phenylhydrazine hydrochloride **1** and tetrahydrothiopyran-4-one **2**, providing a convenient access to tetrahydro-3-thia-9-azafluorenes **3** in good yields (Scheme 1).[92] Subsequently, *N*-benzylation of compounds **3** was accomplished using a methyl 4-(bromomethyl)benzoate in DMF in the presence of sodium hydride and potassium iodide, furnishing the corresponding *N*-(4-methoxycarbonylbenzyl)-1,2,4,9-tetrahydro-3-thia-9-azafluorenes **4**. The final step of the process comprised an ester to hydroxamic acid interconversion, which was realized utilizing an excess of hydroxylamine hydrochloride in the presence of methanolic sodium methoxide in DMF. In this way, the premised *N*-(4-hydroxycarbamoylbenzyl)-1,2,4,9-tetrahydro-3-thia-9-azafluorenes **5** were obtained in an efficient and straightforward approach (Scheme 1, Table 1).

Considering the presence of a (cyclic) sulfone moiety in several drugs and bioactive compounds,[91] the sulfide in systems **3** was oxidized to the corresponding sulfones **6** by means of *meta*-chloroperbenzoic acid treatment in tetrahydrofuran. The thus obtained sulfones **6** were taken further in the synthesis toward the contemplated hydroxamic acids **8** via esters **7** applying a similar strategy to that discussed above for the preparation of hydroxamic acids **5** (Scheme 1, Table 1).
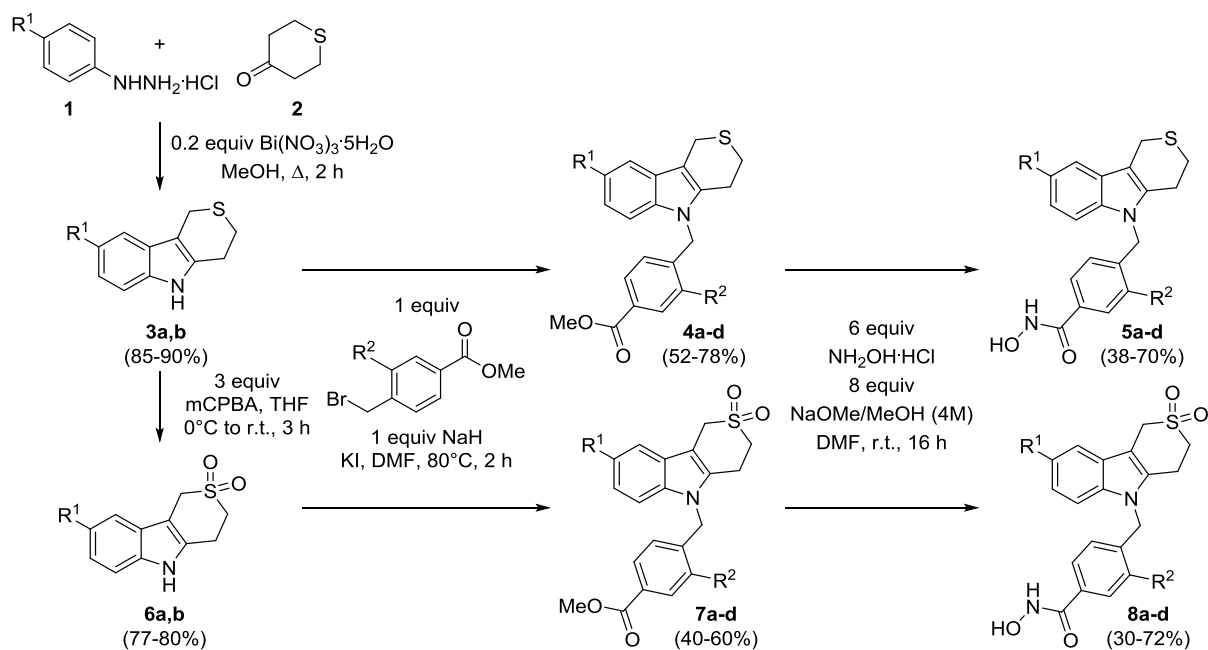
Scheme 1. Synthesis of *N*-(4-hydroxycarbamoylbenzyl)-1,2,4,9-tetrahydro-3-thia-9-azafluorenes **5** and their oxidized analogs **8**.

Table 1. Synthesis of tetrahydro-3-thia-9-azafluorenes **3-5** and their oxidized analogs **6-8**.

R^1	R^2	Compound (yield)^a
H	-	**3a** (85%)
F	-	**3b** (90%)
H	H	**4a** (52%)
H	MeO	**4b** (57%)
F	H	**4c** (69%)
F	MeO	**4d** (78%)
H	H	**5a** (38%)
H	MeO	**5b** (65%)
F	H	**5c** (70%)
F	MeO	**5d** (66%)
H	-	**6a** (77%)
F	-	**6b** (80%)
H	H	**7a** (48%)
H	MeO	**7b** (60%)
F	H	**7c** (47%)
F	MeO	**7d** (40%)
H	H	**8a** (51%)
H	MeO	**8b** (30%)
F	H	**8c** (69%)
F	MeO	**8d** (72%)

^{a} Yields after purification by column chromatography (SiO$_2$) or recrystallization

The binding of the various ligands **5a-d** and **8a-d** in the enzyme's active site was evaluated by means of automated docking. Since the crystal structure of HDAC6 is not available, a homology model was first generated following the example of Kozikowski using the structure of HDAC isozymes as a template (more information on the building of the homology model can be found in the experimental details).[13] Compounds that do not carry a methoxy group on their linker (**5a, 5c**, **8a** and **8c**) were found to fit perfectly in the active site of HDAC6 (Figure 1). In that case, the *p*-tolyl linker is positioned in the tubular access channel, with the carbonyl group of the hydroxamate moiety within chelating distance from the zinc ion at the bottom of the pocket. As the linker fills the access channel almost completely, very little space is left to accommodate a (bulky) substituent such as a methoxy group (Figure 1A), which is in line with previous studies in that respect. In contrast, modifications of the tricyclic cap group do not seem to influence the binding mode very much, since the conformation and orientation of

compounds **5a, 5c**, **8a** and **8c** is nearly identical. However, oxidation of the sulfur atom might generate additional interactions with the enzyme in the form of hydrogen bonds between the introduced oxygen atoms and the backbone nitrogen of residues Asp567 and Gly619 (Figure 1B and Figure 2 in the Experimental Details). The latter observation provided an interesting motive to experimentally assess the HDAC6 inhibitory activity of Tubastatin A analogs in which the NMe moiety is replaced by a sulfone unit.
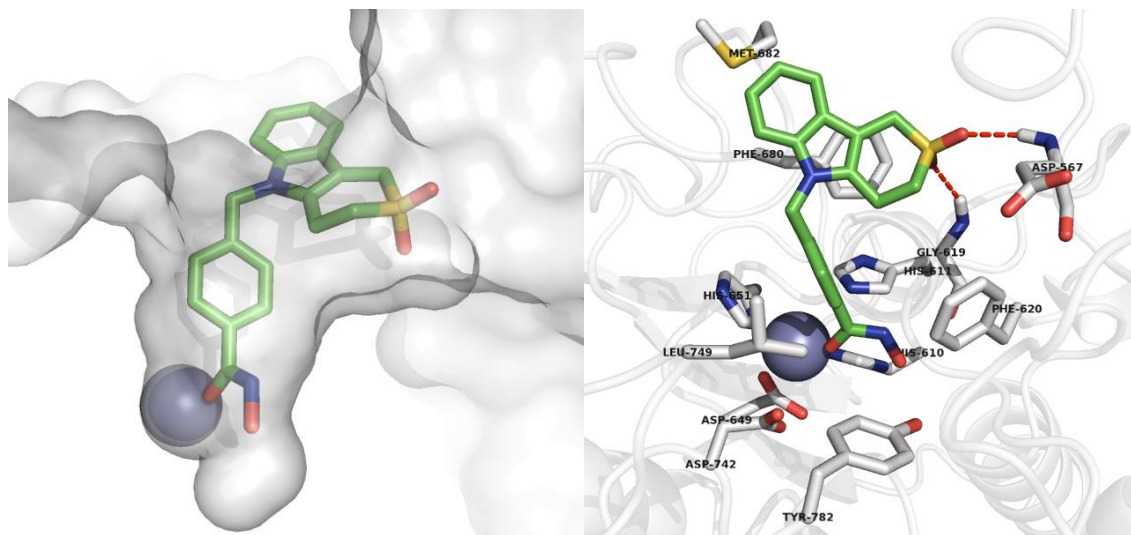

Figure 1. Docking of compound **8a** in the active site of HDAC6. (A) view of the tubular access channel, and (B) additional interactions generated by the oxidation of the sulfur atom (green: carbon; blue: nitrogen; red: oxygen; yellow: sulfur; magenta: zinc ion).

In vitro pharmacology studies of novel hydroxamic acids **5a-d** and **8a-d** with regard to their HDAC1 and HDAC6 inhibitory activity revealed an interesting potency of these compounds as HDAC6 inhibitors (Table 2). In particular, hydroxamic acids **5a**, **5c**, **8a** and **8c** showed complete inhibition at a test concentration of 10 μM, and also compounds **8b** and **8d** exhibited a good profile with an inhibition of 73% and 75%, respectively. In addition, these results pointed to a selectivity of the test compounds toward HDAC6 inhibition, with HDAC1 inhibition percentages ranging from 0% to a maximum of 53%. Furthermore, these data also indicate a detrimental effect of the introduction of a methoxy group in the linker moiety on the bioactivity (compounds **5b,d** and **8b,d**), as indicated by homology modeling. HDAC1 and HDAC6 were chosen for activity comparison in this preliminary test, as these two enzymes have a diverse phylogeny and are members of separate deacetylase classes.

Table 2. % inhibition of control values with regard to HDAC1 and HDAC6 inhibitory activity[a,b]

Compound	% inhibition HDAC1	% inhibition HDAC6	Compound	% inhibition HDAC1	% inhibition HDAC6
5a	26	99	**8a**	51	99
5b	0	38	**8b**	2	73
5c	17	99	**8c**	53	99
5d	0	51	**8d**	8	75

[a] Test concentration: 10 µM; [b] Mean value of two screening sessions

The most promising molecules (those compounds showing an inhibition of >70%) were then selected for determination of their IC_{50} values with respect to HDAC6 inhibition (Table 3). These assessments confirmed the presumption that molecules bearing a methoxy-substituted linker exhibit lower – but still moderate – activities, exemplified by compounds **8b** and **8d** (with IC_{50} values of 2.0 and 1.3 µM, respectively). Furthermore, sulfur oxidation indeed seems to be beneficial for bioactivity, as sulfones **8a** and **8c** show even more potent HDAC6 inhibition as compared to sulfides **5a** and **5c**. Overall, four compounds (**5a**, **5c**, **8a** and **8c**) can be considered to be promising lead templates for further elaborate studies. Sulfides **5a** and **5c** (with IC_{50} values of 15 and 22 nM, respectively) display HDAC6 inhibitory activities similar to the reference compound Trichostatin A and to Tubastatin A, but sulfones **8a** and **8c** are even more potent than sulfides **5a** and **5c** with IC_{50} values of 1.9 and 3.7 nM, respectively.

Table 3. IC_{50} values for HDAC6 inhibition[a]

Compound	IC_{50} (µM)	Compound	IC_{50} (µM)
5a	0.015	**8b**	2.0
5c	0.022	**8c**	0.0037
8a	0.0019	**8d**	1.3

[a] Reference compound: Trichostatin A (IC_{50} = 0.012 µM)

Finally, the HDAC inhibition selectivity of the two most active compounds **8a** ($R^1 = R^2 = H$) and **8c** ($R^1 = F$, $R^2 = H$) against the other HDAC isoform classes was assessed and, to this end, a class I (HDAC1), a class IIa (HDAC4), a class IIb (HDAC6) and a class IV (HDAC11) isozyme was selected. Considering the fact that Tubastatin A has over 1000-fold selectivity against all HDAC isozymes except for HDAC8, where it has only a 57-fold selectivity, the HDAC8 inhibitory activity of compounds **8a** and **8c** was also evaluated.

Table 4. Comparison of HDAC selectivity

Compound	HDAC1 IC$_{50}$ (µM)[a]	HDAC4 IC$_{50}$ (µM)[a]	HDAC6 IC$_{50}$ (µM)[a]	HDAC11 IC$_{50}$ (µM)[b]	HDAC8 IC$_{50}$ (µM)[a]
8a	11	1.6	0.0019	NC	1.7
8c	12	1.9	0.0037	NC	0.93
Tub A[c]	16.4	>30	0.015	>30	0.85

[a] Reference compound: Trichostatin A, [b] Reference compound: Scriptaid, NC = Not Calculable (concentration-response curve shows less than 25% effect at the highest validated testing concentration) [c] Literature values for Tub A (Tubastatin A)[13], caution should be taken when comparing the IC$_{50}$ values of **8a** and **8c** to the literature values for Tubastatin A.

The data in Table 4 point to a good to excellent HDAC6 selectivity of hydroxamic acids **8a** and **8c**, with the HDAC6 *versus* HDAC11 and HDAC1 selectivity being the most pronounced. The HDAC11 inhibitory effect of **8a,c** appeared to be very low and no IC$_{50}$ values could be obtained. Furthermore, a 5789-fold and 3243-fold selectivity against HDAC1 was determined for compounds **8a** and **8c**, respectively, which substantially exceeds the selectivity of Tubastatin A (1093-fold selectivity).[13] In addition, also a high HDAC6 *versus* HDAC4 selectivity was observed for sulfones **8a** and **8c** (842- and 513-fold, respectively). Finally, it is interesting to note that these compounds show a good HDAC6 *versus* HDAC8 selectivity, and both sulfone **8a** (895-fold) and sulfone **8c** (251-fold) exhibited a considerably higher selectivity in that respect as compared to Tubastatin A (57-fold).[13]

The experimental results listed in Tables 2-4 are in line with the structure-activity relationship insights provided by ligand docking. These data show that decoration of the *N*-(4-hydroxycarbamoylbenzyl)-1,2,4,9-tetrahydro-3-thia-9-azafluorene scaffold at the linker unit (*in casu* by a methoxy group) is unfavorable for HDAC6 inhibitory activity. On the other hand, introduction of a substituent (*in casu* a fluoro atom) at the cap group did not appear to have a significant effect on the activity profile. It should also be noted that replacement of the tertiary amine functionality (NMe moiety) in the tetrahydropyrido[4,3-b]indole core structure of Tubastatin A by a sulfide unit results in compounds with a comparable HDAC6 inhibitory activity (at least as concerns the IC$_{50}$ value), whereas replacement by a sulfone moiety (SO$_2$) affords even more potent HDAC6 inhibitors. The *in silico* observed occurrence of hydrogen bonds between the introduced oxygen atoms and the backbone nitrogen atom of residues Asp567 and Gly619 can account for the higher *in vitro* activity of these sulfone derivatives.

In addition to their promising biological potential and their straightforward and easy synthesis and purification, sulfones **8a** and **8c** (designated as Tubathian A and Tubathian B, respectively) also show an interesting profile for further evaluation based on their predicted druglikeness (M$_W$, *c*LogP, solubility).

2.3. Conclusions

N-(4-Hydroxycarbamoylbenzyl)-1,2,4,9-tetrahydro-3-thia-9-azafluorenes were efficiently prepared and shown to be of interest as novel and selective HDAC6 inhibitors, culminating in the identification of two sulfone derivatives as interesting lead structures for further elaboration displaying potent and selective HDAC6 inhibition in the nanomolar range.

The findings described in this chapter thus provide a platform for more elaborate studies with respect to the HDAC6 inhibitory activity of this new class of thiaheterocyclic compounds which, in combination with further optimization of drug-relevant molecular properties, might afford promising new lead structures.

2.4. Experimental Details

2.4.1. Ligand docking

All docking experiments were performed by the Centre for Industrial Biotechnology and Biocatalysis (Prof. Desmet). All manipulations were completed with the molecular modelling program YASARA and the YASARA/WHATIF twinset.[93,94] The HDAC6 sequence was obtained from the UniProt database (www.uniprot.org; UniProt entry Q9UBN7). To increase the accuracy of the model, the sequence was limited to the major functional domain of HDAC6 (Gly482-Gly800). Possible templates were identified by running 3 PSI-BLAST iterations to extract a position specific scoring matrix (PSSM) from UniRef90, and then searching the PDB for a match. To aid the alignment of the HDAC6 sequence and templates, and the modelling of the loops, a secondary structure prediction was performed, followed by multiple sequence alignments. All side chains were ionised or kept neutral according to their predicted pKa values. Initial models were created from different templates, each with several alignment variations and up to hundred conformations tried per loop. After the side-chains had been built, optimised and fine-tuned, all newly modelled parts were subjected to a combined steepest descent and simulated annealing minimisation, i.e. the backbone atoms of aligned residues were kept fixed to preserve the folding, followed by a full unrestrained simulated annealing minimisation for the entire model. The final model was obtained as a hybrid model of the best parts of the initial models, and checked once more for anomalies like incorrect configurations or colliding side chains. Furthermore, it was structurally aligned with known HDAC crystal structures to check if the chelating residues and the zinc atom were arranged correctly.

The HDAC inhibitor structures were created with YASARA and energy minimised with the AMBER03 force field.[95] The grid box used for docking had a dimension of 25 x 25 x 25 angstrom with a grid spacing of 0.2 Å, and comprised the entire catalytic cavity including the Zn ion and the outer surface of the active site entrance. Docking was performed with AutoDock 4.2 using the AMBER03 force field and default parameters.[96] Ligands were allowed to freely rotate during docking. The figure was created with PyMol v1.3.[97]

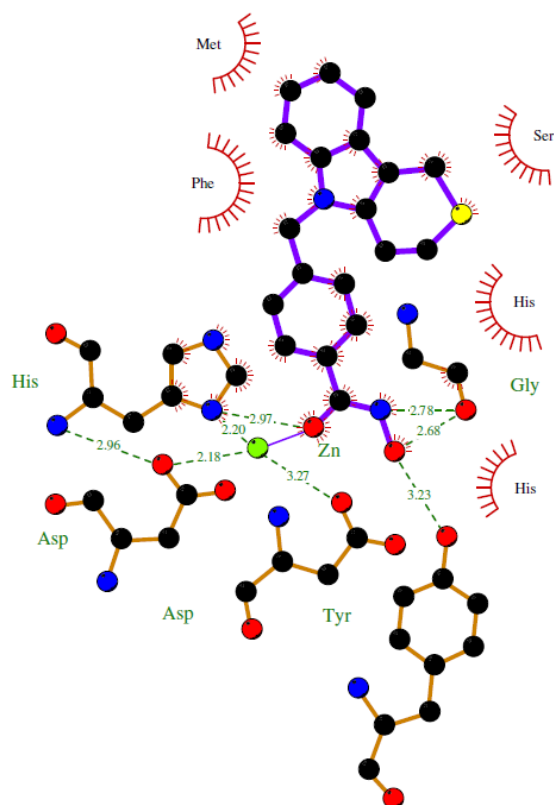Ligplot diagrams were made with LigPlot[+] v1.4.

Figure 2. Ligplot diagram of compound **5a** (black: carbon, blue: nitrogen; red: oxygen; yellow: sulfur; green: zinc ion, values in Å).
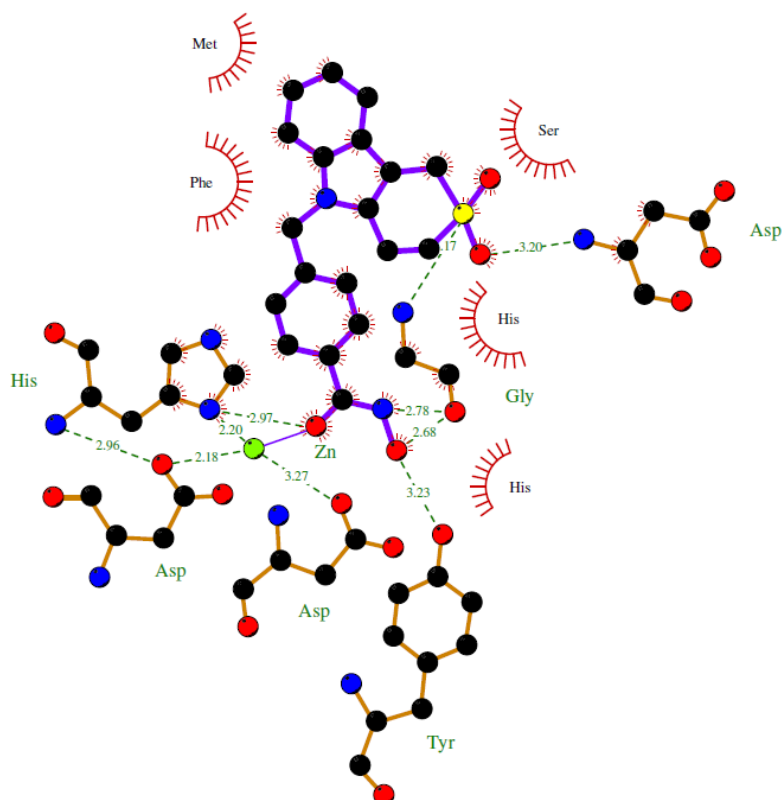

Figure 3. Ligplot diagram of compound **8a** (black: carbon, blue: nitrogen; red: oxygen; yellow: sulfur; green: zinc ion, values in Å). The Glycin hydrogen bond is directed toward the oxygen atom of the sulfone and not to the sulfur atom (value 3.17 Å).

2.4.2. Enzyme inhibition assays

The enzyme inhibition assays were performed by Eurofins Cerep Panlabs. *In vitro* IC_{50} values were determined by using human recombinant HDAC1-11 and fluorogenic HDAC substrate.[98]

2.4.3. Synthetic procedures and spectral data

^{1}H NMR spectra were recorded at 300 MHz (JEOL ECLIPSE+) with $CDCl_3$ or D_6-DMSO as solvent and tetramethylsilane as internal standard. ^{13}C NMR spectra were recorded at 75 MHz (JEOL ECLIPSE+) with $CDCl_3$ or D_6-DMSO as solvent and tetramethylsilane as internal standard. Mass spectra were obtained with a mass spectrometer Agilent 1100, 70 eV. IR spectra were measured with a Spectrum One FT-IR spectrophotometer. High resolution electron spray (ES) mass spectra were obtained with an Agilent Technologies 6210 series time-of-flight instrument. Melting points of crystalline compounds were measured with a Büchi 540 apparatus. The purity of all tested compounds was assessed by HRMS analysis and/or HPLC analysis, confirming a purity of ≥95%.

2.4.2.1. Synthesis of 1,2,4,9-tetrahydro-3-thia-9-azafluorenes 3

General procedure: To a solution of phenyl hydrazine hydrochloride **1** (12 mmol) and tetrahydrothiopyran-4-one **2** (12 mmol) in methanol (50 mL) was added $Bi(NO_3)_3 \cdot 5H_2O$ (2.4 mmol). After being stirred for 2 h under reflux, the reaction mixture was poured into water (100 mL), and bismuth nitrate was removed trough filtration. The crude product was extracted with ethyl acetate (100 mL), washed with saturated $NaHCO_3$ (100 mL), brine (100 mL) and dried over anhydrous $MgSO_4$. Filtration of the drying agent and removal of the solvent *in vacuo* afforded the crude thioether **3**, which was purified by means of recrystallization from ethanol to provide pure 1,2,4,9-tetrahydro-3-thia-9-azafluorene **3** (10.2 mmol, 85%).

1,2,4,9-tetrahydro-3-thia-9-azafluorene 3a (85%)

Spectral data of 1,2,4,9-tetrahydro-3-thia-9-azafluorene **3a** correspond with data described in the literature.[99]

### **1,2,4,9-tetrahydro-3-thia-6-fluoro-9-azafluorene 3b** (90%)
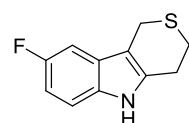
White crystals. Recrystallization from EtOH. Mp = 137.3 °C. ^{1}H NMR (300 MHz, $CDCl_3$): δ 2.98 (4H, s, CH_2CH_2S); 3.79 (2H, s, $C_{quat}CH_2S$); 6.87 (1H, t × d, J = 9.1, 2.8 Hz, CH_{arom}); 7.07 (1H, d × d, J = 9.1, 2.8 Hz, CH_{arom}); 7.16 (1H, d × d, J = 9.1, 4.4 Hz, CH_{arom}); 7.80 (1H, s(br), NH). ^{19}F NMR (282 MHz, $CDCl_3$): δ (-124.46) – (-124.37) (m). ^{13}C NMR (75 MHz, $CDCl_3$): δ 22.7 ($C_{arom,quat}\underline{C}H_2S$), 25.3 and 25.7 ($CH_2CH_2S$), 102.9 (d, J = 24.2 Hz, CH_{arom}), 107.1 (d, J = 4.6 Hz, $C_{arom,quat}$), 109.7 (d, J = 26.6 Hz, CH_{arom}), 111.1 (d, J = 10.4 Hz, CH_{arom}), 127.4 (d, J = 9.2 Hz, $C_{arom,quat}$), 131.0 and

135.3 (2 × $C_{arom,quat}$), 158.0 (d, $J = 234.2$ Hz, $C_{arom,quat}$). IR (ATR, cm^{-1}): $v_{NH} = 3336$; $v_{max} = 1582$, 1480, 1453, 1434, 1330, 1102, 962, 841, 792. MS (70eV): m/z (%) 206 (M$^-$-1, 100). HRMS (ESI) Anal. Calcd. for $C_{11}H_{11}FNS$ 208.0596 [M+H]$^+$, Found 208.0595.

2.4.2.2. Synthesis of sulfones 6

General procedure: To a solution of 1,2,4,9-tetrahydro-3-thia-9-azafluorene **3a** (5 mmol) in tetrahydrofuran (50 mL) was added *m*-chloroperbenzoic acid in tetrahydrofuran (>70%, 15 mmol) at 0°C. The mixture was stirred at room temperature for 2 h. The solvent was removed *in vacuo* and the residue was dissolved in ethyl acetate (100 mL). The solution was washed with saturated aqueous sodium sulfite (30 mL), water (30 mL), brine (2 × 30 mL), and dried over anhydrous MgSO$_4$. Filtration of the drying agent and removal of the solvent *in vacuo* afforded the crude sulfone **6a**, which was purified by recrystallization from EtOH to provide pure 1,2,4,9-tetrahydro-3-thia-9-azafluorene-3,3-dioxide **6a** (3.85 mmol, 77%).

1,2,4,9-Tetrahydro-3-thia-9-azafluoreen-3,3-dioxide 6a (77%)
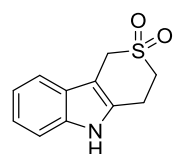
Beige powder. Recrystallization from EtOH. Mp = 245.5 °C. ^{1}H NMR (300 MHz, D$_6$-DMSO): δ 3.26 (2H, t, $J = 6.3$ Hz, C$\underline{H}_2$CH$_2$SO$_2$); 3.48 (2H, t, $J = 6.3$ Hz, CH$_2$C$\underline{H}_2$SO$_2$); 4.44 (2H, s, C$_{quat}$CH$_2$SO$_2$); 6.98-7.02 (1H, m, CH$_{arom}$); 7.07-7.11 (1H, m, CH$_{arom}$); 7.32 (1H, d, $J = 7.9$ Hz, CH$_{arom}$); 7.42 (1H, d, $J = 7.9$ Hz, CH$_{arom}$); 11.15 (1H, s(br), NH). ^{13}C NMR (75 MHz, D$_6$-DMSO): δ 23.1 ($\underline{C}$H$_2$CH$_2$SO$_2$), 47.2 (CH$_2$$\underline{C}H_2SO_2$), 48.9 (C$_{quat}$$\underline{C}H_2SO_2$), 101.9 (C$_{quat,arom}$), 111.4, 117.8, 119.3 and 121.9 (4 × HC$_{arom}$), 127.2, 130.6 and 136.5 (3 × C$_{quat,arom}$). IR (cm^{-1}): $v_{NH} = 3350$; $v_{S=O} = 1114$, 1102; $v_{max} = 1462$, 1315, 1274, 1162, 892, 744 and 645. MS (70 eV): m/z (%) 222 (M$^+$+1, 47); 239 (M$^+$+NH$_4$, 85). HRMS (ESI) Anal. Calcd. for $C_{11}H_{10}NO_2S$ 220.0438 [M-H]$^-$, Found 220.0433.

### 6-Fluoro-1,2,4,9-tetrahydro-3-thia-9-azafluorene-3,3-dioxide 6b (80%)
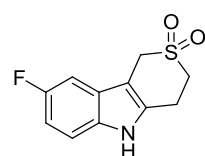
Light brown powder. Recrystallization from EtOH. Mp = 260.4 °C. ^{1}H NMR (300 MHz, D$_6$-DMSO): δ 3.24 and 3.46 (2 × 2H, 2 × t, $J = 6.1$ Hz, CH$_2$CH$_2$S); 4.40 (2H, s, C$_{quat}$CH$_2$S); 6.90 (1H, t × d, $J = 9.1$, 2.8 Hz, CH$_{arom}$); 7.21 (1H, d × d, $J = 9.1$, 2.8 Hz, CH$_{arom}$); 7.30 (1H, d × d, $J = 9.1$, 4.4 Hz, CH$_{arom}$); 11.23 (1H, s(br), NH). ^{19}F NMR (282 MHz, D$_6$-DMSO): δ (-124.67) – (-124.58) (m). ^{13}C NMR (75 MHz, D$_6$-DMSO): δ 23.3 ($\underline{C}$H$_2$CH$_2$S), 47.2 (CH$_2$$\underline{C}H_2$S), 48.9 (C$_{arom,quat}$$\underline{C}H_2$S), 102.4 (d, $J = 4.6$ Hz, C$_{arom,quat}$), 103.0 (d, $J = 24.2$ Hz, CH$_{arom}$), 109.9 (d, $J = 25.4$ Hz, CH$_{arom}$), 112.5 (d, $J = 10.4$ Hz, CH$_{arom}$), 127.6 (d, $J = 10.3$ Hz, C$_{arom,quat}$), 132.9 and 133.3 (2 × C$_{arom,quat}$), 157.4 (d, $J = 231.9$ Hz, C$_{arom,quat}$). IR (ATR, cm^{-1}): $v_{NH} = 3359$; $v_{S=O} = 1119$, 1102. $v_{max} = 1586$, 1489, 1300, 1280, 1170, 1130, 798. MS (70eV): m/z (%) 238 (M$^-$-1, 100). HRMS (ESI) Anal. Calcd. for $C_{11}H_9FNO_2S$ 238.0344 [M-H]$^-$, Found 238.0344.

2.4.2.3. Synthesis of esters 4 and 7

General procedure: 1,2,4,9-Tetrahydro-3-thia-9-azafluorene **3a** (6 mmol) and sodium hydride (60 wt % in mineral oil, 6 mmol) were placed under nitrogen and dissolved in DMF (10 mL).

After stirring for 30 minutes, methyl 4-(bromomethyl)benzoate (6 mmol) and potassium iodide (10 mg) were added to the reaction. The reaction was heated to 80 °C for 2 h, after which the reaction was quenched with water (30 mL) followed by addition of ethyl acetate (30 mL). The aqueous layer was extracted with ethyl acetate (2 × 10 mL) and the combined organic layers were washed with water (2 × 20 mL), brine (15 mL), dried (MgSO₄) and concentrated *in vacuo*. Recrystallization from ethanol afforded pure *N*-(4-methoxycarbonylbenzyl)-1,2,4,9-tetrahydro-3-thia-9-azafluorene **4a** (3.12 mmol, 52%).

N-(4-Methoxycarbonylbenzyl)-1,2,4,9-tetrahydro-3-thia-9-azafluorene 4a (52%)
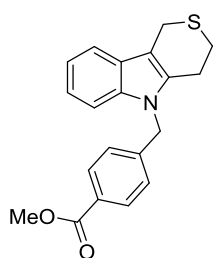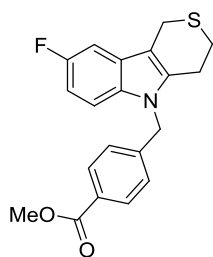
Light brown crystals. Recrystallization from EtOH. Mp = 120.8 °C. ^{1}H NMR (300 MHz, CDCl₃): δ 2.81 and 2.96 (2 × 2H, 2 × t, *J* = 5.7 Hz, CH₂CH₂S); 3.85 (3H, s, CH₃O); 3.88 (2H, s, C$_{quat}$CH₂S); 5.23 (2H, s, CH₂N); 6.99 (2H, d, *J* = 8.2 Hz, 2 × CH$_{arom}$); 7.10-7.15 and 7.47-7.50 (3H and 1H, 2 × m, 4 × CH$_{arom}$); 7.91 (2H, d, *J* = 8.2 Hz, 2 × CH$_{arom}$). ^{13}C NMR (75 MHz, CDCl₃): δ 23.2 (C$_{arom,quat}$CH₂S), 24.1 and 26.0 (CH₂CH₂S), 46.1 (CH₂N), 52.3 (CH₃O), 107.4 (C$_{arom,quat}$), 109.1, 117.9, 119.7 and 121.8 (4 × CH$_{arom}$), 126.2 (2 × CH$_{arom}$), 126.9 and 129.5 (2 × C$_{arom,quat}$), 130.3 (2 × CH$_{arom}$), 134.7, 135.8 and 143.1 (3 × C$_{arom,quat}$), 166.8 (C=O). IR (ATR, cm^{-1}): ν$_{C=O}$ = 1717; ν$_{max}$ = 1462, 1276, 1105, 741, 706. MS (70eV): m/z (%) 338 (M$^+$+1, 65). HRMS (ESI) Anal. Calcd. for C₂₀H₂₀NO₂S 338.1215 [M+H]$^+$, Found 338.1218.

N-(4-Methoxycarbonyl-2-methoxybenzyl)-1,2,4,9-tetrahydro-3-thia-9-azafluorene 4b (57%)
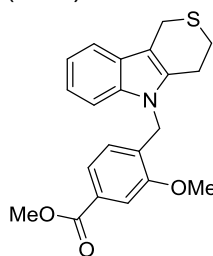
Light yellow crystals. Recrystallization from EtOH/EtOAc (1/1). Mp = 155.1 °C. ^{1}H NMR (300 MHz, CDCl₃): δ 2.86 and 3.00 (2 × 2H, 2 × t, *J* = 5.8 Hz, CH₂CH₂S); 3.88 (3H, s, CH₃O); 3.94 (2H, s, C$_{quat}$CH₂S); 3.98 (3H, s, CH₃O); 5.27 (2H, s, CH₂N); 6.34 (1H, d, *J* = 7.9 Hz, CH$_{arom}$); 7.08-7.19 (3H, m, 3 × CH$_{arom}$); 7.42 (1H, d × d, *J* = 7.9, 1.4 Hz, CH$_{arom}$); 7.50-7.54 (1H, m, CH$_{arom}$); 7.56 (1H, d, *J* = 1.4 Hz, CH$_{arom}$). ^{13}C NMR (75 MHz, CDCl₃): δ 23.2 (C$_{arom,quat}$CH₂S), 23.9 and 26.0 (CH₂CH₂S), 41.6 (CH₂N), 52.3 and 55.7 (2 × CH₃O), 107.1 (C$_{arom,quat}$), 109.1, 110.7, 117.7, 119.5, 121.6, 122.4 and 126.3 (7 × CH$_{arom}$), 126.9, 130.4, 131.3, 134.8 and 135.8 (5 × C$_{arom,quat}$), 156.3 (C$_{arom,quat}$O), 166.9 (C=O). IR (ATR, cm^{-1}): ν$_{C=O}$ = 1716; ν$_{max}$ = 1465, 1435, 1411, 1290, 1269, 1228, 1190, 1099, 1030, 983, 758, 738. MS (70eV): m/z (%) 368 (M$^+$+1, 67). HRMS (ESI) Anal. Calcd. for C₂₁H₂₂NO₃S 368.1320 [M+H]$^+$, Found 368.1318.

### *N*-(4-Methoxycarbonylbenzyl)-6-fluoro-1,2,4,9-tetrahydro-3-thia-9-azafluorene 4c (69%)

White crystals. Recrystallization from EtOH. Mp = 125.4 °C. ^{1}H NMR (300 MHz, CDCl₃): δ 2.86 and 2.99 (2 × 2H, 2 × t, *J* = 5.5 Hz, CH₂CH₂S); 3.85 (2H, s, C$_{quat}$CH₂S); 3.88 (3H, s, CH₃O); 5.28 (2H, s, CH₂N); 6.87 (1H, t × d, *J* = 9.1, 2.8 Hz, CH$_{arom}$); 7.00 (2H, d, *J* = 8.3 Hz, 2 × CH$_{arom}$); 7.07 (1H, d × d, *J* = 9.1, 4.4 Hz, CH$_{arom}$); 7.14 (1H, d × d, *J* = 9.1, 2.8 Hz, CH$_{arom}$); 7.94 (2H, d, *J* = 8.3 Hz, 2 × CH$_{arom}$). ^{19}F NMR (282 MHz, CDCl₃): δ (-124.42) – (-124.34) (m). ^{13}C NMR (75 MHz, CDCl₃): δ 23.0 (C$_{arom,quat}$CH₂S), 24.3 and 25.9 (CH₂CH₂S), 46.3 (CH₂N), 52.3 (CH₃O), 103.1 (d, *J* = 24.2 Hz, CH$_{arom}$),

107.5 (d, J = 4.6 Hz, $C_{arom,quat}$), 109.6 (d, J = 9.2 Hz, CH_{arom}), 109.8 (d, J = 26.5 Hz, CH_{arom}), 126.0 (2 × CH_{arom}), 127.2 (d, J = 10.4 Hz, $C_{arom,quat}$), 129.6 ($C_{arom,quat}$), 130.3 (2 × CH_{arom}), 132.3, 136.4 and 142.6 (3 × $C_{arom,quat}$), 158.0 (d, J = 235.4 Hz, $C_{arom,quat}$), 166.7 (C=O). IR (ATR, cm^{-1}): $v_{C=O}$ = 1712; v_{max} = 1479, 1436, 1416, 1277, 1179, 1136, 1108, 1019, 848, 802, 765, 756. MS (70eV): m/z (%) 356 (M$^+$+1, 30). HRMS (ESI) Anal. Calcd. for $C_{20}H_{19}FNO_2S$ 356.1121 [M+H]$^+$, Found 356.1121.

N-(4-Methoxycarbonyl-2-methoxybenzyl)-6-fluoro-1,2,4,9-tetrahydro-3-thia-9-azafluorene 4d (78%)
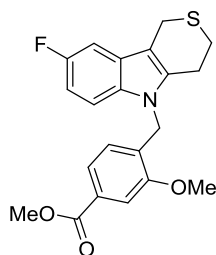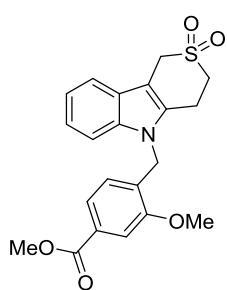
Yellow crystals. Recrystallization from EtOH. Mp = 139.0 °C. ^{1}H NMR (300 MHz, CDCl$_3$): δ 2.86 and 3.00 (2 × 2H, 2 × t, J = 5.7 Hz, CH_2CH_2S); 3.87 (2H, s, $C_{quat}CH_2S$); 3.89 and 3.98 (2 × 3H, 2 × s, 2 × CH_3O); 5.25 (2H, s, CH_2N); 6.31 (1H, d, J = 7.7 Hz, CH_{arom}); 6.86 (1H, t × d, J = 9.1, 2.8 Hz, CH_{arom}); 7.06 (1H, d × d, J = 9.1, 4.4 Hz, CH_{arom}); 7.16 (1H, d × d, J = 9.1, 2.8 Hz, CH_{arom}); 7.43 (1H, d × d, J = 7.7, 1.1 Hz, CH_{arom}); 7.56 (1H, d, J = 1.1 Hz, CH_{arom}). ^{19}F NMR (282 MHz, CDCl$_3$): δ (-124.68) – (-124.60) (m). ^{13}C NMR (75 MHz, CDCl$_3$): δ 23.1 ($C_{arom,quat}\underline{C}H_2S$), 24.1 and 25.9 ($CH_2CH_2S$), 41.8 ($CH_2N$), 52.3 and 55.7 (2 × CH_3O), 103.0 (d, J = 24.2 Hz, CH_{arom}), 107.2 (d, J = 4.6 Hz, $C_{arom,quat}$), 109.6 (d, J = 26.5 Hz, CH_{arom}), 109.7 (d, J = 10.4 Hz, CH_{arom}), 110.7, 122.4 and 126.2 (3 × CH_{arom}), 127.1 (d, J = 9.3 Hz, $C_{arom,quat}$), 130.5, 131.0, 132.3 and 136.6 (4 × $C_{arom,quat}$), 156.3 ($C_{arom,quat}$O), 158.0 (d, J = 235.4 Hz, $C_{arom,quat}$), 166.8 (C=O). IR (ATR, cm^{-1}): $v_{C=O}$ = 1714; v_{max} = 1584, 1480, 1464, 1435, 1411, 1292, 1266, 1231, 1102, 1032, 986, 800, 759. MS (70eV): m/z (%) 386 (M$^+$+1, 100). HRMS (ESI) Anal. Calcd. for $C_{21}H_{21}FNO_3S$ 386.1226 [M+H]$^+$, Found 386.1218.

N-(4-Methoxycarbonylbenzyl)-1,2,4,9-tetrahydro-3-thia-9-azafluorene-3,3-dioxide 7a (48%)
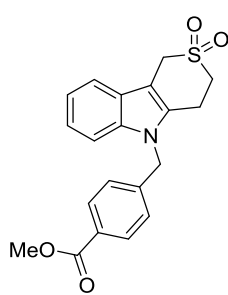
Light brown crystals. Purification by column chromatography (EtOAc/PE 1/2, Rf = 0.15). Mp = 163.1 °C. ^{1}H NMR (300 MHz, CDCl$_3$): δ 3.27 and 3.32 (2 × 2H, 2 × t, J = 4.7 Hz, CH_2CH_2S); 3.89 (3H, s, CH_3O); 4.44 (2H, s, $C_{quat}CH_2S$); 5.34 (2H, s, CH_2N); 7.04 (2H, d, J = 8.2 Hz, 2 × CH_{arom}); 7.15-7.24 and 7.43-7.46 (3H and 1H, 2 × m, 4 × CH_{arom}); 7.96 (2H, d, J = 8.2 Hz, 2 × CH_{arom}). ^{13}C NMR (75 MHz, CDCl$_3$): δ 22.3 ($\underline{C}H_2CH_2S$), 46.6 (CH_2N), 47.5 ($CH_2\underline{C}H_2S$), 49.0 ($C_{arom,quat}\underline{C}H_2S$), 52.3 ($CH_3O$), 102.6 ($C_{arom,quat}$), 109.6, 117.7, 120.6 and 123.1 (4 × CH_{arom}), 126.0 (2 × CH_{arom}), 126.5, 129.9 and 130.1 (3 × $C_{arom,quat}$), 130.5 (2 × CH_{arom}), 137.3 and 142.0 (2 × $C_{arom,quat}$), 166.6 (C=O). IR (ATR, cm^{-1}): $v_{C=O}$ = 1723; $v_{S=O}$ = 1162, 1111; v_{max} = 1461, 1311, 1276, 760, 750, 713. MS (70eV): m/z (%) 370 (M$^+$+1, 100). HRMS (ESI) Anal. Calcd. for $C_{20}H_{20}NO_4S$ 370.1113 [M+H]$^+$, Found 370.1118.

N-(4-Methoxycarbonyl-2-methoxybenzyl)-1,2,4,9-tetrahydro-3-thia-9-azafluorene-3,3-dioxide 7b (60%)

Light brown crystals. Recrystallization from EtOH. Mp = 208.2 °C. ^{1}H NMR (300 MHz, D_6-DMSO): δ 3.17 and 3.47 (2 × 2H, 2 × t, *J* = 5.9 Hz, CH_2CH_2S); 3.81 and 3.92 (2 × 3H, 2 × s, 2 × CH_3O); 4.50 (2H, s, $C_{quat}CH_2S$); 5.38 (2H, s, CH_2N); 6.46 (1H, d, *J* = 7.9 Hz, CH_{arom}); 7.02-7.12 (2H, m, 2 × CH_{arom}); 7.33 (1H, d, *J* = 7.7 Hz, CH_{arom}); 7.40 (1H, d × d, *J* = 7.9, 1.1 Hz, CH_{arom}); 7.49 (1H, d, *J* = 7.2 Hz, CH_{arom}); 7.52 (1H, d, *J* = 1.1 Hz, CH_{arom}). ^{13}C NMR (75 MHz, D_6-DMSO): δ 22.3 ($\underline{C}H_2CH_2S$), 42.1 (CH_2N), 46.9 ($CH_2\underline{C}H_2S$), 48.6 ($C_{quat}CH_2S$), 52.8 and 56.3 (2 × CH_3O), 102.8 ($C_{arom,quat}$), 110.4, 111.4, 118.3, 120.1, 122.2 and 122.5 (6 × CH_{arom}), 126.7 ($C_{arom,quat}$), 127.3 (CH_{arom}), 130.6, 131.6, 131.9 and 137.1 (4 × $C_{arom,quat}$), 157.0 ($C_{arom,quat}O$), 166.5 (C=O). IR (ATR, cm^{-1}): $v_{C=O}$ = 1719; $v_{S=O}$ = 1113, 1105; v_{max} = 1464, 1412, 1312, 1291, 1273, 1234, 1158, 1034, 990, 762, 739. MS (70eV): m/z (%) 400 (M$^+$+1, 100). HRMS (ESI) Anal. Calcd. for $C_{21}H_{22}NO_5S$ 400.1219 [M+H]$^+$, Found 400.1216.

N-(4-Methoxycarbonylbenzyl)-6-fluoro-1,2,4,9-tetrahydro-3-thia-9-azafluorene-3,3-dioxide 7c (47%)
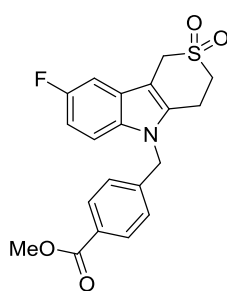
Light yellow crystals. Purification by column chromatography (EtOAc/PE 1/2, Rf = 0.13). Mp = 163.8 °C. ^{1}H NMR (300 MHz, CDCl$_3$): δ 3.27-3.33 (4H, m, CH_2CH_2S); 3.90 (3H, s, CH_3O); 4.38 (2H, s, $C_{quat}CH_2S$); 5.32 (2H, s, CH_2N); 6.96 (1H, t × d, *J* = 9.1, 2.8 Hz, CH_{arom}); 7.02 (2H, d, *J* = 8.8 Hz, 2 × CH_{arom}); 7.09 (1H, d × d, *J* = 9.1, 2.8 Hz, CH_{arom}); 7.12 (1H, d × d, *J* = 9.1, 4.4 Hz, CH_{arom}); 7.97 (2H, d, *J* = 8.8 Hz, 2 × CH_{arom}). ^{19}F NMR (282 MHz, CDCl$_3$): δ (-122.72) – (-122.64) (m). ^{13}C NMR (75 MHz, CDCl$_3$): δ 22.4 ($\underline{C}H_2CH_2S$), 46.8 (CH_2N), 47.3 ($CH_2\underline{C}H_2S$), 48.9 ($C_{arom,quat}\underline{C}H_2S$), 52.4 ($CH_3O$), 102.6 (d, *J* = 4.6 Hz, $C_{arom,quat}$), 103.1 (d, *J* = 24.2 Hz, CH_{arom}), 110.4 (d, *J* = 10.4 Hz, CH_{arom}), 111.4 (d, *J* = 26.5 Hz, CH_{arom}), 125.9 (2 × CH_{arom}), 126.8 (d, *J* = 10.4 Hz, $C_{arom,quat}$), 130.0 ($C_{arom,quat}$), 130.5 (2 × CH_{arom}), 131.8, 133.7 and 141.6 (3 × $C_{arom,quat}$), 158.3 (d, *J* = 237.7 Hz, $C_{arom,quat}$), 166.6 (C=O). IR (ATR, cm^{-1}): $v_{C=O}$ = 1704; $v_{S=O}$ = 1136, 1121; v_{max} = 1480, 1311, 1281, 1258, 1176, 1149, 788. MS (70eV): m/z (%) 386 (M$^-$-1, 100). HRMS (ESI) Anal. Calcd. for $C_{20}H_{19}FNO_4S$ 388.1019 [M+H]$^+$, Found 388.1014.

N-(4-Methoxycarbonyl-2-methoxybenzyl)-6-fluoro-1,2,4,9-tetrahydro-3-thia-9-azafluorene-3,3-dioxide 7d (40%)
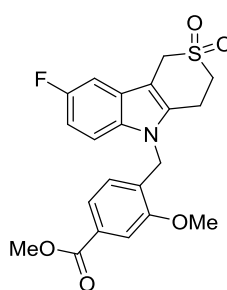

Light yellow crystals. Recrystallization from EtOH. Mp = 259.9 °C. ^{1}H NMR (300 MHz, D_6-DMSO): δ 3.17 and 3.47 (2 × 2H, 2 × t, *J* = 6.1 Hz, CH_2CH_2S); 3.81 and 3.91 (2 × 3H, 2 × s, 2 × CH_3O); 4.47 (2H, s, $C_{quat}CH_2S$); 5.39 (2H, s, CH_2N); 6.49 (1H, d, *J* = 7.7 Hz, CH_{arom}); 6.94 (1H, t × d, *J* = 9.1, 2.8 Hz, CH_{arom}); 7.30 (1H, d × d, *J* = 9.1, 2.8 Hz, CH_{arom}); 7.36 (1H, d × d, *J* = 9.1, 4.4 Hz, CH_{arom}); 7.41 (1H, d × d, *J* = 7.7, 1.6 Hz, CH_{arom}); 7.51 (1H, d, *J* = 1.6 Hz, CH_{arom}). ^{19}F NMR (282 MHz, D_6-DMSO): δ (-124.02) – (-123.94) (m). ^{13}C NMR (75 MHz, D_6-DMSO): δ 22.5 ($\underline{C}H_2CH_2S$), 42.5 (CH_2N), 46.7 ($CH_2\underline{C}H_2S$), 48.4 ($C_{quat}\underline{C}H_2S$), 52.8 and 56.3 (2 × CH_3O), 103.1 (d, *J* = 4.6 Hz, $C_{arom,quat}$), 103.5 (d, *J* = 23.1 Hz, CH_{arom}), 110.3 (d, *J* = 25.4 Hz, CH_{arom}), 111.4 (CH_{arom}), 111.7 (d, *J* = 9.2 Hz, CH_{arom}), 122.2 (CH_{arom}), 127.0 (d, *J* = 10.3 Hz, $C_{arom,quat}$), 127.4 (CH_{arom}), 130.7, 131.4, 133.8 and 133.9 (4 × $C_{arom,quat}$), 157.0 ($C_{arom,quat}O$), 157.8 (d, *J* = 233.1 Hz, $C_{arom,quat}$), 166.4 (C=O). IR (ATR, cm^{-1}): $v_{C=O}$ = 1716; $v_{S=O}$ = 1114, 1104; v_{max} = 1462, 1439, 1414, 1313, 1286, 1274, 1236, 1160, 1147, 1033, 988, 765.

MS (70eV): m/z (%) 418 (M$^+$+1, 100). HRMS (ESI) Anal. Calcd. for C$_{21}$H$_{21}$FNO$_5$S 418.1124 [M+H]$^+$, Found 418.1110.

### 2.4.2.4. Synthesis of hydroxamic acids 5 and 8

General procedure: To a solution of ester **4a** (0.6 mmol) and hydroxylamine hydrochloride (3.6 mmol) in DMF (5 mL) under nitrogen atmosphere was added NaOMe/MeOH (4M, 1.2 mL, 4.8 mmol). The reaction was stirred for 16 h at room temperature and a white precipitate was formed. The reaction mixture was diluted with ethyl acetate (20 mL) and washed with saturated NaHCO$_3$ (10 mL), brine (2 × 10mL), and dried with anhydrous MgSO$_4$. Filtration of the drying agent and removal of the solvent *in vacuo* afforded the crude hydroxamic acid **5a**, which was recrystallized from ethanol to afford pure *N*-(4-hydroxycarbamoylbenzyl)-1,2,4,9-tetrahydro-3-thia-9-azafluorene **5a** (0.23 mmol, 38%).

N-(4-Hydroxycarbamoylbenzyl)-1,2,4,9-tetrahydro-3-thia-9-azafluorene 5a (38%)
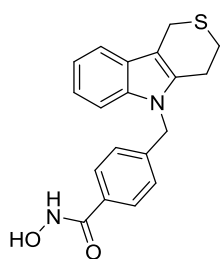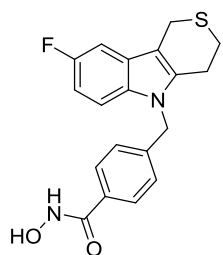

White powder. Crystallization from EtOH. Mp = 149.6 °C. ^{1}H NMR (300 MHz, D$_6$-DMSO): δ 2.87 and 2.98 (2 × 2H, 2 × t, *J* = 5.4 Hz, CH$_2$CH$_2$S); 3.83 (2H, s, C$_{quat}$CH$_2$S); 5.42 (2H, s, CH$_2$N); 6.99-7.10 and 7.39-7.41 (4H and 1H, 2 × m, 5 × CH$_{arom}$); 7.47 (1H, d × d, *J* = 6.9, 1.4 Hz, CH$_{arom}$); 7.65 (2H, d, *J* = 8.3 Hz, 2 × CH$_{arom}$); 9.02 (1H, s(br), OH); 11.14 (1H, s(br), NH). ^{13}C NMR (75 MHz, D$_6$-DMSO): δ 22.8 (C$_{arom,quat}$CH$_2$S), 24.1 and 25.7 (CH$_2$CH$_2$S), 45.7 (CH$_2$N), 107.0 (C$_{arom,quat}$), 110.0, 118.1, 119.5 and 121.7 (4 × CH$_{arom}$), 126.8 (2 × CH$_{arom}$), 126.9 (C$_{arom,quat}$), 127.8 (2 × CH$_{arom}$), 132.4, 135.5, 135.8 and 142.1 (4 × C$_{arom,quat}$), 164.5 (C=O). IR (ATR, cm^{-1}): $v_{NH/OH}$ = 3201; $v_{C=O}$ = 1636; v_{max} = 1612, 1464, 1414, 1356, 1311, 1014, 897, 740. MS (70eV): m/z (%) 339 (M$^+$+1, 100). HRMS (ESI) Anal. Calcd. for C$_{19}$H$_{19}$N$_2$O$_2$S 339.1167 [M+H]$^+$, Found 339.1164.

### *N*-(4-Hydroxycarbamoyl-2-methoxybenzyl)-1,2,4,9-tetrahydro-3-thia-9-azafluorene 5b (65%)
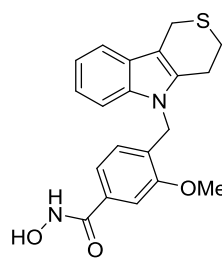
White powder. Crystallization from EtOH. Mp = 191.5 °C. ^{1}H NMR (300 MHz, D$_6$-DMSO): δ 2.82 and 2.96 (2 × 2H, 2 × t, *J* = 5.4 Hz, CH$_2$CH$_2$S); 3.84 (2H, s, C$_{quat}$CH$_2$S); 3.92 (3H, s, CH$_3$O); 5.30 (2H, s, CH$_2$N); 6.22 (1H, d, *J* = 7.7 Hz, CH$_{arom}$); 6.99-7.08 (2H, m, 2 × CH$_{arom}$); 7.15 (1H, d × d, *J* = 7.7, 1.1 Hz, CH$_{arom}$); 7.28-7.30 (1H, m, CH$_{arom}$); 7.39 (1H, d, *J* = 1.1 Hz, CH$_{arom}$); 7.46-7.49 (1H, m, CH$_{arom}$); 9.04 (1H, s(br), OH); 11.16 (1H, s(br), NH). ^{13}C NMR (75 MHz, D$_6$-DMSO): δ 22.9 (C$_{arom,quat}$CH$_2$S), 23.9 and 25.7 (CH$_2$CH$_2$S), 41.4 (CH$_2$N), 56.2 (CH$_3$O), 106.9 (C$_{arom,quat}$), 109.7, 109.9 and 118.1 (3 × CH$_{arom}$), 119.5 (2 × CH$_{arom}$), 121.6 and 126.5 (2 × CH$_{arom}$), 126.8, 129.5, 133.6, 135.7 and 135.8 (5 × C$_{arom,quat}$), 156.6 (C$_{arom,quat}$O), 164.3 (C=O). IR (ATR, cm^{-1}): $v_{NH/OH}$ = 3220; $v_{C=O}$ = 1619; v_{max} = 1574, 1462, 1408, 1362, 1240, 1042, 1026, 824, 744. MS (70eV): m/z (%) 369 (M$^+$+1, 100). HRMS (ESI) Anal. Calcd. for C$_{20}$H$_{21}$N$_2$O$_3$S 369.1273 [M+H]$^+$, Found 369.1280.

N-(4-Hydroxycarbamoylbenzyl)-6-fluoro-1,2,4,9-tetrahydro-3-thia-9-azafluorene 5c
(70%)

White powder. Crystallization from ethanol. Mp = 194.5 °C. ^{1}H NMR (300 MHz, D$_6$-DMSO): δ 2.86 and 2.97 (2 × 2H, 2 × t, *J* = 5.7 Hz, CH$_2$CH$_2$S); 3.80 (2H, s, C$_{quat}$CH$_2$S); 5.42 (2H, s, CH$_2$N); 6.91 (1H, t × d, *J* = 9.1, 2.8 Hz, CH$_{arom}$); 7.03 (2H, d, *J* = 8.3 Hz, 2 × CH$_{arom}$); 7.26 (1H, d × d, *J* = 9.1, 2.8 Hz, CH$_{arom}$); 7.41 (1H, d × d, *J* = 9.1, 4.4 Hz, CH$_{arom}$); 7.65 (2H, d, *J* = 8.3 Hz, 2 × CH$_{arom}$), 9.01 (1H, s(br), OH); 11.13 (1H, s(br), NH). ^{19}F NMR (282 MHz, D$_6$-DMSO): δ (-124.75) – (-124.66) (m). ^{13}C NMR (75 MHz, D$_6$-DMSO): δ 22.7 (C$_{arom,quat}$CH$_2$S), 24.3 and 25.6 (CH$_2$CH$_2$S), 45.9 (CH$_2$N), 103.3 (d, *J* = 23.1 Hz, CH$_{arom}$), 107.3 (d, *J* = 4.6 Hz, C$_{arom,quat}$), 109.4 (d, *J* = 26.5 Hz, CH$_{arom}$), 111.0 (d, *J* = 10.4 Hz, CH$_{arom}$), 126.8 (2 × CH$_{arom}$), 127.1 (d, *J* = 10.4 Hz, C$_{arom,quat}$), 127.8 (2 × CH$_{arom}$), 132.4, 132.5, 137.6 and 141.9 (4 × C$_{arom,quat}$), 157.6 (d, *J* = 230.7 Hz, C$_{arom,quat}$), 164.5 (C=O). IR (ATR, cm^{-1}): ν$_{NH/OH}$ = 3224; ν$_{C=O}$ = 1613; ν$_{max}$ = 1567, 1478, 1459, 1137, 1016, 849, 789. MS (70eV): m/z (%) 355 (M$^-$-1, 100). HRMS (ESI) Anal. Calcd. for C$_{19}$H$_{16}$FN$_2$O$_2$S 355.0922 [M-H]$^-$, Found 355.0924.

### *N*-(4-Hydroxycarbamoyl-2-methoxybenzyl)-6-fluoro-1,2,4,9-tetrahydro-3-thia-9-azafluorene 5d (66%)
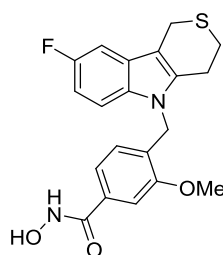
Light yellow powder. Crystallization from EtOH. Mp = 148.1 °C. ^{1}H NMR (300 MHz, D$_6$-DMSO): δ 2.82 and 2.96 (2 × 2H, 2 × t, *J* = 5.5 Hz, CH$_2$CH$_2$S); 3.80 (2H, s, C$_{quat}$CH$_2$S); 3.90 (3H, s, CH$_3$O); 5.30 (2H, s, CH$_2$N); 6.24 (1H, d, *J* = 7.7 Hz, CH$_{arom}$); 6.87 (1H, t × d, *J* = 9.1, 2.8 Hz, CH$_{arom}$); 7.15 (1H, d, *J* = 7.7 Hz, CH$_{arom}$); 7.26 (1H, d × d, *J* = 9.1, 2.8 Hz, CH$_{arom}$); 7.31 (1H, d × d, *J* = 9.1, 4.4 Hz, CH$_{arom}$); 7. 38 (1H, s, CH$_{arom}$); 9.03 (1H, s(br), OH); 11.15 (1H, s(br), NH). ^{19}F NMR (282 MHz, D$_6$-DMSO): δ (-124.81) – (-124.73) (m). ^{13}C NMR (75 MHz, D$_6$-DMSO): δ 22.7 (C$_{arom,quat}$CH$_2$S), 24.1 and 25.6 (CH$_2$CH$_2$S), 41.7 (CH$_2$N), 56.2 (CH$_3$O), 103.2 (d, *J* = 24.3 Hz, CH$_{arom}$), 107.2 (d, *J* = 4.7 Hz, C$_{arom,quat}$), 109.3 (d, *J* = 26.5 Hz, CH$_{arom}$), 109.7 (CH$_{arom}$), 111.0 (d, *J* = 10.4 Hz, CH$_{arom}$), 119.6 and 126.6 (2 × CH$_{arom}$), 127.0 (d, *J* = 10.3 Hz, C$_{arom,quat}$), 129.3, 132.5, 133.7 and 137.8 (4 × C$_{arom,quat}$), 156.7 (C$_{arom,quat}$O), 157.6 (d, *J* = 231.9 Hz, C$_{arom,quat}$), 164.3 (C=O). IR (ATR, cm^{-1}): ν$_{NH/OH}$ = 3209; ν$_{C=O}$ = 1636; ν$_{max}$ = 1576, 1479, 1462, 1409, 1249, 1142, 1034, 829. MS (70eV): m/z (%) 385 (M$^-$-1, 100). HRMS (ESI) Anal. Calcd. for C$_{20}$H$_{20}$FN$_2$O$_3$S 387.1179 [M+H]$^+$, Found 387.1180.

N-(4-Hydroxycarbamoylbenzyl)-1,2,4,9-tetrahydro-3-thia-9-azafluorene-3,3-dioxide 8a
(51%)
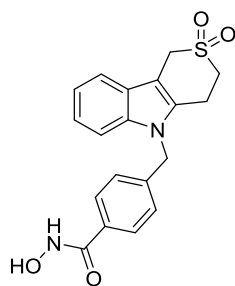
White powder. Crystallization from EtOH. Mp = 200.2 °C. ^{1}H NMR (300 MHz, D$_6$-DMSO): δ 3.21 and 3.50 (2 × 2H, 2 × t, *J* = 6.1 Hz, CH$_2$CH$_2$S); 4.49 (2H, s, C$_{quat}$CH$_2$S); 5.47 (2H, s, CH$_2$N); 7.04-7.16 (4H, m, 4 × CH$_{arom}$); 7.45 (1H, d, *J* = 8.3 Hz, CH$_{arom}$); 7.49 (1H, d, *J* = 7.7 Hz, CH$_{arom}$); 7.66 (2H, d, *J* = 8.2 Hz, 2 × CH$_{arom}$), 9.01 (1H, s(br), OH); 11.15 (1H, s(br), NH). ^{13}C NMR (75 MHz, D$_6$-DMSO): δ 22.5 (CH$_2$CH$_2$S), 46.1 (CH$_2$N), 46.8 (CH$_2$CH$_2$S), 48.6 (C$_{arom,quat}$CH$_2$S), 102.9 (C$_{arom,quat}$), 110.5, 118.3, 120.1 and 122.5 (4 × CH$_{arom}$), 126.7 (C$_{arom,quat}$), 126.9 and 127.9 (4 × CH$_{arom}$), 131.6, 132.5, 137.1 and 141.7 (4 × C$_{arom,quat}$), 164.5 (C=O). IR (ATR, cm^{-1}): ν$_{NH/OH}$ = 3192; ν$_{C=O}$ = 1613; ν$_{S=O}$ = 1126, 1114; ν$_{max}$ = 1467, 1413, 1310, 1284, 1192, 1166, 1016, 885, 741. MS (70eV): m/z (%) 371 (M$^+$+1, 100). HRMS (ESI) Anal. Calcd. for C$_{19}$H$_{19}$N$_2$O$_4$S 371.1066 [M+H]$^+$, Found 371.1062.

N-(4-Hydroxycarbamoyl-2-methoxybenzyl)-1,2,4,9-tetrahydro-3-thia-9-azafluorene-3,3-dioxide 8b (30%)
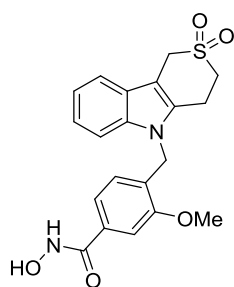
White powder. Crystallization from EtOH. Mp = 174.9 °C. ^{1}H NMR (300 MHz, D_6-DMSO): δ 3.20 and 3.48 (2 × 2H, 2 × t, J = 6.1 Hz, CH_2CH_2S); 3.89 (3H, s, CH_3O); 4.50 (2H, s, $C_{quat}CH_2S$); 5.34 (2H, s, CH_2N); 6.38 (1H, d, J = 7.7 Hz, CH_{arom}); 7.02-7.17 (3H, m, 3 × CH_{arom}); 7,34 (1H, d, J = 7.7 Hz, CH_{arom}); 7.39 (1H, d, J = 1.1 Hz, CH_{arom}); 7.49 (1H, d × d, J = 7.7, 1.1 Hz, CH_{arom}). ^{13}C NMR (75 MHz, D_6-DMSO): δ 22.3 ($\underline{C}H_2CH_2S$), 42.0 (CH_2N), 46.9 ($CH_2\underline{C}H_2S$), 48.6 ($C_{arom,quat}\underline{C}H_2S$), 56.2 ($CH_3O$), 102.7 ($C_{arom,quat}$), 109.8, 110.5, 118.3, 119.5, 120.0 and 122.4 (6 × CH_{arom}), 126.7 ($C_{arom,quat}$), 127.0 (CH_{arom}), 129.0, 131.9, 133.8 and 137.1 (4 × $C_{arom,quat}$), 156.8 ($C_{arom,quat}O$), 164.2 (C=O). IR (ATR, cm^{-1}): $v_{NH/OH}$ = 3186; $v_{C=O}$ = 1631; $v_{S=O}$ = 1126, 1113; v_{max} = 1572, 1463, 1416, 1366, 1330, 1292, 1247, 1163, 1036, 830, 743. MS (70eV): m/z (%) 401 (M$^+$+1, 100). HRMS (ESI) Anal. Calcd. for $C_{20}H_{21}N_2O_5S$ 401.1171 [M+H]$^+$, Found 401.1164.

N-(4-Hydroxycarbamoylbenzyl)-6-fluoro-1,2,4,9-tetrahydro-3-thia-9-azafluorene-3,3-dioxide 8c (69%)
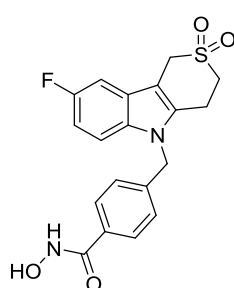
White powder. Crystallization from EtOH. Mp = 170.0 °C. ^{1}H NMR (300 MHz, D_6-DMSO): δ 3.19 and 3.49 (2 × 2H, 2 × t, J = 6.1 Hz, CH_2CH_2S); 4.46 (2H, s, $C_{quat}CH_2S$); 5.47 (2H, s, CH_2N); 6.97 (1H, t × d, J = 9.1, 2.8 Hz, CH_{arom}); 7.06 (2H, d, J = 8.3 Hz, 2 × CH_{arom}); 7.30 (1H, d × d, J = 9.6, 2.8 Hz, CH_{arom}); 7.46 (1H, d × d, J = 9.1, 4.4 Hz, CH_{arom}); 7.65 (2H, d, J = 8.3 Hz, 2 × CH_{arom}), 9.01 (1H, s(br), OH); 11.14 (1H, s(br), NH). ^{19}F NMR (282 MHz, D_6-DMSO): δ (-123.94) – (-123.85) (m). ^{13}C NMR (75 MHz, D_6-DMSO): δ 22.6 ($\underline{C}H_2CH_2S$), 46.3 (CH_2N), 46.7 ($CH_2\underline{C}H_2S$), 48.4 ($C_{arom,quat}\underline{C}H_2S$), 103.1 (d, J = 4.6 Hz, $C_{arom,quat}$), 103.5 (d, J = 24.2 Hz, CH_{arom}), 110.4 (d, J = 25.4 Hz, CH_{arom}), 111.6 (d, J = 9.3 Hz, CH_{arom}), 126.9 (2 × CH_{arom}), 127.0 (d, J = 12.7 Hz, $C_{arom,quat}$), 127.9 (2 × CH_{arom}), 132.5, 133.7, 133.8 and 141.5 (4 × $C_{arom,quat}$), 157.8 (d, J = 233.0 Hz, $C_{arom,quat}$), 164.4 (C=O). IR (ATR, cm^{-1}): $v_{NH/OH}$ = 3200; $v_{C=O}$ = 1619; $v_{S=O}$ = 1146, 1123; v_{max} = 1571, 1480, 1463, 1434, 1311, 1284, 1174, 1016, 896, 864, 786. MS (70eV): m/z (%) 387 (M$^-$-1, 100). HRMS (ESI) Anal. Calcd. for $C_{19}H_{16}FN_2O_4S$ 387.0820 [M-H]$^-$, Found 387.0824.

N-(4-Hydroxycarbamoyl-2-methoxybenzyl)-6-fluoro-1,2,4,9-tetrahydro-3-thia-9-azafluorene-3,3-dioxide 8d (72%)
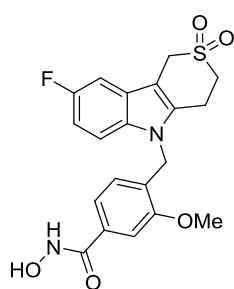
White powder. Crystallization from EtOH. Mp = 236.3 °C. ^{1}H NMR (300 MHz, D_6-DMSO): δ 3.20 and 3.49 (2 × 2H, 2 × t, J = 6.1 Hz, CH_2CH_2S); 3.88 (3H, s, CH_3O); 4.48 (2H, s, $C_{quat}CH_2S$); 5.35 (2H, s, CH_2N); 6.43 (1H, d, J = 8.3 Hz, CH_{arom}); 6.94 (1H, t × d, J = 9.1, 2.8 Hz, CH_{arom}); 7.17 (1H, d, J = 8.3 Hz, CH_{arom}) 7.31 (1H, d × d, J = 9.6, 2.8 Hz, CH_{arom}); 7.34-7.38 (2H, m, 2 × CH_{arom}); 9.04 (1H, s(br), OH); 11.17 (1H, s(br), NH). ^{19}F NMR (282 MHz, D_6-DMSO): δ (-124.07) – (-123.98) (m). ^{13}C NMR (75 MHz, D_6-DMSO): δ 22.5 ($\underline{C}H_2CH_2S$), 42.4 (CH_2N), 46.7 ($CH_2\underline{C}H_2S$), 48.4 ($C_{arom,quat}\underline{C}H_2S$), 56.2 ($CH_3O$), 102.9 (d, J = 3.5 Hz, $C_{arom,quat}$), 103.5 (d, J = 24.3 Hz, CH_{arom}), 109.9 (CH_{arom}), 110.3 (d, J = 25.4 Hz, CH_{arom}), 111.7 (d, J = 9.2 Hz, CH_{arom}), 119.5 (CH_{arom}), 127.0 (d, J = 12.7 Hz, $C_{arom,quat}$), 127.1 (CH_{arom}), 128.8, 133.8, 133.9 and 134.0 (4 × $C_{arom,quat}$), 156.8 ($C_{arom,quat}O$), 157.7 (d, J = 233.1 Hz, $C_{arom,quat}$), 164.2 (C=O). IR (ATR, cm^{-1}): $v_{NH/OH}$ = 3313; $v_{C=O}$ = 1662; $v_{S=O}$ = 1139, 1114; v_{max} = 1578, 1483, 1463, 1407, 1309, 1275,

1246, 1153, 1039, 883, 823, 782. MS (70eV): m/z (%) 417 (M$^-$-1, 100). HRMS (ESI) Anal. Calcd. for $C_{20}H_{18}FN_2O_5S$ 417.0926 [M-H]$^-$, Found 417.0928.

3. Synthesis and SAR assessment of novel Tubathian analogs in the pursuit of potent and selective HDAC6 inhibitors

Abstract: *The synthesis of novel isoform-selective HDAC inhibitors is considered to be an important, emerging field in medicinal chemistry. In this chapter, the preparation and assessment of thirteen selective HDAC6 inhibitors is disclosed, elaborating on the thiaheterocyclic Tubathian series discussed in chapter II. All compounds were evaluated in vitro for their ability to inhibit HDAC6, and a selection of five potent compounds was further screened toward all HDAC isoforms (HDAC1-11). The capability of these Tubathian analogs to inhibit α-tubulin deacetylation was assessed as well, and ADME/Tox data were collected. This thorough SAR evaluation revealed that the oxidized, para-substituted hydroxamic acids can be recognized as valuable lead structures in the pursuit of novel potent and selective HDAC6 inhibitors.*

3.1. Introduction

The interplay between histone acetyltransferases (HATs) and histone deacetylases (HDACs) represents an important epigenetic regulatory mechanism in the biochemistry of life processes.[16] This epigenetic interaction controls the structural transformation of DNA between a compact, inactivated form and a loosely bound, activated form, and thus plays a major role in the functioning of cells.[6] Besides the regulation of histone acetylation, HATs and HDACs mediate the acetylation of other proteins as well, and therefore these enzymes are more correctly referred to as lysine acetyltransferases (KATs) and deacetylases (KDACs).[17] The KDAC family can be divided into four classes (I, IIa/IIb, III and IV), existing of 18 proteins.[100] Selective inhibition of these isoforms could significantly contribute to our knowledge on this family of epigenetic erasers (enzymes known to catalyze the removal of epigenetic marks), and potentially lead to new drugs. One of these proteins, defined as HDAC6, emerged in recent years as a valuable target in drug design and belongs to the class IIb HDACs. Because of its cytoplasmic location, HDAC6 has many interaction partners other than histones, and this feature renders it an interesting protein to study the acetylation status of proteins in cells.[17] The use of small molecule inhibitors of HDAC6 has been proposed as an efficient strategy to block its catalytic activity, and is therefore considered to be a valuable new approach in neurodegenerative diseases,[101] cancer[79] and immunology research.[10,102]

A milestone achievement in the quest for selective HDAC6 inhibitors concerned the development of Tubastatin A (**1**) in 2010, a molecule with a good 'drug-likeness' profile that showed great promise *in vitro* and *in vivo*.[13,34,103] This discovery, together with the growing interest of academia and industry in the design of small molecule inhibitors, prompted us to pursue new analogs of this lead compound with possibly enhanced pharmacological properties. Based on available structure-activity relationships (SAR), sulfur analogs **2** of Tubastatin A (**1**) were constructed in the previous chapter, as shown in Figure 1, and tested for their ability to inhibit HDAC6 *in vitro*.[104] Within this thiaheterocyclic series, sulfone derivatives **2c** and **2d** - designated as Tubathians - exhibited the most pronounced activity and selectivity toward HDAC6.

The first major objective of the present study comprised a full and thorough biological evaluation of this Tubathian family **2** to shed more light on their potential as lead structures for HDAC6 inhibitor design. Furthermore, in view of the promising preliminary results of these Tubathian molecules, an expansion of compound library **2** to general structures **3** was envisioned as a second major objective to study structure-activity relationships in more detail. Guided by in-house docking studies and by the advancing progress made in the literature with regard to selective HDAC6 inhibitor development,[105] three main structural modifications of template molecules **2** were proposed. First, modification of the ring size of the non-aromatic

C-ring (a six-membered *versus* a five-membered thiaheterocyclic ring) was pursued. A second key modification of the core scaffold molecule comprised assessment of the oxidation state of the sulfur atom, implying the selective synthesis of sulfides, sulfoxides and sulfones. Recently, also *meta*-substituted benzohydroxamic acids have been studied and showed dual HDAC6/8 selectivity.[69] Hence, the third structural variation involved the synthesis and evaluation of the *meta*-substituted counterparts of the Tubathian core structure. Once in hand, this set of compounds **2** and **3** will then be subjected to an elaborate biological investigation of their medicinal relevance as potential efficient and selective HDAC6 inhibitors.

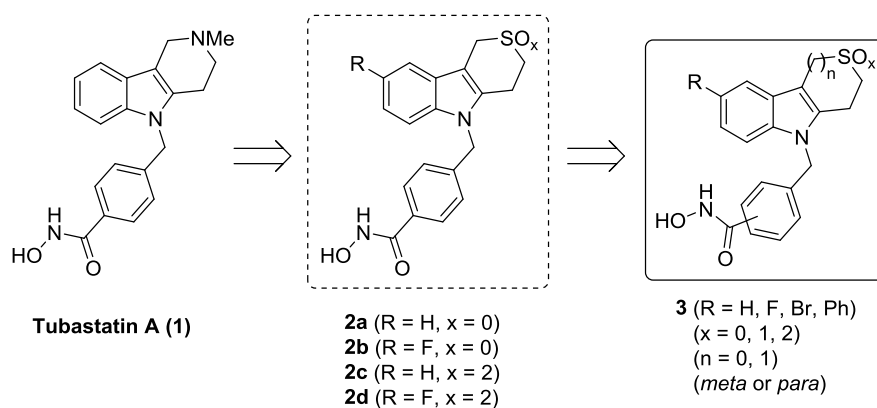**Tubastatin A (1)**

2a (R = H, x = 0)
2b (R = F, x = 0)
2c (R = H, x = 2)
2d (R = F, x = 2)

3 (R = H, F, Br, Ph)
(x = 0, 1, 2)
(n = 0, 1)
(*meta* or *para*)

Figure 1. Expanded SAR of sulfur analogs of Tubastatin A (**1**).

3.2. Synthesis and biological evaluation of Tubathian analogs

In silico docking studies of the proposed compounds **3** using a homology model of HDAC6 revealed that all theoretical structures fit the binding pocket quite well and thus represent compounds worth to be studied (Figure 2). In general, the sulfone derivatives proved to have slightly higher predicted binding energies (better binding) than the corresponding sulfides, due to additional interactions of the sulfone group with surrounding residues. The *para*-substituted compounds resulted in better binding energies than the *meta*-substituted ones, and phenyl substitution (R = Ph) on the aromatic ring seemed to be preferred because of π-stacking interactions with the side chain of a phenylalanine amino acid. However, it must be emphasized that the differences in calculated binding energies of these virtual complexes were small, pointing to the necessity of lab synthesis and detailed biological evaluation *in vitro*.
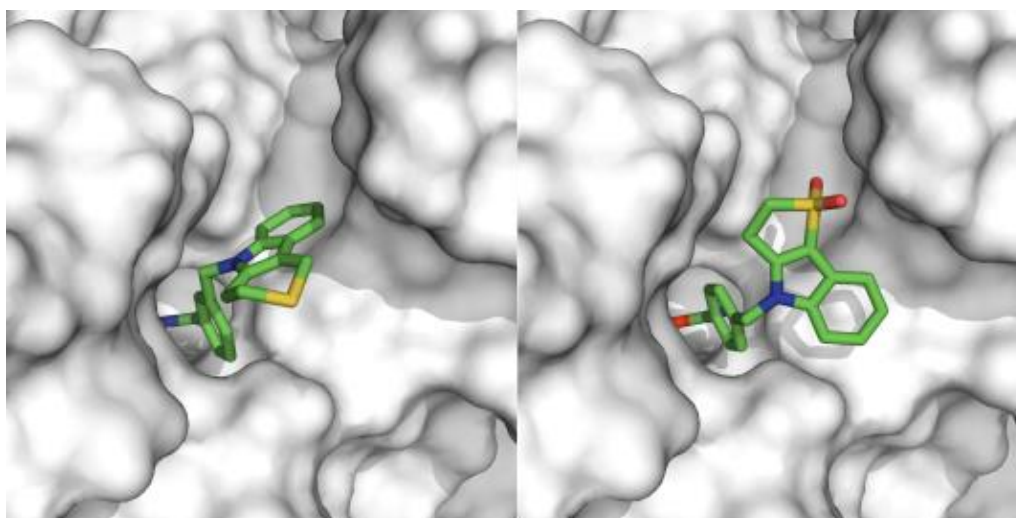

Figure 2. Docking of selected molecules from class **3** (left: **3a**; right: **3l**) in a homology model of HDAC6 (green: carbon, blue: nitrogen, red: oxygen, yellow: sulfur).

The synthesis of compounds **2** has been reported in the previous chapter, and the same approach was used here for the preparation of molecules **3** (Scheme 1, Figure 3).[104] First, the tricyclic indole-containing 'cap'-group was synthesized via a bismuth-nitrate catalyzed Fisher-indole synthesis between aromatic hydrazines **4** and sulfur-containing cyclic ketones **5**.[92] The obtained tricycles **6** were modified through selective oxidation of the sulfur atom employing meta-chloroperbenzoic acid, with or without the addition of boron trifluoride, leading to the corresponding sulfoxides **7** and sulfones **8**, respectively.

7-Bromo-2,3-dihydrothieno[3,2-*b*]indole **6f** (R = Br, n = 0) appeared hard to purify because it contained the corresponding sulfoxide as a side product, which could not be removed by means of column chromatography. Therefore, this compound was used as an intermediate toward direct sulfoxidation, resulting in the synthesis of sulfoxide **7c** (R = Br, n = 0). Phenyl-containing sulfone **8f** (R = Ph, n = 1) was obtained through full oxidation of sulfide **6c** (R = Br, n = 1) to sulfone **8c** (R = Br, n = 1), followed by a Suzuki-Miyaura cross coupling. The obtained thiaheterocycles **6**, **7** and **8** were *N*-deprotonated with sodium hydride and the resulting anion subsequently quenched with methyl 4-(bromomethyl)benzoate or methyl 3-(bromomethyl)benzoate **9** to give methyl esters **10**. In the final step, esters **10** were converted to hydroxamic acids **3** upon treatment with a large excess of hydroxyl amine, which were subsequently used for pharmacological evaluation.
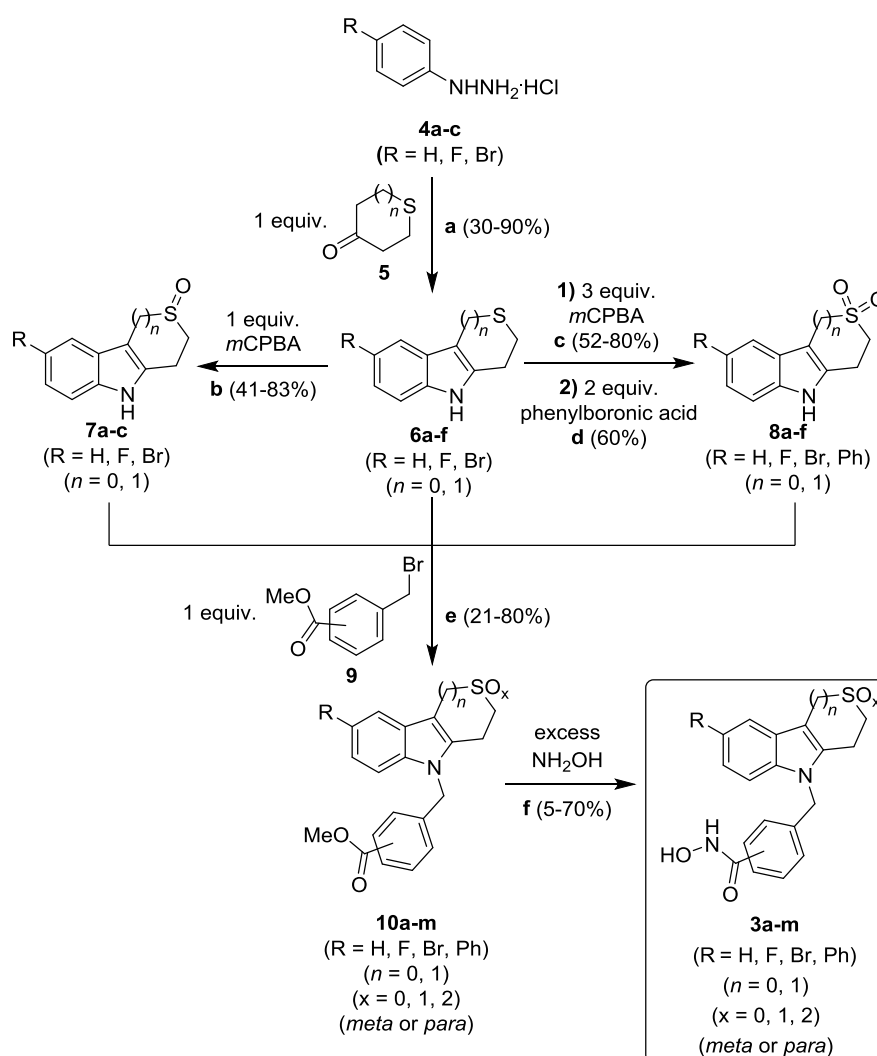
Scheme 1. Synthesis of the expanded Tubathian library **3**. Conditions: **a:** 1 equiv. ketone **5**, 0.2 equiv. Bi(NO$_3$)$_3$·5H$_2$O, MeOH, Δ, 3.5 h (30-90%, **6a-f**). **b:** 1 equiv. *m*CPBA ($\leq$77%), 4 equiv. BF$_3$·O(C$_2$H$_5$)$_2$, THF, -20°C, N$_2$, 2 h (41-83%, **7a-c**). **c:** 3 equiv. *m*CPBA ($\leq$77%), THF, 0°C to rt, 2 h (52-80%, **8a-e**). **d:** 2 equiv. phenylboronic acid, Na$_2$CO$_3$ (7 equiv), 0.04 equiv. Pd(PPh$_3$)$_4$, toluene/ethanol/H$_2$O (2/1/1), Δ, N$_2$, 8 h (60%, **8f**). **e:** 1) 1 equiv. NaH, DMF, rt, N$_2$, 0.5 h 2) 1 equiv. methyl (bromomethyl)benzoate **9**, 0.01 equiv. KI, DMF, 80°C, N$_2$, 2 h (21-80%, **10a-m**). **f:** 100 equiv. NH$_2$OH (50% in H$_2$O), 50 equiv. KOH (4M in MeOH), THF, rt or Δ, 10 min (5-70%, **3a-m**).

As can be seen from Figure 3, no five-membered cyclic thioether-containing hydroxamic acids (with n = 0 and x = 0) were obtained, which was due to the fact that reaction of compound **6d** (R = H, n = 0) with sodium hydride and methyl 3-(bromomethyl)benzoate or methyl 4-(bromomethyl)benzoate always resulted in complex reaction mixtures. To circumvent this problem, an alternative approach toward the synthesis of these molecules was attempted, in which the synthesis of the 'cap'-group was postponed to a later stage in the reaction pathway, however without any success.[106] In total, a set of thirteen novel hydroxamic acids **3a-m** was prepared and, together with the four earlier discovered Tubathian HDAC6 inhibitors **2a-d**, evaluated for their ability to selectively inhibit HDAC6.
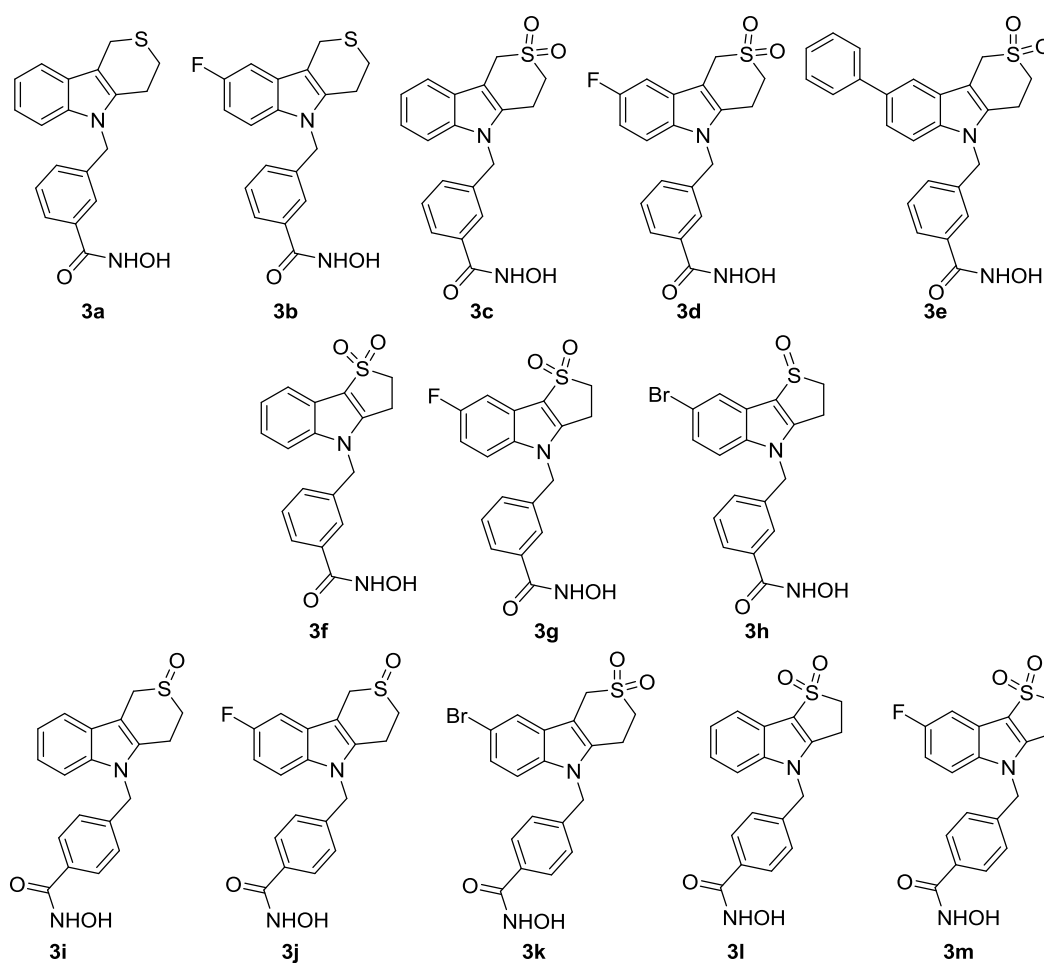

Figure 3. Overview of the newly synthesized hydroxamic acids **3**.

A preliminary *in vitro* screening of their inhibitory potential toward HDAC6 at a concentration of 10 μM learned that the *meta*-substituted compounds **3a-h** inhibited HDAC6 to a lesser extent than the *para*-substituted compounds **2a-d** and **3i-m** (34-74% vs 99-100% inhibition, respectively, Table 1). It must be noted that within the *meta*-substituted series, phenyl-decorated compound **3e** showed the highest inhibition percentage (74%), as predicted by the docking studies. Subsequently, the IC_{50} values of the five new *para*-substituted compounds **3i-**

m were determined and compared with the previously obtained results for compounds **2a-d** (Table 2).[104] All molecules exhibited low nanomolar IC_{50} values toward HDAC6 (≤ 22 nM), and the 6-membered sulfones **2c, 2d** and **3k** displayed the highest HDAC6 inhibitory activity (1.9, 3.7 and 3.4 nM, respectively). As noted in our previous communication,[104] this could be explained (and confirmed *in silico*) through hydrogen bond formation of both oxygen atoms on the sulfone moiety with surrounding residues.

Table 1. % inhibition of control values with regard to HDAC6 inhibitory activity[a,b]

Compound	% inhibition HDAC6	Compound	% inhibition HDAC6	Compound	% inhibition HDAC6
3a	34	**3b**	53	**3c**	65
3d	65	**3e**	74	**3f**	51
3g	40	**3h**	54	**3i**	99
3j	100	**3k**	100	**3l**	99
3m	100	**2a**	99	**2b**	99
2c	99	**2d**	99		

[a] Test concentration: 10 µM; [b] Mean value of two screening sessions

Table 2. *In vitro* enzyme inhibition data: IC_{50} values toward HDAC6

Compound	2a	2b	2c	2d	3i	3j	3k	3l	3m
HDAC6 IC_{50} (nM)	15	22	1.9	3.7	14	9.4	3.4	8.2	16

The selectivity toward HDAC6 was assessed on the enzymatic level through a full-panel HDAC1-11 screening of representative compounds **2b**, **2c**, **2d**, **3j** and **3l**. Compounds **2b**, **2d** and **3j** were selected to compare the influence of the oxidation state of sulfur (R_2S, R_2SO and R_2SO_2) on the selectivity. The influence of the ring size (thiolane vs. thiane) on the inhibitory selectivity was studied by selection of hydroxamic acids **2c** and **3l**. The data in Table 3 reveal that all screened compounds display a similar selectivity profile. These molecular entities inhibit HDAC1, 2, 3, 10 and 11 at IC_{50} values higher than 5 µM, except for the five-membered sulfone **3j**, which also shows a reasonable affinity for HDAC11 (IC_{50} = 0.52 µM). All compounds inhibit HDAC4, 5 and 8 with IC_{50} values around 1 µM, and HDAC7 and 9 at IC_{50} values between 0.1 and 1 µM. In all cases, the lowest values can be observed with respect to HDAC6 inhibition, with IC_{50} values <30 nM. After this in-depth selectivity screening, it can be stated that this set of Tubathian and related compounds selectively inhibit HDAC6 in a potent and pronounced way, but also display some moderate affinity for class IIa HDACs (HDAC4, 5, 7 and 9) and HDAC8.

Table 3. HDAC1-11 screening of selected compounds **2b**, **2c**, **2d**, **3j** and **3l** (IC$_{50}$ values in µM)[a,b]

HDAC	1	2	3	4	5	6	7	8	9	10	11
2b	21	NC	23	1.5	1.8	**0.0220**	0.2	2.8	0.8	21	9.7
2c	11	26	29	1.6	0.5	**0.0019**	0.1	1.7	0.3	7.7	NC
2d	12	29	26	1.9	0.5	**0.0037**	0.1	0.9	0.5	5.9	NC
3j	9.4	>30	24	1.2	1.3	**0.0094**	0.2	2.4	0.5	6.4	0.5
3l	12	>30	NC	0.6	0.4	**0.0082**	0.1	1.9	0.2	13	17
Tub A	16.4	>30	>30	>30	>30	**0.015**	>30	0.85	>30	>30	>30

[a] Reference compound: Trichostatin A (HDAC6 IC$_{50}$ = 0.0093 µM), NC : IC$_{50}$ value not calculable. Concentration-response curve shows less than 25% effect at the highest validated testing concentration (30 µM). >30: IC$_{50}$ value above the highest test concentration. Concentration-response curve shows less than 50 % effect at the highest validated testing concentration (30 µM).
[b] Literature values for Tub A (Tubastatin A)[13], caution should be taken when comparing the IC$_{50}$ values of **2b**, **2c**, **2d**, **3j** and **3l** to the literature values for Tubastatin A.

Next, the potency and selectivity of compounds **2a-d**, **3i-m** together with control substance Tubastatin A was evaluated on a cellular level (Neuro-2a cells) by determining their ability to modify the acetylation level of α-tubulin (a specific HDAC6 substrate) and histones via Western Blots. First, all the compounds were tested at 1 µM for both assays. From Figure 4 it can be seen that the HDAC6 inhibitors clearly hyperacetylate α-tubulin at this concentration and do not affect the acetylation status of histones. Second, Tubathians **2a-d** and control molecule Tubastatin A were tested at a range of concentrations (Figure 5, 10, 50, 100, 500 and 1000 nM), revealing that these compounds already presented a maximal acetyl α-tubulin/α-tubulin ratio at a concentration of 100 nM. Finally, also the newly synthesized Tubathian analogs **3i-m** were tested at a lower concentration of 10 nM, pointing to the conclusion that compound **3k** (together with control substance Tubastatin A) demonstrated an even more pronounced activity than the other compounds (Figure 6).
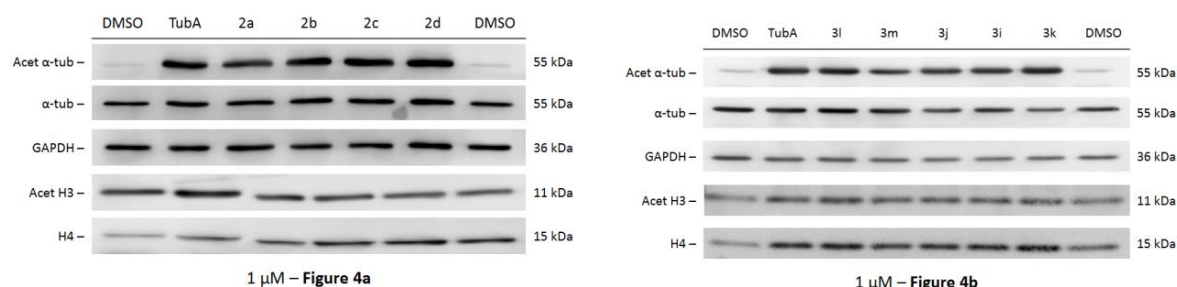

Figure 4a,b. Comparison of α-tubulin and histone hyperacetylation of compounds **2a-d**, **3i-m** and control substance Tubastatin A (TubA, Neuro-2a cells, 1 µM). Acet α-tub (acetyl α-tubuline), GAPDH (Glyceraldehyde 3-phosphate dehydrogenase, loading control), Acet H3 (acetyl histone 3), H4 (histone 4).
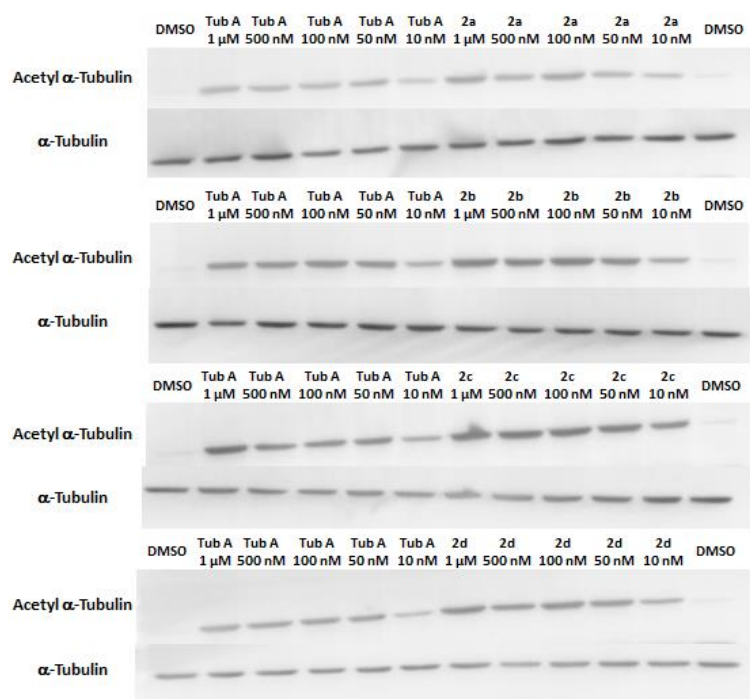
Figure 5. Dose-response Western Blot of the acetalation status of α-tubulin in Neuro-2a-cells for compounds **2a-d** and control substance Tubastatin A (10 - 1000 nM).
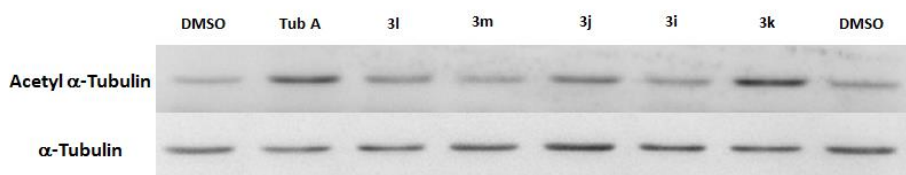

Figure 6. Acetyl α-tubulin Western Blot screening at 10 nM for compounds **3i-k** and control Tubastatin A.

With a strong HDAC inhibition profile for this Tubathian family in hand, the following step involved acquirement of *in vitro* 'ADME' (Absorption, Distribution, Metabolism, and Excretion) and 'Tox' (toxicity) data to know whether further optimization of these compounds in the framework of drug development is appropriate. Therefore, molecules **2a-d** as representative Tubathian 'mother structures' were preliminary screened for their capability to inhibit cytochrome P450 (CYP1A2, CYP2C9, CYP2C19, CYP2D6 and CYP3A4 were evaluated because of their ability to metabolize drugs in the liver, CYP inhibition can cause unanticipated adverse reactions or therapeutic failures), hERG safety (to exclude potential cardiotoxicity, as inhibition of the hERG might result in fatal ventricular tachyarrhythmia), microsomal stability in mouse and human (to measure *in vitro* intrinsic clearance), and plasma protein binding in mouse and human (PPB, the less bound a compound is to proteins in blood plasma, the more efficiently it can diffuse or traverse cell membranes) (Table 4). Apparently, whereas sulfides

2a and **2b** were shown to inhibit the cytochrome P450 enzymes at low micromolar concentrations, which is harmful for possible drug-drug interactions *in vivo*, the sulfones **2c** and **2d** scored much better in this regard. The same can be stated for the hERG safety, showing sulfides **2a** and **2b** to be inferior as compared to sulfones **2c** and **2d**. In the microsomal stability assay and the plasma protein binding assay, sulfides **2a** and **2b** seemed difficult to detect, this in contrast to sulfones **2c** and **2d** which showed acceptable values in both assays. In summary, sulfones **2c** and **2d** clearly demonstrated a much better preliminary ADME/Tox profile than sulfides **2a** and **2b** and might thus be considered as potential lead compounds for further elaboration in future research.

Table 4. Preliminary ADME/Tox screening of representative compounds **2a-d**

compound	CYP1A2 (IC_{50} µM)	CYP2C9 (IC_{50} µM)	CYP2C19 (IC_{50} µM)	CYP2D6 (IC_{50} µM)	CYP3A4 (IC_{50} µM)	hERG (IC_{50} µM)
2a	>50	4.7	1.3	9.6	2.1	9.1
2b	>50	3.7	1.3	9.5	1.8	5.1
2c	>50	>50	19.9	>50	15	>11
2d	>50	11.8	>50	>50	9.7	>11
compound	Mouse MS (µl/min/mg)	Mouse MS $t_{1/2}$ (min)	Human MS (µl/min/mg)	Human MS $t_{1/2}$ (min)	Mouse PPB (%)	Human PPB (%)
2a	<LOQ	<LOQ	<LOQ	<LOQ	<LOQ	<LOQ
2b	58.3	11.9	28.7	24.1	<LOQ	<LOQ
2c	16.2	42.7	26.5	26.1	69.8	62.7
2d	22.6	30.6	47.0	14.7	58.3	52.5

<LOQ: peak areas below limit of quantification, CYP (cytochrome P450), hERG (human ether-a-go-go-related gene channel), MS (microsomal stability), $t_{1/2}$ (half-life) PPB (plasma protein binding)

Additional, a preliminary ADME/Tox screening of compounds **3i-m** concerning cytochrome P450 inhibition and microsomal stability was conducted (Table 5). From the cytochrome P450 inhibition data, it can be concluded that compounds **3j**, **3l** and **3m** display the best profile, with compound **3m** showing no P450 inhibition at all. The microsomal stability assays reveal that six-membered sulfoxides **3i** and **3j**, and five-membered sulfones **3l** and **3m** have an improved stability over six-membered sulfones **2c**, **2d** and **3k**. In summary, further investigation of six-membered sulfoxide **3j** and five-membered sulfones **3l** and **3m** seems appropriate from an ADME/Tox point of view.

Table 5. Preliminary ADME/Tox screening of representative compounds **3i-m**

compound	CYP1A2 (IC$_{50}$ µM)	CYP2C9 (IC$_{50}$ µM)	CYP2C19 (IC$_{50}$ µM)	CYP2D6 (IC$_{50}$ µM)	CYP3A4 (IC$_{50}$ µM)
3i	>50	36.9	15.4	39.8	8.5
3j	>50	>50	>50	>50	28.8
3k	>50	14.9	30.3	14.1	8.2
3l	>50	>50	16.3	>50	>50
3m	>50	>50	>50	>50	>50

compound	Mouse MS (µl/min/mg)	Mouse MS t$_{1/2}$ (min)	Human MS (µl/min/mg)	Human MS t$_{1/2}$ (min)
3i	<2.1	>328	<2.3	>313
3j	8.8	79.1	<2.1	>340
3k	8.2	53.2	13.0	7.6
3l	7.8	89.0	<2.1	>335
3m	10.1	68.9	2.8	247.5

In a final assay, the genotoxicity of six-membered sulfone **2c** and five-membered sulfone **3l** as representative examples was evaluated, bearing in mind the known potential mutagenicity associated with hydroxamic acids.[107,108] The Ames fluctuation test toward four strains of *Salmonella typhimurium* (TA98, TA100, TA1535 and TA1537), with and without metabolic activation by using rat liver S9 fraction, revealed that both compounds were only mutagenic toward strain TA1537, with and without S9, starting at a concentration of 50 µM (more information in the experimental details). No mutagenicity was detected toward the other strains.

3.3. Conclusions

Thirteen novel Tubathian analogs were synthesized and, together with four previously developed analogs, evaluated in depth as HDAC6 inhibitors. The nine *para*-substituted compounds showed the best HDAC6 IC_{50} values and proved to be selective inhibitors in cells. A detailed study of five selected representatives revealed that these Tubathian analogs preferentially inhibit HDAC6, although also a moderate affinity for class IIa HDACs (especially HDAC7 and 9) should be recognized. ADME/Tox evaluation demonstrated that sulfones **2c** and **2d** display a better preliminary ADME/Tox profile than the corresponding sulfides **2a** and **2b** and pointed to six-membered sulfoxide **3j** and five-membered sulfones **3l** and **3m** as promising chemical entities. Therefore, further research should be focused on the oxidized analogs as valuable lead structures in the pursuit of novel selective HDAC6 inhibitors.

3.4. Experimental details

3.4.1. Ligand docking

All docking experiments were performed by the Centre for Industrial Biotechnology and Biocatalysis (Prof. Desmet). All manipulations were completed with the molecular modelling program YASARA and the YASARA/WHATIF twinset,[93,94] and the figure was created with PyMol v1.3.[97] The HDAC6 sequence was obtained from the UniProt database (http://www.uniprot.org, UniProt entry Q9UBN7). To increase the accuracy of the model, the sequence was limited to the major functional domain of HDAC6 (Gly482-Gly800). Possible templates were identified by running 3 PSI-BLAST iterations to extract a position specific scoring matrix (PSSM) from UniRef90, and then searching the PDB for a match. To aid the alignment of the HDAC6 sequence and templates, and the modelling of the loops, a secondary structure prediction was performed, followed by multiple sequence alignments. All side chains were ionised or kept neutral according to their predicted pKa values. Initial models were created from different templates (pdb entry 2VQW, 2VQQ and 3C10), each with several alignment variations and up to hundred conformations tried per loop. After the side-chains had been built, optimised and fine-tuned, all newly modelled parts were subjected to a combined steepest descent and simulated annealing minimisation, i.e. the backbone atoms of aligned residues were kept fixed to preserve the folding, followed by a full unrestrained simulated annealing minimisation for the entire model. The final model was obtained as a hybrid model of the best parts of the initial models, and checked once more for anomalies like incorrect configurations or colliding side chains. Furthermore, it was structurally aligned with known HDAC crystal structures to check if the chelating residues and the zinc atom were arranged correctly.

The HDAC inhibitor structures were created with YASARA Structure and energy minimised with the AMBER03 force field.[95] The grid box used for docking had a dimension of 25 x 25 x 25 angstrom, and comprised the entire catalytic cavity including the zinc ion and the outer surface of the active site entrance. Docking was performed with AutoDock VINA[109] and default parameters. Ligands were allowed to freely rotate during docking. The first conformer from the cluster that has its zinc binding group in the vicinity of the zinc ion, was selected as the binding mode for analysis.

3.4.2. Enzyme inhibition assays

The enzyme inhibition assays were performed by Eurofins Cerep Panlabs. *In vitro* IC_{50} values were determined by using human recombinant HDAC1-11 and fluorogenic HDAC substrate.[98]

3.4.3. ADME/Tox assays

The ADME/Tox Assays were performed by Karus Theraputic Ltd.

3.4.4. Western Blots

The Western Blots were performed by the Laboratory of Neurobiology and Vesalius Research Center, VIB (Prof. Van Den Bosch). Values represent the normalized ratio acetyl α-tubulin/ α-tubulin and acetyl histone 3/histone 4 against Tubastatin A (Tub A) in an established neuronal cell line (Neuro-2a cells: ATCC N° CCL-131).

3.4.4.1. Cell culture

Mouse neuroblastoma (Neuro-2a) cells were grown in a 1:1 mix of D-MEM (Dulbecco's Modified Eagle Medium) and F12 medium supplemented with glutamax (Life Technologies), 100 μg per ml streptomycin, 100 U per ml penicillin (Life Technologies), 10% fetal calf serum (Greiner Bio-one), 1% non-essential amino acids (Life Technologies) and 1.6% $NaHCO_3$ (Life Technologies) at 37 °C and 7.5% CO_2. To split the cells, cells were washed with Versene (Life Technologies) and dissociated with 0.05% Trypsine-EDTA (Life Technologies). The Neuro-2a cells were treated overnight at 37 °C with dosages ranging from 10 nM up to 1 μM of either Tubastatin A (Asclepia, Destelbergen, Belgium) or the candidate HDAC6 inhibitors, and the effect on the acetylation level of α-tubulin is determined by using Western Blot.

3.4.4.2. Western Blot

For sodium dodecyl sulfate-polyacrylamide gel electrophoresis (SDS-PAGE) analysis, treated cells were collected using the EpiQuik Total Histone Extraction Kit (EpiGentek) according to manufacturer's instructions. Protein concentrations were determined using microBCA kit (Thermo Fisher Scientific Inc., Pittsburgh, PA, USA) according to manufacturer's instructions. Before resolving the samples on a 12% SDS-PAGE gel, samples containing equal amounts of protein were supplemented with reducing sample buffer (Thermo Scientific) and boiled at 95 °C for 5 min. After electrophoresis, the proteins were transferred to a polyvinylidene difluoride (PVDF) membrane (Millipore Corp.). The non-specific binding was blocked by incubation of the membrane in 5% bovine serum albumin (BSA), diluted in Tris Buffered Saline Tween (TBST, 50 mM TRIS, 150 mM NaCl, 0.1% Tween-20 (Applichem, Darmstadt, Germany) overnight followed by incubation with primary antibodies during one hour. The antibodies, diluted in TBS-T, were directed against α-tubulin (Sigma-Aldrich, T6199, 1/5000, 1h), against acetylated α-tubulin (Sigma-Aldrich, T6793, 1/5000, 1h), against glyceraldehyde 3-phosphate

dehydrogenase (GAPDH, Life Technologies, AM4300, 1/5000, 1h), against histone H3 acetyl k9-k14 (Cell Signaling, 9677L, 1/500, 1h) and against histone 4 (Abcam, ab10158, 1/500, 1h). The secondary antibodies, coupled to alkaline phosphatase (anti-mouse or anti-rabbit, Sigma-Aldrich, 1/5000, 1h) were used. Blots were visualized by adding the ECF substrate (Enhanced Chemical Fluorescence, GE Healthcare, Uppsala, Sweden) and imaged with the ImageQuant_LAS 4000. A mild reblotting buffer (Millipore) was applied to strip the blots. ImageQuant TL version 7.0-software was used to quantify the blots.

3.4.5. Ames fluctuation assays

The Ames fluctuation assays were performed by Eurofins Cerep Panlabs. Wells that displayed bacteria growth due to the reversion of the histidine mutation (as judged by the ratio of OD430/OD570 being greater than 1.0) are counted and recorded as positive counts. The significance of the positive counts between the treatment (in the presence of test compound) and the control (in the absence of test compound) are calculated using the one-tailed Fisher's exact test.

3.4.6. Synthetic procedures and spectral data

^{1}H NMR, ^{13}C NMR and ^{19}F NMR spectra were recorded at 400, 100.6 or 376.5 MHz (Bruker Avance III) with $CDCl_3$ or D_6-DMSO as the solvent and tetramethylsilane as the internal standard. Mass spectra were obtained with a mass spectrometer Agilent 1100, 70 eV. IR spectra were measured with a Spectrum One FT-IR spectrophotometer. High resolution electron spray (ES) mass spectra were obtained with an Agilent Technologies 6210 series time-of-flight instrument. Melting points of crystalline compounds were measured with a Kofler Bench, type WME Heizbank of Wagner & Munz. The purity of all tested compounds was assessed by ^{1}H NMR analysis and/or HPLC analysis, confirming a purity of ≥95%.

3.4.6.1. Synthesis of sulfides 6a-f

General procedure: To a solution of phenyl hydrazine hydrochloride **4a** (12 mmol) and 4,5-dihydro-3(2*H*)-thiophenone **5b** (12 mmol) in methanol (50 mL), was added Bi(NO$_3$)$_3$·5H$_2$O (2.4 mmol). After being stirred for 3.5 h under reflux, the reaction mixture was poured into water (100 mL), and bismuth nitrate was removed through filtration over celite. The crude product was extracted with ethyl acetate (100 mL), washed with saturated NaHCO$_3$ (100 mL), brine (100 mL) and dried over anhydrous MgSO$_4$. Filtration of the drying agent and removal of the solvent *in vacuo* afforded the crude cyclic thioether **6d**, which was purified by means of column chromatography (EtOAc/PE 1/5) to provide pure 2,3-dihydrothieno[3,2-*b*]indole **6d** (3.7 mmol,

31%). The synthesis of 1,2,4,9-tetrahydro-3-thia-9-azafluorene **6a** and 6-fluoro-1,2,4,9-tetrahydro-3-thia-9-azafluorene **6b** has already been described in the previous chapter. The reaction time for the synthesis of 6-bromo-1,2,4,9-tetrahydro-3-thia-9-azafluorene **6c** was prolonged to 22 h. 7-Bromo-2,3-dihydrothieno[3,2-*b*]indole **6f** was not easily purified because it contained the corresponding sulfoxide as a side product and was therefore used as an intermediate for further transformation.

6-Bromo-1,2,4,9-tetrahydro-3-thia-9-azafluorene 6c (43%)
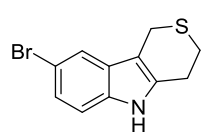
Yellow crystals. Recrystallization from EtOH. Mp = 169.5 °C. ^{1}H NMR (400 MHz, CDCl$_3$): δ 3.00-3.02 (2 × 2H, m, CH$_2$CH$_2$S); 3.80 (2H, s, C$_{quat}$CH$_2$S); 7.16 (1H, d, J = 8.5 Hz, CH$_{arom}$); 7.23 (1H, d × d, J = 8.5, 1.9 Hz, CH$_{arom}$); 7.57 (1H, d, J = 1.9 Hz, CH$_{arom}$); 7.83 (1H, s(br), NH). ^{13}C NMR (100,6 MHz, CDCl$_3$): δ 22.5 (C$_{quat}$CH$_2$S), 25.2 and 25.6 (CH$_2$CH$_2$S), 106.7 (C$_{quat,arom}$), 111.9 (CH$_{arom}$), 112.8 (C$_{quat,arom}$), 120.3 and 124.4 (2 × CH$_{arom}$), 128.7, 133.1 and 134.6 (3 × C$_{quat,arom}$). IR (ATR, cm^{-1}): ν$_{NH}$ = 3396; ν$_{max}$ = 1578, 1464, 1442, 1419, 1325, 1221, 1215, 1173, 1145, 1047, 983, 872, 795, 746, 652. MS (70 eV): m/z (%) 268/70 (M$^+$+1, 58). HRMS (ESI) Anal. Calcd. for C$_{11}$H$_{11}$BrNS 267.9770 [M+H]$^+$, Found 267.9735.

2,3-Dihydrothieno[3,2-*b*]indole 6d (31%)
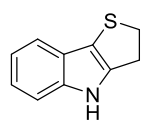
Brown-orange crystals. Purification by column chromatography (EtOAc/PE 1/5, Rf = 0.23). Mp = 144.0 °C. ^{1}H NMR (400 MHz, CDCl$_3$): δ 3.20 and 3.83 (2 × 2H, 2 × t, J = 7.9 Hz, CH$_2$CH$_2$S); 7.07-7.15 (2H, m, 2 × CH$_{arom}$); 7.28-7.31 (1H, m, CH$_{arom}$); 7.36-7.38 (1H, m, CH$_{arom}$); 7.97 (1H, s(br), NH). ^{13}C NMR (100.6 MHz, CDCl$_3$): δ 28.4 and 37.6 (CH$_2$CH$_2$S), 111.6 (CH$_{arom}$),113.1 (C$_{quat,arom}$), 118.7, 120.0 and 121.4 (3 × CH$_{arom}$), 123.1, 137.1 and 140.5 (3 × C$_{quat,arom}$). IR (ATR, cm^{-1}): ν$_{NH}$ = 3375; ν$_{max}$ = 1448, 1423, 1301, 1235, 1043, 1003, 743, 692, 624. MS (70 eV): m/z (%) 174 (M$^-$- 1, 100). HRMS (ESI) Anal. Calcd. for C$_{10}$H$_{10}$NS 176.0528 [M+H]$^+$, Found 176.0526.

### 7-Fluoro-2,3-dihydrothieno[3,2-b]indole 6e (30%)
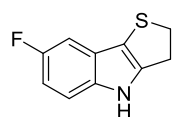
Brown-orange crystals. Purification by column chromatography (EtOAc/PE 1/4, Rf = 0.20). Mp = 133.5 °C. ^{1}H NMR (400 MHz, CDCl$_3$): δ 3.18 and 3.81 (2 × 2H, 2 × t, J = 7.9 Hz, CH$_2$CH$_2$S); 6.86 (1H, t × d, J = 9.0, 2.5 Hz, CH$_{arom}$); 7.02 (1H, d × d, J = 9.4, 2.5 Hz, CH$_{arom}$); 7.18 (1H, d × d, J = 9.0, 4.3 Hz, CH$_{arom}$); 7.95 (1H, s(br), NH). ^{19}F NMR (376.5 MHz, CDCl$_3$): δ (-123.90)-(-123.84) (m). ^{13}C NMR (100.6 MHz, CDCl$_3$): δ 28.4 and 37.6 (CH$_2$CH$_2$S), 103.8 (d, J = 24.3 Hz, CH$_{arom}$), 109.5 (d, J = 26.3 Hz, CH$_{arom}$), 112.1 (d, J = 9.7 Hz, CH$_{arom}$), 113.2 (d, J = 4.4 Hz, C$_{quat,arom}$), 123.2 (d, J = 10.5 Hz, C$_{quat,arom}$), 136.9 and 139.3 (2 × C$_{quat,arom}$), 157.9 (d, J = 234.9 Hz, FC$_{quat,arom}$). IR (ATR, cm^{-1}): ν$_{NH}$ =3396; ν$_{max}$ = 2920, 1574, 1508, 1485, 1474, 1453, 1439, 1426, 1222, 1156, 1038, 844, 825, 795. MS (70 eV): m/z (%) 192 (M$^-$-1, 100). HRMS (ESI) Anal. Calcd. for C$_{10}$H$_7$FNS 192.0289 [M-H]$^-$, Found 192.0291.

### 3.4.6.2. Synthesis of sulfoxides *7a-c*

General procedure: To a solution of 1,2,4,9-tetrahydro-3-thia-9-azafluorene **6a** (5 mmol) in tetrahydrofuran (50 mL) was added boron trifluoride diethyl etherate (20 mmol) at -20 °C under nitrogen atmosphere. Then *meta*-chloroperbenzoic acid was added (5 mmol) at -20 °C and the mixture was stirred at -20 °C for two hours. After two hours the reaction mixture was poured into a saturated solution of $NaHCO_3$ (100 mL) and subsequently extracted with ethyl acetate (100 mL). The organic phase was washed with water (2 × 50 mL), brine (50 mL) and dried over anhydrous $MgSO_4$. Filtration of the drying agent and removal of the solvent in vacuo afforded the crude cyclic sulfoxide **7a**, which was purified by recrystallization from EtOH to provide pure 1,2,4,9-tetrahydro-3-thia-9-azafluorene-3-oxide **7a** (4.15 mmol, 83%).

1,2,4,9-Tetrahydro-3-thia-9-azafluorene-3-oxide 7a (83%)
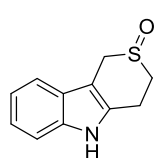
Beige powder. Recrystallization from EtOH. Mp > 260.0 °C. ^{1}H NMR (400 MHz, D_6-DMSO): δ 3.03-3.34 (4H, m, CH_2CH_2SO); 3.93 and 4.21 (2 × 1H, 2 × d, J = 15.1 Hz, C_{quat}(HCH)SO); 6.98 (1H, t, J = 7.5 Hz, CH_{arom}); 7.06 (1H, t, J = 7.5 Hz, CH_{arom}); 7.30 (1H, d, J = 7.5 Hz, CH_{arom}); 7.42 (1H, d, J = 7.5 Hz, CH_{arom}); 11.10 (1H, s(br), NH). ^{13}C NMR (100.6 MHz, D_6-DMSO): δ 17.7 ($\underline{C}H_2CH_2SO$), 44.5 ($CH_2\underline{C}H_2SO$), 45.1 ($C_{quat}\underline{C}H_2SO$), 98.9 ($C_{quat,arom}$), 111.3, 117.7, 119.1 and 121.5 (4 × CH_{arom}), 127.8, 132.3 and 136.1 (3 × $C_{quat,arom}$). IR (ATR, cm^{-1}): v_{NH} = 3190; $v_{S=O}$ = 1027; v_{max} = 1008, 758, 711, 700. MS (70 eV): m/z (%) 206 (M$^+$+1, 90). HRMS (ESI) Anal. Calcd. for $C_{11}H_{12}NOS$ 206.0634 [M+H]$^+$, Found 206.0638.

6-Fluoro-1,2,4,9-tetrahydro-3-thia-9-azafluorene-3-oxide 7b (68%)
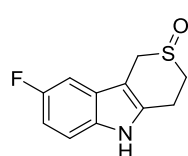
Yellow powder. Recrystallization from EtOH. Mp = 242.0 °C. ^{1}H NMR (400 MHz, D_6-DMSO): δ 3.02-3.33 (4H, m, CH_2CH_2SO); 3.93 and 4.16 (2 × 1H, 2 × d, J = 15.2 Hz, C_{quat}(HCH)SO); 6.89 (1H, t × d, J = 9.0, 2.6 Hz, CH_{arom}); 7.22 (1H, d × d, J = 9.9, 2.6 Hz, CH_{arom}); 7.29 (1H, d × d, J = 9.0, 4.5 Hz, CH_{arom}); 11.14 (1H, s(br), NH). ^{19}F NMR (376.5 MHz, D_6-DMSO): δ (-125.11)-(-125.05) (m). ^{13}C NMR (100.6 MHz, D_6-DMSO): δ 17.5 ($\underline{C}H_2CH_2SO$), 44.2 ($CH_2\underline{C}H_2SO$), 44.8 ($C_{quat}\underline{C}H_2SO$), 99.4 (d, J = 4.4 Hz, $C_{quat,arom}$), 102.8 (d, J = 23.6 Hz, CH_{arom}), 109.3 (d, J = 25.9 Hz, CH_{arom}), 112.2 (d, J = 9.7 Hz, CH_{arom}), 128.2 (d, J = 10.0 Hz, $C_{quat,arom}$), 132.7 and 134.5 (2 × $C_{quat,arom}$), 157.3 (d, J = 231.4 Hz, $FC_{quat,arom}$). IR (ATR, cm^{-1}): v_{NH} = 3176; $v_{S=O}$ = 1022; v_{max} =1455, 1410, 1169, 1126, 1106, 991, 944, 838, 817, 710, 690. MS (70 eV): m/z (%) 224 (M$^+$+1, 100). HRMS (ESI) Anal. Calcd. for $C_{11}H_{11}FNOS$ 224.0540 [M+H]$^+$, Found 224.0548.

#### 7-Bromo-2,3-dihydrothieno[3,2-*b*]indole-1-oxide 7c (41%)
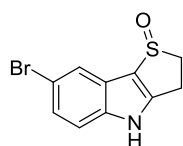
Black powder. Recrystallization from EtOH. Mp = 191.0 °C. ^{1}H NMR (400 MHz, D6-DMSO): δ 3.15-3-22, 3.28-3.33, 3.59-3.67 and 3.96-4.03 (4 × 1H, 4 × m, CH_2CH_2S); 7.33 (1H, d × d, J = 8.6, 1.9 Hz, CH_{arom}); 7.43 (1H, d, J = 8.6 Hz, CH_{arom}); 7.83 (1H, d, J = 1.9 Hz, CH_{arom}); 12.07 (1H, s(br), NH). ^{13}C NMR (100.6 MHz, D6-DMSO): δ 24.0 and 59.0 (CH_2CH_2S), 113.9 ($C_{arom,quat}$), 115.0 and 120.8 (2 × CH_{arom}), 120.9 and 124.5 (2 × $C_{arom,quat}$), 125.3 (CH_{arom}), 140.1 and 153.4 (2 × $C_{arom,quat}$). IR (ATR, cm^{-1}): v_{NH} = 3466; $v_{S=O}$ = 986; v_{max} = 1590, 1485, 1454, 1438, 1294, 1236,

1126, 1071,1040, 954, 815, 802, 715. MS (70eV): m/z (%) 270/2 (M$^+$+1, 100). HRMS (ESI) Anal. Calcd. for C$_{10}$H$_9$BrNOS 269.9583 [M+H]$^+$, Found 269.9593.

3.4.6.3. Synthesis of sulfones 8a-e

General procedure: To a solution of 6-bromo-1,2,4,9-tetrahydro-3-thia-9-azafluorene **6c** (5 mmol) in tetrahydrofuran (50 mL) was added *meta*-chloroperbenzoic acid in tetrahydrofuran (15 mmol) at 0 °C. The mixture was stirred at room temperature for two hours. The solvent was removed *in vacuo* and the residue was dissolved in ethyl acetate (100 mL). The solution was washed with saturated aqueous sodium sulfite (30 mL), water (30 mL), brine (2 × 30 mL), and dried over anhydrous MgSO$_4$. Filtration of the drying agent and removal of the solvent *in vacuo* afforded the crude cyclic sulfone **8c**, which was purified by recrystallization from EtOH to provide pure 6-bromo-1,2,4,9-tetrahydro-3-thia-9-azafluorene-3,3-dioxide **8c** (3.05 mmol, 61%). The synthesis of 1,2,4,9-tetrahydro-3-thia-9-azafluorene-3,3-dioxide **8a** and 6-fluoro-1,2,4,9-tetrahydro-3-thia-9-azafluorene-3,3-dioxide **8b** has been described in the previous chapter.

6-Bromo-1,2,4,9-tetrahydro-3-thia-9-azafluorene-3,3-dioxide 8c (61%)
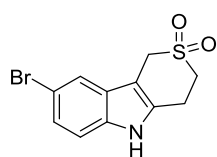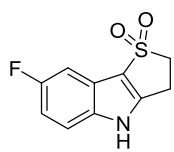
Brown powder. Recrystallization from EtOH. Mp = 215.0 °C. ^{1}H NMR (400 MHz, D6-DMSO): δ 3.27 and 3.48 (2 × 2H, 2 × t, *J* = 6.1Hz, CH$_2$CH$_2$S); 4.44 (2H, s, C$_{quat}$CH$_2$S); 7.20 (1H, d × d, *J* = 8.6, 1.5 Hz, CH$_{arom}$); 7.30 (1H, d, *J* = 8.6 Hz, CH$_{arom}$); 7.65 (1H, d, *J* = 1.5 Hz, CH$_{arom}$); 11.36 (1H, s(br), NH). ^{13}C NMR (100.6 MHz, D6-DMSO): δ 23.1 and 47.1 (CH$_2$CH$_2$S), 48.6 (C$_{arom,quat}$CH$_2$S), 101.9 and 111.9 (2 × C$_{arom,quat}$), 113.4, 120.3 and 124.3 (3 × CH$_{arom}$), 129.1, 132.4 and 135.2 (3 × C$_{arom,quat}$). IR (ATR, cm^{-1}): v$_{NH}$ = 3350; v$_{S=O}$ = 1100; v$_{max}$ = 1585, 1470, 1454, 1432, 1311, 1273, 1252, 1162, 1048, 953, 894, 861, 802, 786, 769, 743. MS (70eV): m/z (%) 322/4 (M$^+$+23, 55). HRMS (ESI) Anal. Calcd. for C$_{11}$H$_{10}$BrNO$_2$S 297.9543 [M-H]$^-$, Found 297.9541.

### 2,3-Dihydrothieno[3,2-*b*]indole-1,1-dioxide 8d (52%)
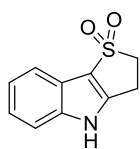
Beige powder. Recrystallization from EtOH. Mp = 260.0 °C. ^{1}H NMR (400 MHz, D$_6$-DMSO): δ 3.44 (2H, t, *J* = 6.6 Hz, CH$_2$CH$_2$SO$_2$); 3.90 (2H, t, *J* = 6.6 Hz, CH$_2$CH$_2$SO$_2$); 7.17-7.21 (1H, m, CH$_{arom}$); 7.24-7.28 (1H, m, CH$_{arom}$); 7.48-7.50 (1H, m, CH$_{arom}$); 7.54-7.56 (1H, m, CH$_{arom}$); 12.00 (1H, s(br), NH). ^{13}C NMR (100.6 MHz, D$_6$-DMSO): δ 21.4 (CH$_2$CH$_2$SO$_2$), 57.6 (CH$_2$CH$_2$SO$_2$), 113.3 (CH$_{arom}$), 116.1 (C$_{quat,arom}$); 118.4 (CH$_{arom}$), 119.4 (C$_{quat,arom}$), 121.9 and 123.7 (2 × CH$_{arom}$), 140.8 and 147.7 (2 × C$_{quat,arom}$). IR (ATR, cm^{-1}): v$_{NH}$ =3355; v$_{S=O}$ = 1121, 1104; v$_{max}$ = 1306, 1275, 1238, 1220, 1134, 766, 658. MS (70 eV): m/z (%) 208 (M$^+$+1, 30); 225 (M+NH$_4^+$, 100). HRMS (ESI) Anal. Calcd. for C$_{10}$H$_{10}$NO$_2$S 208.0427 [M+H]$^+$, Found 208.0429.

7-Fluoro-2,3-dihydrothieno[3,2-*b*]indole-1,1-dioxide 8e (70%)

Pink powder. Recrystallization from EtOH. Mp > 260.0 °C. ^{1}H NMR (400 MHz, D$_6$-DMSO): δ 3.44 (2H, t, J = 6.6 Hz, C$\underline{H}_2$CH$_2$SO$_2$); 3.89 (2H, t, J = 6.6 Hz, CH$_2$C$\underline{H}_2$SO$_2$); 7.12 (1H, t × d, J = 9.1, 2.5 Hz, CH$_{arom}$); 7.33 (1H, d × d, J = 9.3, 2.5 Hz, CH$_{arom}$); 7.51 (1H, d × d, J = 9.1, 4.5 Hz, CH$_{arom}$); 12.10 (1H, s(br), NH). ^{19}F NMR (376.5 MHz, D$_6$-DMSO): δ (-121.35)-(-121.29) (m). ^{13}C NMR (100.6 MHz, D$_6$-DMSO): δ 21.5 ($\underline{C}$H$_2$CH$_2$SO$_2$), 57.6 (CH$_2$$\underline{C}H_2SO_2$), 103.8 (d, J = 25.1 Hz, CH$_{arom}$), 111.7 (d, J = 25.7 Hz, CH$_{arom}$), 114.6 (d, J = 9.8 Hz, CH$_{arom}$), 116.2 (d, J = 4.4 Hz, C$_{quat,arom}$), 119.6 (d, J = 11.3 Hz, C$_{quat,arom}$), 137.4 (C$_{quat,arom}$), 149.3 (C$_{quat,arom}$), 158.3 (d, J = 235.3 Hz, FC$_{quat,arom}$). IR (ATR, cm^{-1}): ν$_{NH}$ =3243; ν$_{S=O}$ = 1123, 1103; ν$_{max}$ = 1442, 1434, 1275, 1238, 1228, 1193, 1163, 1142, 1054, 995, 847, 816, 749. MS (70 eV): m/z (%) 243 (M+NH$_4$$^+$, 100). HRMS (ESI) Anal. Calcd. for C$_{10}$H$_9$FNO$_2$S 226.0333 [M+H]$^+$, Found 226,0334.

3.4.6.4. Synthesis of 6-phenyl-1,2,4,9-tetrahydro-3-thia-9-azafluorene-3,3-dioxide 8f

6-Bromo-1,2,4,9-tetrahydro-3-thia-9-azafluorene-3,3-dioxide **8c** (2 mmol) was dissolved in toluene (15 mL), and to this solution an aqueous solution of sodium carbonate (7 mL, 2 M) and a solution of phenylboronic acid (4 mmol) in ethanol (7 mL) were added. This mixture was then flushed with nitrogen gas for 10 minutes before tetrakis(triphenylphosphine)palladium(0) (0.08 mmol) was added, and the reaction mixture was heated under reflux for 8 hour. The reaction mixture was then poured into brine (20 mL) and extracted with EtOAc (3 × 20 mL). The combined organic fraction was washed with brine (3 × 15 mL), dried (MgSO$_4$), filtered and evaporated under vacuum. Purification through recrystallization from EtOH yielded 6-phenyl-1,2,4,9-tetrahydro-3-thia-9-azafluorene-3,3-dioxide **8f** (1.2 mmol, 60%) as a light brown powder.

6-Phenyl-1,2,4,9-tetrahydro-3-thia-9-azafluorene-3,3-dioxide 8f (60%)
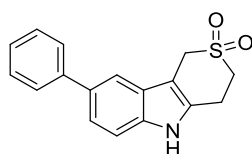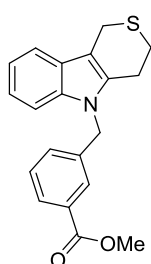
Light brown powder. Recrystallization from EtOH. Mp = 237.0 °C. ^{1}H NMR (400 MHz, D6-DMSO): δ 3.29 and 3.50 (2 × 2H, 2 × t, J = 6.2 Hz, CH$_2$CH$_2$S); 4.51 (2H, s, C$_{quat}$CH$_2$S); 7.30 (1H, t, J = 7.4 Hz, CH$_{arom}$); 7.39-7.43 (2H, m, 2 × CH$_{arom}$); 7.45 (2H, t, J = 7.4 Hz, 2 × CH$_{arom}$); 7.68 (2H, d, J = 7.4 Hz, 2 × CH$_{arom}$); 7.74 (1H, s, CH$_{arom}$); 11.21 (1H, s(br), NH). ^{13}C NMR (100.6 MHz, D6-DMSO): δ 23.2 and 47.2 (CH$_2$CH$_2$S), 48.9 (C$_{arom,quat}$$\underline{C}H_2$S), 102.5 (C$_{arom,quat}$), 111.8, 116.1, 121.2, 126.8 and 127.1 (6 × CH$_{arom}$), 127.9 (C$_{arom,quat}$), 129.2 (2 × CH$_{arom}$), 131.4, 131.9, 136.2 and 142.1 (4 × C$_{arom,quat}$). IR (ATR, cm^{-1}): ν$_{NH}$ = 3347; ν$_{S=O}$ = 1100; ν$_{max}$ = 1594, 1474, 1437, 1311, 1272, 1217, 1162, 895, 876, 812, 783, 760, 748, 696, 640. MS (70eV): m/z (%) 298 (M$^+$+1, 40). HRMS (ESI) Anal. Calcd. for C$_{17}$H$_{16}$NO$_2$S 298.0896 [M+H]$^+$, Found 298.0902.

3.4.6.5. Synthesis of esters 10a-m

General procedure: 1,2,4,9-Tetrahydro-3-thia-9-azafluorene **6a** (6 mmol) and sodium hydride (60 wt% in mineral oil, 6 mmol) were placed under nitrogen and dissolved in DMF (10 mL).
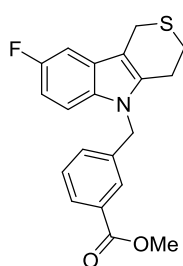
After stirring for 30 minutes, methyl 3-(bromomethyl)benzoate **9** (6 mmol) and potassium iodide (0.06 mmol) were added. The mixture was heated to 80 °C for 2 h, after which it was quenched with water (30 mL), followed by addition of ethyl acetate (30 mL). The aqueous layer was extracted with ethyl acetate (2 × 10 mL) and the combined organic layers were washed with water (2 × 20 mL) and brine (15 mL), dried (MgSO₄) and concentrated *in vacuo.* Purification by means of column chromatography (EtOAc/PE 1/10, R$_f$ = 0.18) afforded pure *N*-(3-methoxycarbonylbenzyl)-1,2,4,9-tetrahydro-3-thia-9-azafluorene **10a** (2.46 mmol, 41%).

N-(3-Methoxycarbonylbenzyl)-1,2,4,9-tetrahydro-3-thia-9-azafluorene 10a (41%)

White-yellow crystals. Purification by column chromatography (EtOAc/PE 1/10, Rf = 0.18). Mp = 115.0 °C. ^{1}H NMR (400 MHz, CDCl₃): δ 2.92 and 3.04 (2 × 2H, 2 × t, J = 5.8 Hz, CH₂CH₂S); 3.93 (3H, s, CH₃O); 3.95 (2H, s, C$_{quat}$CH₂S); 5.33 (2H, s, CH₂N); 7.03-7.05 (1H, m, CH$_{arom}$); 7.13-7.20 (2H, m, 2 × CH$_{arom}$); 7.24-7.26 (1H, m, CH$_{arom}$); 7.33 (1H, t, J = 7.7 Hz, CH$_{arom}$); 7.52-7.55 (1H, m, CH$_{arom}$); 7.90-7.95 (2H, m, 2 × CH$_{arom}$). ^{13}C NMR (100.6 MHz, CDCl₃): δ 23.1 (C$_{quat}$<u>C</u>H₂S), 24.1 and 25.9 (CH₂CH₂S), 46.0 (CH₂N), 52.3 (CH₃O), 107.3 (C$_{quat,arom}$), 108.9, 117.7, 119.5 and 121.7 (4 × CH$_{arom}$), 126.8 (C$_{quat,arom}$), 127.4, 128.7, 129.1 and 130.5 (4 × CH$_{arom}$), 130.6, 134.5, 135.7 and 138.2 (4 × C$_{quat,arom}$), 166.8 (C=O). IR (ATR, cm^{-1}): ν$_{C=O}$ = 1714; ν$_{max}$ = 2923, 1467, 1448, 1434, 1284, 1258, 1200, 1188, 1175, 992, 740. MS (70 eV): m/z (%) 338 (M⁺+1, 90); 376 (M+K⁺, 100). HRMS (ESI) Anal. Calcd. for C₂₀H₂₀NO₂S 338.1209 [M+H]⁺, Found 338.1219.

N-(3-Methoxycarbonylbenzyl)-6-fluoro-1,2,4,9-tetrahydro-3-thia-9-azafluorene 10b (50%)


White-yellow crystals. Purification by column chromatography (EtOAc/PE 1/10, Rf = 0.16). Mp = 97.0 °C. ^{1}H NMR (400 MHz, CDCl₃): δ 2.89 and 3.00 (2 × 2H, 2 × t, J = 5.7 Hz, CH₂CH₂S); 3.85 (2H, s, C$_{quat}$CH₂S); 3.90 (3H, s, CH₃O); 5.27 (2H, s, CH₂N); 6.87 (1H, t × d, J = 9.1, 2.5 Hz, CH$_{arom}$); 6.99-7.01 (1H, m, CH$_{arom}$); 7.08-7.15 (2H, m, 2 × CH$_{arom}$); 7.32 (1H, t, J = 7.7 Hz, CH$_{arom}$); 7.84 (1H, s, CH$_{arom}$); 7.90-7.93 (1H, m, CH$_{arom}$). ^{19}F NMR (376.5 MHz, CDCl₃): δ (-124.64)-(-124.52) (m). ^{13}C NMR (100.6 MHz, CDCl₃): δ 22.9 (C$_{quat}$<u>C</u>H₂S), 24.2 and 25.8 (CH₂CH₂S), 46.2 (CH₂N), 52.3 (CH₃O), 103.0 (d, J = 23.6 Hz, CH$_{arom}$), 107.4 (d, J = 4.4 Hz, C$_{quat,arom}$), 109.5 (d, J = 9.6 Hz, CH$_{arom}$), 109.7 (d, J = 26.0 Hz, CH$_{arom}$), 127.1 (d, J = 9.7 Hz, C$_{quat,arom}$), 127.3, 128.8, 129.2 and 130.4 (4 × CH$_{arom}$), 130.8, 132.2, 136.3 and 137.9 (4 × C$_{quat,arom}$), 157.9 (d, J = 235.0 Hz, FC$_{quat,arom}$), 166.7 (C=O). IR (ATR, cm^{-1}): ν$_{C=O}$ = 1717; ν$_{S=O}$ = 1147, 1134; ν$_{max}$ = 3415, 2923, 1583, 1479, 1449, 1431, 1300, 1284, 1260, 1196, 1184, 1122, 1104, 857, 844, 780, 763, 473. MS (70 eV): m/z (%) 356 (M⁺+1, 100). HRMS (ESI) Anal. Calcd. for C₂₀H₁₉FNO₂S 356.1115 [M+H]⁺, Found 356.1131.

N-(3-Methoxycarbonylbenzyl)-1,2,4,9-tetrahydro-3-thia-9-azafluorene-3,3-dioxide   10c (21%)

Dark yellow powder. Purification by column chromatography (EtOAc/PE 4/5, R_f = 0.26). Mp = 200.0 °C. ^{1}H NMR (400 MHz, D_6-DMSO): δ 3.21 (2H, t, J = 6.2 Hz, C$\underline{H}_2$CH$_2$SO$_2$); 3.51 (2H, t, J = 6.2 Hz, CH$_2$C$\underline{H}_2$SO$_2$); 3.82 (3H, s, CH$_3$O); 4.51 (2H, s, C$_{quat}$CH$_2$SO$_2$); 5.53 (2H, s, CH$_2$N); 7.06-7.10 (1H, m, CH$_{arom}$); 7.14-7.18 (1H, m, CH$_{arom}$); 7.22-7.25 (1H, m, CH$_{arom}$); 7.45-7.52 (3H, m, 3 × CH$_{arom}$); 7.78 (1H, s, CH$_{arom}$); 7.85 (1H, d, J = 7.9 Hz, CH$_{arom}$). ^{13}C NMR (100.6 MHz, D_6-DMSO): δ 22.4 ($\underline{C}$H$_2$CH$_2$SO$_2$), 45.9 (CH$_2$N), 46.7 (CH$_2$$\underline{C}H_2SO_2$), 48.4 (CH$_2SO_2$), 52.7 (CH$_3$O), 102.8 (C$_{quat,arom}$), 110.3, 118.3, 120.0 and 122.5 (4 × CH$_{arom}$), 126.6 (C$_{quat,arom}$), 127.7, 128.6 and 129.8 (3 × CH$_{arom}$), 130.5 (C$_{quat,arom}$), 131.5 (CH$_{arom}$), 131.6, 137.1 and 139.3 (3 × C$_{quat,arom}$), 166.4 (C=O). IR (ATR, cm^{-1}): $v_{C=O}$ = 1712; $v_{S=O}$ = 1125, 1113; v_{max} = 2922, 2852, 1464, 1302, 1283, 1237, 1205, 1188, 1162, 1083, 750, 713, 702. MS (70 eV): m/z (%) 370 (M$^+$+1, 7); 387 (M+NH$_4^+$, 100). HRMS (ESI) Anal. Calcd. for C$_{20}$H$_{20}$NO$_4$S 370.1108 [M+H]$^+$, Found 370.1111.
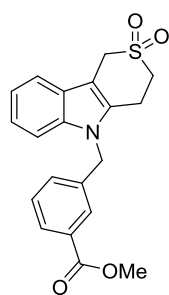
### *N*-(3-Methoxycarbonylbenzyl)-6-fluoro-1,2,4,9-tetrahydro-3-thia-9-azafluorene-3,3-dioxide 10d (67%)
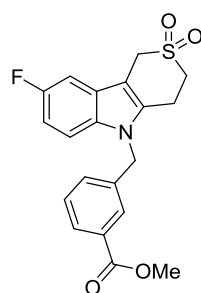
Beige powder. Recrystallization from EtOH. Mp = 214.0 °C. 1H NMR (400 MHz, D_6-DMSO): δ 3.21 (2H, t, J = 6.1 Hz, C$\underline{H}_2$CH$_2$SO$_2$); 3.50 (2H, t, J = 6.1 Hz, CH$_2$C$\underline{H}_2$SO$_2$); 3.83 (3H, s, CH$_3$O); 4.48 (2H, s, C$_{quat}$CH$_2$SO$_2$); 5.54 (2H, s, CH$_2$N); 7.01 (1H, t × d, J = 9.2, 2.5 Hz, CH$_{arom}$); 7.22 (1H, d, J = 7.9 Hz, CH$_{arom}$); 7.33 (1H, d × d, J = 9.3, 2.5 Hz, CH$_{arom}$); 7.47 (1H, t, J = 7.9 Hz, CH$_{arom}$); 7.51 (1H, d × d, J = 9.2, 4.3 Hz, CH$_{arom}$); 7.77 (1H, s, CH$_{arom}$); 7.86 (1H, d, J = 7.9 Hz, CH$_{arom}$). ^{19}F NMR (376.5 MHz, D_6-DMSO): δ (-124.05)-(-123.99) (m). ^{13}C NMR (100.6 MHz, D_6-DMSO): δ 22.5 ($\underline{C}$H$_2$CH$_2$SO$_2$), 46.1 (CH$_2$N), 46.6 (CH$_2$$\underline{C}H_2SO_2$), 48.3 (C$_{quat}$$\underline{C}H_2SO_2$), 52.7 (CH$_3$O), 103.1 (d, J = 4.6 Hz, C$_{quat,arom}$), 103.5 (d, J = 24.0 Hz, CH$_{arom}$), 110.4 (d, J = 25.9 Hz, CH$_{arom}$), 111.5 (d, J = 9.6 Hz, CH$_{arom}$), 126.9 (d, J = 10.3 Hz, C$_{quat,arom}$), 127.7, 128.7 and 129.8 (3 × CH$_{arom}$), 130.5 (C$_{quat,arom}$), 131.6 (CH$_{arom}$), 133.5, 133.8 and 139.1 (3 × C$_{quat,arom}$), 157.7 (d, J = 233.0 Hz, FC$_{quat,arom}$), 166.4 (C=O). IR (ATR, cm^{-1}): $v_{C=O}$ = 1713; $v_{S=O}$ = 1128, 1112; v_{max} = 2951, 1480, 1459, 1427, 1312, 1283, 1242, 1206, 1165, 1150, 1128, 1112, 1083, 877, 790, 739. MS (70 eV): m/z (%) 405 (M+NH$_4^+$, 100). HRMS (ESI) Anal. Calcd. for C$_{20}$H$_{19}$FNO$_4$S 388.1013 [M+H]$^+$, Found 388.1019.

N-(3-Methoxycarbonylbenzyl)-6-phenyl-1,2,4,9-tetrahydro-3-thia-9-azafluorene-3,3-dioxide 10e (60%)
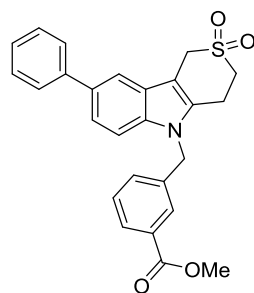
Light brown powder. Recrystallization from EtOH. Mp = 201.0 °C. ^{1}H NMR (400 MHz, D6-DMSO): δ 3.24 and 3.52 (2 × 2H, 2 × t, J = 5.9 Hz, CH$_2$CH$_2$S); 3.83 (3H, s, CH$_3$O); 4.57 (2H, s, C$_{quat}$CH$_2$S); 5.57 (2H, s, CH$_2$N); 7.26 (1H, d, J = 7.7 Hz, CH$_{arom}$); 7.32 (1H, t, J = 7.3 Hz, CH$_{arom}$); 7.44-7.50 (4H, m, 4 × CH$_{arom}$); 7.58 (1H, d, J = 8.6 Hz, CH$_{arom}$); 7.70 (2H, d, J = 7.3 Hz, 2 × CH$_{arom}$); 7.81-7.83 (2H, m, 2 × CH$_{arom}$); 7.87 (1H, d, J = 7.7 Hz, CH$_{arom}$). ^{13}C NMR (100.6 MHz, D6-DMSO): δ 22.5 ($\underline{C}$H$_2$CH$_2$S), 46.1 (CH$_2$N), 46.7 (CH$_2$$\underline{C}H_2$S), 48.5 (C$_{arom,quat}$$\underline{C}H_2$S), 52.7 (CH$_3$O), 103.4 (C$_{arom,quat}$), 110.7, 116.6, 121.7 and 126.9 (4 × CH$_{arom}$), 127.2 (2 × CH$_{arom}$ and C$_{arom,quat}$), 127.7, 128.6, 129.3 and 129.8 (5 × CH$_{arom}$), 130.5 (C$_{arom,quat}$), 131.6 (CH$_{arom}$), 132.3, 132.6, 136.7, 139.3 and 141.8 (5 × C$_{arom,quat}$), 166.4 (C=O). IR (ATR, cm^{-1}): $v_{C=O}$ = 1716; $v_{S=O}$ = 1117; v_{max} = 1473, 1446, 1430, 1313, 1286, 1260, 1233, 1198, 1167, 1135, 982, 890,
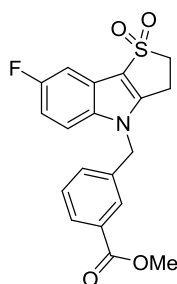
878, 758, 745, 723, 693. MS (70eV): m/z (%) 446 (M$^+$+1, 80). HRMS (ESI) Anal. Calcd. for C$_{26}$H$_{27}$N$_2$O$_4$S 463.1686 [M+NH$_4$]$^+$, Found 463.1694.

### *N*-(3-Methoxycarbonylbenzyl)-2,3-dihydrothieno[3,2-*b*]indole-1,1-dioxide 10f (72%)
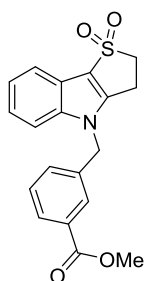
White powder. Recrystallization from EtOH. Mp = 210.5 °C.^{1}H NMR (400 MHz, D$_6$-DMSO): δ 3.44 (2H, t, *J* = 6.5 Hz, C$\underline{H}_2$CH$_2$SO$_2$); 3.84 (3H, s, OCH$_3$); 3.95 (2H, t, *J* = 6.5 Hz, CH$_2$C$\underline{H}_2$SO$_2$); 5.57 (2H, s, CH$_2$N); 7.23-7.32 (2H, m, 2 × CH$_{arom}$); 7.42-7.45 (1H, m, CH$_{arom}$); 7.49-7.53 (1H, m, CH$_{arom}$); 7.59-7.62 (2H, m, 2 × CH$_{arom}$); 7.88-7.91 (2H, m, 2 × CH$_{arom}$). ^{13}C NMR (100.6 MHz, D$_6$-DMSO): δ 21.0 ($\underline{C}$H$_2$CH$_2$SO$_2$), 46.9 (CH$_2$N), 52.7 (CH$_3$O), 57.4 (CH$_2$$\underline{C}H_2SO_2$), 112.3 (CH$_{arom}$), 116.2 (C$_{quat,arom}$), 118.8 (CH$_{arom}$), 119.3 (C$_{quat,arom}$), 122.5, 124.0, 128.2, 129.0 and 129.9 (5 × CH$_{arom}$), 130.6 (C$_{quat,arom}$), 132.3 (CH$_{arom}$), 137.9, 141.0 and 148.5 (3 × C$_{quat,arom}$), 166.4 (C=O). IR (ATR, cm^{-1}): ν$_{C=O}$ = 1718; ν$_{S=O}$ = 1124, 1107; ν$_{max}$ = 2948, 2923, 2854, 1292, 1277, 1261, 1235, 1195, 755, 746. MS (70 eV): m/z (%) 373 (M+NH$_4^+$, 100). HRMS (ESI) Anal. Calcd. for C$_{19}$H$_{18}$NO$_4$S 356.0951 [M+H]$^+$, Found 356.0958.

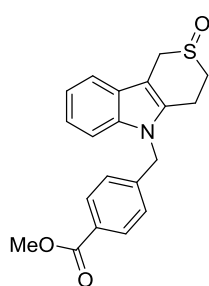### *N*-(3-Methoxycarbonylbenzyl)-7-fluoro-2,3-dihydrothieno[3,2-*b*]indole-1,1-dioxide 10g (60%)

White powder. Recrystallization from EtOH. Mp = 222.0 °C.^{1}H NMR (400 MHz, D$_6$-DMSO): δ 3.44 (2H, t, *J* = 6.5 Hz, C$\underline{H}_2$CH$_2$SO$_2$); 3.84 (3H, s, OCH$_3$); 3.95 (2H, t, *J* = 6.5 Hz, CH$_2$C$\underline{H}_2$SO$_2$); 5.57 (2H, s, CH$_2$N); 7.18 (1H, t × d, *J* = 9.2, 2.5 Hz, CH$_{arom}$); 7.39-7.44 (2H, m, 2 × CH$_{arom}$); 7.49-7.53 (1H, m, CH$_{arom}$); 7.63 (1H, d × d, *J* = 9.2, 4.3 Hz, CH$_{arom}$); 7.89-7.91 (2H, m, 2 × CH$_{arom}$). ^{19}F NMR (376.5 MHz, D$_6$-DMSO): δ (-120.57)-(-120.50) (m). ^{13}C NMR (100.6 MHz, D$_6$-DMSO): δ 21.1 ($\underline{C}$H$_2$CH$_2$SO$_2$), 47.1 (CH$_2$N), 52.7 (CH$_3$O), 57.3 (CH$_2$$\underline{C}H_2SO_2$), 104.3 (d, *J* = 25.2 Hz, CH$_{arom}$), 112.1 (d, *J* = 26.0 Hz, CH$_{arom}$), 113.7 (d, *J* = 9.9 Hz, CH$_{arom}$), 116.2 (d, *J* = 4.4 Hz, C$_{quat,arom}$), 119.5 (d, *J* = 11.2 Hz, C$_{quat,arom}$), 128.2, 129.1 and 130.0 (3 × CH$_{arom}$), 130.6 (C$_{quat,arom}$), 132.3 (CH$_{arom}$), 137.6, 137.7 and 150.1 (3 × C$_{quat,arom}$), 158.7 (d, *J* = 236.9 Hz, FC$_{quat,arom}$), 166.4 (C=O). IR (ATR, cm^{-1}): ν$_{C=O}$ = 1723; ν$_{S=O}$ = 1127, 1111; ν$_{max}$ = 2980, 1479, 1443, 1287, 1265, 1198, 1188, 1145, 748. MS (70 eV): m/z (%) 391 (M+NH$_4^+$, 100). HRMS (ESI) Anal. Calcd. for C$_{19}$H$_{17}$FNO$_4$S 374.0857 [M+H]$^+$, Found 374.0857.
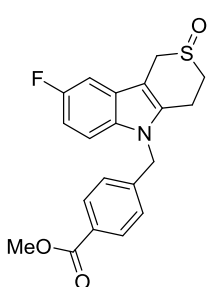
N-(3-Methoxycarbonylbenzyl)-7-bromo-2,3-dihydrothieno[3,2-*b*]indole-1-oxide 10h (54%)
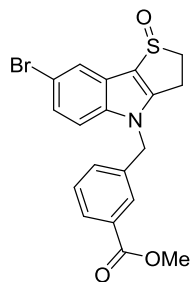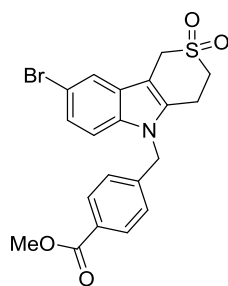
Brown powder. Purification by column chromatography (acetone/PE 1/1, Rf = 0.23). Mp = 187.5 °C. ^{1}H NMR (400 MHz, CDCl$_3$): δ 3.01-3-07, 3.45-3.51, 3.61-3.69 and 3.91-4.00 (4 × 1H, 4 × m, CH$_2$CH$_2$S); 3.91 (3H, s, CH$_3$O); 5.29 and 5.35 (2 × 1H, 2 × d, *J* = 16.4 Hz, CH$_2$N); 7.13 (1H, d, *J* = 8.8 Hz, CH$_{arom}$); 7.19 (1H, d, *J* = 7.7 Hz, CH$_{arom}$); 7.34 (1H, d × d, *J* = 8.8, 1.8 Hz, CH$_{arom}$); 7.40 (1H, t, *J* = 7.7 Hz, CH$_{arom}$); 7.90 (1H, s, CH$_{arom}$); 7.96 (1H, d, *J* = 1.8 Hz, CH$_{arom}$); 7.99 (1H, d, *J* = 7.7 Hz, CH$_{arom}$). ^{13}C NMR (100.6 MHz, CDCl$_3$): δ 23.8 ($\underline{C}$H$_2$CH$_2$S), 48.9 (CH$_2$N), 52.4 (CH$_3$O), 58.3 (CH$_2$$\underline{C}H_2$S), 112.0 (CH$_{arom}$), 115.5 and 120.9 (2 × C$_{arom,quat}$), 122.1 (CH$_{arom}$), 124.3 (C$_{arom,quat}$), 126.3, 127.8, 129.5, 129.6 and 130.9 (5 × CH$_{arom}$), 131.2, 135.8, 140.1 and 152.4 (4 × C$_{arom,quat}$), 166.4 (C=O). IR (ATR, cm^{-1}): ν$_{C=O}$ = 1715; ν$_{S=O}$ = 1032; ν$_{max}$ = 1435, 1424, 1352, 1303, 1258, 1198, 1100, 1084, 1050, 973, 926, 805, 748, 691. MS (70eV): m/z (%) 418/20 (M$^+$+1, 100). HRMS (ESI) Anal. Calcd. for C$_{19}$H$_{17}$BrNO$_3$S 418.0107 [M+H]$^+$, Found 418.0125.

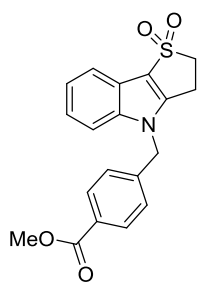### *N*-(4-Methoxycarbonylbenzyl)-1,2,4,9-tetrahydro-3-thia-9-azafluorene-3-oxide 10i (47%)

Brown powder. Recrystallization from EtOH. Mp = 78.0 °C. ^{1}H NMR (400 MHz, D$_6$-DMSO): δ 2.98-3.16 and 3.28-3.38 (3H and 1H, 2 × m, CH$_2$CH$_2$SO); 3.82 (3H, s, CH$_3$O); 4.03 and 4.23 (2 × 1H, 2 × d, *J* = 15.4 Hz, C$_{quat}$(HCH)SO); 5.53 (2H, s, CH$_2$N); 7.05-7.14 (2H, m, 2 × CH$_{arom}$); 7.17 (2H, d, J = 8.3 Hz, 2 × CH$_{arom}$); 7.43 (1H, d, *J* = 8.0 Hz, CH$_{arom}$); 7.52 (1H, d, *J* = 7.5 Hz, CH$_{arom}$); 7.90 (2H, d, *J* = 8.3 Hz, 2 × CH$_{arom}$). ^{13}C NMR (100.6 MHz, D$_6$-DMSO): δ 16.6 (CH$_2$CH$_2$SO), 44.0 (CH$_2$CH$_2$SO), 44.8 (C$_{quat}$CH$_2$SO), 45.9 (CH$_2$N), 52.6 (CH$_3$O), 99.8 (C$_{quat,arom}$), 110.1, 118.1, 119.8 and 122.0 (4 × CH$_{arom}$), 127.1 (2 × CH$_{arom}$), 127.6 and 129.1 (2 × C$_{quat,arom}$), 130.1 (2 × CH$_{arom}$), 133.2, 136.7 and 144.2 (3 × C$_{quat,arom}$), 166.4 (C=O). IR (ATR, cm^{-1}): ν$_{C=O}$ = 1715 ; ν$_{S=O}$ = 1107; ν$_{max}$ = 1464, 1434, 1414, 1277, 1174, 1038, 1018, 999, 744, 713. MS (70 eV): m/z (%) 354 (M$^+$+1, 70). HRMS (ESI) Anal. Calcd. for C$_{20}$H$_{20}$NO$_3$S 354.1158 [M+H]$^+$, Found 354.1153.

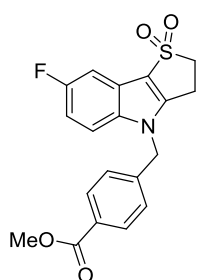### *N*-(4-Methoxycarbonylbenzyl)-6-fluoro-1,2,4,9-tetrahydro-3-thia-9-azafluorene-3-oxide 10j (42%)

Brown powder. Recrystallization from EtOH. Mp = 135.5 °C. ^{1}H NMR (400 MHz, D$_6$-DMSO): δ 2.97-3.14 and 3.32-3.36 (3H and 1H, 2 × m, CH$_2$CH$_2$SO); 3.82 (3H, s, CH$_3$O); 4.02 and 4.18 (2 × 1H, 2 × d, *J* = 15.3 Hz, C$_{quat}$(HCH)SO); 5.53 (2H, s, CH$_2$N); 6.96 (1H, t × d, *J* = 9.0, 2.5 Hz, CH$_{arom}$); 7.16 (2H, d, *J* = 8.3 Hz, 2 × CH$_{arom}$); 7.33 (1H, d × d, *J* = 9.7, 2.5 Hz, CH$_{arom}$); 7.45 (1H, d × d, *J* = 9.0, 4.3 Hz, CH$_{arom}$); 7.90 (2H, d, *J* = 8.3 Hz, 2 × CH$_{arom}$). ^{19}F NMR (376.5 MHz, D$_6$-DMSO): δ (-124.41)-(-124.34) (m). ^{13}C NMR (100.6 MHz, D$_6$-DMSO): δ 16.5 (CH$_2$CH$_2$SO), 43.7 (CH$_2$CH$_2$SO), 44.6 (C$_{quat}$CH$_2$SO), 46.1 (CH$_2$N), 52.6 (CH$_3$O), 100.1 (d, *J* = 4.4 Hz, C$_{quat,arom}$), 103.3 (d, *J* = 23.8 Hz, CH$_{arom}$), 109.8 (d, *J* = 26.0 Hz, CH$_{arom}$), 111.2 (d, *J* = 9.6 Hz, CH$_{arom}$), 127.1 (2 × CH$_{arom}$), 128.0 (d, *J* = 10.2 Hz, C$_{quat,arom}$), 129.1 (C$_{quat,arom}$), 130.1 (2 × CH$_{arom}$), 133.4, 135.3 and 143.9 (3 × C$_{quat,arom}$), 157.7 (d, *J* = 232.6 Hz, FC$_{quat,arom}$), 166.4 (C=O). IR (ATR, cm^{-1}): ν$_{C=O}$ = 1709; ν$_{S=O}$ = 1035; ν$_{max}$ = 1478, 1464, 1438, 1417, 1307, 1282, 1256, 1181, 1147, 1139, 1109, 1018, 860, 795, 770, 722. MS (70 eV): m/z (%) 372 (M$^+$+1, 77). HRMS (ESI) Anal. Calcd. for C$_{20}$H$_{19}$FNO$_3$S 372.1064 [M+H]$^+$, Found 372.1065.

N-(4-Methoxycarbonylbenzyl)-6-bromo-1,2,4,9-tetrahydro-3-thia-9-azafluorene-3,3-dioxide 10k (80%)

Light brown powder. Purification by column chromatography (EtOAc/PE 1/1, Rf = 0.25). Mp = 191.0 °C. ^{1}H NMR (400 MHz, CDCl$_3$): δ 3.25-3.28 and 3.30-3.33 (2 × 2H, 2 × m, C$\underline{H}_2$C$\underline{H}_2$S); 3.90 (3H, s, CH$_3$O); 4.37 (2H, s, C$_{quat}$C$\underline{H}_2$S); 5.32 (2H, s, CH$_2$N); 7.01 (2H, d, J = 8.5 Hz, 2 × CH$_{arom}$); 7.09 (1H, d, J = 8.7 Hz, CH$_{arom}$); 7.30 (1H, d × d, J = 8.7, 1.8 Hz, CH$_{arom}$); 7.57 (1H, d, J = 1.8 Hz, CH$_{arom}$); 7.97 (2H, d, J = 8.5 Hz, 2 × CH$_{arom}$). ^{13}C NMR (100.6 MHz, CDCl$_3$): δ 22.2 ($\underline{C}$H$_2$CH$_2$S), 46.7 (CH$_2$N), 47.2 (CH$_2\underline{C}$H$_2$S), 48.7 (C$_{arom,quat}\underline{C}H_2$S), 52.3 (CH$_3$O), 102.2 (C$_{arom,quat}$), 111.0 (CH$_{arom}$), 113.8 (C$_{arom,quat}$), 120.4, 125.8 and 125.9 (4 × CH$_{arom}$), 128.0 and 130.0 (2 × C$_{arom,quat}$), 130.5 (2 × CH$_{arom}$), 131.4, 135.9 and 141.3 (3 × C$_{arom,quat}$), 166.4 (C=O). IR (ATR, cm^{-1}): $\nu_{C=O}$ = 1715; $\nu_{S=O}$ = 1113; ν_{max} = 1463, 1433, 1408, 1315, 1277, 1240, 1190, 1160, 1058, 888, 868, 802, 779, 769, 760, 718. MS (70eV): m/z (%) 448/50 (M$^+$+1, 70). HRMS (ESI) Anal. Calcd. for C$_{20}$H$_{22}$BrN$_2$O$_4$S 465.0478 [M+NH$_4$]$^+$, Found 465.0473.

N-(4-Methoxycarbonylbenzyl)-2,3-dihydrothieno[3,2-*b*]indole-1,1-dioxide 10l (60%)

White powder. Recrystallization from EtOH. Mp = 226.5 °C. ^{1}H NMR (400 MHz, D$_6$-DMSO): δ 3.44 (2H, t, J = 6.5 Hz, C$\underline{H}_2$CH$_2$SO$_2$); 3.83 (3H, s, OCH$_3$); 3.95 (2H, t, J = 6.5 Hz, CH$_2$C$\underline{H}_2$SO$_2$); 5.57 (2H, s, CH$_2$N); 7.23-7.31 (2H, m, 2 × CH$_{arom}$); 7.35 (2H, d, J = 8.4 Hz, 2 × CH$_{arom}$); 7.55-7.62 (2H, m, 2 × CH$_{arom}$); 7.94 (2H, d, J = 8.4 Hz, 2 × CH$_{arom}$). ^{13}C NMR (100.6 MHz, D$_6$-DMSO): δ 20.9 ($\underline{C}$H$_2$CH$_2$SO$_2$), 47.0 (CH$_2$N), 52.6 (CH$_3$O), 57.4 (CH$_2\underline{C}$H$_2$SO$_2$), 112.2 (CH$_{arom}$), 116.3 (C$_{quat,arom}$), 118.8 (CH$_{arom}$), 119.3 (C$_{quat,arom}$), 122.5 and 124.0 (2 × CH$_{arom}$), 127.8 (2 × CH$_{arom}$), 129.5 (C$_{quat,arom}$), 130.2 (2 × CH$_{arom}$), 141.0, 142.5 and 148.6 (3 × C$_{quat,arom}$), 166.3 (C=O). IR (ATR, cm^{-1}): $\nu_{C=O}$ = 1714; $\nu_{S=O}$ = 1131, 1107; ν_{max} = 1446, 1432, 1277, 1237, 757, 741, 708. MS (70 eV): m/z (%) 356 (M$^+$+1, 41); 373 (M+NH$_4^+$, 100). HRMS (ESI) Anal. Calcd. for C$_{19}$H$_{18}$NO$_4$S 356.0951 [M+H]$^+$, Found 356.0954.
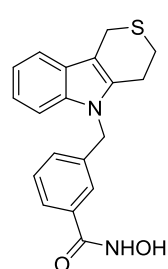
N-(4-Methoxycarbonylbenzyl)-7-fluoro-2,3-dihydrothieno[3,2-*b*]indole-1,1-dioxide 10m (80%)

White powder. Recrystallization from EtOH. Mp = 243.0 °C. ^{1}H NMR (400 MHz, D$_6$-DMSO): δ 3.44 (2H, t, J = 6.5 Hz, C$\underline{H}_2$CH$_2$SO$_2$); 3.84 (3H, s, OCH$_3$); 3.95 (2H, t, J = 6.5 Hz, CH$_2$C$\underline{H}_2$SO$_2$); 5.57 (2H, s, CH$_2$N); 7.16 (1H, t × d, J = 9.2, 2.5 Hz, CH$_{arom}$); 7.34 (2H, d, J = 8.3 Hz, 2 × CH$_{arom}$); 7.41 (1H, d × d, J = 9.1, 2.5 Hz, CH$_{arom}$); 7.59 (1H, d × d, J = 9.2, 4.3 Hz, CH$_{arom}$); 7.94 (2H, d, J = 8.3 Hz, 2 × CH$_{arom}$). ^{19}F NMR (376.5 MHz, D$_6$-DMSO): δ (-120.57)-(-120.51) (m). ^{13}C NMR (100.6 MHz, D$_6$-DMSO): δ 21.0 ($\underline{C}$H$_2$CH$_2$SO$_2$), 47.2 (CH$_2$N), 52.7 (CH$_3$O), 57.3 (CH$_2\underline{C}$H$_2$SO$_2$), 104.3 (d, J = 25.1 Hz, CH$_{arom}$), 112.1 (d, J = 25.8 Hz, CH$_{arom}$), 113.7 (d, J = 9.9 Hz, CH$_{arom}$), 116.3 (d, J = 4.5 Hz, C$_{quat,arom}$), 119.5 (d, J = 11.3 Hz, C$_{quat,arom}$), 127.8 (2 × CH$_{arom}$), 129.6 (C$_{quat,arom}$), 130.2 (2 × CH$_{arom}$), 137.6, 142.2 and 150.1 (3 × C$_{quat,arom}$), 158.7 (d, J = 236.9 Hz, FC$_{quat,arom}$), 166.3 (C=O). IR (ATR, cm^{-1}): $\nu_{C=O}$ = 1708; $\nu_{S=O}$ = 1124, 1105; ν_{max} = 1729, 1483, 1442, 1430, 1288, 1270, 1235, 1188, 1145, 850, 808, 802, 768, 724, 699. MS (70 eV): m/z (%) 391 (M+NH$_4^+$, 100). HRMS (ESI) Anal. Calcd. for C$_{19}$H$_{17}$FNO$_4$S 374.0857 [M+H]$^+$, Found 374.0852.

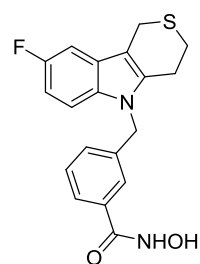### 3.4.6.6. Synthesis of hydroxamic acids *3a-m*

General procedure: *N*-(3-Methoxycarbonylbenzyl)-1,2,4,9-tetrahydro-3-thia-9-azafluorene **10a** (1 mmol) was dissolved in THF (10 mL), and to this solution was added hydroxylamine (100 mmol) and subsequently potassium hydroxide in methanol (4 M, 50 mmol). The resulting mixture was stirred for an additional 10 minutes at room temperature, before it was poured into a saturated aqueous solution of $NaHCO_3$ (10 mL). This aqueous solution was extracted two times with ethyl acetate, after which the combined organic fractions were washed with water (10 mL) and a saturated brine solution (10 mL), dried ($MgSO_4$), filtered and evaporated. Purification through crystallization from EtOH yielded *N*-(3-hydroxycarbamoylbenzyl)-1,2,4,9-tetrahydro-3-thia-9-azafluorene **3a** (0.57 mmol, 57%) as a white-yellow powder. Note: the mixture was stirred at reflux temperature for the synthesis of hydroxamic acids **3d**, **3g** and **3m**.

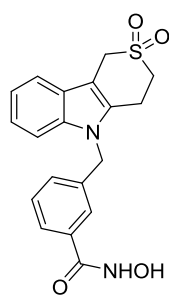### *N*-(3-Hydroxycarbamoylbenzyl)-1,2,4,9-tetrahydro-3-thia-9-azafluorene 3a (57%)

White-yellow powder. Crystallization from EtOH. Mp = 124.5 °C. ^1H NMR (400 MHz, D_6-DMSO): δ 2.90 and 3.00 (2 × 2H, 2 × t, *J* = 5.5 Hz, CH_2CH_2S); 3.84 (2H, s, $C_{quat}CH_2S$); 5.42 (2H, s, CH_2N); 7.01-7.05 (1H, m, CH_{arom}); 7.07-7.11 (2H, m, 2 × CH_{arom}); 7.36 (1H, t, *J* = 7.7 Hz, CH_{arom}); 7.42 (1H, d, *J* = 7.7 Hz, CH_{arom}); 7.48 (1H, d, *J* = 7.3 Hz, CH_{arom}); 7.54 (1H, s, CH_{arom}); 7.58 (1H, d, *J* = 7.7, CH_{arom}); 9.00 (1H, s(br), OH); 11.19 (1H, s(br), NH). ^{13}C NMR (100.6 MHz, D_6-DMSO): δ 22.7 ($C_{quat}\underline{C}H_2S$), 24.0 and 25.6 ($CH_2CH_2S$), 45.7 ($CH_2N$), 106.8 ($C_{quat,arom}$), 109.9, 118.0, 119.4, 121.5, 125.8 and 125.9 (6 × CH_{arom}), 126.7 ($C_{quat,arom}$), 129.2 and 129.5 (2 × CH_{arom}), 133.7, 135.4, 135.7 and 139.3 (4 × $C_{quat,arom}$), 164.6 (C=O). IR (ATR, cm^{-1}): v_{NHOH} = 3182; $v_{C=O}$ = 1634; v_{max} = 1584, 1464, 1417, 1345, 907, 734. MS (70 eV): m/z (%) 339 (M^++1, 100). HRMS (ESI) Anal. Calcd. for $C_{19}H_{19}N_2O_2S$ 339.1162 $[M+H]^+$, Found 339.1159.

N-(3-Hydroxycarbamoylbenzyl)-6-fluoro-1,2,4,9-tetrahydro-3-thia-9-azafluorene 3b (63%)

Yellow powder. Crystallization from diethyl ether. Mp = 190.0 °C. ^1H NMR (400 MHz, D_6-DMSO): δ 2.89 and 2.99 (2 × 2H, 2 × t, *J* = 5.4 Hz, CH_2CH_2S); 3.81 (2H, s, $C_{quat}CH_2S$); 5.42 (2H, s, CH_2N); 6.92 (1H, t × d, *J* = 9.1, 2.5 Hz, CH_{arom}); 7.07 (1H, d, *J* = 7.7 Hz, CH_{arom}); 7.26 (1H, d × d, *J* = 9.7, 2.5 Hz, CH_{arom}); 7.36 (1H, t, *J* = 7.7 Hz, CH_{arom}); 7.44 (1H, d × d, *J* = 9.1, 4.4 Hz, CH_{arom}); 7.51 (1H, s, CH_{arom}); 7.59 (1H, d, *J* = 7.7 Hz, CH_{arom}); 9.04 (1H, s(br), OH); 11.14 (1H, s(br), NH). ^{19}F NMR (376.5 MHz, D_6-DMSO): δ (-124.92)-(-124.86) (m). ^{13}C NMR (100.6 MHz, D_6-DMSO): δ 22.6 ($C_{quat}\underline{C}H_2S$), 24.2 and 25.5 ($CH_2CH_2S$), 45.9 ($CH_2N$), 103.1 (d, *J* = 23.4 Hz, CH_{arom}), 107.1 (d, *J* = 4.4 Hz, $C_{quat,arom}$), 109.3 (d, *J* = 25.8 Hz, CH_{arom}), 110.9 (d, *J* = 9.8 Hz, CH_{arom}), 125.7 and 125.9 (2 × CH_{arom}), 127.0 (d, *J* = 10.1 Hz, $C_{quat,arom}$), 129.2 and 129.4 (2 × CH_{arom}), 132.4, 133.7, 137.5 and 139.0 (4 × $C_{quat,arom}$), 157.5 (d, *J* = 232.0 Hz, $FC_{quat,arom}$), 164.5 (C=O). IR (ATR, cm^{-1}): v_{NHOH} = 3222; $v_{C=O}$ = 1581; v_{max} = 1612, 1598, 1538, 1478, 1458, 1435, 1418, 1182, 1145, 1135, 1035. MS (70 eV): m/z (%) 357 (M^++1, 100). HRMS (ESI) Anal. Calcd. for $C_{19}H_{18}FN_2O_2S$ 357.1068 $[M+H]^+$, Found 357.1062.
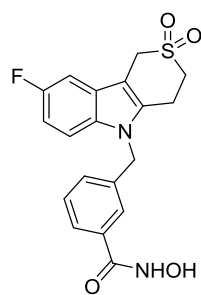
N-(3-Hydroxycarbamoylbenzyl)-1,2,4,9-tetrahydro-3-thia-9-azafluorene-3,3-dioxide 3c
(32%)

Yellow powder. Crystallization from diethyl ether. Mp = 229.5 °C. ^{1}H NMR (400 MHz, D_6-DMSO): δ 3.24 (2H, t, *J* = 6.0 Hz, C$\underline{H}_2$CH$_2$SO$_2$); 3.51 (2H, t, *J* = 6.0 Hz, CH$_2$C$\underline{H}_2$SO$_2$); 4.50 (2H, s, C$_{quat}$CH$_2$SO$_2$); 5.47 (2H, s, CH$_2$N); 7.06-7.11 (2H, m, 2 × CH$_{arom}$); 7.14-7.18 (1H, m, CH$_{arom}$); 7.37 (1H, t, *J* = 7.9 Hz, CH$_{arom}$); 7.48-7.51 (2H, m, 2 × CH$_{arom}$); 7.59-7.61 (2H, m, 2 × CH$_{arom}$); 9.04 (1H, s(br), OH); 11.22 (1H, s(br), NH). ^{13}C NMR (100.6 MHz, D_6-DMSO): δ 22.4 ($\underline{C}$H$_2$CH$_2$SO$_2$), 46.2 (CH$_2$N), 46.7 (CH$_2$$\underline{C}H_2SO_2$), 48.4 (C$_{quat}$$\underline{C}H_2SO_2$), 102.7 (C$_{quat,arom}$), 110.4, 118.2, 120.0, 122.4, 126.0 and 126.1 (6 × CH$_{arom}$), 126.6 (C$_{quat,arom}$), 129.3 and 129.5 (2 × CH$_{arom}$), 131.5, 133.8, 137.1 and 138.9 (4 × C$_{quat,arom}$), 164.5 (C=O). IR (ATR, cm^{-1}): v_{NHOH} = 3196; $v_{C=O}$ = 1641; $v_{S=O}$ = 1124, 1113; v_{max} = 1466, 1307, 1282, 1165, 1038, 744, 714. MS (70 eV): m/z (%) 371 (M$^+$+1, 95). HRMS (ESI) Anal. Calcd. for C$_{19}$H$_{19}$N$_2$O$_4$S 371.1060 [M+H]$^+$, Found 371.1066.
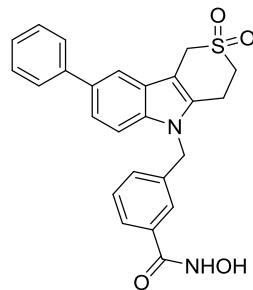
N-(3-Hydroxycarbamoylbenzyl)-6-fluoro-1,2,4,9-tetrahydro-3-thia-9-azafluorene-3,3-dioxide 3d (35%)

White powder. Crystallization from EtOH. Mp = 237.0 °C. ^{1}H NMR (400 MHz, D_6-DMSO): δ 3.23 (2H, t, *J* = 5.9 Hz, C$\underline{H}_2$CH$_2$SO$_2$); 3.50 (2H, t, *J* = 5.9 Hz, CH$_2$C$\underline{H}_2$SO$_2$); 4.48 (2H, s, C$_{quat}$CH$_2$SO$_2$); 5.47 (2H, s, CH$_2$N); 7.00 (1H, t × d, *J* = 9.1, 2.5 Hz, CH$_{arom}$); 7.08 (1H, d, *J* = 7.5 Hz, CH$_{arom}$); 7.32 (1H, d × d, *J* = 9.7, 2.5 Hz, CH$_{arom}$); 7.34-7.38 (1H, m, CH$_{arom}$); 7.50 (1H, d × d, *J* = 9.1, 4.3 Hz, CH$_{arom}$); 7.58 (1H, s, CH$_{arom}$); 7.61 (1H, d, *J* = 7.5 Hz, CH$_{arom}$); 9.05 (1H, s(br), OH); 11.21 (1H, s(br), NH). ^{19}F NMR (376.5 MHz, D_6-DMSO): δ (-124.15)-(-124.09) (m). ^{13}C NMR (100.6 MHz, D_6-DMSO): δ 22.5 ($\underline{C}$H$_2$CH$_2$SO$_2$), 46.4 (CH$_2$N), 46.6 (CH$_2$$\underline{C}H_2SO_2$), 48.3 (C$_{quat}$$\underline{C}H_2SO_2$), 102.9 (d, *J* = 4.6 Hz, C$_{quat,arom}$), 103.4 (d, *J* = 24.0 Hz, CH$_{arom}$), 110.3 (d, *J* = 26.1 Hz, CH$_{arom}$), 111.5 (d, *J* = 9.5 Hz, CH$_{arom}$), 125.9 and 126.1 (2 × CH$_{arom}$), 126.9 (d, *J* = 10.2 Hz, C$_{quat,arom}$), 129.2 and 129.4 (2 × CH$_{arom}$), 133.5, 133.7, 133.8 and 138.6 (4 × C$_{quat,arom}$), 157.7 (d, *J* = 232.9 Hz, FC$_{quat,arom}$), 164.3 (C=O). IR (ATR, cm^{-1}): v_{NHOH} = 3252; $v_{C=O}$ = 1627; $v_{S=O}$ = 1146, 1114; v_{max} = 1481, 1461, 1316, 1284, 1260, 1165, 793. MS (70 eV): m/z (%) 389 (M$^+$+1, 100). HRMS (ESI) Anal. Calcd. for C$_{19}$H$_{18}$FN$_2$O$_4$S 389.0966 [M+H]$^+$, Found 389.0967.

N-(3-Hydroxycarbamoylbenzyl)-6-phenyl-1,2,4,9-tetrahydro-3-thia-9-azafluorene-3,3-dioxide 3e (63%)

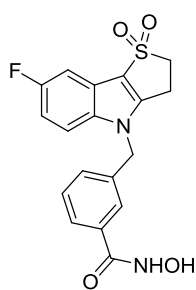White powder. Crystallization from CH$_2$Cl$_2$. Mp = 214 °C. ^{1}H NMR (400 MHz, D6-DMSO): δ 3.25 and 3.52 (2 × 2H, 2 × t, *J* = 5.8 Hz, CH$_2$CH$_2$S); 4.57 (2H, s, C$_{quat}$CH$_2$S); 5.49 (2H, s, CH$_2$N); 7.10 (1H, d, *J* = 7.4 Hz, CH$_{arom}$); 7.30-7.36 (2H, m, 2 × CH$_{arom}$); 7.44-7.48 (3H, m, 3 × CH$_{arom}$); 7.57 (1H, d, *J* = 8.6 Hz, CH$_{arom}$); 7.61-7.63 (2H, m, 2 × CH$_{arom}$); 7.70 (2H, d, *J* = 7.2 Hz, 2 × CH$_{arom}$); 7.81 (1H, s, CH$_{arom}$) 9.02 (1H, s(br), OH); 11.17 (1H, s(br), NH). ^{13}C NMR (100.6 MHz, D6-DMSO): δ 22.5 ($\underline{C}$H$_2$CH$_2$S), 46.4 (CH$_2$N), 46.7 (CH$_2$$\underline{C}H_2$S), 48.5 (C$_{arom,quat}$$\underline{C}H_2$S), 103.2 (C$_{arom,quat}$), 110.8, 116.5, 121.6, 125.7, 126.0 and 126.9 (6 × CH$_{arom}$), 127.17 (C$_{arom,quat}$), 127.20 (2 × CH$_{arom}$), 129.1, 129.2 and 129.3 (4 × CH$_{arom}$), 132.3, 132.5, 134.2, 136.7, 138.6 and 141.8 (6 × C$_{arom,quat}$), 164.0 (C=O). IR (ATR, cm^{-1}): $v_{NH/OH}$ = 3240; $v_{C=O}$ = 1614; $v_{S=O}$ = 1116; v_{max} = 1583, 1472, 1315, 1283, 1164, 1044, 889, 806, 762, 724, 698. MS (70eV): m/z (%) 447 (M$^+$+1, 85). HRMS (ESI) Anal. Calcd. for C$_{25}$H$_{23}$N$_2$O$_4$S 447.1373 [M+H]$^+$, Found 447.1361.

N-(3-Hydroxycarbamoylbenzyl)-2,3-dihydrothieno[3,2-*b*]indole-1,1-dioxide 3f (25%)
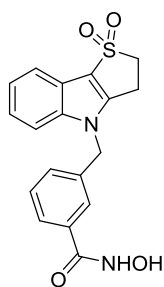
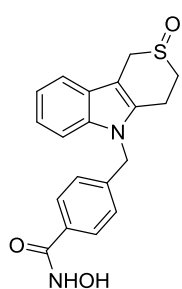White powder. Crystallization from EtOH. Mp = 236.5 °C. ^{1}H NMR (400 MHz, D$_6$-DMSO): δ 3.47 (2H, t, *J* = 6.5 Hz, C$\underline{H}_2$CH$_2$SO$_2$); 3.96 (2H, t, *J* = 6.5 Hz, CH$_2$C$\underline{H}_2$SO$_2$); 5.50 (2H, s, CH$_2$N); 7.22-7.34 (3H, m, 3 × CH$_{arom}$); 7.43 (1H, t, *J* = 7.9 Hz, CH$_{arom}$); 7.58-7.61 (2H, m, 2 × CH$_{arom}$); 7.65-7.66 (2H, m, 2 × CH$_{arom}$); 9.04 (1H, s(br), OH); 11.24 (1H, s(br), NH). ^{13}C NMR (100.6 MHz, D$_6$-DMSO): δ 21.0 ($\underline{C}$H$_2$CH$_2$SO$_2$), 47.1 (CH$_2$N), 57.4 (CH$_2\underline{C}$H$_2$SO$_2$), 112.3 (CH$_{arom}$), 116.1 (C$_{quat,arom}$), 118.7 (CH$_{arom}$), 119.3 (C$_{quat,arom}$), 122.5, 123.9, 126.3, 126.6, 129.4 and 130.3 (6 × CH$_{arom}$), 133.8, 137.4, 141.0 and 148.5 (4 × C$_{quat,arom}$), 164.3 (C=O). IR (ATR, cm^{-1}): ν$_{NHOH}$ = 3330; ν$_{C=O}$ = 1655; ν$_{S=O}$ = 1123, 1108; ν$_{max}$ = 2954, 2921, 2853, 1584, 1544, 1474, 1443, 1374, 1326, 1269, 1235, 1036, 1018, 914, 744, 702. MS (70 eV): m/z (%) 357 (M$^+$+1, 100). HRMS (ESI) Anal. Calcd. for C$_{18}$H$_{17}$N$_2$O$_4$S 357.0904 [M+H]$^+$, Found 357.0907.

N-(3-Hydroxycarbamoylbenzyl)-7-fluoro-2,3-dihydrothieno[3,2-*b*]indole-1,1-dioxide 3g (40%)

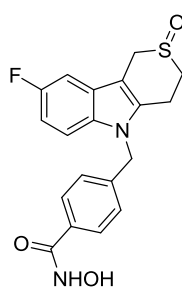White powder. Crystallization from diethyl ether. Mp > 260.0 °C. ^{1}H NMR (400 MHz, D$_6$-DMSO): δ 3.47 (2H, t, *J* = 6.5 Hz, C$\underline{H}_2$CH$_2$SO$_2$); 3.96 (2H, t, *J* = 6.5 Hz, CH$_2$C$\underline{H}_2$SO$_2$); 5.51 (2H, s, CH$_2$N); 7.17 (1H, t × d, *J* = 9.2, 2.5 Hz, CH$_{arom}$); 7.33 (1H, d, *J* = 7.8 Hz, CH$_{arom}$); 7.38-7.45 (2H, m, 2 × CH$_{arom}$); 7.61 (1H, d × d, *J* = 9.2, 4.3 Hz, CH$_{arom}$); 7.65-7.67 (2H, m, 2 × CH$_{arom}$); 9.04 (1H, s(br), OH); 11.23 (1H, s(br), NH). ^{19}F NMR (376.5 MHz, D$_6$-DMSO): δ (-120.64)-(-120.58) (m). ^{13}C NMR (100.6 MHz, D$_6$-DMSO): δ 21.1 ($\underline{C}$H$_2$CH$_2$SO$_2$), 47.3 (CH$_2$N), 57.3 (CH$_2\underline{C}$H$_2$SO$_2$), 104.2 (d, *J* = 25.4 Hz, CH$_{arom}$), 112.0 (d, *J* = 25.8 Hz, CH$_{arom}$), 113.8 (d, *J* = 9.7 Hz, CH$_{arom}$), 116.1 (d, *J* = 4.4 Hz, C$_{quat,arom}$), 119.5 (d, *J* = 11.2 Hz, C$_{quat,arom}$), 126.3, 126.7, 129.5 and 130.3 (4 × CH$_{arom}$), 133.9, 137.2, 137.6 and 150.1 (4 × C$_{quat,arom}$), 158.7 (d, *J* = 236.6 Hz, FC$_{quat,arom}$), 164.3 (C=O). IR (ATR, cm^{-1}): ν$_{NHOH}$ = 3238; ν$_{C=O}$ = 1630; ν$_{S=O}$ = 1126, 1109; ν$_{max}$ = 1585, 1482, 1442, 1276, 1145, 692. MS (70 eV): m/z (%) 375 (M$^+$+1, 87). HRMS (ESI) Anal. Calcd. for C$_{18}$H$_{16}$FN$_2$O$_4$S 375.0809 [M+H]$^+$, Found 375.0810.

### *N*-(3-Hydroxycarbamoylbenzyl)-7-bromo-2,3-dihydrothieno[3,2-*b*]indole-1-oxide 3h (70%)
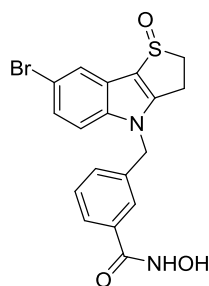
White powder. Crystallization from CH$_2$Cl$_2$. Mp = 218.5 °C. ^{1}H NMR (400 MHz, D6-DMSO): δ 3.24-3-31, 3.36-3.43, 3.57-3.64 and 4.00-4.07 (4 × 1H, 4 × m, CH$_2$CH$_2$S); 5.51 and 5.57 (2 × 1H, 2 × d, *J* = 16.3 Hz, CH$_2$N); 7.31 (1H, d, *J* = 7.9 Hz, CH$_{arom}$); 7.38 (1H, d × d, *J* = 8.8, 1.9 Hz, CH$_{arom}$); 7.42 (1H, t, *J* = 7.9 Hz, CH$_{arom}$); 7.56 (1H, d, *J* = 8.8 Hz, CH$_{arom}$); 7.64-7.66 (2H, m, 2 × CH$_{arom}$); 7.90 (1H, d, *J* = 1.9 Hz, CH$_{arom}$); 9.04 (1H, s(br), OH); 11.23 (1H, s(br), NH). ^{13}C NMR (100.6 MHz, D6-DMSO): δ 23.9 ($\underline{C}$H$_2$CH$_2$S), 48.5 (CH$_2$N), 58.5 (CH$_2\underline{C}$H$_2$S), 114.1 (CH$_{arom}$), 114.6 and 120.4 (2 × C$_{arom,quat}$), 121.2 (CH$_{arom}$), 124.4 (C$_{arom,quat}$), 125.5, 126.3, 126.6, 129.4 and 130.2 (5 × CH$_{arom}$), 133.9, 137.4, 140.2 and 154.6 (4 × C$_{arom,quat}$), 166.3 (C=O). IR (ATR, cm^{-1}): ν$_{NH/OH}$ = 3235; ν$_{C=O}$ = 1646; ν$_{S=O}$ = 987; ν$_{max}$ = 1604, 1588, 1531, 1478, 1428, 1353, 1328, 1135, 955, 921, 791, 741, 704. MS (70eV): m/z (%) 419/21 (M$^+$+1, 100). HRMS (ESI) Anal. Calcd. for C$_{18}$H$_{16}$BrN$_2$O$_3$S 419.0060 [M+H]$^+$, Found 419.0056.

N-(4-Hydroxycarbamoylbenzyl)-1,2,4,9-tetrahydro-3-thia-9-azafluorene-3-oxide 3i (13%)
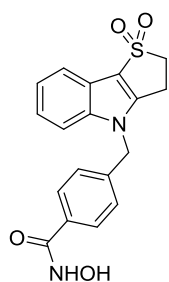
White powder. Crystallization from ethanol. Mp = 258.5 °C. ^{1}H NMR (400 MHz, D$_6$-DMSO): δ 3.02-3.16 and 3.32-3.38 (3H and 1H, 2 × m, CH$_2$CH$_2$SO); 4.03 and 4.22 (2 × 1H, 2 × d, J = 15.2 Hz, C$_{quat}$(HCH)SO); 5.48 (2H, s, CH$_2$N); 7.04-7.15 (4H, m, 4 × CH$_{arom}$); 7.44 (1H, d, J = 8.1 Hz, CH$_{arom}$); 7.51 (1H, d, J = 7.6 Hz, CH$_{arom}$); 7.66 (2H, d, J = 8.2 Hz, 2 × CH$_{arom}$); 9.00 (1H, s(br), OH); 11.14 (1H, s(br), NH). ^{13}C NMR (100.6 MHz, D$_6$-DMSO): δ 16.6 and 43.9 (CH$_2$CH$_2$SO), 44.8 (C$_{quat}$CH$_2$SO), 45.9 (CH$_2$N), 99.7 (C$_{quat,arom}$), 110.1, 118.1, 119.8 and 122.0 (4 × CH$_{arom}$), 126.8 (2 × CH$_{arom}$), 127.6 (C$_{quat,arom}$), 127.7 (2 × CH$_{arom}$), 132.3, 133.2, 136.7 and 141.7 (4 × C$_{quat,arom}$), 164.4 (C=O). IR (ATR, cm^{-1}): ν$_{NHOH}$ = 3172; ν$_{C=O}$ = 1639; ν$_{S=O}$ = 1014; ν$_{max}$ = 1465, 1314, 896, 743. MS (70 eV): m/z (%) 355 (M$^+$+1, 100). HRMS (ESI) Anal. Calcd. for C$_{19}$H$_{19}$N$_2$O$_3$S 355.1111 [M+H]$^+$, Found 255.1112.

N-(4-Hydroxycarbamoylbenzyl)-6-fluoro-1,2,4,9-tetrahydro-3-thia-9-azafluorene-3-oxide 3j (28%)
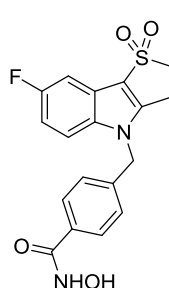
White powder. Crystallization from ethanol. Mp = 244.5 °C. ^{1}H NMR (400 MHz, D$_6$-DMSO): δ 3.01-3.15 and 3.28-3.38 (3H and 1H, 2 × m, CH$_2$CH$_2$SO); 4.02 and 4.17 (2 × 1H, 2 × d, J = 15.6 Hz, C$_{quat}$(HCH)SO); 5.44 (2H, s, CH$_2$N); 6.95 (1H, t × d, J = 9.0, 2.5 Hz, CH$_{arom}$); 7.09 (2H, d, J = 8.2 Hz, 2 × CH$_{arom}$); 7.32 (1H, d × d, J = 9.7, 2.5 Hz, CH$_{arom}$); 7.45 (1H, d × d, J = 9.0, 4.3 Hz, CH$_{arom}$); 7.67 (2H, d, J = 8.2 Hz, 2 × CH$_{arom}$); 9.00 (1H, s(br), OH); 11.15 (1H, s(br), NH). ^{19}F NMR (376.5 MHz, D$_6$-DMSO): δ (-124.45)-(-124.39) (m). ^{13}C NMR (100.6 MHz, D$_6$-DMSO): δ 16.5 and 43.7 (CH$_2$CH$_2$SO), 44.6 (C$_{quat}$CH$_2$SO), 46.0 (CH$_2$N), 100.0 (d, J = 4.3 Hz, C$_{quat,arom}$), 103.3 (d, J = 23.7 Hz, CH$_{arom}$), 109.8 (d, J = 26.1 Hz, CH$_{arom}$), 111.2 (d, J = 9.7 Hz, CH$_{arom}$), 126.8 (2 × CH$_{arom}$), 127.8 (2 × CH$_{arom}$), 128.0 (d, J = 10.0 Hz, C$_{quat,arom}$), 132.4, 133.3, 135.3 and 141.5 (4 × C$_{quat,arom}$), 157.7 (d, J = 231.9 Hz, FC$_{quat,arom}$), 164.4 (C=O). IR (ATR, cm^{-1}): ν$_{NHOH}$ = 3180; ν$_{C=O}$ = 1636; ν$_{S=O}$ = 1013; ν$_{max}$ = 1480, 1459, 1414, 1307, 1143, 1123, 895, 848, 796. MS (70 eV): m/z (%) 373 (M$^+$+1, 100). HRMS (ESI) Anal. Calcd. for C$_{19}$H$_{18}$FN$_2$O$_3$S 373, 1017 [M+H]$^+$, Found 373.1014.

N-(4-Hydroxycarbamoylbenzyl)-6-bromo-1,2,4,9-tetrahydro-3-thia-9-azafluorene-3,3-dioxide 3k (70%)
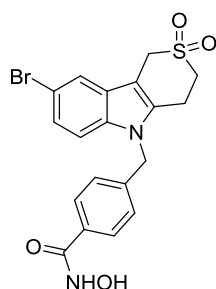
White powder. Crystallization from CH$_2$Cl$_2$. Mp = 230.0 °C. ^{1}H NMR (400 MHz, D$_6$-DMSO): δ 3.22 and 3.51 (2 × 2H, 2 × t, J = 5.9 Hz, CH$_2$CH$_2$S); 4.51 (2H, s, C$_{quat}$CH$_2$S); 5.50 (2H, s, CH$_2$N); 7.07 (2H, d, J = 8.2 Hz, 2 × CH$_{arom}$); 7.27 (1H, d × d, J = 8.7, 1.7 Hz, CH$_{arom}$); 7.47 (1H, d, J = 8.7 Hz, CH$_{arom}$); 7.67 (2H, d, J = 8.2 Hz, 2 × CH$_{arom}$); 7.75 (1H, d, J = 1.7 Hz, CH$_{arom}$); 9.01 (1H, s(br), OH); 11.16 (1H, s(br), NH). ^{13}C NMR (100.6 MHz, D$_6$-DMSO): δ 22.4 (CH$_2$CH$_2$S), 46.2 (CH$_2$N), 46.5 (CH$_2$CH$_2$S), 48.2 (C$_{arom,quat}$CH$_2$S), 102.7 (C$_{arom,quat}$), 112.5 (CH$_{arom}$), 112.7 (C$_{arom,quat}$), 120.8, 124.8, 126.8 and 127.8 (6 × CH$_{arom}$), 128.3, 132,5, 133.3, 135.8 and 141.2 (5 × C$_{arom,quat}$), 164.3 (C=O). IR (ATR, cm^{-1}): ν$_{NH/OH}$ = 3371; ν$_{C=O}$ = 1645; ν$_{S=O}$ = 1114; ν$_{max}$ = 1533, 1463, 1428, 1348, 1312, 1284, 1240, 1163, 1013, 885, 864, 852, 798, 779, 762, 700, 662. MS (70eV): m/z (%) 449/51 (M$^+$+1, 5). HRMS (ESI) Anal. Calcd. for C$_{19}$H$_{18}$BrN$_2$O$_4$S 449.0165 [M+H]$^+$, Found 449.0148.

N-(4-Hydroxycarbamoylbenzyl)-2,3-dihydrothieno[3,2-*b*]indole-1,1-dioxide 3l (25%)

White powder. Crystallization from ethanol. Mp = 198.0 °C. ^{1}H NMR (400 MHz, D$_6$-DMSO): δ 3.46 (2H, t, *J* = 6.3 Hz, CH$_2$CH$_2$SO$_2$); 3.96 (2H, t, *J* = 6.3 Hz, CH$_2$CH$_2$SO$_2$); 5.51 (2H, s, CH$_2$N); 7.22-7.30 (4H, m, 4 × CH$_{arom}$); 7.56-7.61 (2H, m, 2 × CH$_{arom}$); 7.71 (2H, d, *J* = 8.2 Hz, 2 × CH$_{arom}$); 9.03 (1H, s(br), OH); 11.17 (1H, s(br), NH). ^{13}C NMR (100.6 MHz, D$_6$-DMSO): δ 20.9 (CH$_2$CH$_2$SO$_2$), 47.0 (CH$_2$N), 57.4 (CH$_2$CH$_2$SO$_2$), 112.3 (CH$_{arom}$), 116.1 (C$_{quat,arom}$), 118.7 (CH$_{arom}$), 119.3 (C$_{quat,arom}$), 122.5 and 123.9 (2 × CH$_{arom}$), 127.5 (2 × CH$_{arom}$), 127.9 (2 × CH$_{arom}$), 132.7, 140.1, 140.9 and 148.5 (4 × C$_{quat,arom}$), 164.2 (C=O). IR (ATR, cm^{-1}): ν$_{NHOH}$ = 3316; ν$_{C=O}$ = 1668; ν$_{S=O}$ = 1123, 1094; ν$_{max}$ = 1446, 1436, 1412, 1260, 1012, 749. MS (70 eV): m/z (%) 357 (M$^+$+1, 33); 374 (M+NH$_4^+$, 100). HRMS (ESI) Anal. Calcd. for C$_{18}$H$_{17}$N$_2$O$_4$S 357.0904 [M+H]$^+$, Found 357.0900.

N-(4-Hydroxycarbamoylbenzyl)-7-fluoro-2,3-dihydrothieno[3,2-*b*]indole-1,1-dioxide 3m (5%)

White powder. Crystallization from diethyl ether. Mp = 240.5 °C. ^{1}H NMR (400 MHz, D$_6$-DMSO): δ 3.47 (2H, t, *J* = 6.5 Hz, CH$_2$CH$_2$SO$_2$); 3.96 (2H, t, *J* = 6.5 Hz, CH$_2$CH$_2$SO$_2$); 5.51 (2H, s, CH$_2$N); 7.16 (1H, t × d, *J* = 9.2, 2.5 Hz, CH$_{arom}$); 7.29 (2H, d, *J* = 8.2 Hz, 2 × CH$_{arom}$); 7.40 (1H, d × d, *J* = 9.1, 2.5 Hz, CH$_{arom}$); 7.60 (1H, d × d, *J* = 9.2, 4.3 Hz, CH$_{arom}$); 7.72 (2H, d, *J* = 8.2 Hz, 2 × CH$_{arom}$); 9.03 (1H, s(br), OH); 11.19 (1H, s(br), NH). ^{19}F NMR (376.5 MHz, D$_6$-DMSO): δ (-120.60)-(-120.54) (m). ^{13}C NMR (100.6 MHz, D$_6$-DMSO): δ 21.0 (CH$_2$CH$_2$SO$_2$), 47.2 (CH$_2$N), 57.3 (CH$_2$CH$_2$SO$_2$), 104.3 (d, *J* = 25.3 Hz, CH$_{arom}$), 112.0 (d, *J* = 26.2 Hz, CH$_{arom}$), 113.7 (d, *J* = 9.8 Hz, CH$_{arom}$), 116.2 (d, *J* = 5.3 Hz, C$_{quat,arom}$), 119.5 (d, *J* = 11.1 Hz, C$_{quat,arom}$), 127.5 (2 × CH$_{arom}$), 127.9 (2 × CH$_{arom}$), 132.8, 137.6, 139.9 and 150.1 (4 × C$_{quat,arom}$), 158.7 (d, *J* = 235.5 Hz, FC$_{quat,arom}$), 164.2 (C=O). IR (ATR, cm^{-1}): ν$_{NHOH}$ = 3417; ν$_{C=O}$ = 1614; ν$_{S=O}$ = 1127, 1110; ν$_{max}$ = 3092, 1476, 1441, 1282, 1144, 853, 806, 699. MS (70 eV): m/z (%) 392 (M+NH$_4^+$, 100). HRMS (ESI) Anal. Calcd. for C$_{18}$H$_{19}$FN$_3$O$_4$S 392.1075 [M+NH$_4$]$^+$, Found 392.1075.

4. Synthesis of benzothiophene-based hydroxamic acids as potent and selective HDAC6 inhibitors

Abstract: *A small library of 3-[(4-hydroxycarbamoylphenyl)aminomethyl]benzothiophenes was prepared and assessed as a novel class of HDAC6 inhibitors, leading to the identification of three representatives as potent and selective HDAC6 inhibitors. Further tests with regard to inflammatory responses indicated that HDAC6 inhibition can be uncoupled from transcriptional inhibition at the level of activated NF-κB, AP-1, and GR.*

4.1. Introduction

The research field dealing with histone deacetylases (HDACs) has expanded rapidly in recent years, initiated by the original identification of HDAC1 in 1996.[110] Although HDACs were initially recognized as enzymes responsible for the removal of acetyl groups from ε-*N*-acetylated lysine residues of histones, it is now established that HDACs1-11 not only employ histones as substrates but also many non-histone proteins (hormone receptors, chaperone proteins, transcription factors,. . .).[3,111] In that respect, HDACs are sometimes referred to as lysine deacetylases to better reflect their substrate scope.[5] Although HDAC inhibitors recently emerged as promising new drugs, the consequences of inhibiting this family of enzymes are not yet fully understood, and potential toxicities associated with non-selective inhibitors hamper their clinical usefulness.[75,112] Of particular interest is the mainly cytoplasmic deacetylase HDAC6, as inhibition of this HDAC isoform is believed to be accompanied by minimal toxicity to the cell.[11] Furthermore, its impact on various cellular functions, such as arranging the acetylation status of α-tubulin and Hsp90, has contributed to the rise of HDAC6 as an attractive drug target for the treatment of *e.g.* neurodegenerative disorders, autoimmunity and cancer.[113] The development of potent and selective HDAC6 inhibitors thus represent an important challenge in chemical research, as witnessed by the high interest of scientists active in diverse therapeutic fields (oncology, immunology, neurology,. . .) and the pharmaceutical industry in new HDAC6 inhibitors.

HDAC inhibitors are typically composed of a zinc-binding group (ZBG), a linker and a group for protein surface recognition or interaction (cap group). The hydroxamate functional group has amply proven its good zinc chelating properties, as exemplified by the marketed hydroxamate suberanilohydroxamic acid (SAHA, Zolinza, vorinostat). Recent studies have also shown that a branched sp_2 carbon atom in α-position with respect to the hydroxamate ZBG gives rise to a good HDAC6 selectivity profile.[23] This has been confirmed by different recently developed HDAC6 selective inhibitors with an *N*-hydroxybenzamide group in their molecular structure.[13,24,31,32,38,104] On the other hand, exploring the chemical space with regard to the cap groups seems to provide an excellent anchor point within the quest for new HDAC6 inhibitors. In that respect, the evaluation of benzothiophene as a template for cap group design could provide new opportunities. Benzothiophene is more hydrophobic as compared to the 'privileged' scaffolds indole and benzofuran, and this hydrophobic character could possibly allow for an improved binding profile since the protein surface in the area of the cap group accommodates several hydrophobic amino acid residues. The known use of benzothiophene as a scaffold in drug development, for example as a central part in the commercial pharmaceuticals raloxifene, zileuton, and sertaconazole, further supported the selection of this heterocycle as a building block to develop new bioactive molecules. Furthermore,

benzothiophene has been used as a cap group in a cinnamyl hydroxamide scaffold for HDAC inhibition, where it showed interesting potency.[114]

In this part, the synthesis and evaluation of 3-[(4-hydroxycarbamoylphenyl)-aminomethyl]benzothiophenes **1** as a new class of potential HDAC6 inhibitors was proposed (Figure 1). A short linker between the benzothiophene ring and the benzenehydroxamic acid should account for optimal interactions with the surface of the enzyme, and the presence of a nitrogen atom could be employed as a handle for further derivatization.
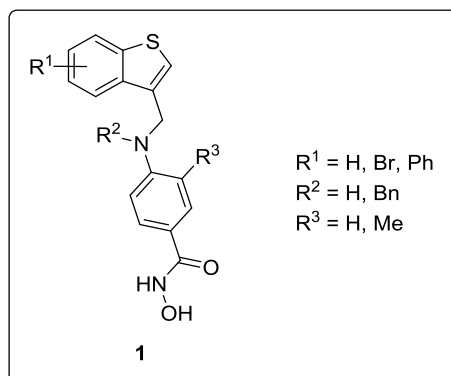
Figure 1. Proposed new family of benzothiophene-based hydroxamic acids as potential HDAC6 inhibitors.

4.2. Synthesis and biological evaluation of benzothiophene-based benzohydroxamic acids

In order to explore the theoretical potential of these new compounds *in silico*, a set of representative virtual structures was subjected to docking studies. These studies acknowledged the inhibitory potential of structures **1** and revealed that expansion of the cap group (R^1 = Ph) and the introduction of a benzylic group (R^2 = Bn) could result in a more complete occupation of the binding pocket (Figure 2). Three new compounds were also subjected toward docking studies in the catalytic pocket of HDAC2 and 4 to address the selectivity *in silico*. This revealed a clear preference for HDAC6, with significantly lower affinities for the other isoforms (more information can be found in the experimental details).
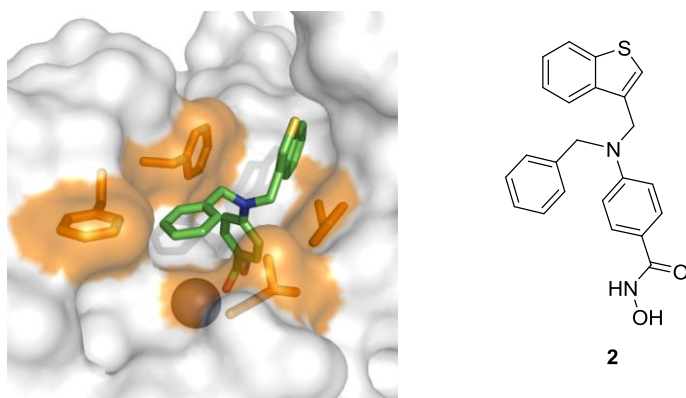

Figure 2. Docking of *N*-benzyl substituted hydroxamic acid **2** in a homology model of HDAC6 (green = carbon, blue = nitrogen, red = oxygen, yellow = sulfur, magenta = zinc) and presence of the hydrophobic amino acid residues in the vicinity of the catalytic pocket (orange, Phe620, Phe679, Phe680 and Leu749).

Given the *in silico* predicted good affinities, the focus was pointed toward the synthesis of this family of structures **1**. In addition, the indole counterpart of the 'mother' structure was pursued as well to verify the hypothesis that the protein surface close to the cap group preferably binds to a more hydrophobic scaffold. Finally, also the influence of a methyl group in the aromatic linker part was assessed.

To that end, the commercially available benzothiophene-3-carbaldehyde **3a** (R^1 = H) and 5-bromobenzothiophene-3-carbaldehyde **3b** (R^1 = Br) were used as substrates. First, 5-phenylbenzothiophene-3-carbaldehyde **4** was prepared via a Suzuki-Miyaura cross-coupling using 5-bromobenzothiophene **3b**, Pd(PPh$_3$)$_4$, phenylboronic acid and Na$_2$CO$_3$ in a toluene/EtOH/H$_2$O (2/1/1) mixture. Reductive amination of carbaldehydes **3a-b** and **4** employing methyl 4-aminobenzoates and NaCNBH$_3$ resulted in the synthesis of methyl 4-aminobenzoate esters **5a-d**.[114] Secondary amines **5a-c** were further *N*-benzylated using benzyl bromide and NaH in DMF to give tertiary amines **6a-c**. As a last step, hydroxamic acids

7a-d and **8a-c** were synthesized upon treatment of methyl esters **5a-d** and **6a-c** with an excess of hydroxyl amine and potassium hydroxide in THF (Scheme 1).
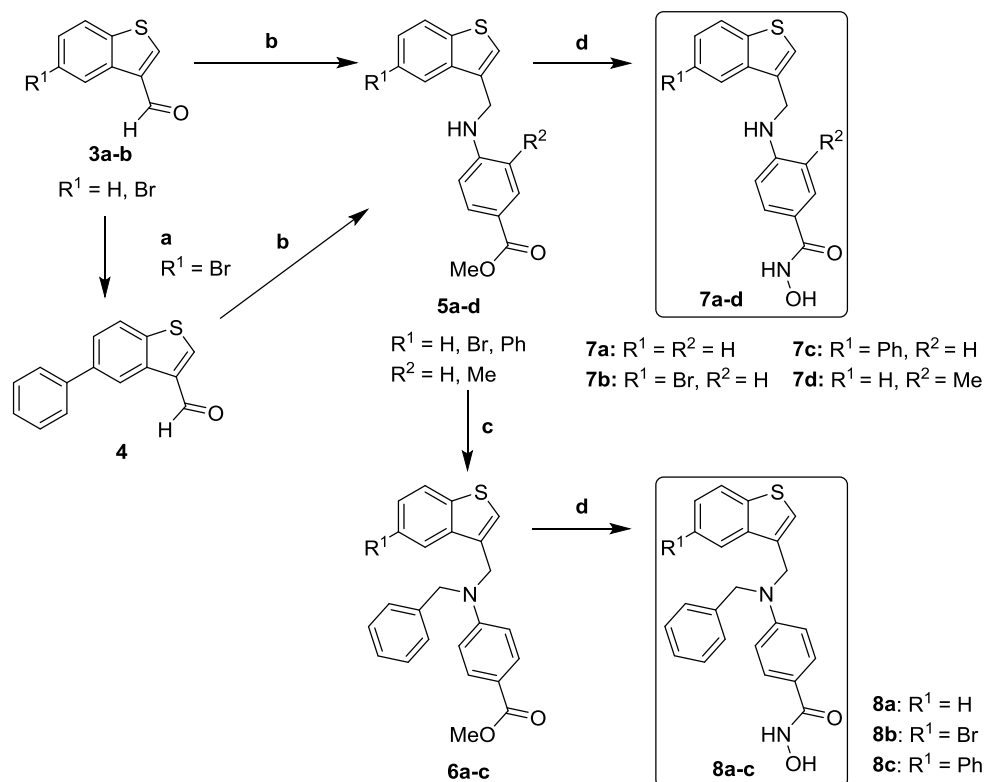
Scheme 1. **a:** phenylboronic acid (2 equiv), Na_2CO_3 (6.5 equiv), $Pd(PPh_3)_4$ (4 mol %), toluene/ethanol/H_2O (2/1/1), Δ, 8h, N_2, 72%. **b**: methyl 4-aminobenzoate or methyl 4-amino-3-methylbenzoate (1.2 equiv), glacial acetic acid (5 equiv), ethanol or ethanol/CH_2Cl_2, Δ, 1h -> $NaCNBH_3$ (3 equiv), 0°C -> r.t., 1h, 50-75%. **c**: NaH (60% in mineral oil, 1.2 equiv), DMF, r.t., 30' -> benzyl bromide (2 equiv), KI (5 mg), 2h, r.t., 65-79%. **d:** NH_2OH (50% in H_2O, 100 equiv), KOH (4M in MeOH, 50 equiv), THF, r.t., 10', 13-85%.

The synthesis of the second group of substituted benzothiophene-based hydroxamic acids commenced with the bromination of benzothiophene-3-carbaldehyde **3a** in CH_3CN to yield 6-bromobenzothiophene-3-carbaldehyde **9** as the main isomer (60%, ^{1}H NMR, $CDCl_3$) in an isolated yield of 40%.[115] The latter aldehyde **9** was subjected to the same strategy as described above (involving (b) Suzuki-Miyaura coupling, (c) reductive amination, (d) *N*-benzylation, and (e) ester to hydroxamic acid conversion) and provided novel compounds **10**, **11a-b**, **12a-b**, **13a-b** and **14a-b** (Scheme 2).
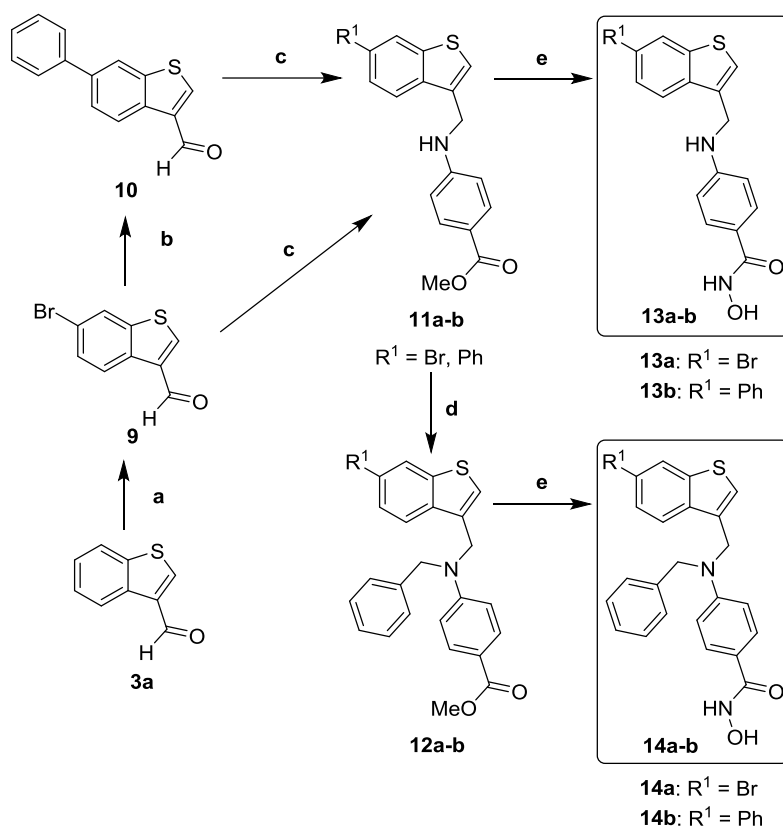
Scheme 2. a: Br$_2$ (5 equiv), CH$_3$CN, r.t., 18h, 40%. **b**: phenylboronic acid (2 equiv), Na$_2$CO$_3$ (6.5 equiv), Pd(PPh$_3$)$_4$ (4 mol %), toluene/ethanol/H$_2$O (2/1/1), Δ, 8h, N$_2$, 96%. **c**: methyl 4-aminobenzoate (1.2 equiv), glacial acetic acid (5 equiv), ethanol, Δ, 1h -> NaCNBH$_3$ (3 equiv), 0°C -> r.t., 1h, 50-66%. **d**: NaH (60% in mineral oil, 1.2 equiv), DMF, r.t., 30' -> benzyl bromide (2 equiv), KI (5 mg), 2h, r.t., 87-91%. **e**: NH$_2$OH (50% in H$_2$O, 100 equiv), KOH (4M in MeOH, 50 equiv), THF, r.t., 10', 56-80%.

Application of these strategies (Scheme 1 and 2) thus resulted in a small set of eleven novel benzothiophene-based hydroxamic acids with potential HDAC6 inhibitory activity. The short and easy synthetic route toward these compounds provides an added value in terms of upscaling and industrial synthesis.

Several attempts to obtain **18** as the indole counterpart of benzothiophene **7a** starting from indole-3-carbaldehyde **15** using the procedure described above failed at the imination stage. However, a Dean Stark-mediated procedure using a catalytic amount of *p*TsOH did effect the desired imination, and NaBH$_4$-assisted reduction of the latter imine then afforded the indole-based methyl 4-aminobenzoate ester **17**. Finally, ester to hydroxamic acid conversion produced the desired target structure **18** in a good yield (Scheme 3).
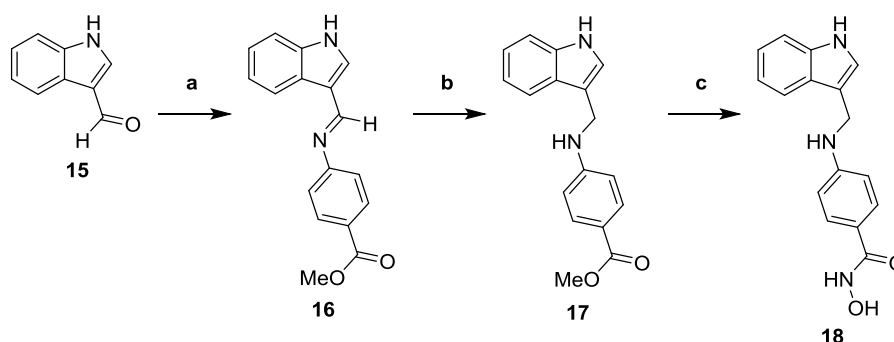
Scheme 3. a: methyl 4-aminobenzoate (1.2 equiv), *p*-toluenesulfonic acid monohydrate (0.05 equiv), toluene, Dean Stark, 18h, 85%. **b:** NaBH$_4$ (5 equiv), MeOH, Δ, 90', 88%. **c:** NH$_2$OH (50% in H$_2$O, 100 equiv), KOH (4M in MeOH, 50 equiv), THF, r.t., 10', 77%.

In vitro studies of novel hydroxamic acids **7a-d**, **8a-c**, **13a-b**, **14a-b** and **18** with regard to their HDAC6 inhibitory activity revealed interesting SAR information (Table 1). Surprisingly, and in contrast with the predicted binding mode in Figure 2, *N*-benzylation of secondary amines drastically reduced the inhibitory activity. The same holds for the introduction of a phenyl group on the benzothiophene ring and a methyl group in the linker. The indole-containing hydroxamic acid **18** showed promising HDAC6 inhibitory activity with an IC$_{50}$ value of 0.2 µM, albeit considerably less as compared to its benzothiophene counterpart **7a** (IC$_{50}$ = 0.014 µM).

Table 1. *In vitro* pharmacological data: HDAC6 inhibition[a]

Compound	R^1	R^2	% Inhibition (10 µM)	IC$_{50}$ (µM)
7a	H	H	99.8	0.014
7b	Br	H	99.2	0.037
7c	Ph	H	95.1	0.31
7d	H	Me	73.4	2.4
8a	H	-	89.9	0.47
8b	Br	-	84.9	0.85
8c	Ph	-	47.9	N.D.[b]
13a	Br	-	99.3	0.064
13b	Ph	-	89.8	0.66
14a	Br	-	70.7	2.1
14b	Ph	-	61.1	N.D.[b]
18	-	-	99.0	0.2

[a] Reference compound: Trichostatin A (IC$_{50}$ = 0.014 µM) [b] Not Determined (< 70% inhibition at 10 µM)

The selectivity of the most potent HDAC6 inhibitors **7a**, **7b** and **13a** was then assessed through screening of their affinity toward all zinc-containing HDAC isozymes (Table 2). These results reveal an explicit selectivity profile for all three molecules taking their low nanomolar HDAC6

IC$_{50}$ values (< 100 nM) and micromolar IC$_{50}$ values for all other HDAC isozymes into account. The least pronounced selectivity is observed toward HDAC8, which is in line with the activity of other HDAC6 inhibitors.[13,24,31,32,38,104] For example, Tubastatin A (HDAC6 IC$_{50}$ = 0.015 µM) displays a high selectivity against all HDAC isozymes except for HDAC8, where it has only a 57-fold selectivity (data compared with literature data).[10] In that respect, benzothiophene **7a** (HDAC6 IC$_{50}$ = 0.014 µM) performs very well with a 100-fold selectivity toward HDAC8 and high selectivities toward all other HDAC isoforms.

Table 2. *In vitro* enzyme inhibition data: IC$_{50}$ values for **7a**, **7b** and **13a** toward HDAC1-11 (µM)[a,b]

Compound	1	2	3	4	5
7a	7.5	30	10	10	17
7b	>10	N.C.	>10	N.C.	N.C.
13a	3.4	20	6.6	31	45
Tub A	16.4	>30	>30	>30	>30
6	**7**	**8**	**9**	**10**	**11**
0.014	5.2	1.4	7.1	9.9	31
0.037	>10	2.1	N.C.	33	15
0.064	12	1.9	25	7.6	1.2
0.015	>30	0.85	>30	>30	>30

[a] Reference compound: trichostatin A. N.C.: IC$_{50}$ value not calculable. Concentration-response curve shows less than 25% effect at the highest validated testing concentration (100 µM). Conc.: IC$_{50}$ value above the highest test concentration. Concentration-response curve shows less than 50% effect at the highest validated testing concentration (100 µM). [b] Literature values for Tub A (Tubastatin A)[13], caution should be taken when comparing the IC$_{50}$ values of **7a**, **7b** and **13a** to the literature values for Tubastatin A.

Next, the ability of the most potent HDAC6 inhibitors **7a**, **7b** and **13a** to modify the acetylation level of α-tubulin in Neuro-2a cells was compared with Tubastatin A. Neuro-2a cells were treated overnight with different concentrations of the HDAC6 inhibitors and the effect on the acetylation level of α-tubulin was determined using Western Blots (Figure 3). These results showed that compounds **7a**, **7b** and **13a** have the same effect on the acetylation level of α-tubulin as Tubastatin A, proving that the compounds inhibit the deacetylation of acetylated α-tubulin in a more complex cellular environment.
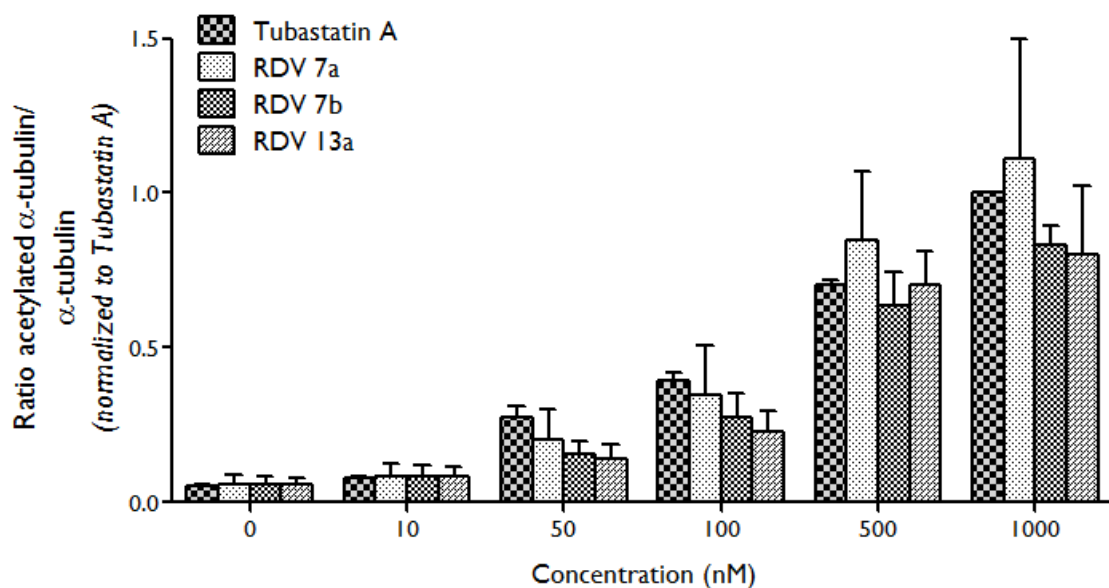
Figure 3. Potency of inhibiting the deacetylation of acetylated α-tubulin by compounds **7a**, **7b**, **13a** and Tubastatin A in Neuro-2a cells. ImageQuant TL version 7.0-software was used to quantify the blots.

HDAC6 is known to regulate Hsp90 acetylation and consequently also controls the chaperone-dependent activation of the glucocorticoid receptor, GR.[116] This means that hypoacetylated Hsp90 complexes with the GR and assists the translocation of the GR to the nucleus when a glucocoticoid binds the GR. Hyperacetylated Hsp90 (due to the absence or inhibition of HDAC6) on the contrary is not able to bind the GR and therefore the transcriptional activation of the GR is compromised. To study whether compounds **7a**, **7b** and **13a** exhibit a direct effect on the transcriptional activity of GR, we used a glucocorticoid response element-dependent promoter fragment coupled to luciferase, stably integrated in A549 cells (adenocarcinomic human alveolar basal epithelial cells). As expected, the strong GR agonist dexamethasone (DEX) is able to activate the reporter gene (Figure 4A). In accord with previous findings, the selective GR modulator compound A (CpdA),[117] which does not support transactivation, is able to partially compete with DEX and as such able to lower the GRE-dependent reporter gene activity. Remarkably, none of the HDAC6-inhibiting compounds were able to significantly inhibit DEX-activated GR-driven gene expression. On the contrary, both **7a** and **7b** were able to significantly stimulate GRE-dependent promoter activities, with **13a** showing the same trend at the same concentration. These results indicate that compounds **7a**, **7b** and **13a** are able to inhibit HDAC6 at a concentration that does not influence the transcriptional activity of GR in a negative manner. With regard to inflammatory responses, the HDAC6 inhibitor Tubastatin A has been reported to significantly inhibit TNF-α and IL-6 in LPS stimulated human THP-1 macrophages.[118] Therefore, we addressed whether compounds **7a**, **7b** and **13a** are able to interfere with the activity of pro-inflammatory transcription factors, NF-κB and AP-1 (Figure 4B

and C). As NF-κB was identified before as the main key transcription factor driving IL-6,[119] we investigated first whether the HDAC6 inhibitors may directly target this pro-inflammatory transcription factor. Surprisingly and in contrast to the reference compounds DEX and CpdA, **7a**, **7b** and **13a** were not able to block the activity of NF-κB and by extension, did not show any anti-inflammatory activity, at least at the transcriptional level. Since besides NF-κB, both the IL-6 and TNF-α promoters also contain response elements for the transcription factor AP-1, we decided to also test whether the compounds could target this transcription factor instead, potentially explaining the previously reported inhibitory effect of HDAC6 inhibitors on cytokine production. On the AP1-dependent luciferase reporter gene construct, pCollagenase-luc, treatment with the AP-1 activating phorbol ester PMA (phorbol 12-myristate 13-acetate) resulted in enhanced promoter activity, as expected. It was published before that CpdA does not target AP-1-driven promoters, in contrast to DEX. None of the hydroxamic acid HDAC6 inhibitors were able to repress the AP-1-driven reporter gene. On the contrary, compounds **7b** and **13a**, both at 10 µM, clearly induced the AP1-dependent promoter activity as compared to solvent control (DMSO).
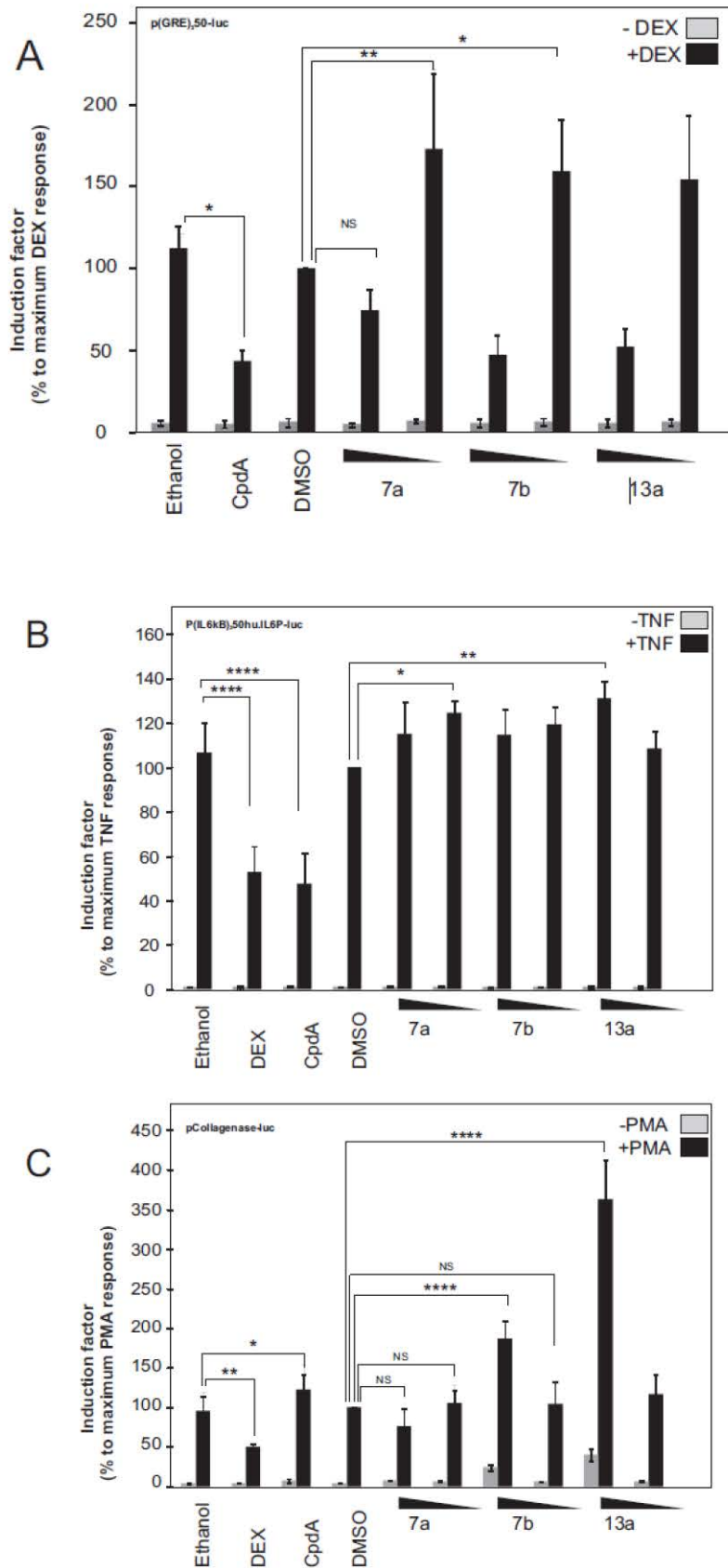
Figure 4. Influence of HDAC6 inhibitors **7a**, **7b** and **13a** on the transcriptional level of a GRE-dependent luciferase reporter gene construct (A), an NF-κB-dependent recombinant promoter construct (B) and an AP1-dependent luciferase reporter gene construct (C). Averaged results of four independent experiments are shown ± SD. ****$p < 0.0001$; *** $p < 0.001$; ** $p < 0.01$; * $p < 0.05$.

As an extra control, we tested the effect of Tubastatin A on the same reporter genes (Figure 5). Also for this well-known HDAC6 inhibitor, we could not find any evidence that NF-κB or AP-1 are directly targeted at the transcriptional level. Only at the highest dose of 50 µM, an inhibition of the luciferase activity could be noted. However, since this was apparent for all reporter genes tested, and since the corresponding dilution of DMSO (1/200) also gave rise to a substantial inhibition, we regard this effect as potentially nonspecific and given the high dose, also as non-physiological. Of note, none of the compounds at all concentrations used demonstrated cell toxicity, as assayed using a Cell Titer Glo assay (Promega, data not shown). Overall, our results indicate that HDAC6 inhibition by the hydroxamic structures or Tubastatin A targets neither NF-κB nor AP-1 in a direct manner, i.e. at the transcriptional level. Overall, our results demonstrate that a potent HDAC6 inhibition can be uncoupled from transcriptional inhibition at the level of activated NF-κB, AP-1, and GR. These preliminary results require further in-depth investigation, which will be the topic of an elaborate study in the future.

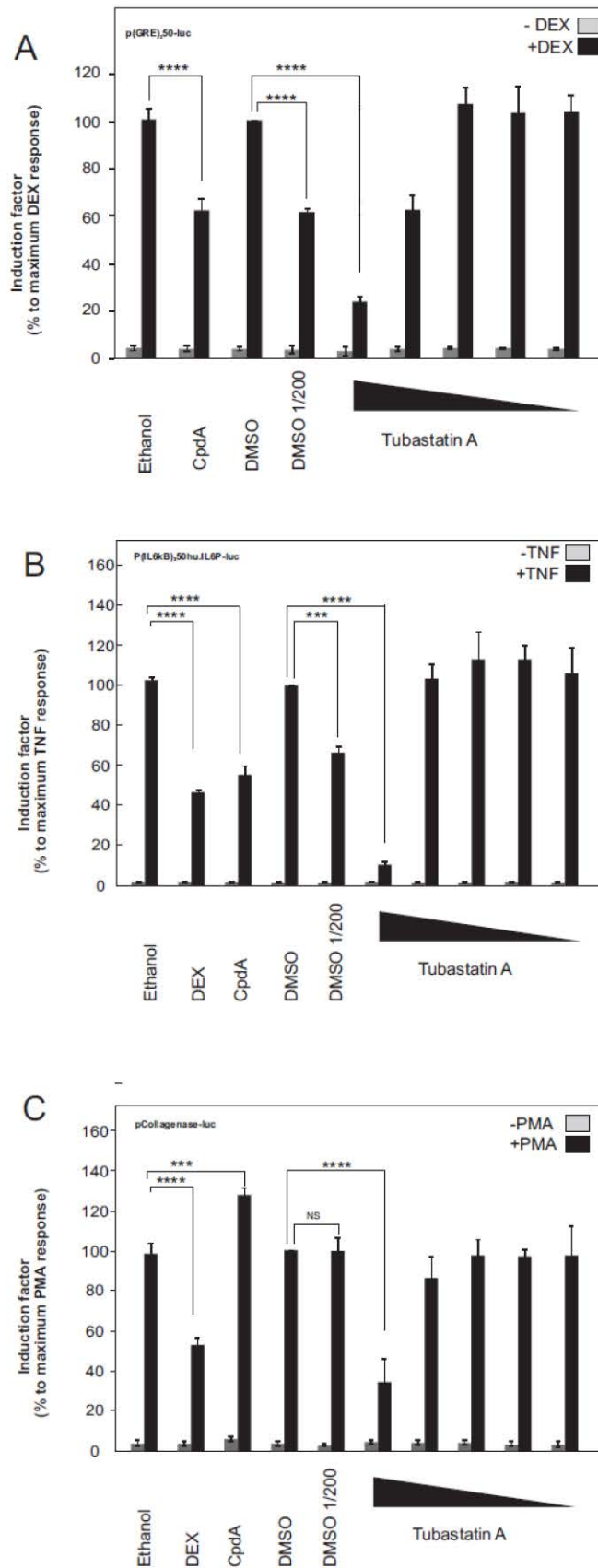**Figure 5.** Influence of HDAC6 inhibitor Tubastatin A on the transcriptional level of a GRE-dependent luciferase reporter gene construct (A), an NF-κB-dependent recombinant promoter construct (B) and an AP1-dependent luciferase reporter gene construct (C). Averaged results of four independent experiments are shown ± SD. ****$p < 0.0001$; *** $p < 0.001$; ** $p < 0.01$; * $p < 0.05$.

A concern with regard to the use of hydroxamic acid-based pharmaceuticals is the potential mutagenicity associated with these compounds.[107,108] Assessment of the novel 'mother structure' benzothiophene **7a** in the Ames fluctuation test toward four strains of *Salmonella typhimurium* (TA98, TA100, TA1535 and TA1537), with and without metabolic activation by using rat liver S9 fraction, revealed no mutagenicity at first sight. However, as cytotoxicity was observed at concentrations of ≥ 50 μM, this result can obscure the genotoxicity of the compound, and further evaluation by other assay systems is advisable to ensure that the compound is not mutagenic.

4.3. Conclusions

In summary, a set of novel 3-[(4-hydroxycarbamoylphenyl)aminomethyl]benzothiophenes was prepared, leading to the identification of three potent HDAC6 inhibitors as interesting lead structures with an activity/selectivity profile comparable to Tubastatin A. Adding additional substituents decreased the affinity for HDAC6, this in contrast to what was expected from docking studies (also pointing to the limitations associated with homology-based ligand docking in the HDAC6 area). The three most potent HDAC6 inhibitors performed well at α-tubulin acetylation and demonstrated that HDAC6 inhibition can be uncoupled from transcriptional inhibition at the level of activated NF-κB, AP-1, and GR.

4.4. Experimental details

4.4.1. Ligand docking

All docking experiments were performed by the Centre for Industrial Biotechnology and Biocatalysis (Prof. Desmet). All manipulations were performed with the molecular modelling program YASARA and the YASARA/WHATIF[93,94] twinset and the figure was created with PyMol v1.3.[97] The HDAC6 sequence was obtained from the UniProt database (www.uniprot.org; UniProt entry Q9UBN7). To increase the accuracy of the model, the sequence was limited to the major functional domain of HDAC6 (Gly482-Gly800). Possible templates were identified by running 3 PSI-BLAST iterations to extract a position specific scoring matrix (PSSM) from UniRef90, and then searching the PDB for a match. To aid the alignment of the HDAC6 sequence and templates, and the modelling of the loops, a secondary structure prediction was performed, followed by multiple sequence alignments. All side chains were ionised or kept neutral according to their predicted pKa values. Initial models were created from different templates (pdb entry 2VQW, 2VQQ and 3C10), each with several alignment variations and up to hundred conformations tried per loop. After the side-chains had been built, optimised and fine-tuned, all newly modelled parts were subjected to a combined steepest descent and simulated annealing minimisation, i.e. the backbone atoms of aligned residues were kept fixed to preserve the folding, followed by a full unrestrained simulated annealing minimisation for the entire model. The final model was obtained as a hybrid model of the best parts of the initial models, and checked once more for anomalies like incorrect configurations or colliding side chains. Furthermore, it was structurally aligned with known HDAC crystal structures to check if the chelating residues and the zinc atom were arranged correctly.

The HDAC inhibitor structures were created with YASARA Structure and energy minimised with the AMBER03 force field.[95] The grid box used for docking had a dimension of 25 x 25 x 25 angstrom, and comprised the entire catalytic cavity including the Zn ion and the outer surface of the active site entrance. Docking was performed with AutoDock VINA[109] and default parameters. Ligands were allowed to freely rotate during docking. The first conformer from the cluster that has its zinc binding group in the vicinity of the zinc ion, was selected as the binding mode for further analysis. The associated cluster was moreover always the highest populated and had the highest average binding energy, proving that the selected docking pose is highly preferred. Docking was in addition redone with a grid covering the whole protein extended by 5 Å on each side (~60x60x60) and the results were consistent with those obtained with the smaller grid. The docking experiments thus showed that the preferred binding mode is the one in which the phenylhydroxamate group occupies the tubular access channel (with the zinc binding group close to the zinc atom) and the cap group interacts with the protein surface. For

the most potent inhibitors (**7a**, **7b** and **13a**), the cap group was somehow sandwiched between Phe620 and Phe680, interacting via pi-pi stacking and hydrophobic contacts. Similar interactions were found for the cap group of the less potent *N*-substituted compounds, with additional contacts between the extra phenyl group and Phe679 and Leu749. There is accordingly no obvious reason for the lower *in vitro* activity. The selectivity for HDAC6 in contrast could be captured by molecular docking experiments. To that end, the most potent and selective HDAC6 inhibitors (**7a**, **7b** and **13a**) were docked in HDAC2 (class I) and HDAC4 (class IIa) and predicted binding energies were compared with HDAC6 (class IIb) (Figure 6). A clear preference for HDAC6 was observed, with significantly lower affinities for the other isoforms (in accordance with the *in vitro* tests).
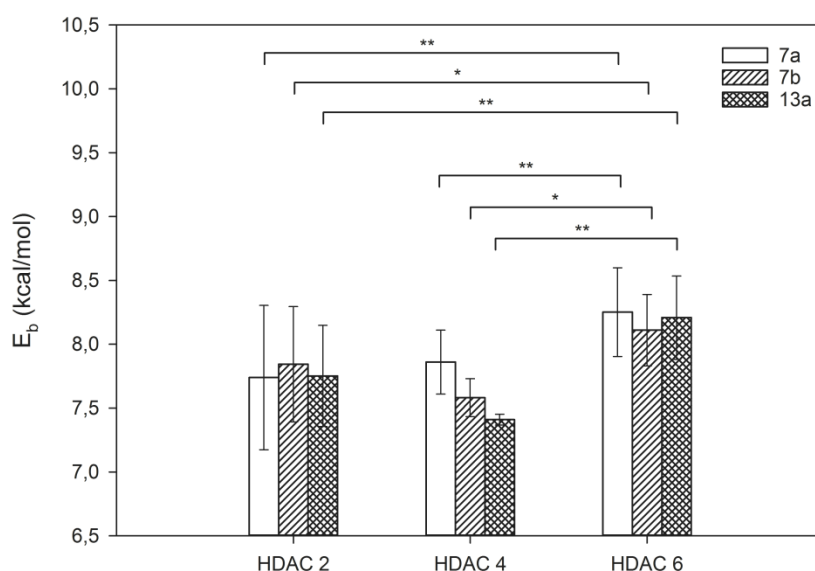
Figure 6. Predicted binding energies for the most potent and selective HDAC6 inhibitors (**7a**, **7b** and **13a**) against HDAC2 (class I), HDAC4 (class IIa) and HDAC6 (class IIb) (structures used for ligand docking: pdb entry 4LY1 chain A (HDAC2), 4CBY chain A (HDAC4) and the model created in this study (HDAC6); average binding energy from the cluster having its zinc binding group in the vicinity of the zinc ion (the higher the E_b the better the binding); ** $p < 0.01$, * $p < 0.05$).

4.4.2. Enzyme inhibition assays

The enzyme inhibition assays were performed by Eurofins Cerep Panlabs. *In vitro* IC_{50} values were determined by using human recombinant HDAC1-11 and fluorogenic HDAC substrate.[98]

4.4.3. Western Blots

The Western Blots were performed by the Laboratory of Neurobiology and Vesalius Research Center, VIB (Prof. Van Den Bosch). Values represent the normalized ratio Acetyl α-Tubulin/α-Tubulin against Tubastatin A (Tub A) in an established neuronal cell line (Neuro-2a cells: ATCC

N° CCL-131). Neuro-2a cells are treated overnight with different concentrations of the HDAC6 inhibitors and the effect on the acetylation level of α-tubulin is determined by using Western Blot.

4.4.3.1. Cell culture

Mouse neuroblastoma (Neuro-2a) cells were grown in a 1:1 mix of D-MEM (Dulbecco's Modified Eagle Medium) and F12 medium supplemented with glutamax (Invitrogen), 100 µg/ml streptomycin, 100 U/ml penicillin (Invitrogen), 10% fetal calf serum (Greiner Bio-one), 1% non-essential amino acids (Invitrogen) and 1.6% $NaHCO_3$ (Invitrogen) at 37 °C and 7.5% CO_2. To split the cells, cells were washed with Versene (Invitrogen) and dissociated with 0.05% Trypsine-EDTA (Invitrogen). The Neuro-2a cells were treated overnight at 37°C with dosages ranging from 10 nM up to 1 µM of either Tubastatin A (Sigma-Aldrich) or the candidate HDAC6 inhibitors.

4.4.3.2. Western Blot

For sodium dodecyl sulfate-polyacrylamide gel electrophoresis (SDS-PAGE) analysis, transfected cells were collected using the EpiQuik Total Histone Extraction Kit (EpiGentek) according to manufacturer's instructions. Protein concentrations were determined using microBCA kit (Thermo Fisher Scientific Inc., Pittsburgh, PA, USA) according to manufacturer's instructions. Before resolving the samples on a 12% SDS-PAGE gel, samples containing equal amounts of protein were supplemented with reducing sample buffer (Thermo Scientific) and boiled at 95 °C for 5 min. After electrophoresis, the proteins were transferred to a polyvinylidene difluoride (PVDF) membrane (Millipore Corp., Bedford, MA, USA). The non-specific binding was blocked by incubation of the membrane in 5% bovine serum albumin (BSA), diluted in Tris Buffered Saline Tween (TBST, 50 mM TRIS, 150 mM NaCl, 0,1% Tween-20 (Applichem, Darmstadt, Duitsland) for 1h at room temperature followed by incubation with primary antibodies overnight. The antibodies, diluted in TBS-T, were directed against α-tubulin (1/5000, T6199, Sigma-Aldrich), and acetylated α-tubulin (1/5000, T6793 monoclonal, Sigma-Aldrich). The secondary antibodies, coupled to alkaline phosphatase (anti-mouse or anti-rabbit, 1/5000, Sigma-Aldrich) were used. Blots were visualized by adding the ECF substrate (Enhanced Chemical Fluorescence, GE Healthcare, Uppsala, Sweden) and imaged with the ImageQuant_LAS 4000. A mild reblotting buffer (Millipore) was applied to strip the blots. ImageQuant TL version 7.0-software was used to quantify the blots.

4.4.4. GRE/NF-κB/AP-1 assays

These bioassays were performed by the Cytokine Receptor Lab, VIB (Prof. De Bosscher). A549 cells with the stably integrated recombinant reporter gene p(GRE)2-50-luc (**A**) were pre-incubated with respective solvents, the selective Glucocorticoid Receptor modulator CpdA (10 µM), **7a** (1µM or 10µM), **7b** (1µM or 10µM), **13a** (1µM or 10µM) and Tubastatin A (0.5, 1, 5, 10, 50 µM) for 1h after which the synthetic glucocorticoid dexamethasone (DEX,1µM) was added, where indicated, for 5h. An extra DMSO control at the highest dose was included (1/200), whereas the level of DMSO for the other concentrations corresponded to the one-before highest dose, i.e. of the 10 µM set-up. A549 cells with the stably integrated recombinant reporter gene p(IL6κB)350hu.IL6P-luc (**B**)[120] or Collagenase-luc (**C**) were pre-incubated with respective solvents, DEX (1µM), CpdA (10 µM), **7a** (1µM or 10 µM), **7b** (1µM or 10 µM), **13a** (1µM or 10 µM) and Tubastatin A (0.5, 1, 5, 10, 50 µM) for 1h after which TNF (2000 units/ml) or PMA (20 nM) were added, where indicated, for 5h. Cell lysates were assayed for luciferase activities. Promoter activities are expressed as relative induction factor calculated as percentage of maximal DEX (**A**), TNF (**B**) or PMA (**C**) responses. Averaged results of four independent experiments are shown ± SD. ****$p < 0.0001$; *** $p < 0.001$; ** $p < 0.01$; * $p < 0.05$. Statistical significance was determined on the averaged results, and analysis performed using one-way ANOVA tests followed by a Tukey multiple comparison post test.

4.4.5. Ames fluctuation assays

The Ames fluctuation assays were performed by Eurofins Cerep Panlabs. Wells that displayed bacteria growth due to the reversion of the histidine mutation (as judged by the ratio of OD430/OD570 being greater than 1.0) are counted and recorded as positive counts. The significance of the positive counts between the treatment (in the presence of test compound) and the control (in the absence of test compound) are calculated using the one-tailed Fisher's exact test.

### 4.4.6. Synthetic procedures and spectral data

^{1}H NMR spectra were recorded at 300 MHz (JEOL ECLIPSE+) or 400 MHz (Bruker Avance III) with $CDCl_3$ or D_6-DMSO as solvent and tetramethylsilane as internal standard. ^{13}C NMR spectra were recorded at 75 MHz (JEOL ECLIPSE+) or 100.6 MHz (Bruker Avance III) with $CDCl_3$ or D_6-DMSO as solvent and tetramethylsilane as internal standard. Mass spectra were obtained with a mass spectrometer Agilent 1100, 70 eV. IR spectra were measured with a Spectrum One FT-IR spectrophotometer. High resolution electron spray (ES) mass spectra were obtained with an Agilent Technologies 6210 series time-of-flight instrument. Melting points of crystalline compounds were measured with a Büchi 540 apparatus or with a Kofler

Bench, type WME Heizbank of Wagner & Munz. The purity of all tested compounds was assessed by HRMS analysis and/or HPLC analysis, confirming a purity of ≥95%.

4.4.6.1. Synthesis of 6-bromobenzothiophene-3-carbaldehyde 9[115]

Benzothiophene-3-carbaldehyde (811 mg, 5 mmol, 1 equiv) **3a** was dissolved in acetonitrile (15 mL) and to this solution was slowly added bromine (1,29 mL, 25 mmol, 5 equiv). The resulting reaction mixture was stirred at room temperature for 18 hour after which it was partitioned between an aqueous sodium bicarbonate solution (50 mL) and EtOAc (50 mL). To this biphasic solution was added dropwise, under vigorous stirring, a saturated aqueous sodium thiosulfate solution until discoloration of the organic medium. The organic layer was separated, and the aqueous layer was extracted with EtOAc (25 mL). The organic fractions were combined, dried (MgSO$_4$), filtered and concentrated under vacuum. Purification through column chromatography yielded 6-bromobenzothiophene-3-carbaldehyde **9** (482 mg, 2 mmol, 40%) as a white powder.

6-Bromobenzothiophene-3-carbaldehyde 9 (40%)
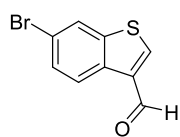
White powder. Purification by column chromatography (EtOAc/PE 1/13, Rf = 0.14). Mp = 111 °C. ^{1}H NMR (400 MHz, CDCl$_3$): δ 7.63 (1H, d × d, J = 8.7, 1.7 Hz, CH$_{arom}$); 8.04 (1H, d, J = 1.7 Hz, CH$_{arom}$); 8.30 (1H, s, CH$_{arom}$S); 8.56 (1H, d, J = 8.7 Hz, CH$_{arom}$); 10.12 (1H, s, CHO). ^{13}C NMR (100.6 MHz, CDCl$_3$): δ 120.2 (C$_{quat,arom}$), 125.0, 125.9 and 129.6 (3 × CH$_{arom}$), 134.0, 136.1 and 141.8 (3 × C$_{quat,arom}$), 143.2 (CH$_{arom}$), 185.1 (C=O). IR (ATR, cm^{-1}): v$_{C=O}$ = 1662; v$_{max}$ = 3074, 2851, 1583, 1492, 1454, 1389, 1358, 1182, 1135, 1110, 1040, 862, 854, 809, 796, 727, 714. Anal. Calcd. For C$_9$H$_5$BrOS: C 44.84 H 2.09. Found C 45.17 H 1.71.

4.4.6.2. Synthesis of phenylbenzothiophene-3-carbaldehydes 4 and 10

General procedure: 5-Bromobenzothiophene-3-carbaldehyde **3b** (482 mg, 2 mmol, 1 equiv) was dissolved in toluene (15 mL) and to this solution were added an aqueous solution of sodium carbonate (7 mL, 2M) and a solution of phenylboronic acid (488 mg, 4 mmol, 2 equiv) in ethanol (7 mL). This mixture was flushed with nitrogen for 10 minutes before tetrakis(triphenylphosphine)palladium(0) (92 mg, 0.08 mmol, 0.04 equiv) was added and the reaction mixture was heated to its boiling temperature for 8 hour. The reaction mixture was poured in to brine (20 mL) and three times extracted with EtOAc (20 mL). The combined organic fraction was thereafter three times washed with brine (15 mL), dried (MgSO$_4$), filtered and evaporated under vacuum. Purification through column chromatography yielded 5-phenylbenzothiophene-3-carbaldehyde **4** (343 mg, 1.44 mmol, 72%) as an orange powder.

5-Phenylbenzothiophene-3-carbaldehyde 4 (72%)
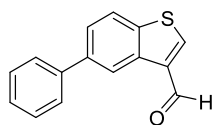
Orange powder. Purification by column chromatography (EtOAc/PE 1/5, Rf = 0.35). Mp = 102 °C. ^{1}H NMR (300 MHz, CDCl$_3$): δ 7.36-7.41, 7.46-7.51 and 7.69-7.72 (1H, 2H and 3H, 3 × m, 6 × CH$_{arom}$); 7.94 (1H, d, J = 8.3 Hz, CH$_{arom}$); 8.35 and 8.92 (2 × 1H, 2 × s, 2 × CH$_{arom}$); 10.17 (1H, s, CHO). ^{13}C NMR (75 MHz, CDCl$_3$): δ 122.7, 123.3, 125.9, 127.6, 127.7 and 129.0 (8 × CH$_{arom}$), 135.9, 136.7, 139.5, 139.8 and 140.8 (5 × C$_{quat,arom}$), 144.0 (CH$_{arom}$), 185.5 (C=O). IR (ATR, cm^{-1}): $v_{C=O}$ = 1671; v_{max} = 3076, 2923, 2796, 2718, 1600, 1507, 1494, 1451, 1428, 1381, 1284, 1246, 1156, 1104, 904, 856, 802, 765, 729, 702, 664. MS (70 eV): m/z (%) 239 (M$^+$+1, 35). HRMS (ESI) Anal. Calcd. for C$_{15}$H$_{11}$OS 239.0525 [M+H]$^+$, Found 239.0524.

6-Phenylbenzothiophene-3-carbaldehyde 10 (96%)
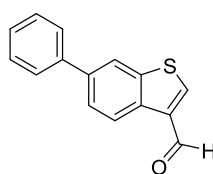
Orange powder. Purification by column chromatography (EtOAc/PE 1/13, Rf = 0.20). (96%). Mp = 94 °C. ^{1}H NMR (400 MHz, CDCl$_3$): δ 7.37-7.41, 7.46-7.50 and 7.65-7.68 (1H, 2H and 2H, 3 × m, 5 × CH$_{arom}$); 7.76 (1H, d × d, J = 8.4, 1.4 Hz, CH$_{arom}$); 8.08 (1H, d, J = 1.4 Hz, CH$_{arom}$); 8.33 (1H, s, CH$_{arom}$); 8.72 (1H, d, J = 8.4 Hz, CH$_{arom}$); 10.16 (1H, s, CHO). ^{13}C NMR (100.6 MHz, CDCl$_3$): δ 120.6, 125.0, 125.8, 127.4, 127.7 and 129.0 (8 × CH$_{arom}$), 134.2, 136.4, 139.6, 140.5 and 141.3 (5 × C$_{quat,arom}$), 143.2 (CH$_{arom}$), 185.4 (C=O). IR (ATR, cm^{-1}): $v_{C=O}$ = 1662; v_{max} = 3082, 1542, 1491, 1463, 1390, 1147, 1102, 1052, 856, 821, 761, 715, 691. MS (70 eV): m/z (%) 239 (M$^+$+1, 100). HRMS (ESI) Anal. Calcd. for C$_{15}$H$_{11}$OS 239.0525 [M+H]$^+$, Found 239.0524.

#### *4.4.6.3. Synthesis of methyl 4-aminobenzoate esters 5a-d and 11a-b*

General procedure: Benzothiophene-3-carbaldehyde **3a** (406 mg, 2.5 mmol, 1 equiv) was dissolved in ethanol (15 mL) and to this solution were added glacial acetic acid (751 mg, 12.5 mmol, 5 equiv) and methyl 4-aminobenzoate (454 mg, 3 mmol, 1.2 equiv). This reaction mixture was stirred for one hour at refluxing conditions after which it was cooled to 0°C. Sodium cyanoborohydride (471 mg, 7.5 mmol, 3 equiv) was added and the reaction mixture was allowed to warm to room temperature. After one hour the mixture was poured in to brine (15 mL) and three times extracted with EtOAc (15 mL). The combined organic fraction was thereafter three times washed with brine (15 mL), dried (MgSO$_4$), filtered and evaporated under vacuum. Purification through recrystallization from ethanol yielded 3-[(4-methoxycarbonylphenyl)aminomethyl]-benzothiophene **5a** (520 mg, 1.75 mmol, 70%) as a white powder. For secondary amine **5b** a solvent mixture of ethanol/CH$_2$Cl$_2$ (1/1) was used as solvent for the reaction.

### 3-[(4-Methoxycarbonylphenyl)aminomethyl]benzothiophene 5a (70%)
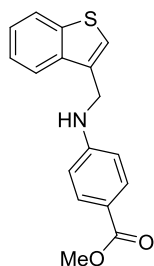
White powder. Recrystallization from EtOH. Mp = 127 °C. ^{1}H NMR (300 MHz, CDCl$_3$): δ 3.84 (3H, s, CH$_3$O); 4.48 (1H, s(br), NH); 4.58 (2H, d, J = 5.0 Hz, CH$_2$NH); 6.62 (2H, d, J = 8.8 Hz, 2 × CH$_{arom}$); 7.32 (1H, s, CHS); 7.35-7.43, 7.73-7.81 and 7.86-7.90 (2H, 1H and 3H, 3 × m, 6 × CH$_{arom}$). ^{13}C NMR (75 MHz, CDCl$_3$): δ 42.2 (CH$_2$NH), 51.7 (CH$_3$O), 111.8 (2 × CH$_{arom}$), 119.0 (C$_{quat,arom}$), 121.7 and 123.2 (2 × CH$_{arom}$), 124.1 (CHS), 124.4, 124.8 and 131.7 (4 × CH$_{arom}$), 132.8, 137.8, 141.0 and 151.7 (4 × C$_{quat,arom}$), 167.4 (C=O). IR (ATR, cm^{-1}): ν$_{NH}$ = 3379; ν$_{C=O}$ = 1685; ν$_{max}$ = 2944, 1598, 1524, 1431, 1334, 1275, 1260, 1170, 1113, 840, 769, 756, 732. MS (70 eV): m/z (%) 296 (M$^-$-1, 100). HRMS (ESI) Anal. Calcd. for C$_{17}$H$_{14}$NO$_2$S 296.0751 [M-1]$^-$, Found 296.0760.

5-Bromo-3-[(4-methoxycarbonylphenyl)aminomethyl]benzothiophene 5b (70%)
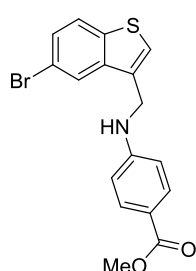
Brown powder. Recrystallization from EtOH. Mp = 143 °C. ^{1}H NMR (300 MHz, CDCl$_3$): δ 3.86 (3H, s, CH$_3$O); 4.48 (1H, s(br), NH); 4.56 (2H, s, CH$_2$NH); 6.64 (2H, d, J = 8.5 Hz, 2 × CH$_{arom}$); 7.37 (1H, s, CHS); 7.48 (1H, d, J = 8.3 Hz, CH$_{arom}$); 7.74 (1H, d, J = 8.3 Hz, CH$_{arom}$); 7.89 (2H, d, J = 8.5 Hz, CH$_{arom}$); 7.92 (1H, s, CH$_{arom}$). ^{13}C NMR (75 MHz, CDCl$_3$): δ 42.1 (CH$_2$NH), 51.7 (CH$_3$O), 111.9 (2 × CH$_{arom}$), 118.6 and 119.3 (2 × C$_{quat,arom}$), 124.4, 124.5, 125.8, 127.9 and 131.7 (6 × CH$_{arom}$), 132.3, 139.4, 139.6 and 151.5 (4 × C$_{quat,arom}$), 167.3 (C=O). IR (ATR, cm^{-1}): ν$_{NH}$ = 3376; ν$_{C=O}$ = 1683; ν$_{max}$ = 2945, 1600, 1576, 1532, 1434, 1341, 1315, 1286, 1273, 1195, 1174, 1118, 1068, 970, 769, 698. MS (70 eV): m/z (%) 374/6 (M$^-$-1, 100). HRMS (ESI) Anal. Calcd. for C$_{17}$H$_{13}$BrNO$_2$S 373.9856 [M-H]$^-$, Found 373.9869.

### 3-[(4-Methoxycarbonylphenyl)aminomethyl]-5-phenylbenzothiophene 5c (75%)
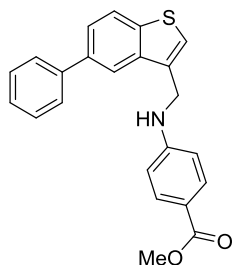
Brown powder. Purification by column chromatography (EtOAc/PE 1/5, Rf = 0.29). Mp = 154° C. ^{1}H NMR (300 MHz, CDCl$_3$): δ 3.85 (3H, s, CH$_3$O); 4.49 (1H, s(br), NH); 4.65 (2H, d, J = 4.9 Hz, CH$_2$NH); 6.65 (2H, d, J = 8.8 Hz, 2 × CH$_{arom}$); 7.33-7.48, 7.62-7.65 and 7.88-7.96 (4H, 3H and 4H, 3 × m, 11 × CH$_{arom}$). ^{13}C NMR (75 MHz, CDCl$_3$): δ 42.3 (CH$_2$NH), 51.7 (CH$_3$O), 111.9 (2 × CH$_{arom}$), 119.1 (C$_{quat,arom}$), 120.0, 123.4, 124.5, 124.9, 127.5, 127.6, 129.0 and 131.7 (11 × CH$_{arom}$), 133.0, 138.1, 138.3, 140.0, 141.2 and 151.7 (6 × C$_{quat,arom}$), 167.3 (C=O). IR (ATR, cm^{-1}): ν$_{NH}$ = 3389; ν$_{C=O}$ = 1697; ν$_{max}$ = 3076, 2922, 2852, 1609, 1530, 1496, 1445, 1430, 1350, 1310, 1285, 1170, 1104, 1081, 1020, 832, 767, 756, 694. MS (70 eV): m/z (%) 372 (M$^-$-1, 25). HRMS (ESI) Anal. Calcd. for C$_{23}$H$_{18}$NO$_2$S 372.1064 [M-H]$^-$, Found 372.1069.

3-[(4-Methoxycarbonyl-2-methylphenyl)aminomethyl]benzothiophene 5d (50%)
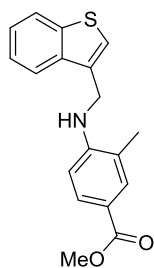
White powder. Recrystallization from EtOH. Mp = 148 °C. ^{1}H NMR (300 MHz, CDCl$_3$): δ 2.15 (3H, s, CH$_3$C$_{quat}$); 3.85 (3H, s, CH$_3$O); 4.29 (1H, s(br), NH); 4.64 (2H, s, CH$_2$NH); 6.66 (1H, d, J = 8.8 Hz, CH$_{arom}$); 7.33 (1H, s, CHS); 7.37-7.43 and 7.78-7.89 (2H and 4H, 2 × m, 6 × CH$_{arom}$). ^{13}C NMR (75 MHz, CDCl$_3$): δ 17.5 (CH$_3$C$_{quat}$), 42.4 (CH$_2$NH), 51.7 (CH$_3$O), 108.9 (CH$_{arom}$), 118.5 and 121.2 (2 × C$_{quat,arom}$), 121.7 and 123.2 (2 × CH$_{arom}$), 124.2 (CHS), 124.5, 124.8, 129.9 and 131.7 (4 × CH$_{arom}$), 132.8, 137.8, 141.0 and 149.8 (4 × C$_{quat,arom}$), 167.6 (C=O). IR (ATR, cm^{-1}): ν$_{NH}$ = 3442; ν$_{C=O}$ = 1702; ν$_{max}$ = 2939, 1601, 1513, 1459, 1430, 1379, 1342, 1286, 1266, 1258, 1230, 1189, 1146, 1113, 1004, 828, 771, 762, 728. MS (70

eV): m/z (%) 310 (M$^-$-1, 100). HRMS (ESI) Anal. Calcd. for $C_{18}H_{16}NO_2S$ 310.0907 [M-H]$^-$, Found 310.0917.

6-Bromo-3-[(4-methoxycarbonylphenyl)aminomethyl]benzothiophene 11a (50%)
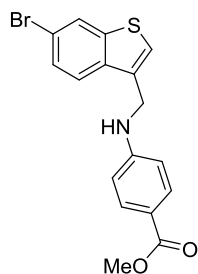
Light yellow powder. Recrystallization from EtOH. Mp = 155 °C. ^{1}H NMR (400 MHz, D$_6$-DMSO): δ 3.74 (3H, s, CH$_3$O); 4.57 (2H, d, J = 5.5 Hz, CH$_2$NH); 6.70 (2H, d, J = 8.8 Hz, 2 × CH$_{arom}$); 7.12 (1H, t, J = 5.5 Hz, CH$_2$NH); 7.58 (1H, d × d, J = 8.6, 1.8 Hz, CH$_{arom}$); 7.65 (1H, s, CH$_{arom}$); 7.69 (2H, d, J = 8.8 Hz, 2 × CH$_{arom}$); 7.89 (1H, d, J = 8.6 Hz, CH$_{arom}$); 8.30 (1H, d, J = 1.8 Hz, CH$_{arom}$). ^{13}C NMR (100.6 MHz, D$_6$-DMSO): δ 41.1 (CH$_2$NH), 51.7 (CH$_3$O), 111.8 (2 × CH$_{arom}$), 116.6 and 118.1 (2 × C$_{quat,arom}$), 124.2, 125.7, 125.8, 127.7 and 131.4 (6 × CH$_{arom}$), 133.8, 137.4, 142.4 and 153.0 (4 × C$_{quat,arom}$), 166.8 (C=O). IR (ATR, cm^{-1}): ν$_{NH}$ = 3346; ν$_{C=O}$ = 1672; ν$_{max}$ = 1600, 1526, 1431, 1337, 1287, 1264, 1176, 1114, 1057, 837, 820, 772. MS (70 eV): m/z (%) 374/6 (M$^-$-1, 20). HRMS (ESI) Anal. Calcd. for $C_{17}H_{13}BrNO_2S$ 373.9856 [M-1]$^-$, Found 373.9862.

### 3-[(4-Methoxycarbonylphenyl)aminomethyl]-6-phenyl-benzothiophene 11b (66%)
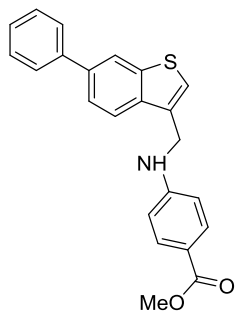
White powder. Recrystallization from EtOH. Mp = 169 °C. ^{1}H NMR (400 MHz, CDCl$_3$): δ 3.86 (3H, s, CH$_3$O); 4.48 (1H, t, J = 5.0 Hz, NH); 4.64 (2H, d, J = 5.0 Hz, CH$_2$NH); 6.66 (2H, d, J = 8.8 Hz, 2 × CH$_{arom}$); 7.36-7.40 (2H, m, 2 × CH$_{arom}$); 7.48 (2H, t, J = 7.6 Hz, 2 × CH$_{arom}$); 7.64-7.67 (3H, m, 3 × CH$_{arom}$); 7.85 (1H, d, J = 8.4 Hz, CH$_{arom}$); 7.90 (2H, d, J = 8.8 Hz, 2 × CH$_{arom}$); 8.09 (1H, d, J = 1.2 Hz, CH$_{arom}$). ^{13}C NMR (100.6 MHz, CDCl$_3$): δ 42.2 (CH$_2$NH), 51.6 (CH$_3$O), 111.7 (2 × CH$_{arom}$), 119.0 (C$_{quat,arom}$), 121.4, 121.8, 124.1, 124.4, 127.4, 127.5, 128.9 and 131.6 (11 × CH$_{arom}$), 132.5, 136.8, 138.2, 140.8, 141.6 and 151.6 (6 × C$_{quat,arom}$), 167.3 (C=O). IR (ATR, cm^{-1}): ν$_{NH}$ = 3390; ν$_{C=O}$ = 1683; ν$_{max}$ = 1600, 1524, 1490, 1436, 1341, 1310, 1275, 1177, 1105, 1074, 784, 764, 692. MS (70 eV): m/z (%) 396 (M+Na$^+$, 30).

4.4.6.4. Synthesis of tertiary amines 6a-c and 12a-b

General procedure: 3-[(4-Methoxycarbonylphenyl)aminomethyl]-benzothiophene **5a** (297 mg, 1 mmol, 1 equiv) was dissolved in DMF (10 mL) and to this solution was sodium hydride (40 mg, 60 % dispersion in mineral oil, 1 mmol, 1 equiv) added. The reaction mixture was stirred for 30 minutes at room temperature under nitrogen atmosphere after which benzyl bromide (342 mg, 2 mmol, 2 equiv) and potassium iodide (5 mg) were added. After two hours the reaction mixture was poured in to brine (20 mL) and three times extracted with EtOAc (20 mL). The combined organic fraction was thereafter three times washed with brine (15 mL), dried (MgSO$_4$), filtered and evaporated under vacuum. Purification through column chromatography yielded 3-[*N*-benzyl-*N*-(4-methoxycarbonylphenyl)-aminomethyl]benzothiophene **6a** (271 mg,0.7 mmol, 70%) as a yellow powder.

3-[*N*-Benzyl-*N*-(4-methoxycarbonylphenyl)aminomethyl]-benzothiophene 6a (70%)
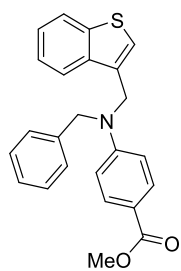
Yellow powder. Purification by column chromatography (EtOAc/PE 1/5, Rf = 0.30). Mp = 126 °C. ^{1}H NMR (300 MHz, CDCl$_3$): δ 3.84 (3H, s, CH$_3$O); 4.76 and 4.87 (2 × 2H, 2 × s, 2 × CH$_2$N); 6.76 (2H, d, *J* = 8.8 Hz, 2 × CH$_{arom}$); 7.11 (1H, s, CHS); 7.21-7.40, 7.65-7.68 and 7.85-7.90 (7H, 1H and 3H, 3 × m, 11 × CH$_{arom}$). ^{13}C NMR (75 MHz, CDCl$_3$): δ 49.6 (CH$_2$N), 51.7 (CH$_3$O), 54.0 (CH$_2$N), 111.5 (2 × CH$_{arom}$), 118.3 (C$_{quat,arom}$), 121.3, 122.8, 123.2, 124.3, 124.8, 126.6, 127.4 and 129.0 (10 × CH$_{arom}$), 131.4 (C$_{quat,arom}$), 131.6 (2 × CH$_{arom}$), 137.5, 137.6, 141.3 and 152.4 (4 × C$_{quat,arom}$), 167.3 (C=O). IR (ATR, cm^{-1}): ν$_{C=O}$ = 1701; ν$_{max}$ = 2921, 2852, 1602, 1520, 1494, 1432, 1398, 1357, 1318, 1282, 1234, 1183, 1109, 1072, 1026, 962, 946, 817, 768, 729, 696. MS (70 eV): m/z (%) 388 (M$^+$+1, 85). HRMS (ESI) Anal. Calcd. for C$_{24}$H$_{22}$NO$_2$S 388.1366 [M+H]$^+$, Found 388.1374.

5-Bromo-3-[*N*-benzyl-*N*-(4-methoxycarbonylphenyl)aminomethyl]-benzothiophene 6b (79%)
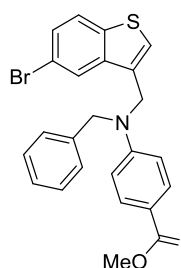
Yellow powder. Purification by column chromatography (EtOAc/PE 1/5, Rf = 0.37). Mp = 130 °C. ^{1}H NMR (300 MHz, CDCl$_3$): δ 3.84 (3H, s, CH$_3$O); 4.76 and 4.87 (2 × 2H, 2 × s, 2 × CH$_2$N); 6.76 (2H, d, *J* = 8.8 Hz, 2 × CH$_{arom}$); 7.11 (1H, s, CHS); 7.22-7.41, 7.65-7.68 and 7.85-7.91 (6H, 1H and 3H, 3 × m, 10 × CH$_{arom}$). ^{13}C NMR (75 MHz, CDCl$_3$): δ 49.4 (CH$_2$N), 51.7 (CH$_3$O), 54.1 (CH$_2$N), 111.5 (2 × CH$_{arom}$), 118.5 (2 × C$_{quat,arom}$), 124.2, 124.5, 126.6, 127.5, 127.8 and 129.0 (9 × CH$_{arom}$), 130.9 (C$_{quat,arom}$), 131.6 (2 × CH$_{arom}$), 137.3, 139.2, 139.9 and 152.2 (4 × C$_{quat,arom}$), 167.3 (C=O). IR (ATR, cm^{-1}): ν$_{C=O}$ = 1702; ν$_{max}$ = 2943, 1598, 1522, 1451, 1434, 1410, 1365, 1318, 1280, 1231, 1186, 1109, 1073, 943, 818, 769, 742, 728, 698. MS (70 eV): m/z (%) 466/8 (M$^+$+1, 100). HRMS (ESI) Anal. Calcd. for C$_{24}$H$_{21}$BrNO$_2$S 466.0471 [M+H]$^+$, Found 466.0483.

### 3-[*N*-Benzyl-*N*-(4-methoxycarbonylphenyl)aminomethyl]-5-phenyl-benzothiophene 6c (65%)
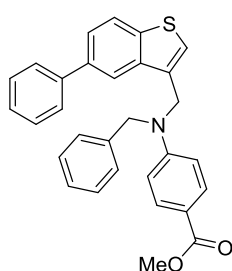
Yellow powder. Purification by column chromatography (EtOAc/PE 1/5, Rf = 0.31). Mp = 82 °C. ^{1}H NMR (300 MHz, CDCl$_3$): δ 3.83 (3H, s, CH$_3$O); 4.76 and 4.90 (2 × 2H, 2 × s, 2 × CH$_2$N); 6.76 (2H, d, *J* = 8.8 Hz, 2 × CH$_{arom}$); 7.13 (1H, s, CHS); 7.22-7.46, 7.59-7.63 and 7.83-7.93 (8H, 3H and 4H, 3 × m, 15 × CH$_{arom}$). ^{13}C NMR (75 MHz, CDCl$_3$): δ 49.7 (CH$_2$N), 51.7 (CH$_3$O), 54.1 (CH$_2$N), 111.6 (2 × CH$_{arom}$), 118.4 (C$_{quat,arom}$), 119.8, 123.4, 123.5, 124.5, 126.6, 127.4, 127.5 and 129.0 (14 × HC$_{arom}$), 131.6 (C$_{quat,arom}$), 131.7 (2 × HC$_{arom}$), 137.5, 138.0, 138.2, 140.4, 141.2 and 152.4 (6 × C$_{quat,arom}$), 167.3 (C=O). IR (ATR, cm^{-1}): ν$_{C=O}$ = 1702; ν$_{max}$ = 2969, 2923, 1604, 1519, 1494, 1451, 1434, 1396, 1360, 1317, 1279, 1233, 1183, 1155, 1108, 1074, 1026, 947, 895, 819, 759, 730, 696. MS (70 eV): m/z (%) 464 (M$^+$+1, 70). HRMS (ESI) Anal. Calcd. for C$_{30}$H$_{26}$NO$_2$S 464.1679 [M+H]$^+$, Found 464.1698.

6-Bromo-3-[*N*-benzyl-*N*-(4-methoxycarbonylphenyl)aminomethyl]-benzothiophene 12a
(87%)
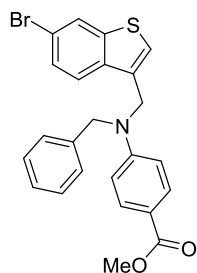
White powder. Purification by column chromatography (EtOAc/PE 1/10, Rf = 0.21). Mp = 63 °C. ^{1}H NMR (400 MHz, D$_6$-DMSO): δ 3.74 (3H, s, CH$_3$O); 4.83 and 5.01 (2 × 2H, 2 × s, 2 × CH$_2$N); 6.79 (2H, d, J = 9.1 Hz, 2 × CH$_{arom}$); 7.24-2.28 and 7.32-7.36 (3H and 2H, 2 × m, 5 × CH$_{arom}$); 7.38 (1H, s, CH$_{arom}$); 7.58 (1H, d × d, J = 8.6, 1.8 Hz, CH$_{arom}$); 7.71 (2H, d, J = 9.1 Hz, 2 × CH$_{arom}$); 7.80 (1H, d, J = 8.6 Hz, CH$_{arom}$); 8.31 (1H, d, J = 1.8 Hz, CH$_{arom}$). ^{13}C NMR (100.6 MHz, D$_6$-DMSO): δ 49.7 (CH$_2$N), 51.8 (CH$_3$O), 54.1 (CH$_2$N), 112.1 (2 × CH$_{arom}$), 117.1 and 118.2 (2 × C$_{quat,arom}$), 124.0, 124.6, 125.9, 127.0, 127.4, 127.7, 129.1 and 131.3 (11 × CH$_{arom}$), 132.4, 137.0, 138.5, 142.6 and 152.2 (5 × C$_{quat,arom}$), 166.6 (C=O). IR (ATR, cm^{-1}): ν$_{C=O}$ = 1702; ν$_{max}$ = 2922, 1602, 1520, 1433, 1281, 1233, 1184, 1109, 946, 808, 797, 768, 730, 696. MS (70 eV): m/z (%) 466/8 (M$^+$+1, 100). HRMS (ESI) Anal. Calcd. for C$_{24}$H$_{21}$BrNO$_2$S 466.0471 [M+H]$^+$, Found 466.0482.

3-[*N*-Benzyl-*N*-(4-methoxycarbonylphenyl)aminomethyl]-6-phenyl-benzothiophene 12b
(91%)
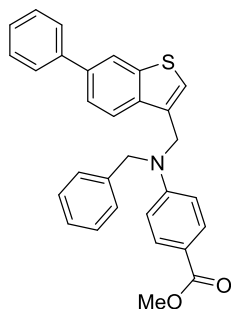
White powder. Purification by column chromatography (EtOAc/PE 1/10, Rf = 0.13). Mp = 66 °C. ^{1}H NMR (400 MHz, CDCl$_3$): δ 3.84 (3H, s, CH$_3$O); 4.76 and 4.88 (2 × 2H, 2 × s, 2 × CH$_2$N); 6.77 (2H, d, J = 9.1 Hz, 2 × CH$_{arom}$); 7.11 (1H, s, CHS); .7.23-7.39, 7.45-7.48, 7.61-7.66 and 7.70-7.72 (6H, 2H, 3H and 1H, 4 × m, 12 × CH$_{arom}$); 7.87 (2H, d, J = 9.1 Hz, 2 × CH$_{arom}$); 8.08 (1H, d, J = 1.0 Hz, CH$_{arom}$). ^{13}C NMR (100.6 MHz, CDCl$_3$): δ 49.5 (CH$_2$N), 51.6 (CH$_3$O), 53.9 (CH$_2$N), 111.5 (2 × CH$_{arom}$), 118.2 (C$_{quat,arom}$), 121.4, 121.5, 123.1, 124.0, 126.5, 127.36, 127.42, 127.5, 128.92 and 128.94 (14 × CH$_{arom}$), 131.2 (C$_{quat,arom}$), 131.6 (2 × CH$_{arom}$), 136.6, 137.4, 138.1, 140.9, 142.0 and 152.3 (6 × C$_{quat,arom}$), 167.2 (C=O). IR (ATR, cm^{-1}): ν$_{C=O}$ = 1702; ν$_{max}$ = 2923, 1601, 1521, 1495, 1451, 1433, 1398, 1318, 1282, 1233, 1184, 1109, 945, 823, 767, 731, 696. MS (70 eV): m/z (%) 464 (M$^+$+1, 100). HRMS (ESI) Anal. Calcd. for C$_{30}$H$_{26}$NO$_2$S 464.1679 [M+H]$^+$, Found 464.1672.

### *4.4.6.5. Synthesis of 3-[(4-methoxycarbonylphenyl)iminomethyl]indole 16*

Indole-3-carbaldehyde **15** (435 mg, 3 mmol, 1 equiv), methyl 4-aminobenzoate (544 mg, 3.6 mmol, 1.2 equiv) and *p*-toluenesulfonic acid monohydrate (29 mg, 0.15 mmol, 0.05 equiv) were added to toluene (25 mL) in a Dean Stark apparatus. After 18 hour refluxing the mixture was extracted with EtOAc (25 mL) and washed with a saturated aqueous solution of sodium bicarbonate (25 mL), water (25 mL) and brine (25 mL). Drying (MgSO$_4$), filtering and evaporating of the organic layer yielded a yellow crude reaction mixture which was recrystallized from EtOAc/hexane to obtain 3-[(4-methoxycarbonylphenyl)iminomethyl]indole **16** (710 mg, 2.55 mmol, 85%) as a light yellow powder.

3-[(4-Methoxycarbonylphenyl)iminomethyl]indole 16 (85%)
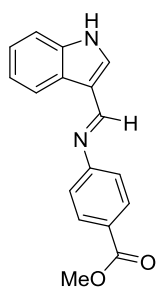
Light yellow powder. Recrystallization from EtOAc/Hexane. Mp = 159 °C. ^{1}H NMR (400 MHz, CDCl$_3$): δ 3.92 (3H, s, CH$_3$O); 7.24 (2H, d, J = 8.2 Hz, 2 × CH$_{arom}$); 7.29-7.31 and 7.38-7.40 (2H and 1H, 2 × m, 3 × CH$_{arom}$); 7.64 (1H, s, C$\underline{H}$NH); 8.07 (2H, d, J = 8.2 Hz, 2 × CH$_{arom}$); 8.49-8.51 (1H, m, CH$_{arom}$); 8.62 (1H, s, CHN); 8.83 (1H, s(br), NH). ^{13}C NMR (100.6 MHz, CDCl$_3$): δ 52.0 (CH$_3$O), 111.4 (CH$_{arom}$), 116.5 (C$_{quat,arom}$), 120.9, 122.1, 122.3 and 123.9 (5 × CH$_{arom}$), 125.1 and 126.3 (2 × C$_{quat,arom}$), 130.9 and 131.2 (3 × CH$_{arom}$), 136.9 (C$_{quat,arom}$), 155.7 (C=N), 157.7 (C$_{quat,arom}$), 167.2 (C=O). IR (ATR, cm^{-1}): ν$_{NH}$ = 3292; ν$_{C=O}$ = 1698; ν$_{max}$ = 1622, 1586, 1573, 1431, 1415, 1367, 1310, 1280, 1247, 1194, 1165, 1115, 1101, 851, 772, 748, 700. MS (70 eV): m/z (%) 279 (M$^+$+1, 100). HRMS (ESI) Anal. Calcd. for C$_{17}$H$_{15}$N$_2$O$_2$ 279.1128 [M+H]$^+$, Found 279.1135.

4.4.6.6. Synthesis of 3-[(4-methoxycarbonylphenyl)aminomethyl]indole 17

3-[(4-Methoxycarbonylphenyl)iminomethyl]indole **16** (417 mg, 1.5 mmol, 1 equiv) was dissolved in methanol (20 mL). To this solution was sodium borohydride (284 mg, 7.5 mmol, 5 equiv) added after which the mixture was heated to its boiling point. After 90 minutes of stirring the mixture was cooled to room temperature and quenched with water. The obtained mixture was extracted with EtOAc (2 x 25 mL), washed with water (25 mL) and brine (25 mL), dried (MgSO$_4$), filtered and evaporated under vacuum. After recrystallization from EtOAc/hexane 3-[(4-methoxycarbonylphenyl)-aminomethyl]indole **17** (370 mg, 1.32 mmol, 88%) was obtained as a yellow powder.

**3-[(4-Methoxycarbonylphenyl)aminomethyl]indole 17** (88%)
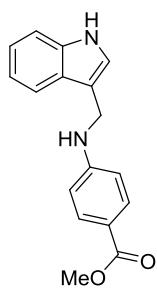
Yellow powder. Recrystallization from EtOAc/Hexane. Mp = 115.5 °C. ^{1}H NMR (400 MHz, D$_6$-DMSO): δ 3.74 (3H, s, CH$_3$O); 4.45 (2H, d, J = 5.3 Hz, C$\underline{H}_2$NH); 6.72 (2H, d, J = 8.8 Hz, 2 × CH$_{arom}$); 6.87 (1H, t, J = 5.3 Hz, CH$_2$N$\underline{H}$); 7.01 and 7.10 (2 × 1H, 2 × t, J = 7.5 Hz, 2 × CH$_{arom}$); 7.35-7.39 and 7.62-7.64 (2H and 1H, 2 × m, 3 × CH$_{arom}$); 7.70 (2H, d, J = 8.8 Hz, 2 × CH$_{arom}$); 10.95 (1H, s(br), NH) . ^{13}C NMR (100.6 MHz, D$_6$-DMSO): δ 38.7 (CH$_2$NH), 51.6 (CH$_3$O), 111.6 and 111.9 (3 × CH$_{arom}$), 112.2 and 116.0 (2 × C$_{quat,arom}$), 119.0, 119.2, 121.6 and 124.4 (4 × CH$_{arom}$), 127.1 (C$_{quat,arom}$), 131.3 (2 × CH$_{arom}$), 136.9 and 153.4 (2 × C$_{quat,arom}$), 166.9 (C=O). IR (ATR, cm^{-1}): ν$_{NH}$ = 3408, 3360; ν$_{C=O}$ = 1685; ν$_{max}$ = 1598, 1526, 1438, 1422, 1345, 1314, 1279, 1241, 1194, 1169, 1114, 1094, 840, 765, 738, 700. MS (70 eV): m/z (%) 279 (M$^-$-1, 20). HRMS (ESI) Anal. Calcd. for C$_{17}$H$_{15}$N$_2$O$_2$ 279.1139 [M-H]$^-$, Found 279.1146.

4.4.6.7. Synthesis of hydroxamic acids 7a-d, 8a-c, 13a-b, 14a-b and 18

General procedure: 3-[(4-Methoxycarbonylphenyl)aminomethyl]benzothiophene **6a** (400 mg, 1.35 mmol, 1 equiv) was dissolved in ethanol (10 mL) and to this solution was firstly hydroxylamine (8.3 mL, 50% in water, 135 mmol, 100 equiv) added and secondly potassium

hydroxide (16.9 mL, 4M in methanol, 67.5 mmol, 50 equiv). The resulting mixture was stirred for an additional 10 minutes at room temperature before it was poured in a saturated aqueous solution of sodium bicarbonate (10 mL). This aqueous solution was extracted two times with ethyl acetate, after which the combined organic fractions were washed with water (10 mL) and brine (10 mL). After drying (MgSO$_4$), filtering and evaporating a very viscous colorless liquid was obtained which was recrystallized overnight from CHCl$_3$ to obtain 3-[(4-hydroxycarbamoylphenyl)aminomethyl]benzothiophene **7a** (161 mg, 0.54 mmol, 40%) as a white powder. For hydroxamic acids **7b-d** and **8a-c** the mixture was stirred for 10 minutes in ethanol at refluxing conditions and for hydroxamic acids **13a-b**, **14a-b** and **18** the mixture was stirred for 10 minutes in THF at room temperature.

### 3-[(4-Hydroxycarbamoylphenyl)aminomethyl]benzothiophene 7a (40%)
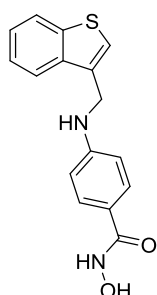
White powder. Crystallization from CHCl$_3$. Mp = 191 °C. ^{1}H NMR (300 MHz, D$_6$-DMSO): δ 4.53 (2H, d, J = 5.5 Hz, CH$_2$NH); 6.64 (2H, d, J = 8.6 Hz, 2 × CH$_{arom}$); 6.78 (1H, t, J = 5.5 Hz, CH$_2$NH); 7.35-7.43 (2H, m, 2 × CH$_{arom}$); 7.50 (2H, d, J = 8.6 Hz, 2 × CH$_{arom}$); 7.59 (1H, s, CHS); 7.90-8.00 (2H, m, 2 × CH$_{arom}$); 8.67 (1H, s(br), NHOH); 10.76 (1H, s(br), NHOH). ^{13}C NMR (75 MHz, D$_6$-DMSO): δ 41.4 (CH$_2$NH), 111.7 (2 × CH$_{arom}$), 120.1 (C$_{quat,arom}$), 122.7 and 123.5 (2 × CH$_{arom}$), 124.5 (CHS), 124.7, 125.0 and 128.8 (4 × CH$_{arom}$), 134.5, 138.5, 140.6 and 151.6 (4 × C$_{quat,arom}$), 165.5 (C=O). IR (ATR, cm^{-1}): $v_{NH/OH}$ = 3380, 3255, 3105; $v_{C=O}$ = 1600; v_{max} = 2862, 1620, 1568, 1500, 1480, 1464, 1340, 1314, 1307, 1259, 1156, 1022, 899, 831, 760, 729, 678. MS (70 eV): m/z (%) 299 (M$^+$+1, 100). HRMS (ESI) Anal. Calcd. for C$_{16}$H$_{15}$N$_2$O$_2$S 299.0849 [M+H]$^+$, Found 299.0862.

5-Bromo-3-[(4-hydroxycarbamoylphenyl)aminomethyl]benzothiophene 7b (85%)
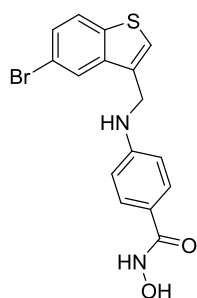
White powder. Crystallization from CHCl$_3$. Mp = 199 °C. ^{1}H NMR (300 MHz, D$_6$-DMSO): δ 4.52 (2H, d, J = 5.5 Hz, CH$_2$NH); 6.64 (2H, d, J = 8.5 Hz, 2 × CH$_{arom}$); 6.82 (1H, t, J = 5.5 Hz, CH$_2$NH); 7.50 (2H and 1H, d, J = 8.5 Hz, 3 × CH$_{arom}$); 7.69 (1H, s, CH$_{arom}$); 7.96 (1H, d, J = 8.5 Hz, CH$_{arom}$); 8.17 (1H, s, CH$_{arom}$); 8.67 (1H, s(br), NHOH); 10.75 (1H, s(br), NHOH). ^{13}C NMR (75 MHz, D$_6$-DMSO): δ 41.2 (CH$_2$NH), 111.8 (2 × CH$_{arom}$), 118.2 and 120.2 (2 × C$_{quat,arom}$), 125.3, 125.5, 126.7, 127.7 and 128.8 (6 × CH$_{arom}$), 134.1, 139.6, 140.4 and 151.5 (4 × C$_{quat,arom}$), 165.5 (C=O). IR (ATR, cm^{-1}): $v_{NH/OH}$ = 3376, 3235; $v_{C=O}$ = 1604; v_{max} = 2928, 1512, 1433, 1418, 1357, 1322, 1269, 1227, 1192, 1153, 1132, 1063, 1024, 970, 896, 873, 828, 807, 775, 621. MS (70 eV): m/z (%) 377/9 (M$^+$+1, 100). HRMS (ESI) Anal. Calcd. for C$_{16}$H$_{14}$BrN$_2$O$_2$S 376.9954 [M+H]$^+$, Found 376.9943.

3-[(4-Hydroxycarbamoylphenyl)aminomethyl]-5-phenyl-benzothiophene 7c (33%)
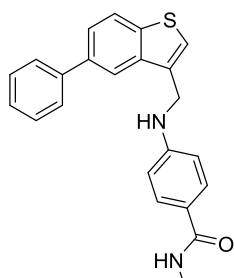
White powder. Crystallization from CHCl$_3$. Mp = 181 °C. ^{1}H NMR (300 MHz, D$_6$-DMSO): δ 4.62 (2H, d, J = 5.5 Hz, CH$_2$NH); 6.68 (2H, d, J = 8.8 Hz, 2 × CH$_{arom}$); 6.87 (1H, t, J = 5.5 Hz, CH$_2$NH); 7.35-7.40, 7.46-7.53 and 7.65-7.76 (1H, 4H and 4H, 3 × m, 9 × CH$_{arom}$); 8.05 (1H, d, J = 8.8 Hz, CH$_{arom}$); 8.19 (1H, s, CH$_{arom}$); 8.67 (1H, s(br), NHOH); 10.76 (1H, s(br), NHOH). ^{13}C NMR (75 MHz, D$_6$-DMSO): δ 41.4 (CH$_2$NH), 111.8 (2 × CH$_{arom}$), 120.0 (C$_{quat,arom}$), 120.8, 123.9, 124.1, 125.3, 127.7, 127.9, 128.8 and 129.5 (11 × CH$_{arom}$), 134.8, 137.1, 139.2, 139.8, 140.9 and 151.7 (6 × C$_{quat,arom}$), 165.5 (C=O). IR (ATR, cm^{-1}): ν$_{NH/OH}$ = 3403, 3202; ν$_{C=O}$ = 1608; ν$_{max}$ = 3056, 2902, 1661, 1573, 1505, 1442, 1422, 1342, 1319, 1299, 1279, 1260, 1162, 1135, 1033, 898, 830, 758, 698. MS (70 eV): m/z (%) 375 (M$^+$+1, 100). HRMS (ESI) Anal. Calcd. for C$_{22}$H$_{19}$N$_2$O$_2$S 375.1162 [M+H]$^+$, Found 375.1171.

3-[(4-Hydroxycarbamoyl-2-methylphenyl)aminomethyl]benzothiophene 7d (40%)
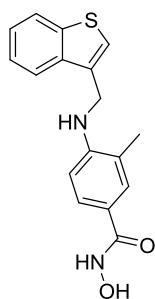
White powder. Crystallization from CHCl$_3$. Mp = 190 °C. ^{1}H NMR (300 MHz, D$_6$-DMSO): δ 2.16 (3H, s, CH$_3$); 4.63 (2H, d, J = 5.5 Hz, CH$_2$NH); 6.17 (1H, t, J = 5.5 Hz, CH$_2$NH); 6.51 (1H, d, J = 8.2 Hz, CH$_{arom}$); 7.36-7.43 (4H, m, 4 × CH$_{arom}$); 7.51 (1H, s, CH$_{arom}$); 7.96 (1H, d, J = 7.7 Hz, CH$_{arom}$); 8.05 (1H, d, J = 7.7 Hz, CH$_{arom}$); 8.66 (1H, s(br), NHOH); 10,73 (1H, s(br), NHOH). ^{13}C NMR (75 MHz, D$_6$-DMSO): δ 18.5 (CH$_3$), 41.7 (CH$_2$NH), 109.0 (CH$_{arom}$), 119.9 and 121.6 (2 × C$_{quat,arom}$), 122.7, 123.5, 124.1, 124.6, 125.0, 126.5 and 129.4 (7 × CH$_{arom}$), 134.7, 138.4, 140.7 and 149.2 (4 × C$_{quat,arom}$), 165.6 (C=O). IR (ATR, cm^{-1}): ν$_{NH/OH}$ = 3396, 3366, 3260; ν$_{C=O}$ = 1604; ν$_{max}$ = 3078, 2900, 2860, 1564, 1498, 1479, 1429, 1339, 1316, 1289, 1233, 1128, 1035, 983, 975, 832, 812, 798, 756, 724, 665. MS (70 eV): m/z (%) 313 (M$^+$+1, 100). HRMS (ESI) Anal. Calcd. for C$_{17}$H$_{17}$N$_2$O$_2$S 313.1005 [M+H]$^+$, Found 313.1019.

3-[N-Benzyl-N-(4-hydroxycarbamoylphenyl)aminomethyl]benzothiophene 8a (17%)
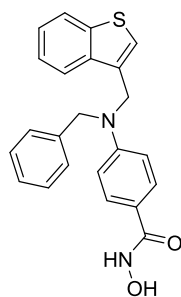
Brown powder. Purification by column chromatography (CH$_2$Cl$_2$/MeOH/Et$_3$N 95/5/2, Rf = 0.14). Mp = 178 °C. ^{1}H NMR (300 MHz, CDCl$_3$): δ 4.74 and 4.85 (2 × 2H, 2 × s, 2 × CH$_2$N); 6.74-6.76 (2H, m, 2 × CH$_{arom}$); 7.09 (1H, s, CHS); 7.20-7.40, 7.57-7.67 and 7.87-7.90 (7H, 3H and 1H, 3 × m, 11 × CH$_{arom}$). ^{13}C NMR (75 MHz, CDCl$_3$): δ 49.5 and 54.0 (2 × CH$_2$N), 111.9 (2 × CH$_{arom}$), 118.6 (C$_{quat,arom}$), 121.4, 122.8, 123.2, 124.3, 124.8, 126.6, 127.4, 128.8 and 128.9 (12 × CH$_{arom}$), 131.4, 137.5, 137.6, 141.3 and 151.8 (5 × C$_{quat,arom}$), 167.4 (C=O). IR (ATR, cm^{-1}): ν$_{NH/OH}$ = 3059; ν$_{C=O}$ = 1604; ν$_{max}$ = 3029, 2970, 2929, 2871, 1702, 1556, 1519, 1494, 1451, 1434, 1396, 1357, 1280, 1233, 1184, 1155, 1108, 1073, 1026, 947, 894, 821, 758, 730, 696. MS (70 eV): m/z (%) 389 (M$^+$+1, 100). HRMS (ESI) Anal. Calcd. for C$_{23}$H$_{21}$N$_2$O$_2$S 389.1318 [M+H]$^+$, Found 389.1334.

5-Bromo-3-[*N*-benzyl-*N*-(4-hydroxycarbamoylphenyl)aminomethyl]-benzothiophene 8b
(13%)
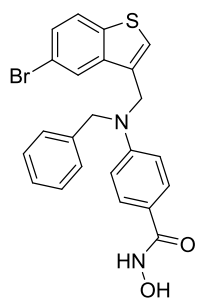
White powder. Purification by column chromatography (CH$_2$Cl$_2$/MeOH/Et$_3$N 95/5/2, Rf = 0.14). Mp = 179 °C. ^{1}H NMR (300 MHz, (CD$_3$)$_2$CO): δ 4.84 and 5.03 (2 × 2H, 2 × s, 2 × CH$_2$N); 6.82 (2H, d, *J* = 8.8 Hz, 2 × CH$_{arom}$); 7.24-7.37 (6H, m, 6 × CH$_{arom}$); 7.53 (1H, d, *J* = 8.8 Hz, CH$_{arom}$); 7.66 (2H, d, *J* = 8.8 Hz, 2 × CH$_{arom}$); 7.93 (1H, d, *J* = 8.8 Hz, CH$_{arom}$); 8.05 (1H, s, CH$_{arom}$); 10.45 (1H, s(br), NHOH). ^{13}C NMR (75 MHz, (CD$_3$)$_2$CO): δ 49.6 and 54.1 (2 × CH$_2$N), 111.9 (2 × CH$_{arom}$), 117.9 and 119.7 (2 × C$_{quat,arom}$), 124.7, 124.8, 126.7, 127.0, 127.5, 128.4 and 128.7 (11 × CH$_{arom}$), 132.2, 138.5, 139.8, 140.0 and 151.2 (5 × C$_{quat,arom}$), 165.7 (C=O). IR (ATR, cm^{-1}): ν$_{NH/OH}$ = 3199; ν$_{C=O}$ = 1605; ν$_{max}$ = 2970, 2924, 1703, 1556, 1513, 1505, 1494, 1452, 1393, 1359, 1232, 1203, 1154, 1072, 1026, 946, 894, 863, 818, 732, 696. MS (70 eV): m/z (%) 465/7 (M$^-$-1, 22). HRMS (ESI) Anal. Calcd. for C$_{23}$H$_{18}$BrN$_2$O$_2$S 465.0278 [M-H]$^-$, Found 465.0287.

### 3-[*N*-Benzyl-*N*-(4-hydroxycarbamoylphenyl)aminomethyl]-5-phenyl-benzothiophene 8c
(13%)
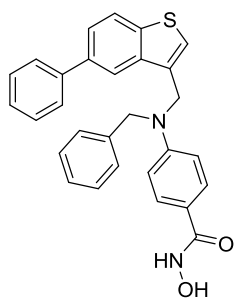
Yellow powder. Purification by column chromatography (CH$_2$Cl$_2$/MeOH/Et$_3$N 95/5/2, Rf = 0.14). Mp = 126 °C. ^{1}H NMR (300 MHz, CDCl$_3$): δ 4.73 and 4.88 (2 × 2H, 2 × s, 2 × CH$_2$N); 6.73-3.79 (2H, m, 2 × CH$_{arom}$); 7.11-7.46 and 7.59-7.63 (10H and 4H, 2 × m, 14 × CH$_{arom}$); 7.81 (1H, s, CH$_{arom}$); 7.92 (1H, d, *J* = 8.3 Hz, CH$_{arom}$); 8.63 (1H, s(br), NHOH). ^{13}C NMR (75 MHz): δ 49.7 and 54.0 (2 × CH$_2$N), 112.0 (2 × CH$_{arom}$), 118.4 (C$_{quat,arom}$), 119.8, 123.4, 123.5, 124.4, 126.6, 127.4, 127.5, 128.8 and 129.0 (16 × CH$_{arom}$), 131.5, 137.4, 137.9, 138.1, 140.3, 141.1 and 152.0 (7 × C$_{quat,arom}$), 167.6 (C=O). IR (ATR, cm^{-1}): ν$_{NH/OH}$ = 3198; ν$_{C=O}$ = 1604; ν$_{max}$ = 2969, 2926, 1702, 1556, 1519, 1494, 1451, 1434, 1396, 1357, 1318, 1280, 1233, 1184, 1155, 1108, 1073, 1026, 947, 894, 822, 758, 730, 696. MS (70 eV): m/z (%) 465 (M$^+$+1, 100). HRMS (ESI) Anal. Calcd. for C$_{29}$H$_{25}$N$_2$O$_2$S 465.1631 [M+H]$^+$, Found 465.1639.

6-Bromo-3-[(4-hydroxycarbamoylphenyl)aminomethyl]benzothiophene 13a (80%)
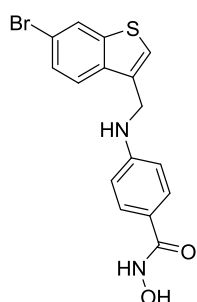
White powder. Crystallization from CHCl$_3$. Mp = 179.5 °C. ^{1}H NMR (400 MHz, D$_6$-DMSO): δ 4.54 (2H, d, *J* = 5.5 Hz, CH$_2$NH); 6.65 (2H, d, *J* = 8.6 Hz, 2 × CH$_{arom}$); 6.80 (1H, t, *J* = 5.5 Hz, CH$_2$NH); 7.52 (2H, d, *J* = 8.6 Hz, 2 × CH$_{arom}$); 7.58 (1H, d × d, *J* = 8.6, 1.7 Hz, CH$_{arom}$); 7.64 (1H, s, CH$_{arom}$); 7.90 (1H, d, *J* = 8.6 Hz, CH$_{arom}$); 8.30 (1H, d, *J* = 1.6 Hz, CH$_{arom}$); 8.69 (1H, s(br), NHOH); 10,78 (1H, s(br), NHOH). ^{13}C NMR (100.6 MHz, D$_6$-DMSO): δ 41.2 (CH$_2$NH), 111.6 (2 × CH$_{arom}$), 118.0 and 120.0 (2 × C$_{quat,arom}$), 124.2, 125.5, 125.8, 127.6 and 128.7 (6 × CH$_{arom}$), 134.2, 137.4, 142.4 and 151.5 (4 × C$_{quat,arom}$), 165.3 (C=O). IR (ATR, cm^{-1}): ν$_{NH/OH}$ = 3417, 3220; ν$_{C=O}$ = 1604; ν$_{max}$ = 1501, 1466, 1426, 1312, 1261, 1224, 1196, 1155, 1022, 891, 834, 812, 793, 765. MS (70 eV): m/z (%) 375/7 (M$^-$-1, 100). HRMS (ESI) Anal. Calcd. for C$_{16}$H$_{12}$BrN$_2$O$_2$S 374.9808 [M-1]$^-$, Found 374.9815.

3-[(4-Hydroxycarbamoylphenyl)aminomethyl]-6-phenyl-benzothiophene 13b (68%)
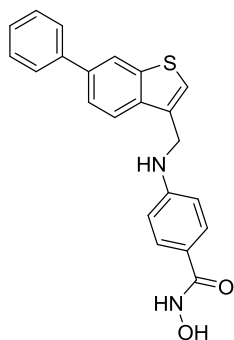
White powder. Crystallization from CHCl$_3$. Mp = 190.5 °C. ^{1}H NMR (400 MHz, D$_6$-DMSO): δ 4.58 (2H, d, J = 5.6 Hz, C$\underline{H}_2$NH); 6.68 (2H, d, J = 8.8 Hz, 2 × CH$_{arom}$); 6.82 (1H, t, J = 5.6 Hz, CH$_2$N$\underline{H}$); 7.39 (1H, t, J = 7.3 Hz, CH$_{arom}$); 7.48-7.55 (4H, m, 4 × CH$_{arom}$); 7.64 (1H, s, CH$_{arom}$); 7.72-7.78 (3H, m, 3 × CH$_{arom}$); 8.03 (1H, d, J = 8.4 Hz , CH$_{arom}$); 8.67 (1H, s(br), NHO$\underline{H}$); 10.77 (1H, s(br), N$\underline{H}$OH). ^{13}C NMR (100.6 MHz, D$_6$-DMSO): δ 41.4 (CH$_2$NH), 111.7 (2 × CH$_{arom}$), 120.0 (C$_{quat,arom}$), 121.3, 123.0, 123.7, 125.0, 127.4, 127.9, 128.7 and 129.5 (11 × CH$_{arom}$), 134.2, 137.1, 137.7, 140.5, 141.5 and 151.5 (6 × C$_{quat,arom}$), 165.4 (C=O). IR (ATR, cm^{-1}): ν$_{NH/OH}$ = 3411, 3254; ν$_{C=O}$ = 1604; ν$_{max}$ = 1567, 1499, 1462, 1420, 1336, 1308, 1259, 1195, 1153, 1020, 892, 829, 765, 745, 692. MS (70 eV): m/z (%) 375 (M$^+$+1, 35). HRMS (ESI) Anal. Calcd. for C$_{22}$H$_{19}$N$_2$O$_2$S 375.1162 [M+H]$^+$, Found 375.1154.

6-Bromo-3-[*N*-benzyl-*N*-(4-hydroxycarbamoylphenyl)aminomethyl]benzothiophene 14a (56%)

Light brown powder. Recrystallization from CHCl$_3$/ether. Mp = 97.5 °C. ^{1}H NMR (400 MHz, CDCl$_3$): δ 4.73 and 4.83 (2 × 2H, 2 × s, 2 × CH$_2$N); 6.76 (2H, d, J = 8.2 Hz, 2 × CH$_{arom}$); 7.08 (1H, s, CH$_{arom}$); 7.21 (2H, d, J = 7.1 Hz, 2 × CH$_{arom}$); 7.29-7.36 (3H, m, 3 × CH$_{arom}$); 7.50 (2H, s, 2 × CH$_{arom}$); 7.59 (2H, d, J = 8.2 Hz, 2 × CH$_{arom}$); 8.02 (1H, s, CH$_{arom}$). ^{13}C NMR (100.6 MHz, CDCl$_3$): δ 49.3 and 53.9 (2 × CH$_2$N), 111.9 (2 × CH$_{arom}$), 118.2 and 118.8 (2 × C$_{quat,arom}$), 122.3, 123.2, 125.6, 126.4, 127.4, 127.7, 128.7 and 128.9 (11 × CH$_{arom}$), 131.1, 136.2, 137.1, 142.6 and 151.8 (5 × C$_{quat,arom}$), 167.6 (C=O). IR (ATR, cm^{-1}): ν$_{NH/OH}$ = 3061; ν$_{C=O}$ = 1602; ν$_{max}$ = 2873, 2924, 1494, 1451, 1397, 1375, 1355, 1310, 1233, 1157, 1027, 944, 823, 811, 797, 755, 732, 696. MS (70 eV): m/z (%) 467/9 (M$^+$+1, 100). HRMS (ESI) Anal. Calcd. for C$_{23}$H$_{18}$BrN$_2$O$_2$S 467.0423 [M+H]$^+$, Found 467.0423.

3-[*N*-Benzyl-*N*-(4-hydroxycarbamoylphenyl)aminomethyl]-6-phenyl-benzothiophene 14b (74%)

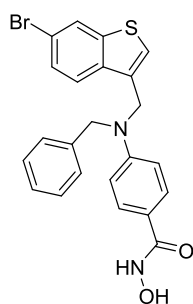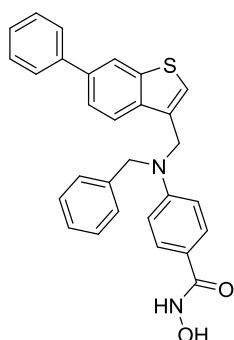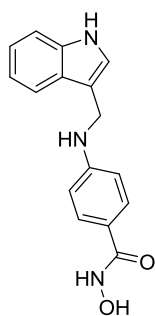White powder. Recrystallization from CHCl$_3$/ether. Mp = 102 °C. ^{1}H NMR (400 MHz, D$_6$-DMSO): δ 4.82 and 5.02 (2 × 2H, 2 × s, 2 × CH$_2$N); 6.75 (2H, d, J = 9.0 Hz, 2 × CH$_{arom}$); 7.24-7.41 (7H, m, 7 × CH$_{arom}$); 7.50 (2H, t, J = 7.6 Hz, 2 × CH$_{arom}$); 7.55 (2H, d, J = 9.0 Hz, 2 × CH$_{arom}$); 7.74 (1H, d × d, J = 8.4, 1.6 Hz, CH$_{arom}$); 7.77 (2H, d, J = 7.3 Hz, 2 × CH$_{arom}$); 7.94 (1H, d, J = 8.4 Hz, CH$_{arom}$); 8.33 (1H, s, CH$_{arom}$); 8.76 (1H, s(br), NHO$\underline{H}$); 10.82 (1H, s(br), N$\underline{H}$OH). ^{13}C NMR (100.6 MHz, D$_6$-DMSO): δ 49.9 and 54.1 (2 × CH$_2$N), 112.0 (2 × CH$_{arom}$), 120.4 (C$_{quat,arom}$), 121.4, 122.8, 123.8, 124.1, 127.0, 127.3, 127.4, 127.9, 128.7, 129.0 and 129.5 (16 × CH$_{arom}$), 132.8, 137.2, 137.3, 139.0, 140.4, 141.7 and 150.7 (7 × C$_{quat,arom}$), 165.1 (C=O). IR (ATR, cm^{-1}): ν$_{NH/OH}$ = 3026; ν$_{C=O}$ = 1602; ν$_{max}$ = 1556, 1519, 1495, 1461, 1397, 1376, 1356, 1287, 1232, 1186, 1157, 1027, 945, 897, 823, 762, 732, 696. MS (70 eV): m/z (%) 465 (M$^+$+1, 100). HRMS (ESI) Anal. Calcd. for C$_{29}$H$_{25}$N$_2$O$_2$S 465.1631 [M+H]$^+$, Found 465.1640.

3-[(4-Hydroxycarbamoylphenyl)aminomethyl]indole 18 (77%)

Yellow powder. Crystallization from $CHCl_3$. Mp = 132.5 °C. ^{1}H NMR (400 MHz, D_6-DMSO): δ 4.40 (2H, d, J = 5.3 Hz, C$\underline{H}_2$NH); 6.52 (1H, t, J = 5.3 Hz, $CH_2N\underline{H}$); 6.66 (2H, d, J = 8.8 Hz, 2 × CH_{arom}); 6.97-7.01, 7.06-7.10 and 7.33-7.37 (1H, 1H and 2H, 3 × m, 4 × CH_{arom}); 7.51 (2H, d, J = 8.8 Hz, 2 × CH_{arom}); 7.62 (1H, d, J = 7.8 Hz, CH_{arom}); 8.66 (1H, s(br), OH); 10.74 and 10.93 (2 × 1H, 2 × s(br), 2 × NH). ^{13}C NMR (100.6 MHz, D_6-DMSO): δ 38.8 (CH_2NH), 111.5 and 111.9 (3 × CH_{arom}), 112.5 ($C_{quat,arom}$), 118.9 and 119.2 (2 × CH_{arom}), 119.4 ($C_{quat,arom}$), 121.6 and 124.3 (2 × CH_{arom}), 127.1 ($C_{quat,arom}$), 128.6 (2 × CH_{arom}), 136.8 and 151.8 (2 × $C_{quat,arom}$), 165.5 (C=O). IR (ATR, cm^{-1}): $v_{NH/OH}$ = 3407; $v_{C=O}$ = 1601; v_{max} = 2860, 1567, 1524, 1456, 1419, 1346, 1319, 1284, 1241, 1160, 1034, 896, 826, 741. MS (70 eV): m/z (%) 282 (M$^+$+1, 20). HRMS (ESI) Anal. Calcd. for $C_{16}H_{16}N_3O_2$ 282.1237 [M+H]$^+$, Found 282.1236.

136

5. Synthesis of potent and selective HDAC6 inhibitors bearing a cyclohexane- or cycloheptane-annulated 1,5-benzothiazepine scaffold

Abstract: In this chapter, the synthesis of ten new benzohydroxamic acids, constructed by employing the tetrahydrobenzothiazepine core as a privileged pharmacophoric unit, is described. This is the first report on the synthesis and isolation of octahydrodibenzothiazepines and octahydro-6H-benzocycloheptathiazepines, which were then used to develop a new class of HDAC6 inhibitors. Evaluations of their HDAC-inhibiting activity resulted in the identification of cis-N-(4-hydroxycarbamoylbenzyl)-1,2,3,4,4a,5,11,11a-octahydrodibenzo[b,e][1,4]-thiazepine-10,10-dioxide and cis-N-(4-hydroxycarbamoylbenzyl)-7-trifluoromethyl-1,2,3,4,4a,5,11,11a-octahydrodibenzo[b,e][1,4]-thiazepine-10,10-dioxide as highly potent and selective HDAC6 inhibitors with activity in the low nanomolar range, which also show excellent selectivity on the enzymatic and cellular levels. Furthermore, four promising inhibitors were subjected to an Ames fluctuation assay, which revealed no mutagenic effects associated with these structures.*

5.1. Introduction

Histone deacetylases (HDACs), together with histone acetyltransferases (HATs), regulate the acetylation status of histones and other proteins through lysine acetylation and deacetylation.[121-123] This ability to modify the ε-amino tail of lysine residues allows the net charge of proteins to be changed, which makes HDACs valuable regulatory enzymes and explains the broad biological relevance of HDAC inhibitors, which have potential applications in the treatment of cancer, neurodegenerative diseases, depression, inflammatory diseases, and so forth.[19,124-128] Unfortunately, commercially available pan-HDAC inhibitors, which inhibit multiple classes of zinc-dependent HDACs (class I: HDAC1, 2, 3, and 8; class IIa: HDAC4, 5, 7, and 9; class IIb: HDAC6 and 10; class IV: HDAC11), have been reported to show toxic side effects, which hamper their broad clinical usability.[129,130] Therefore, many efforts are now devoted to the design and discovery of isozyme-selective HDAC inhibitors, which potentially have fewer toxic side effects while maintaining pronounced specific activity. In this regard, HDAC6, a member of HDAC class IIb, has been identified as an interesting pharmaceutical target, since its activity is associated with biological pathways operating in neurodegenerative diseases, cancer, and immunology.[8,10,79,101,105,131] Because of its cytoplasmic location, HDAC6 has several non-histone substrates (α-tubulin, cortactin, etc.), and this makes it an interesting protein for studying the acetylation status of proteins in cells. Hence, several groups embarked on a journey to discover selective HDAC6 inhibitors, which resulted in a variety of new compounds with promising potencies, as exemplified by inhibitors **1-8** (Figure 1).[13,23,24,30,36,82,132-140]
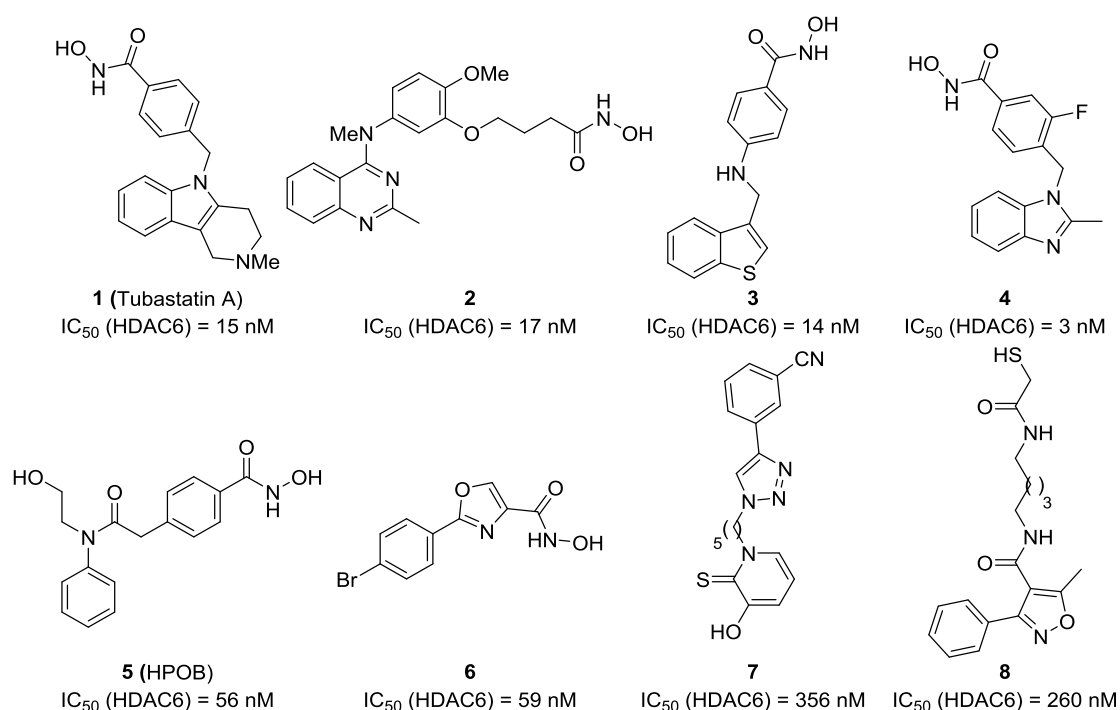
Figure 1. A selection of selective HDAC6 inhibitors reported in the literature.[13,24,36,82,132-135]

Of these compounds, our attention was initially drawn by Tubastatin A (**1**), a highly potent and selective HDAC6 inhibitor accommodating a tricyclic protein-surface recognition group (cap group) and a benzohydroxamic acid linker/zinc-binding group. In our first attempts to pursue new potent and selective HDAC6 inhibitors, the nitrogen-containing tricyclic tetrahydropyridoindole group in **1** was replaced by a sulfur-containing tetrahydrothiopyranoindole framework in compounds **9** (Figure 2) to give several *S*-oxidized analogues (denoted Tubathians) demonstrating excellent *in vitro* potency, selectivity, and pharmacokinetics.[104,141] The higher potency of these *S*-oxidized analogues with respect to HDAC6 was rationalized *in silico* through ligand-docking studies, which showed that sulfoxides **9** (x=1) and sulfones **9** (x=2) can establish an additional hydrogen bond with the surface of HDAC6. Inspired by these interesting findings, the present work aimed at expanding our thiaheterocyclic library of HDAC6 inhibitors through the design of new structures bearing a benzohydroxamic acid functionality and an unprecedented sulfur-containing tricyclic cap group. In this respect, 1,5-benzothiazepine was identified and selected as a suitable privileged scaffold for elaboration into a new class of HDAC6 inhibitors. Indeed, 1,5-benzothiazepine is a well-known pharmacophore exhibiting a broad range of biological activities (Ca^{2+} channel blockers, CNS-acting agents, anti-platelet aggregation, anti-HIV, angiotensin-converting enzyme inhibitors, antimicrobial, antifungal, calmodulin antagonist, bradykinin receptor agonist, anticancer) and is present in several FDA-approved drugs (diltiazem, clentiazem, thiazesim, quetiapine hemifumarate, and clotiapine).[142-144] Moreover, tetrahydro-1,5-benzothiazepine contains a secondary amino group and an oxidizable sulfur atom, which makes it an ideal building block for further synthetic elaboration into functionalized target structures. Considering that the cap group in previously developed HDAC6 inhibitors consists of a tricyclic structure bearing an aromatic A ring, an azaheterocyclic B ring, and a saturated C ring, the main objective of the present study was the development of a new tricyclic scaffold by annulation of a cyclohexane or cycloheptane ring to the 1,5-benzothiazepine unit *en route* to the synthesis of a series of octahydrodibenzo- (n=1) or octahydro-6*H*-benzocycloheptathiazepine-based (n=2) HDAC6 inhibitors **10**.

1 Tubastatin A

9
R^1 = H, F, Br
R^2 = H, OMe
n = 0, 1
x = 0, 1, 2

10
R = H, Cl, CF$_3$
x = 0, 1, 2
n = 1, 2
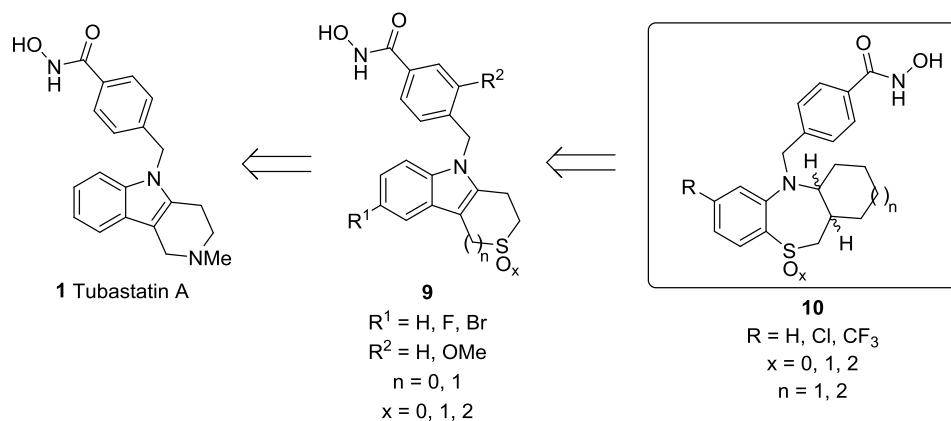
Figure 2. Synthesis rationale of this chapter.

5.2. Synthesis and biological evaluation of benzothiazepine-based benzohydroxamic acids

Only one report on the synthesis of tricyclic benzothiazepine **14** is available in the literature, starting from 2-(piperidin-1-ylmethyl)cyclohexan-1-one **11** or its HCl salt (Scheme 1).[145] Mannich base **11** was treated with 2-aminothiophenol **12** in refluxing benzene to furnish tricyclic imine **13** in 80% yield. After hydride reduction of cyclic imine **13**, the corresponding thiazepine **14** was obtained, although no reaction details were provided in the original report. We made several attempts to reproduce these results by using the same or slightly modified protocols, but we could never obtain cyclic imine **13**.
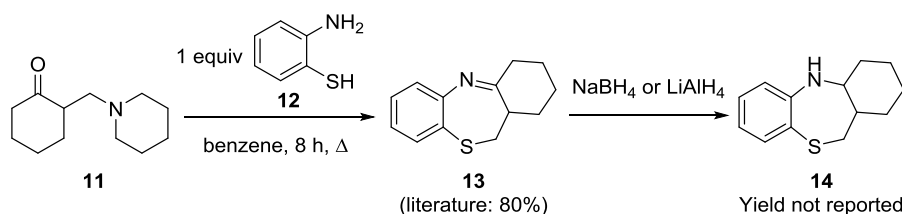
Scheme 1. Synthesis of octahydrodibenzo[*b*,*e*][1,4]thiazepine **14** reported by Hideg *et al.*[145]

Therefore, the literature procedure was modified, and 2-(tosyloxymethyl)cyclohexanone **17** was evaluated as starting material for the synthesis of secondary amines **19a-c**, bearing in mind the better leaving-group potential of the tosyloxy group compared to the piperidine ring (Scheme 2). To synthesize 2-(tosyloxymethyl)cyclohexanone **17**, β-hydroxyketone **16a** first had to be prepared from cyclohexanone **15a** (n=1). To that end, a literature procedure using paraformaldehyde instead of 37% aqueous formaldehyde was applied, and 2-(hydroxymethyl)cyclohexanone **16a** was obtained in 30% yield after column chromatography.[146] Ketone **16a** was subsequently tosylated in pyridine with 1.5 equiv of *p*-toluenesulfonyl chloride to provide **17** in 70% yield. We then attempted to produce imine **13** by heating tosylate **17** to reflux in toluene in the presence of 2-aminothiophenol **18a**. Although the formation of tricyclic imine **13** could be observed by LC-MS, only a mixture of products was obtained after workup. To circumvent this problem, a one-pot reductive amination was performed by treatment of tosyloxyketone **17** with 2-aminothiophenol **18a** in toluene under reflux for 45 min, after which the mixture was cooled to room temperature and 3 equiv of sodium cyanoborohydride were added. Then, the reaction medium was heated to boiling temperature, and after 1 h a mixture of diastereomers **19a1** and **19a2** was formed with a **19a1**/**19a2** ratio of 65:35 (determined by ^{1}H NMR and based on the correct assignment of the relative stereochemistry of diastereomer **19a1** by X-ray crystallography).

Separation and purification by column chromatography provided pure samples of both diastereomers **19a1** and **19a2** in 12% and 3% yield, respectively. The same protocol was used for the attempted synthesis of chloro- and trifluoromethyl-substituted benzothiazepines **19b**,**c**, but no conversion toward products **19b**,**c** could be realized. Moreover, during the synthesis of **19a1**,**a2**, β-tosyloxyketone **17** appeared to be unstable at elevated temperatures; therefore, the one-pot approach was expanded (scheme 2), and β-hydroxyketone **16a** was converted to 1,5-benzothiazepine **19a** via β-tosyloxyketone **17** prepared *in situ*. It was necessary to quench the excess of *p*-toluenesulfonyl chloride with water to prevent side reactions with 2-aminothiophenol. In this way, and after column-chromatographic purification, all six compounds **19a1-c2** (n=1) were obtained in pure form and acceptable yields (11-39%), taking into account the losses during chromatography resulting from similar R_f-values for all diastereomers. Moreover, a cycloheptanone derivative **19d** (n=2) was assembled from seven-membered β-hydroxyketone **16b**, which was synthesized in 15% yield from cycloheptanone **15b** (n=2) in the same manner as β-hydroxyketone **16a**, except the reaction solvent was changed from water to ethanol. In total, four pairs of diastereomers **19a1-d2** were thus prepared and isolated, whereby *cis* isomers **19a1-c1** were formed as the major products (d.r. *cis*/*trans* = 60-70:30-40, determined via ^{1}H NMR spectroscopy), except for diastereomers **19d**, which were obtained in a 1:1 ratio. The relative stereochemistry of heterotricyclic compounds **19a1-d2** was secured by X-ray crystallography of 1,5-benzothiazepine **19a1** and based on the characteristic signals present in the ^{1}H NMR spectra (CDCl$_3$) of compounds **19a1-d2** (Figure 3).
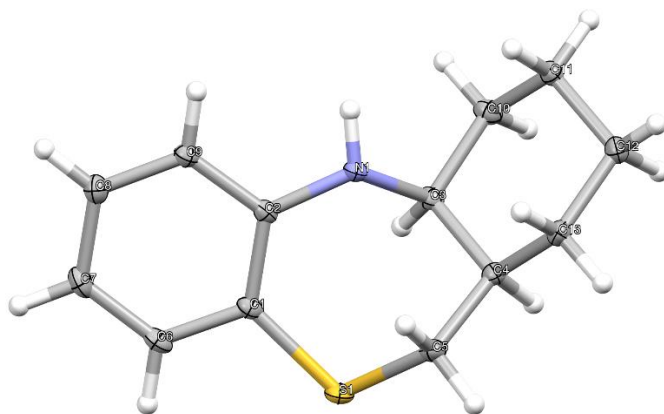
Figure 3. X-ray structure of 1,5-benzothiazepine **19a1**.
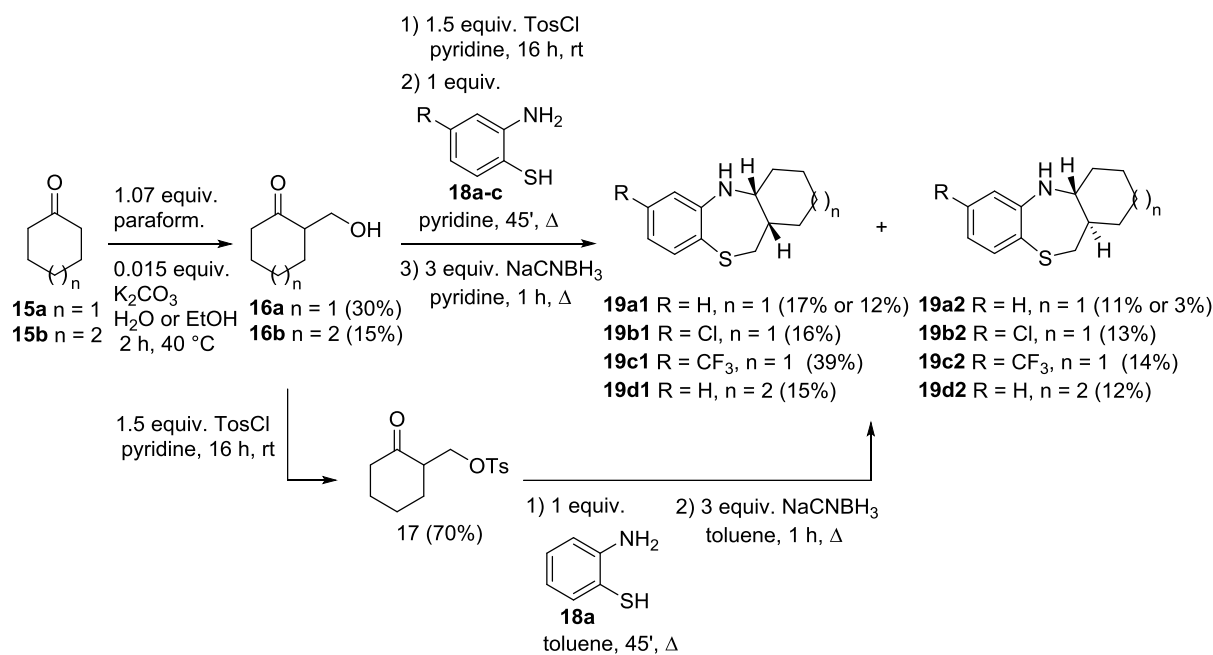
Scheme 2. Synthesis of 1,5-benzothiazepines **19a1**-**d2**.

In a following step, the tricyclic core fragment was connected to methyl 4-(bromomethyl)benzoate by a nucleophilic substitution reaction at nitrogen (Scheme 3). To efficiently perform this transformation a broad range of reaction conditions was tested, including the use of different bases (K_2CO_3, Cs_2CO_3, triethylamine, NaH, KHMDS, LiHMDS, butyllithium), solvents (THF, CH_3CN, DMF, DMSO), varying amounts of electrophile, and methyl 4-(iodomethyl)benzoate as a substitute electrophile; however, none of the tested conditions could affect the desired *N*-functionalization of 1,5-benzothiazepines **19a1-d2** to an extent greater than 50% (determined by ^{1}H NMR, $CDCl_3$). The highest conversion was obtained with 5 equiv of potassium carbonate in DMF at 120 °C after 16 h of reaction. To improve this degree of conversion, 1 equiv of methyl 4-(bromomethyl)benzoate was treated with 1,5-benzothiazepine **19a1** under neat conditions in the melt at 120 °C. After 2 h of reaction at 120 °C, 85% conversion was observed by ^{1}H NMR spectroscopy ($CDCl_3$). Unfortunately, due to the release of hydrogen bromide, traces of carboxylic acid were formed as well. Hence, the released hydrogen bromide was trapped by means of 3 equiv of potassium carbonate. Finally, an excellent conversion of 99% could be achieved, without the formation of any carboxylic acid, under neat reaction conditions for 3 h at 120 °C. By utilizing a similar strategy, esters **20a-d** and **23a,b** were also obtained from secondary amines **19a1-d1,b2** and **d2** in acceptable yields after column chromatography by varying the reaction time and temperature (37-66%, Scheme 3).

Oxidized sulfur analogues (e.g., sulfoxides and sulfones) of hydroxamic acids **10** could be of great value, given our previous observations that sulfur-oxidized analogues show a higher affinity for HDAC6 than their non-oxidized counterparts due to additional hydrogen bonding.[104] First, compounds **19a1-c1** were converted to the corresponding sulfones by using 3 equiv of *m*-chloroperbenzoic acid (*m*CPBA, Scheme 3). In this way, three sulfones **21a-c** were obtained in low to moderate yields (22-48%) after crystallization from ethanol. However, only **21a** could be transformed into *N*-benzylated compound **22a** by using a high reaction temperature (205 °C). This could be attributed to the high melting points of **21a-c** (234, 260 and 252 °C, respectively), and the fact that compounds **21b,c**, as opposed to sulfone **21a**, did not form a liquefied reaction mixture at 205 °C. In addition, the introduction of a strongly electron withdrawing sulfonyl group in *ortho* position with respect to the aromatic amino group results in a significant decrease in nucleophilicity of the nitrogen lone pair, which hinders smooth nucleophilic substitution. Higher reaction temperatures could possibly overcome this problem, but we chose to investigate the possibility to obtain sulfones **22b,c** by direct oxidation of esters **20b,c** instead. Thus, esters **20a-c** were subjected to the same conditions as cyclic sulfides **19a1-c1**, and as a result sulfones **22a-c** (x=2) were produced and isolated in high to excellent yields after crystallization from ethanol (73-97 %, Scheme 3). This strategy is clearly superior to the previous approach, since higher yields were obtained for the oxidation step (22-48 versus 73-97 %), and the sulfur derivatization takes place in a later stage of the synthesis pathway. When only 1 equiv of *m*CPBA was added to sulfide **20a** at 20 °C and a reaction time of 2 h was applied, sulfoxide **22d** (x=1) was obtained in 26% yield after crystallization from ethanol. The selective synthesis of these *S*-oxidized analogues provides the opportunity to compare the influence of the oxidation state of sulfur (sulfide, sulfoxide, or sulfone) on the biological profile of these compounds.
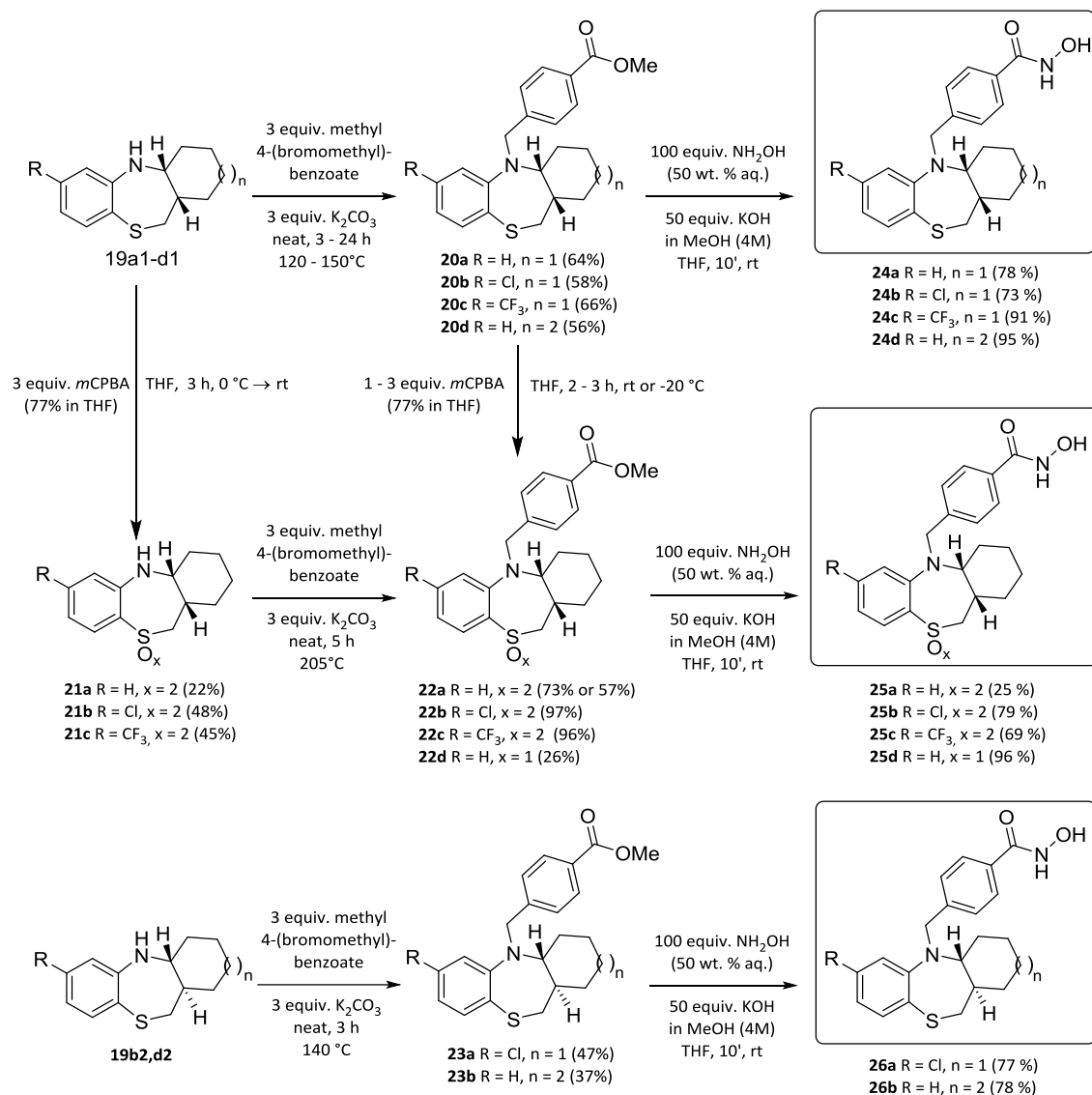
Scheme 3. Synthesis of the target hydroxamic acids **24**-**26**.

The synthesis of the cap group and the formation of the linker unit to furnish methyl esters **20/22/23** starting from the diastereomerically pure cyclohexane- or cycloheptane-annulated 1,5-benzothiazepine scaffolds **19a1-d1** and **19b2,d2** was described above. Hence, only the zinc complexing hydroxamic acid moiety had to be introduced through functional group conversion of esters **20/22/23** to complete the synthesis (Scheme 3). By using an excess of hydroxylamine and potassium hydroxide, methyl carboxylates **20/22/23** were converted to the target hydroxamic acids **24-26** in good yields (69-96 %, except 25% for **25a**). Thus, ten 1,5-benzothiazepine-containing benzohydroxamic acids **24-26** were prepared starting from tricyclic 1,5-benzothiazepines **19a1-d2**. These compounds were biologically screened for their capability to selectively inhibit HDAC6.

First, hydroxamic acids **24-26** were tested for their *in vitro* potential to inhibit HDAC6 at a concentration of 10 µM. This preliminary evaluation revealed that all compounds **24-26** strongly inhibited HDAC6 at this concentration (96-100% inhibition, Table 1), and hence their IC_{50} values toward HDAC6 were determined (Table 1). Compounds **24-26** are highly potent inhibitors with IC_{50} values in the nanomolar range, and the *S*-oxidized compounds **25** have even higher HDAC6 inhibitory activity than their non-oxidized analogues **24** (6.3-68 nM for **25** and 33-650 nM for **24**). The unsubstituted compounds **24a** and **25a** (R=H) have better IC_{50} values (36 and 8.3 nM, respectively) than the trifluoromethyl-substituted compounds **24c** and **25c** (R=CF$_3$; 200 and 11 nM, respectively), and chlorinated compounds **24b** and **25b** (R=Cl) show the lowest, yet still submicromolar, activity (650 and 68 nM, respectively). Hydroxamic acid **24d** containing a seven-membered ring shows the strongest inhibition of all sulfides (33 nM), and trans isomers **26** show intermediate potency with respect to the other compounds.

Table 1. *In vitro* enzyme inhibition data toward HDAC6

Compound	24a	24b	24c	24d	25a	25b	25c	25d	26a	26b
% inhibition of HDAC6 (10 µM)	98	97	96	100	99	98	100	99	99	97
HDAC6 IC$_{50}$ (µM)	0.036	0.650	0.200	0.033	0.008	0.068	0.011	0.006	0.160	0.092

Next, the selectivity of the five most potent HDAC6 inhibitors **24a,d** and **25a,c,d** was evaluated by determining the IC_{50} values toward the other zinc-dependent HDAC isoforms (HDAC1-11, Table 2). Sulfides **24a** and **d** show similar selectivity profiles, with high micromolar IC_{50} values for HDAC1-5, 7, 9 and 10 ($IC_{50} \geq 25$ µM) and low micromolar activities for HDAC8 and 11 (5.3-6.7 µM and 1.2-1.5 µM, respectively). Sulfones **25a,c** and sulfoxide **25d** show a somewhat lower selectivity profile compared to compounds **24a,d**, but still should be regarded as highly selective HDAC6 inhibitors. These compounds show low micromolar IC_{50} values for HDAC8 and 11 (1.1-2.9 and 0.54-2.4 µM, respectively), and exhibit some affinity for HDAC1 (4.9-8.8 µM). For HDAC2-5, 7, 9, and 10, higher IC_{50} values were obtained ($IC_{50} \geq 8.9$ µM). In general, taking the low nanomolar (toward HDAC6) and (high) micromolar (toward all other HDAC isozymes) IC_{50} values into account, it is fair to conclude that tricyclic benzothiazepine-based hydroxamic acids **24a,d** and **25a,c,d** can be regarded as highly potent and selective HDAC6 inhibitors suitable for further assessment.

Table 2. HDAC1-11 screening of selected compounds **24a,d** and **25a,c,d** (IC_{50} values in µM)[a,b,c]

HDAC1-11	1	2	3	4	5	6	7	8	9	10	11
24a	>30	N.C.	N.C.	>30	27	**0.036**	>30	5.3	25	>30	1.5
24d	>30	N.C.	>30	>30	>30	**0.033**	N.C.	6.7	>30	>30	1.2
25a	8.1	24	24	>30	9.1	**0.008**	22	1.1	13	10	2.4
25c	8.8	16	18	N.C.	22	**0.011**	15	2.0	>30	9.4	0.82
25d	4.9	26	>30	>30	12	**0.006**	>30	2.9	8.9	14	0.54
Tub A	16.4	>30	>30	>30	>30	**0.015**	>30	0.85	>30	>30	>30

[a] Reference compound: Trichostatin A (HDAC6 IC_{50} = 0.0093 µM). [b] NC: IC_{50} value not calculable. Concentration-response curve shows less than 25% effect at the highest validated testing concentration (30 µM). >30: IC_{50} value above the highest test concentration. Concentration-response curve shows less than 50% effect at the highest validated testing concentration (30 µM). [c] Literature values for Tub A (Tubastatin A)[13], caution should be taken when comparing the IC_{50} values of **24a**, **24d**, **25a**, **25c** and **25d** to the literature values for Tubastatin A.

The obtained in vitro HDAC6 inhibition data also confirmed the suggested improved affinity of oxidized analogues **25** in contrast to their non-oxidized counterparts **24** and **26**. This was further rationalized by *in silico* ligand docking and molecular dynamics simulation. Ligand docking was performed with a homology model of the functional domain of HDAC6 (Gly482-Gly800). Three initial models were built from different templates (pdb entry 2VQW, 2VQQ, 3C10), after which the best parts of each were combined into one hybrid model. The most likely conformation for both compounds was found to have the hydroxamate group positioned near the zinc ion, the linker in the tubular access channel and the cap group contacting the protein surface, which is in agreement with previous docking studies. The positions of the hydroxamate and linker groups in the docked structures of **24a** and **25a** are very similar, whereas the cap groups are rotated with respect to each other and form a few different apolar interactions. However, these do not result in significantly different binding energies (8.4 ± 0.5 and 8.5 ± 0.5 kcal mol^{-1}). Because docking alone could not explain the preference of HDAC6 for inhibitors carrying a sulfone moiety in the cap group, a molecular dynamics simulation was run. The entrance to the active site is surrounded by a few highly flexible loops that may influence binding, but this dynamic structure was not taken into account during the ligand docking experiment. The simulation of the complex with HDAC6 inhibitor **25a** revealed that a serine residue at position 564 has a clear tendency to move toward one of the oxygen atoms of the sulfone group, forming a hydrogen bond (Figure 4 and Figure 7 in the Experimental Details). This additional interaction might increase the affinity of HDAC6 for sulfone **25a** and other sulfone ligands, and account for experimentally observed lower IC_{50} values.
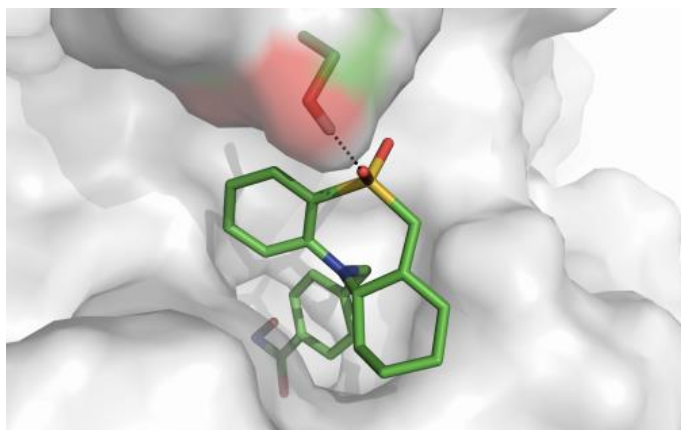
Figure 4. Molecular dynamics simulation of compound **25a** in HDAC6.

To evaluate the effectiveness of these compounds on a cellular level, HDAC6 inhibitors **24a,d** and **25a,c,d** were tested in N2a cells, a neuronal cell line, to determine their potency toward HDAC6 and their selectivity against class I HDACs. This was done by using Western Blots to detect the acetylation status of known substrates of HDAC6 and class I HDACs, that is, α-tubulin and histones, respectively. In vehicle-treated cells, α-tubulin is mainly present in its non-acetylated form (Figure 5A). Tubastatin A (1) was used as a positive control, as it increased the acetylation of α-tubulin at 1 µM (Figure 5A). Additionally, a sub-optimal concentration of 10 nM was chosen for the further characterization of the potency of the compounds. HDAC6 inhibitors **24a,d** and **25a,c,d** induced a significant increase in α-tubulin acetylation, as shown by Western Blot (Figure 5A, B). At the lower concentration of 10 nM, **25a** and **25c** induced a significant increase in the acetylation of α-tubulin (Figure 5A, C). Although for **25a,c,d** a low nanomolar potency toward HDAC6 was measured in the enzymatic assay, **25d** failed to induce a similar increase in α-tubulin acetylation at 10 nM, as compared to **25a** and **25c**. This indicates that in this more complex cellular environment additional cues, such as cell permeability, may lower the inhibitory capacity of **25d**.

Figure 5. Assessment of the potency of the HDAC6 inhibitors **24a,d** and **25a,c,d** in a neuronal cell line (N2a cells). **A**. Using Western Blot, the acetylation of α-tubulin was checked in N2a cells treated with different HDAC6 inhibitors. Tubastatin A (tubA) was used as a positive control. **B,C**. Densitometry was used to quantify the levels of acetylated α-tubulin relative to the amount of total α-tubulin present in the cells, treated with 1 µM or 10 nM of the HDAC6 inhibitors or tubastatin A. All values were normalized to the tubA-samples. N = 4. One-way Analysis-of-Covariance. $*p<0.05$, $**p<0.01$.

To evaluate the specificity of these compounds, the acetylation of histone 3 was also determined by Western blot as an indicator of class I HDAC inhibition. The rationale for this experiment relates to the fact that Tubastatin A, as a known selective HDAC6 inhibitor, does not affect the acetylation of histones (Figure 6A). None of the HDAC6 inhibitors tested interfered with histone acetylation, as expected and desired (Figure 6A, B). This observation further confirms the selectivity of the compounds toward HDAC6.

There is increasing concern about the potential genotoxicity of hydroxamic acids and their clinical use beyond oncology. Indeed, already in 1977 hydroxamic acids were reported to possibly exert genotoxic effects,[107,108] and mutagenic activities have been documented for three approved hydroxamic acid HDAC inhibitors (Vorinostat, Belinostat, and Panobinostat), which is less of an issue in cancer therapy.[147] Hence, compounds **24a,d** and **25a,c** were tested in the Ames fluctuation test against four strains of *Salmonella typhimurium* (TA98, TA100, TA1535, and TA1537), with and without the addition of rat liver S9 fraction. Surprisingly, no statistically significant positive effects could be detected in this *in vitro* reverse mutation assay at the concentrations tested (5, 10, 50 and 100 µM). This leads to the conclusion that our tricyclic benzothiazepine-based hydroxamic acids − in contrast to other hydroxamic acids described in the literature − may have a beneficial profile for further optimization studies toward new HDAC6 inhibitors for oncological and non-oncological applications. No bacterial cytotoxicity was observed at these concentrations, but other and more elaborate genotoxic

tests, for example, *in vitro* micronucleus and comet assays, should be performed in the future to exclude any potential genotoxicity of these compounds.
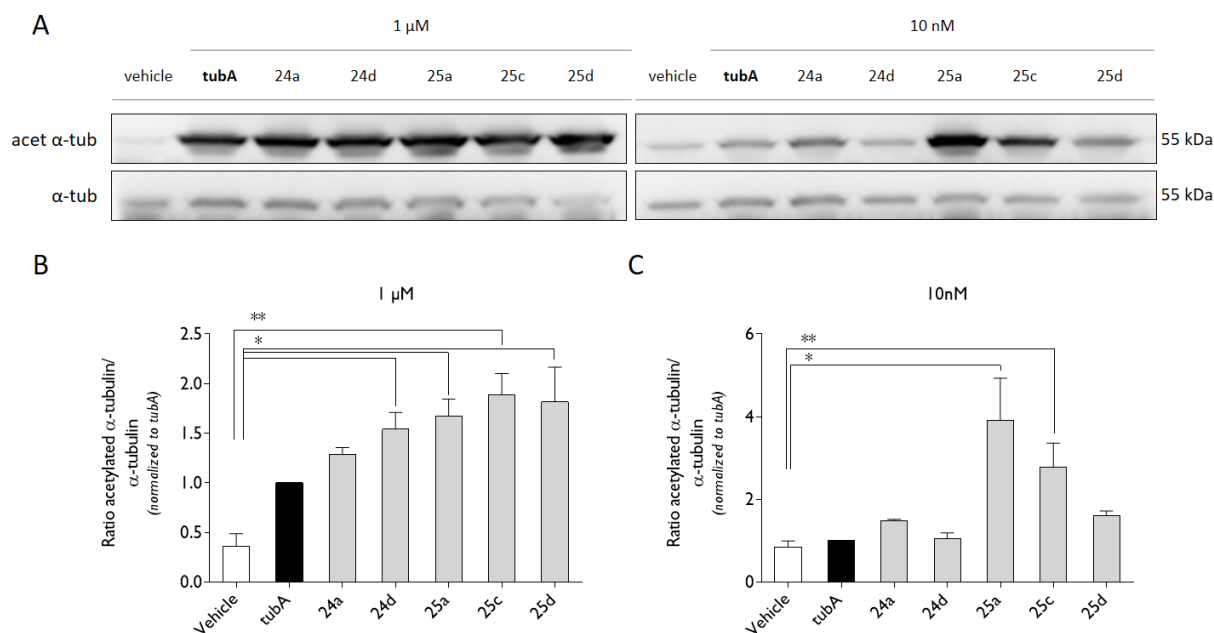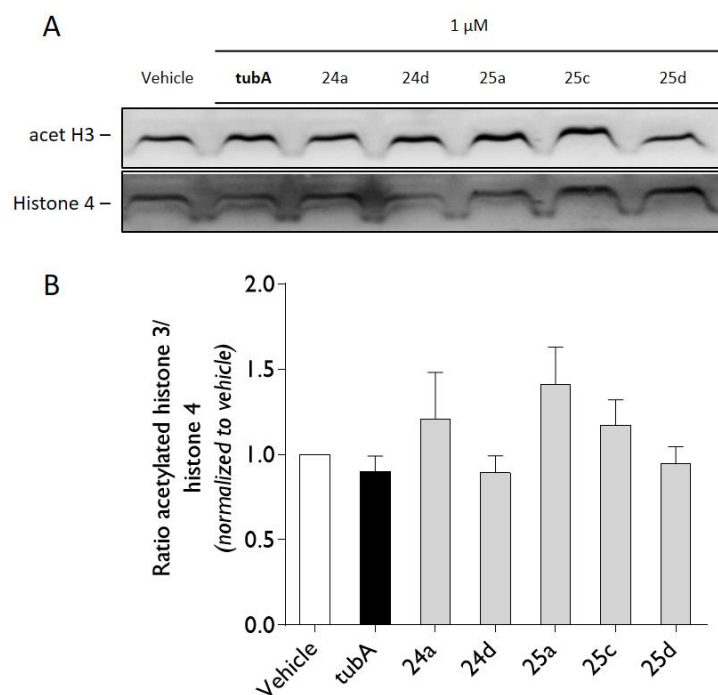

Figure 6. Assessment of the selectivity of the HDAC6 inhibitors **24a,d** and **25a,c,d** in a neuronal cell line. **A**. Using Western Blot, the acetylation of histone 3 (H3) was checked in N2a cells treated with different HDAC6 inhibitors (1 µM). Tubastatin A (tubA) was used as a control and an antibody directed against histone 4 was used as a loading control. **B**. Densitometry was used to quantify the levels of acetylated histone 3 relative to the amount histone 4 present in the cells, treated with 1 µM of the HDAC6 inhibitors or tubastatin A. All values were normalized to the vehicle-samples. N = 5. One-way Analysis-of-Covariance.

5.3. Conclusions

This is the first report on a detailed synthesis and isolation of both diastereomers of tricyclic cyclohexane- and cycloheptane-fused tetrahydrobenzothiazepines as new heterocyclic scaffolds, for which the correct structure was secured by X-ray crystallography. Starting from benzothiazepine building blocks **19a1-d2**, ten benzohydroxamic acids **24-26** were efficiently synthesized and tested for their ability to inhibit HDAC6. In accordance with previous observations regarding the effect of *S*-oxidation, oxidized sulfur analogues **25** proved to be more potent HDAC6 inhibitors than their non-oxidized counterparts **24** and **26**. This superior HDAC6 inhibitory activity of sulfoxide and sulfones **25** was supported by a molecular dynamics simulation, which revealed an additional hydrogen bond between the sulfur-bound oxygen atom and a serine residue. The most promising HDAC6 inhibitors **24a,d** and **25a,c,d** were further tested to assess their selectivity on both an enzymatic and a cellular level, and these studies revealed that compounds **25a** (*cis-N*-(4-hydroxycarbamoylbenzyl)-1,2,3,4,4a,5,11,11a-octahydrodibenzo[*b,e*][1,4]thiazepine-10,10-dioxide) and **25c** (*cis-N*-(4-hydroxycarbamoylbenzyl)-7-trifluoromethyl-1,2,3,4,4a,5,11,11a-octahydrodibenzo[*b,e*][1,4]-thiazepine-10,10-dioxide) demonstrated very potent activity and selectivity in both assays. Considering the reported genotoxicity of hydroxamic acids, four representatives **24a,d** and **25a,c** were tested in an Ames fluctuation assay, which showed safe profiles in that respect. This new class of tricyclic tetrahydrobenzothiazepine hydroxamic acids can thus be considered to be a valuable pool of new lead structures for further medicinal chemistry optimization studies in the pursuit of new therapeutic HDAC6 inhibitors.

5.4. Experimental details

5.4.1. Ligand docking

All docking experiments were performed by the Centre for Industrial Biotechnology and Biocatalysis (Prof. Desmet). All manipulations were performed with the molecular modelling program YASARA and the YASARA/WHATIF twinset[93,94] and the figure was created with PyMol v1.3.[97] The HDAC6 sequence was obtained from the UniProt database (www.uniprot.org, UniProt entry Q9UBN7). To increase the accuracy of the model, the sequence was limited to the major functional domain of HDAC6 (Gly482-Gly800). Possible templates were identified by running 3 PSI-BLAST iterations to extract a position specific scoring matrix (PSSM) from UniRef90, and then searching the PDB for a match. To aid the alignment of the HDAC6 sequence and templates, and the modelling of the loops, a secondary structure prediction was performed, followed by multiple sequence alignments. All side chains were ionised or kept neutral according to their predicted pKa values. Initial models were created from different templates (pdb entry 2VQW, 2VQQ and 3C10), each with several alignment variations and up to hundred conformations tried per loop. After the side-chains had been built, optimised and fine-tuned, all newly modelled parts were subjected to a combined steepest descent and simulated annealing minimisation, i.e. the backbone atoms of aligned residues were kept fixed to preserve the folding, followed by a full unrestrained simulated annealing minimisation for the entire model. The final model was obtained as a hybrid model of the best parts of the initial models, and checked once more for anomalies like incorrect configurations or colliding side chains. Furthermore, it was structurally aligned with known HDAC crystal structures to check if the chelating residues and the zinc atom were arranged correctly.

The HDAC inhibitor structures were created with YASARA Structure and energy minimised with the AMBER03 force field.[95] The grid box used for docking had a dimension of 25 x 25 x 25 angstrom, and comprised the entire catalytic cavity including the zinc ion and the outer surface of the active site entrance. Docking was performed with AutoDock VINA[109] and default parameters. Ligands were allowed to freely rotate during docking. The first conformer from the cluster that has its zinc binding group in the vicinity of the zinc ion, was selected as the binding mode for further analysis.

A 2ns MD simulation of the complex with HDAC6 inhibitor **25a** was conducted using the md_run macro implemented within YASARA with the AMBER03 force field. The standard parameters were maintained. Snapshots of the simulation were taken at regular time intervals.

Ligplot diagrams were made with LigPlot+ v1.4.
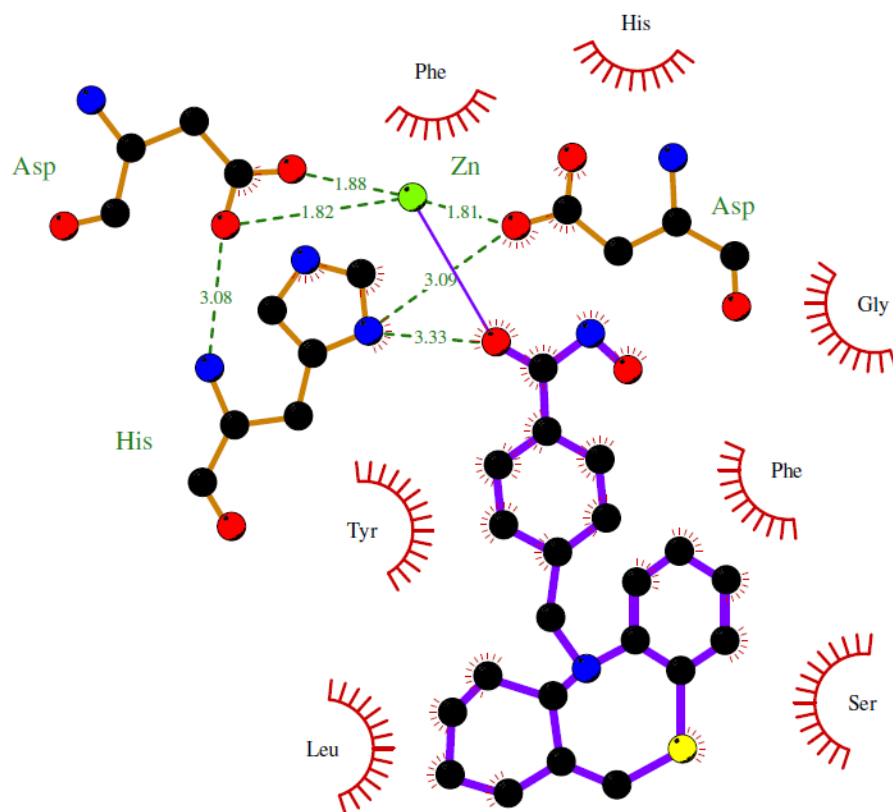
Figure 7. Ligplot diagram of compound **24a** (black: carbon, blue: nitrogen; red: oxygen; yellow: sulfur; green: zinc ion, values in Å).
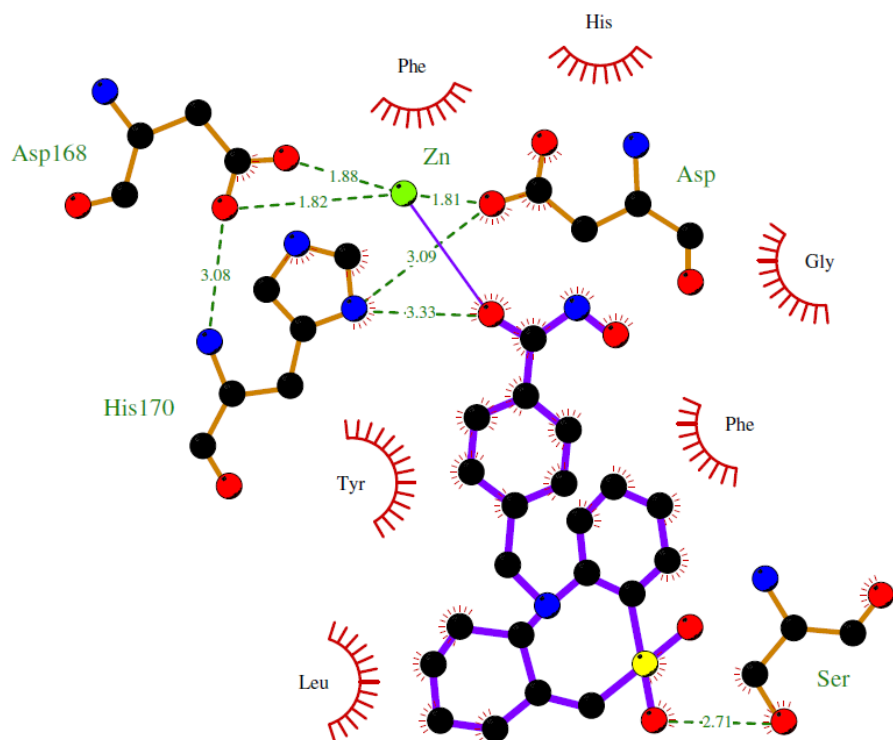
Figure 8. Ligplot diagram of compound **25a** (black: carbon, blue: nitrogen; red: oxygen; yellow: sulfur; green: zinc ion, values in Å).

5.4.2. Enzyme inhibition assays

The enzyme inhibition assays were performed by Eurofins Cerep Panlabs. *In vitro* IC$_{50}$ values were determined by using human recombinant HDAC1-11 and fluorogenic HDAC substrate.[98]

5.4.3. Western Blots

The Western Blots were performed by the Laboratory of Neurobiology and Vesalius Research Center, VIB (Prof. Van Den Bosch). Values represent the normalized ratio acetyl α-tubulin/α-tubulin and acetyl histone 3/histone 4 against Tubastatin A (Tub A) in an established neuronal cell line (Neuro-2a cells: ATCC N° CCL-131). Neuro-2a cells are treated overnight with different concentrations of the HDAC6 inhibitors and the effect on the acetylation level of α-tubulin is determined by using Western blot.

5.4.3.1. Cell culture

Mouse neuroblastoma (Neuro-2a) cells were grown in a 1:1 mix of D-MEM (Dulbecco's Modified Eagle Medium) and F12 medium supplemented with glutamax (Thermo Fisher Scientific, Waltham, MA, USA), 100 µg/ml streptomycin (Thermo Fisher Scientific), 100 U/ml penicillin (Thermo Fisher Scientific), 10% fetal calf serum (Greiner Bio-one, Kremsmünster, Austria), 1% non-essential amino acids (Thermo Fisher Scientific) and 1.6% NaHCO$_3$ (Thermo Fisher Scientific) at 37 °C and 7.5% CO$_2$. To split the cells, cells were washed with Versene (Thermo Fisher Scientific) and dissociated with 0.05% Trypsine-EDTA (Thermo Fisher Scientific). The Neuro-2a cells were treated overnight at 37°C with dosages ranging from 10 nM up to 1 µM of either Tubastatin A (Destelbergen, Belgium) or the candidate HDAC6 inhibitors.

4.4.3.2. Western Blot

For sodium dodecyl sulfate-polyacrylamide gel electrophoresis (SDS-PAGE) analysis, transfected cells were collected using the EpiQuik Total Histone Extraction Kit (EpiGentek, Farmingdale, NY, USA) according to manufacturer's instructions. Protein concentrations were determined using microBCA kit (Thermo Fisher Scientific) according to manufacturer's instructions. Before resolving the samples on a 12% SDS-PAGE gel, samples containing equal amounts of protein were supplemented with reducing sample buffer (Thermo Scientific) and boiled at 95 °C for 5 min. After electrophoresis, the proteins were transferred to a polyvinylidene difluoride (PVDF) membrane (Millipore Corp., Bedford, MA, USA). The non-specific binding was blocked by incubation of the membrane in 5% bovine serum albumin

(BSA), diluted in Tris Buffered Saline Tween (TBST, 50 mM TRIS, 150 mM NaCl, 0,1% Tween-20 (Applichem, Darmstadt, Duitsland) for 1h at room temperature followed by incubation with primary antibodies overnight. The antibodies, diluted in TBS-T, were directed against α-tubulin (1/5000, T6199, Sigma-Aldrich), and acetylated α-tubulin (1/5000, T6793 monoclonal, Sigma-Aldrich). The secondary antibodies, coupled to horseradish peroxidase (anti-mouse or anti-rabbit, 1/5000, Dako) were used. Blots were visualized by adding the ECF substrate (Enhanced Chemical Fluorescence, GE Healthcare, Uppsala, Sweden) and imaged with the ImageQuant_LAS 4000. A mild reblotting buffer (Millipore) was applied to strip the blots. ImageQuant TL version 7.0-software was used to quantify the blots.

5.4.4. Ames fluctuation assays

The Ames fluctuation assays were performed by Eurofins Cerep Panlabs. Wells that displayed bacteria growth due to the reversion of the histidine mutation (as judged by the ratio of OD430/OD570 being greater than 1.0) are counted and recorded as positive counts. The significance of the positive counts between the treatment (in the presence of test compound) and the control (in the absence of test compound) are calculated using the one-tailed Fisher's exact test.

5.4.5. X-ray crystallography

X-ray analysis was performed by the Department of Inorganic and Physical Chemistry (Ghent University, Prof. K. Van Hecke). For the structure of **19a1**, X-ray intensity data were collected at 100 K on an Agilent Supernova Dual Source (Cu at zero) diffractometer equipped with an Atlas CCD detector using ω scans and CuKα (λ = 1.54184 Å) radiation. The images were interpreted and integrated with the program CrysAlisPro (Agilent Technologies, Agilent, CrysAlis Pro; Agilent Technologies UK Ltd, Yarnton, England: 2013). Using Olex2,[148] the structure was solved by direct methods using the ShelXS structure solution program and refined by full-matrix least-squares on F^2 using the ShelXL program package.[149] Non-hydrogen atoms were anisotropically refined and the hydrogen atoms in the riding mode and isotropic temperature factors fixed at 1.2 times U(eq) of the parent atoms. The amine N-H hydrogen atom was unrestrained refined with an isotropic temperature factors fixed at 1.2 times U(eq) of the parent atom. The asymmetric unit has chirality at C3 (*S*) and C4 (*R*), but because of the centro-symmetric space group, also the inverse configuration is present in the crystal structure.

*Crystal data for compound **19a1***. $C_{13}H_{17}NS$, *M* = 219.34, monoclinic, space group *P*2$_1$/c (No. 14), *a* = 6.94615(11) Å, *b* = 15.8167(3) Å, *c* = 10.49482(20) Å, *β* = 103.9924(18), *V* = 1118.80(4) Å^3, *Z* = 4, *T* = 100 K, ρ_{calc} = 1.302 g cm^{-3}, μ(Cu-Kα) = 2.261 mm^{-1}, *F*(000) = 472,

10704 reflections measured, 2270 unique (R_{int} = 0.0317) which were used in all calculations. The final R1 was 0.0336 ($I > 2\sigma$ (I)) and wR2 was 0.0891 (all data).

CCDC 1494789 contains the supplementary crystallographic data for this molecule and can be obtained free of charge via www.ccdc.cam.ac.uk/conts/retrieving.html (or from the Cambridge Crystallographic Data Centre, 12, Union Road, Cambridge CB2 1EZ, UK; fax: +44-1223-336033; or deposit@ccdc.cam.ac.uk).

5.4.6. Synthetic procedures and spectral data

^{1}H, ^{13}C and ^{19}F NMR spectra were recorded at 400, 100.6, and 376.5 MHz (Bruker Avance III) with $CDCl_3$ or D_6-DMSO as solvent and TMS as internal standard. Mass spectra were obtained with an Agilent 1100 mass spectrometer (70 eV). IR spectra were measured with a Spectrum One FTIR spectrophotometer. High-resolution ES mass spectra were obtained with an Agilent Technologies 6210 series time-of-flight instrument. Melting points of crystalline compounds were measured with a Kofler Bench, type WME Heizbank of Wagner & Munz. Column chromatography was performed on silica gel (SiO_2), by using TLC plates and a UV lamp to identify the correct products. The purity of all tested compounds was assessed by ^{1}H NMR analysis and/or HPLC analysis, which confirmed a purity of ≥95%.

5.4.6.1. Synthesis of (hydroxymethyl)cycloalkanones *16*

General procedure: A mixture of cycloheptanone (22.43 g, 0.2 mol) and K_2CO_3 (0.41 g, 2.97 mmol, 0.015 equiv) in 50 mL of ethanol was stirred vigorously at 40 °C while paraformaldehyde (6.42 g, 0.214 mol, 1.07 equiv.) was added. Stirring was continued for 2 h, after which the cooled reaction mixture was extracted with 100 mL ethyl acetate and 100 mL water. The aqueous phase was three times extracted with 50 mL of ethyl acetate, and then the combined organic fractions were dried ($MgSO_4$) and concentrated under reduced pressure. The crude product was purified by column chromatography (SiO_2) to give 2-(hydroxymethyl)cycloheptan-1-one **16b** (4.26 g, 0.03 mmol, 15 %). For the synthesis of 2-(hydroxymethyl)cyclohexan-1-one **16a** water was used as the reaction solvent.

2-(Hydroxymethyl)cyclohexan-1-one 16a (30%)

Spectral data of 1,2,4,9-tetrahydro-3-thia-9-azafluorene **16a** correspond with data described in the literature.[146]

2-(Hydroxymethyl)cycloheptan-1-one 16b (15%)
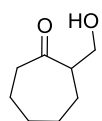
Colorless liquid. Purification by column chromatography (EtOAc/PE 1/1, Rf = 0.29). ^{1}H NMR (400 MHz, CDCl$_3$): δ 1.31-1.44, 1.50-1.60, 1.65-1.77 and 1.79-1.96 (2H, 1H, 2H and 3H, 4 × m, CH$_2$CH$_2$CH$_2$CH$_2$); 2.42-2.50 and 2.55-2.62 (2 × 1H, 2 × m, CH$_2$C=O); 2.75-2.82 (1H, m, CHC=O); 3.61 (1H, d × d, J = 11.2, 4.2 Hz, (HCH)O); 3.78 (1H, d × d, J = 11.2, 7.9 Hz, (HCH)O). ^{13}C NMR (100.6 MHz, CDCl$_3$): δ 23.8, 27.9, 29.1 and 29.6 (CH$_2$CH$_2$CH$_2$CH$_2$), 43.9 (CH$_2$C=O), 53.4 (CHC=O), 64.1 (CH$_2$O), 217.4 (C=O). IR (ATR, cm^{-1}): v_{OH} = 3402; $v_{C=O}$ = 1688; v_{max} = 1454, 1377, 1344, 1217, 1167, 1138, 1057, 1015, 984, 935, 920, 752. MS (70eV): m/z (%) 143 (M$^+$+1, 55).

5.4.6.2. Synthesis of 2-tosyloxymethylcyclohexanone 17a

In a 250 mL flask was added α-(hydroxymethyl)cyclohexanone **16a** (6.70 g, 52 mmol) dissolved in 67 mL of pyridine. To this solution was added *para*-toluenesulfonyl chloride (14.87 g, 78 mmol, 1.5 equiv.), and the reaction mixture was stirred at room temperature for 16 hours. The resulting mixture was quenched with 20 mL of ice water to convert the excess of *para*-toluenesulfonyl chloride to *para*-toluenesulfonic acid. The mixture was dissolved in 100 mL of ethyl acetate, and washed with 100 mL of HCl solution (1M), 100 mL of water and 100 mL of a saturated brine solution, dried over magnesium sulfate, filtered and evaporated. This afforded pure α-(tosyloxymethyl)cyclohexanone **17a**. (10.16 g, 36 mmol, 70 %).

2-(Tosyloxymethyl)cyclohexanone 17a (70%)
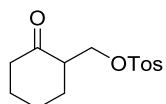
Colorless liquid. No purification needed. ^{1}H NMR (400 MHz, CDCl$_3$): δ 1.32-1.43, 1.56-1.71, 1.89-1.93, 2.05-2.13, 2.24-2.33 and 2.35-2.40 (1H, 2H, 1H, 1H, 2H and 1H, 6 × m, CH$_2$CH$_2$CH$_2$CH$_2$); 2.45 (3H, s, CH$_3$); 2.67-2.75 (1H, m, CHC=O); 3.95 (1H, d × d, J = 10.1, 7.6 Hz, (HCH)O); 4.32 (1H, d × d, J = 10.1, 5.0 Hz, (HCH)O); 7.35 and 7.80 (2 × 2H, 2 × d, J = 8.1 Hz, 4 × CH$_{arom}$). ^{13}C NMR (100.6 MHz, CDCl$_3$): δ 21.7 (CH$_3$), 24.5, 27.5, 30.9 and 42.0 (CH$_2$CH$_2$CH$_2$CH$_2$), 49.6 (CHC=O), 69.3 (CH$_2$O), 128.1 and 129.9 (4 × CH$_{arom}$), 132.7 and 144.9 (2 × C$_{arom,quat}$), 209.5 (C=O). IR (ATR, cm^{-1}): $v_{C=O}$ = 1707; $v_{S=O}$ = 1173; v_{max} = 1450, 1357, 1188, 1121, 1096, 960, 863, 814, 791, 750, 706, 644. MS (70eV): m/z (%) 300 (M$^+$+NH$_4$, 100). HRMS (ESI) Anal. Calcd. for C$_{14}$H$_{22}$NO$_4$S 300.1264 [M+NH$_4$]$^+$, Found 300.1259.

5.4.6.3. Synthesis of benzothiazepines 19

General procedure: α-(Hydroxymethyl)cyclohexanone **16a** (6.70 g, 52 mmol) was dissolved in pyridine (67 mL). *p*-Toluenesulfonyl chloride (14.87 g, 78 mmol, 1.5 equiv) was added to this solution, and the reaction mixture was stirred at room temperature for 16 h. Then, the reaction mixture was quenched with ice water (20 mL), after which 2-aminothiophenol (5.6 mL, 52 mmol, 1 equiv) was added. After stirring for 45 min under reflux conditions, the reaction mixture was cooled, and sodium cyanoborohydride (9.80 g, 0.156 mol, 3 equiv) was added portion-wise. After a reaction time of 1 h under reflux conditions, the reaction mixture was quenched

with water (20 mL) and then extracted with ethyl acetate (100 mL). The organic phase was washed with water (100 mL), a solution of NaCl (100 mL), and then dried with magnesium sulfate, filtered, and evaporated. Purification by column chromatography yielded *cis*-1,2,3,4,4a,5,11,11a-octahydrodibenzo[*b*,*e*][1,4]thiazepine **19a1** (1.94 g, 8.84 mmol, 17%) and *trans*-1,2,3,4,4a,5,11,11a-octahydrodibenzo[*b*,*e*][1,4]thiazepine **19a2** (1.25 g, 5.72 mmol, 11%).

cis-1,2,3,4,4a,5,11,11a-Octahydrodibenzo[*b*,*e*][1,4]thiazepine 19a1 (17%)
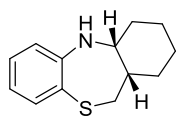
Yellow crystals. Purification by column chromatography (EtOAc/PE 3/97, Rf = 0.19). Mp = 82 °C. ^{1}H NMR (400 MHz, CDCl$_3$): δ 1.20-1.89 (9H, m, CH$_2$CH$_2$CH$_2$CH$_2$CH); 2.77 (1H, d × d, J = 14.3, 5.4 Hz, (HCH)S); 3.11 (1H, d × d, J = 14.3, 9.6 Hz, (HCH)S); 3.18 (1H, s(br), NH); 4.35 (1H, s(br), CHN); 6.55 (1H, d × d, J = 7.7, 1.4 Hz, CH$_{arom}$); 6.66 (1H, t × d, J = 7.7, 1.4 Hz, CH$_{arom}$); 6.94 (1H, t × d, J = 7.7, 1.4 Hz, CH$_{arom}$); 7.16 (1H, d × d, J = 7.7, 1.4 Hz, CH$_{arom}$). ^{13}C NMR (100.6 MHz, CDCl$_3$): δ 20.8, 25.4, 27.8 and 32.6 (CH$_2$CH$_2$CH$_2$CH$_2$), 37.4 (CH$_2$S), 40.2 (CHCH$_2$S), 52.7 (CHN), 118.6 and 119.4 (2 × CH$_{arom}$), 122.6 (C$_{arom,quat}$), 126.9 and 131.7 (2 × CH$_{arom}$), 148.9 (C$_{arom,quat}$). IR (ATR, cm^{-1}): ν_{NH} = 2914; ν_{max} = 1584, 1468, 1456, 1446, 1420, 1407, 1368, 1299, 1260, 1246, 1238, 1124, 1041, 740, 716. MS (70eV): m/z (%) 220 (M$^+$+1, 100). HRMS (ESI) Anal. Calcd. for C$_{13}$H$_{18}$NS 220.1155 [M+H]$^+$, Found 220.1162.

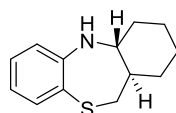### *trans*-1,2,3,4,4a,5,11,11a-Octahydrodibenzo[*b*,*e*][1,4]thiazepine 19a2 (11%)

White crystals. Purification by column chromatography (EtOAc/PE 3/97, Rf = 0.11). Mp = 97 °C. ^{1}H NMR (400 MHz, CDCl$_3$): δ 1.09-1.19, 1.24-1.40, 1.44-1.54 and 1.64-1.90 (1H, 2H, 1H and 5H, 4 × m, CH(CH$_2$)$_4$); 2.36 (1H, d × d, J = 14.4, 7.2 Hz, (HCH)S); 2.92-2.98 (1H, m, CHN); 3.14 (1H, d × d, J = 14.4, 3.8 Hz, (HCH)S); 3.36 (1H, s(br), NH); 6.71 (1H, d, J = 7.6 Hz, CH$_{arom}$); 6.78 (1H, t, J = 7.6 Hz, CH$_{arom}$); 7.04 (1H, t × d, J = 7.6, 1.2 Hz, CH$_{arom}$); 7.34 (1H, d × d, J = 7.6, 1.2 Hz, CH$_{arom}$). ^{13}C NMR (100.6 MHz, CDCl$_3$): δ 25.5, 25.6, 32.0 and 34.6 ((CH$_2$)$_4$), 38.3 (CH$_2$S), 47.4 (CHCH$_2$S), 60.5 (CHN), 120.2 and 120.8 (2 × CH$_{arom}$), 125.5 (C$_{arom,quat}$), 127.7 and 132.4 (2 × CH$_{arom}$), 150.2 (C$_{arom,quat}$). IR (ATR, cm^{-1}): ν_{NH} = 3332; ν_{max} = 2915, 2848, 1471, 1442, 1367, 1302, 1238, 1072, 870, 746, 732, 717. MS (70eV): m/z (%) 220 (M$^+$+1, 100). HRMS (ESI) Anal. Calcd. for C$_{13}$H$_{18}$NS 220.1155 [M+H]$^+$, Found 220.1162.

cis-7-Chloro-1,2,3,4,4a,5,11,11a-octahydrodibenzo[*b*,*e*][1,4]thiazepine 19b1 (16%)
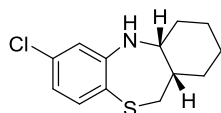
White crystals. Purification by column chromatography (EtOAc/PE 3/97, Rf = 0.19). Mp = 132 °C. ^{1}H NMR (400 MHz, CDCl$_3$): δ 1.20-1.32, 1.34-1.45, 1.51-1.61 and 1.65-1.88 (1H, 1H, 3H and 4H, 4 × m, CH(CH$_2$)$_4$); 2.78 (1H, d × d, J = 14.4, 5.7 Hz, (HCH)S); 3.09 (1H, d × d, J = 14.4, 9.8 Hz, (HCH)S); 3.22 (1H, s(br), NH); 4.46 (1H, s(br), CHN); 6.54 (1H, d, J = 2.2 Hz, CH$_{arom}$); 6.61 (1H, d × d, J = 8.3, 2.2 Hz, CH$_{arom}$); 7.04 (1H, d, J = 8.3 Hz, CH$_{arom}$). ^{13}C NMR (100.6 MHz, CDCl$_3$): δ 20.6, 25.3, 27.8 and 32.3 ((CH$_2$)$_4$), 37.5 (CH$_2$S), 40.1 (CHCH$_2$S), 52.4 (CHN), 117.9 and 119.0 (2 x CH$_{arom}$), 120.7 and 132.1 (2 × C$_{arom,quat}$), 132.5 (CH$_{arom}$), 149.7 (C$_{arom,quat}$). IR (ATR, cm^{-1}): ν_{NH} = 3387; ν_{max} = 2926, 1582, 1564, 1469, 1436, 1372, 1309, 1245, 1229, 1098, 1050, 1008, 846,

780. MS (70eV): m/z (%) 254 (M$^+$+1, 100). HRMS (ESI) Anal. Calcd. for C$_{13}$H$_{17}$ClNS 254.0765 [M+H]$^+$, Found 254.0764.

trans-7-Chloro-1,2,3,4,4a,5,11,11a-octahydrodibenzo[*b,e*][1,4]thiazepine 19b2 (13%)

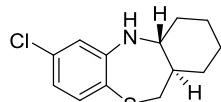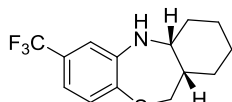White crystals. Purification by column chromatography (EtOAc/PE 3/97, Rf = 0.11). Mp = 158 °C. ^{1}H NMR (400 MHz, CDCl$_3$): δ 1.12-1.51, 1.64-1.75 and 1.81-1.89 (4H, 3H and 2H, 3 × m, CH(CH$_2$)$_4$); 2.36 (1H, d × d, *J* = 14.4, 6.5 Hz, (HCH)S); 3.06-3.13 (1H, m, CHN); 3.20 (1H, d × d, *J* = 14.4, 4.1 Hz, (HCH)S); 3.37 (1H, s(br), NH); 6.69 (1H, d, *J* = 2.1 Hz, CH$_{arom}$); 6.72 (1H, d × d, *J* = 8.2, 2.1 Hz, CH$_{arom}$); 7.21 (1H, d, *J* = 8.2 Hz, CH$_{arom}$). ^{13}C NMR (100.6 MHz, CDCl$_3$): δ 25.4, 25.5, 31.9 and 34.3 ((CH$_2$)$_4$), 38.2 (CH$_2$S), 47.0 (CHCH$_2$S), 60.0 (CHN), 119.5 and 120.4 (2 x CH$_{arom}$), 123.4 and 132.8 (2 × C$_{arom,quat}$), 133.2 (CH$_{arom}$), 150.9 (C$_{arom,quat}$). IR (ATR, cm^{-1}): ν$_{NH}$ = 3318; ν$_{max}$ = 2931, 1574, 1462, 1443, 1234, 1098, 1073, 893, 870, 799, 754, 716. MS (70eV): m/z (%) 254/6 (M$^+$+1, 100). HRMS (ESI) Anal. Calcd. for C$_{13}$H$_{17}$ClNS 254.0765 [M+H]$^+$, Found 254.0781.

cis-7-Trifluoromethyl-1,2,3,4,4a,5,11,11a-octahydrodibenzo[*b,e*][1,4]thiazepine 19c1 (38%)

White crystals. Purification by column chromatography (EtOAc/PE 3/97, Rf = 0.5). Mp = 120 °C. ^{1}H NMR (400 MHz, CDCl$_3$): δ 1.20-1.52, 1.56-1.62, 1.67-1.77 and 1.81-1.87 (3H and 3 × 2H, 4 × m, CH(CH$_2$)$_4$); 2.80 (1H, d × d, *J* = 14.4, 5.8 Hz, (HCH)S); 3.19 (1H, d × d, *J* = 14.4, 10.2 Hz, (HCH)S); 3.34 (1H, s(br), NH); 4.59 (1H, s(br), CHN); 6.73 (1H, s, CH$_{arom}$); 6.84 (1H, d, *J* = 8.0 Hz, CH$_{arom}$); 7.18 (1H, d, *J* = 8.0 Hz, CH$_{arom}$). ^{19}F NMR (376.5 MHz, CDCl$_3$): δ (-62.8) (s). ^{13}C NMR (100.6 MHz, CDCl$_3$): δ 20.5, 25.3, 28.0 and 32.1 ((CH$_2$)$_4$), 37.2 (CH$_2$S), 39.5 (CHCH$_2$S), 52.1 (CHN), 114.4 (q, *J* = 3.7 Hz, CH$_{arom}$), 115.3 (q, *J* = 3.7 Hz, CH$_{arom}$), 124.1 (q, *J* = 271.9 Hz, F$_3$C$_{quat}$), 126.1 (C$_{arom,quat}$), 128.8 (q, *J* = 32.3 Hz, F$_3$CC$_{arom,quat}$), 131.7 (CH$_{arom}$), 148.5 (C$_{arom,quat}$). IR (ATR, cm^{-1}): ν$_{NH}$ = 3398, ν$_{max}$ = 2935, 1471, 1334, 1310, 1296, 1232, 1164, 1131, 1108, 1086, 1037, 1009, 856, 810. MS(70eV): m/z (%) 288 (M$^+$+1, 100). HRMS (ESI) Anal. Calcd. for C$_{14}$H$_{17}$F$_3$NS 288.1028 [M+H]$^+$, Found 288.1025.

trans-7-Trifluoromethyl-1,2,3,4,4a,5,11,11a-octahydrodibenzo[*b,e*][1,4]thiazepine 19c2 (14%)
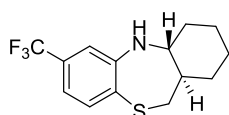
White crystals. Purification by column chromatography (EtOAc/PE 3/97, Rf = 0.36). Mp = 132 °C. ^{1}H NMR (400 MHz, CDCl$_3$): δ 1.21-1.53, 1.65-1.79 and 1.84-1.93 (4H, 3H and 2H, 3 x m, CH(CH$_2$)$_4$); 2.43 (1H, d x d, *J* = 14.5, 5.4 Hz, (HCH)S); 3.32-3.38 (1H, m, CHN); 3.44 (1H, d x d, *J* = 14.5, 4.5 Hz, (HCH)S); 3.51 (1H, s(br), NH); 6.87 (1H, d, *J* = 1.3 Hz, CH$_{arom}$); 6.96 (1H, d × d, *J* = 8.1, 1.3 Hz, CH$_{arom}$); 7.37 (1H, d, *J* = 8.1 Hz, CH$_{arom}$). ^{19}F NMR (376.5 MHz, CDCl$_3$): δ (-62.7) (s). ^{13}C NMR (100.6 MHz, CDCl$_3$): δ 25.4, 25.5, 31.7 and 34.0 ((CH$_2$)$_4$), 38.0 (CH$_2$S), 46.4 (CHCH$_2$S), 59.5 (CHN), 115.8 (q, *J* = 3.7 Hz, CH$_{arom}$), 116.4 (q, *J* = 3.7 Hz, CH$_{arom}$), 123.8 (q, *J* = 271.9 Hz, F$_3$C$_{quat}$), 128.4 (C$_{arom,quat}$), 129.5 (q, *J* = 32.3 Hz, F$_3$CC$_{arom,quat}$), 132.4 (CH$_{arom}$), 149.5 (C$_{arom,quat}$). IR (ATR, cm^{-1}): ν$_{NH}$ = 3329; ν$_{max}$ = 2937, 1330, 1292, 1236, 1162, 1140, 1123, 1108, 1090, 1080, 1055, 735. MS (70eV): m/z (%) 288 (M$^+$+1, 100). HRMS (ESI) Anal. Calcd. for C$_{14}$H$_{17}$F$_3$NS 288.1028 [M+H]$^+$, Found 288.1033.

### *cis*-6,6a,7,8,9,10,11,11a-Octahydro-12*H*-benzo[*b*]cyclohepta[*e*][1,4]thiazepine 19d1 (15%)
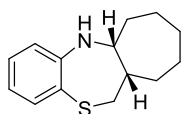
Yellow crystals. Purification by column chromatography (EtOAc/PE 2/98, Rf = 0.27). Mp = 87 °C. ^{1}H NMR (400 MHz, CDCl$_3$): δ 1.23-1.44, 1.58-1.76, 1.83-1.89, 2.03-2.11 and 2.18-2.25 (5H, 2H, 2H, 1H and 1H, 5 × m, CH$_2$CH$_2$CH$_2$CH$_2$CH$_2$CH); 2.73 (1H, d × d, *J* = 14.1, 5.4 Hz, (<u>H</u>CH)S); 2.92 (1H, s(br), NH); 3.51 (1H, d × d, *J* = 14.1, 11.4 Hz, (HC<u>H</u>)S); 4.58-4.64 (1H, m, CHN); 6.48 (1H, d × d, *J* = 7.9, 1.3 Hz, CH$_{arom}$); 6.65 (1H, t × d, *J* = 11.3, 1.3 Hz, CH$_{arom}$); 6.91 (1H, t × d, *J* = 11.3, 1.3 Hz, CH$_{arom}$); 7.09 (1H, d × d, *J* = 7.9, 1.3 Hz, CH$_{arom}$). ^{13}C NMR (100.6 MHz, CDCl$_3$): δ 23.3, 28.6, 29.3, 31.1 and 35.6 (CH$_2$CH$_2$CH$_2$CH$_2$CH$_2$), 37.0 (CH$_2$S), 45.0 (<u>C</u>HCH$_2$S), 56.3 (CHN), 118.2 and 119.2 (2 × CH$_{arom}$), 121.1 (C$_{arom,quat}$), 126.3 and 130.5 (2 × CH$_{arom}$), 147.9 (C$_{arom,quat}$). IR (ATR, cm^{-1}): ν$_{NH}$ = 3375; ν$_{max}$ = 1584, 1458, 1312, 1300, 1246, 1120, 743, 721, 446. MS (70eV): m/z (%) 234 (M$^+$+1, 100).

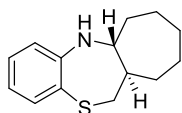### *trans*-6,6a,7,8,9,10,11,11a-Octahydro-12*H*-benzo[*b*]cyclohepta[*e*][1,4]thiazepine 19d2 (12%)

Yellow crystals. Purification by column chromatography (EtOAc/PE 2/98, Rf = 0.21). Mp < 50 °C. ^{1}H NMR (400 MHz, CDCl$_3$): δ 1.54-1.64, 1.66-1.75 and 1.91-2.00 (6H, 3H and 2H, 3 × m, CH$_2$CH$_2$CH$_2$CH$_2$CH$_2$CH); 2.45 (1H, d × d, *J* = 14.0, 3.5 Hz, (<u>H</u>CH)S); 3.13 (1H, s(br), NH); 3.71-3.77 (1H, m, CHN); 3.88 (1H, d × d, *J* = 14.0, 4.3 Hz, (HC<u>H</u>)S); 6.49 (1H, d × d, *J* = 7.8, 1.4 Hz, CH$_{arom}$); 6.65-6.69 (1H, m, CH$_{arom}$); 6.90-6.94 (1H, m, CH$_{arom}$); 7.11 (1H, d × d, *J* = 7.8, 1.4 Hz, CH$_{arom}$). ^{13}C NMR (100.6 MHz, CDCl$_3$): δ 24.8, 26.4, 26.6, 32.8 and 37.6 (CH$_2$CH$_2$CH$_2$CH$_2$CH$_2$), 39.2 (CH$_2$S), 45.2 (<u>C</u>HCH$_2$S), 61.3 (CHN), 118.5 and 119.7 (2 × CH$_{arom}$), 121.4 (C$_{arom,quat}$), 126.4 and 130.6 (2 × CH$_{arom}$), 148.3 (C$_{arom,quat}$). IR (ATR, cm^{-1}): ν$_{NH}$ = 3395; ν$_{max}$ = 1585, 1466, 1414, 1371, 1302, 1244, 1082, 1069, 745, 669, 420. MS (70eV): m/z (%) 234 (M$^+$+1, 100).

5.4.6.4. *Synthesis of sulfones and sulfoxide 21 and 22*

General procedure: *m*-Chloroperbenzoic acid (≤77%, 3.36 g, 15 mmol) was added to a solution of **19a1** (1.10 g, 5 mmol) in THF (50 mL) at 0 °C, and the mixture was stirred at room temperature for 2 h. The solvent was then removed *in vacuo* and the residue was dissolved in ethyl acetate (100 mL). Afterwards, the solution was washed with saturated aqueous sodium sulfite (30 mL), water (30 mL) and brine (2 × 30 mL), and dried with anhydrous magnesium sulfate. Filtration to remove the drying agent and removal of the solvent *in vacuo* afforded crude sulfone **21a**, which was purified by recrystallization from EtOH to provide pure *cis*-1,2,3,4,4a,5,11,11a-octahydrodibenzo[*b,e*][1,4]thiazepine-10,10-dioxide **21a** (0.27 g, 1.05 mmol, 22%). For the synthesis of sulfoxide **22d**, only 1 equiv of *m*-chloroperbenzoic acid was added and the reaction temperature was maintained at -20 °C.

cis-1,2,3,4,4a,5,11,11a-Octahydrodibenzo[*b*,*e*][1,4]thiazepine-10,10-dioxide 21a (22%)
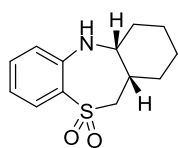
Light brown crystals. Recrystallization from EtOH. Mp = 234 °C. ^{1}H NMR (400 MHz, CDCl$_3$): δ 1.30-1.69 and 1.75-1.90 (5H and 3H, 2 × m, (CH$_2$)$_4$); 2.29-2.38 (1H, m, CHCH$_2$S); 3.19 (1H, d × d, *J* = 15.0, 10.6 Hz, (HCH)S); 3.37 (1H, d × d, *J* = 15.0, 6.2 Hz, (HCH)S); 3.99 (1H, s(br), NH); 4.22 (1H, s(br), CHN); 6.75 (1H, d × d, *J* = 7.9, 0.7 Hz, CH$_{arom}$); 6.92 (1H, t × d , *J* = 7.9, 0.7 Hz, CH$_{arom}$); 7.28 (1H, t × d, *J* = 7.9, 1.4 Hz, CH$_{arom}$); 7.91 (1H, d × d, *J* = 7.9, 1.4 Hz, CH$_{arom}$). ^{13}C NMR (100.6 MHz, CDCl$_3$): δ 20.8, 24.7, 27.2 and 31.3 ((CH$_2$)$_4$), 37.7 (CHCH$_2$S), 54.2 (CHN), 58.1 (CH$_2$S), 118.7 and 119.2 (2 × CH$_{arom}$), 126.9 (CH$_{arom}$), 128.8 (C$_{arom,quat}$), 132.8 (CH$_{arom}$), 146.8 (C$_{arom,quat}$). IR (ATR, cm^{-1}): ν$_{NH}$ = 3349; ν$_{max}$ = 2932, 1599, 1478, 1279, 1252, 1177, 1123, 1098, 932, 788, 764, 642. MS (70eV): m/z (%) 252 (M$^+$+1, 100). HRMS (ESI) Anal. Calcd. for C$_{13}$H$_{18}$NO$_2$S 252.1053 [M+H]$^+$, Found 252.1042.

cis-7-Chloro-1,2,3,4,4a,5,11,11a-octahydrodibenzo[*b*,*e*][1,4]thiazepine-10,10-dioxide 21b (48%)
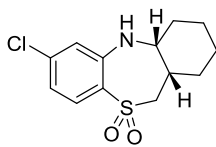
White crystals. Recrystallization from EtOH. Mp = 260 °C. ^{1}H NMR (400 MHz, CDCl$_3$): δ 1.25-1.53, 1.60-1.67 and 1.73-1.87 (3H, 2H and 3H, 3 × m, (CH$_2$)$_4$); 2.29-2.31 (1H, m, CHCH$_2$S); 3.12 (1H, d × d, *J* = 15.0, 10.6 Hz, (HCH)S); 3.36 (1H, d × d, *J* = 15.0, 6.4 Hz, (HCH)S); 4.02 (1H, s(br), NH); 4.25 (1H, s(br), CHN); 6.75 (1H, d, *J* = 1.5 Hz, CH$_{arom}$); 6.85 (1H, d × d, *J* = 8.6, 1.5 Hz, CH$_{arom}$); 7.81 (1H, d, *J* = 8.6 Hz, CH$_{arom}$). ^{13}C NMR (100.6 MHz, CDCl$_3$): δ 20.6, 24.7, 27.1 and 31.2 ((CH$_2$)$_4$), 37.7 (CHCH$_2$S), 54.0 (CHN), 58.1 (CH$_2$S), 118.0 and 119.3 (2 x CH$_{arom}$), 127.2 (C$_{arom,quat}$), 128.5 (CH$_{arom}$), 138.7 and 147.8 (2 × C$_{arom,quat}$). IR (ATR, cm^{-1}): ν$_{NH}$ = 3346; ν$_{max}$ = 2938, 1588, 1451, 1283, 1253, 1126, 1094, 1007, 864, 783. MS (70eV): m/z (%) 286/8 (M$^+$+1, 100). HRMS (ESI) Anal. Calcd. for C$_{13}$H$_{17}$ClNO$_2$S 286.0663 [M+H]$^+$, Found 286.0669.

cis-7-Trifluoromethyl-1,2,3,4,4a,5,11,11a-octahydrodibenzo[*b*,*e*][1,4]thiazepine-10,10-dioxide 21c (45%)
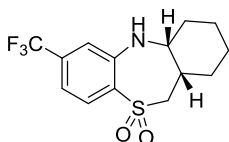
White crystals. Recrystallization from EtOH. Mp = 252 °C. ^{1}H NMR (400 MHz, CDCl$_3$): δ 1.30-1.55, 1.63-1.70, 1.76-1.84 and 1.88-1.92 (3H, 2H, 2H and 1H, 4 × m, (CH$_2$)$_4$); 2.29-2.38 (1H, m, CHCH$_2$S); 3.14 (1H, d × d, *J* = 15.1, 10.7 Hz, (HCH)S); 3.40 (1H, d × d, *J* = 15.1, 6.4 Hz, (HCH)S); 4.19 (1H, s(br), NH); 4.32 (1H, s(br), CHN); 7.00 (1H, s, CH$_{arom}$); 7.10 (1H, d , *J* = 8.4 Hz, CH$_{arom}$); 8.00 (1H, d, *J* = 8.4 Hz, CH$_{arom}$). ^{19}F NMR (376.5 MHz, CDCl$_3$): δ (-63.6) (s). ^{13}C NMR (100.6 MHz, CDCl$_3$): δ 20.5, 24.8, 27.1 and 31.3 ((CH$_2$)$_4$), 37.9 (CHCH$_2$S), 54.1 (CHN), 58.1 (CH$_2$S), 115.2 (q, *J* = 3.4 Hz, CH$_{arom}$), 115.5 (q, *J* = 3.4 Hz, CH$_{arom}$), 123.0 (q, *J* = 273.0 Hz, F$_3$C$_{quat}$), 128.2 (CH$_{arom}$), 131.1 (C$_{arom,quat}$), 134.6 (q, *J* = 33.0 Hz, F$_3$CC$_{arom,quat}$), 147.0 (C$_{arom,quat}$). IR (ATR, cm^{-1}): ν$_{NH}$ = 3350; ν$_{max}$ = 2933, 1346, 1305, 1286, 1261, 1173, 1138, 1122, 1087, 1007, 884, 808, 784, 688. MS (70eV): m/z (%) 320 (M$^+$+1, 100). HRMS (ESI) Anal. Calcd. for C$_{14}$H$_{17}$F$_3$NO$_2$S 320.0927 [M+H]$^+$, Found 320.0939.

cis-*N*-(4-Methoxycarbonylbenzyl)-1,2,3,4,4a,5,11,11a-octahydrodibenzo[*b,e*][1,4]-thiazepine-10,10-dioxide 22a (73%)
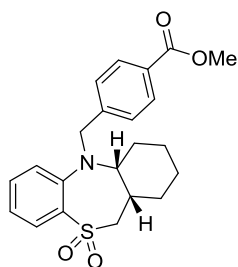
White powder. Recrystallization from EtOH. Mp = 78 °C. ^{1}H NMR (400 MHz, CDCl$_3$): δ 0.83-0.94, 1.01-1.13, 1.17-1.28, 1.37-1.48, 1.57-1.60 and 1.70-1.74 (3 × 1H, 3H, 2 × 1H, 6 × m, (CH$_2$)$_4$); 2.68-2.71 (1H, m, C<u>H</u>CH$_2$SO$_2$); 3.06-3.12 (2H, m, (HC<u>H</u>)S and CHN); 3.42 (1H, d × d, J = 14.7, 13.4 Hz, (<u>H</u>CH)S); 3.91 (3H, s, CH$_3$O); 4.38 and 4.59 (2 × 1H, 2 × d, J = 14.1 Hz, CH$_2$N); 7.16-7.19 (2H, m, CH$_{arom}$); 7.48-7.52 (1H, m, CH$_{arom}$); 7.69 (2H, d, J = 8.2 Hz, CH$_{arom}$); 8.02-8.05 (3H, m, CH$_{arom}$). ^{13}C NMR (100.6 MHz, CDCl$_3$): δ 19.9, 23.8, 26.2 and 31.2 ((CH$_2$)$_4$); 35.1 (<u>C</u>HCH$_2$S); 52.1 (CH$_3$O); 53.1 (CH$_2$S); 58.9 (CH$_2$N); 62.0 (CHN); 122.9, 123.8, 128.3 and 128.5 (5 × CH$_{arom}$); 129.4 (C$_{arom,quat,}$); 129.9 and 134.2 (3 × CH$_{arom}$); 135.4, 144.2 and 147.6 (3 × C$_{arom,quat}$); 167.0 (C=O). IR (ATR, cm^{-1}): $v_{C=O}$ = 1717; v_{max} = 2931, 1478, 1438, 1308, 1277, 1152, 1131, 1071, 878, 770, 743, 702. MS (70eV): m/z (%) 400 (M$^+$+1, 100). HRMS (ESI) Anal. Calcd. for C$_{22}$H$_{26}$NO$_4$S 400.1577 [M+H]$^+$, Found 400.1581.

cis-7-Chloro-*N*-(4-methoxycarbonylbenzyl)-1,2,3,4,4a,5,11,11a-octahydrodibenzo[*b,e*]-[1,4]thiazepine-10,10-dioxide 22b (97%)
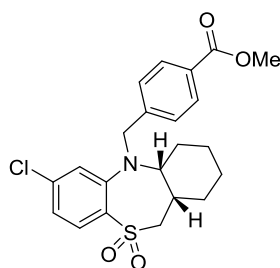
White powder. Recrystallization from EtOH. Mp = 182 °C. ^{1}H NMR (400 MHz, CDCl$_3$): δ 0.91-0.98, 1.03-1.12, 1.39-1.51 and 1.73-1.76 (1H, 2H, 4H and 1H, 4 × m, (CH$_2$)$_4$); 2.64-2.67 (1H, m, C<u>H</u>CH$_2$S); 3.07-3.13 (2H, m, (<u>H</u>CH)S and CHN); 2.38-2.45 (1H, m, (HC<u>H</u>)S); 3.92 (3H, s, CH$_3$O); 4.35 and 4.56 (2 × 1H, 2 × d, J = 13.9 Hz, CH$_2$N); 7.11-7.15 (2H, m, CH$_{arom}$); 7.66 (2H, d, J = 8.2 Hz, CH$_{arom}$); 7.96 (1H, d, J = 9.1 Hz, CH$_{arom}$); 8.05 (2H, d, J = 8.2 Hz, CH$_{arom}$). ^{13}C NMR (100.6 MHz, CDCl$_3$): δ 19.8, 23.8, 26.2 and 31.2 ((CH$_2$)$_4$), 34.9 (<u>C</u>HCH$_2$S), 52.1 (CH$_3$O), 52.9 (CH$_2$S), 58.8 (CH$_2$N), 62.3 (CHN), 123.0, 123.8, 128.5, 129.6, 129.6 and 130.0 (7 × CH$_{arom}$), 133.6, 140.5, 143.4 and 148.9 (4 × C$_{arom,quat}$), 167.0 (C=O). IR (ATR, cm^{-1}): $v_{C=O}$ = 1716; v_{max} = 2930, 1579, 1309, 1278, 1151, 1132, 1094, 1071, 889, 792, 760, 729. MS (70eV): m/z (%) 434/436 (M$^+$+1, 100). HRMS (ESI) Anal. Calcd. for C$_{22}$H$_{25}$ClNO$_4$S 434.1187 [M+H]$^+$, Found 434.1170.

### *cis*-*N*-(4-Methoxycarbonylbenzyl)-7-trifluoromethyl-1,2,3,4,4a,5,11,11a-octahydro-dibenzo[*b,e*][1,4]thiazepine-10,10-dioxide 22c (96%)
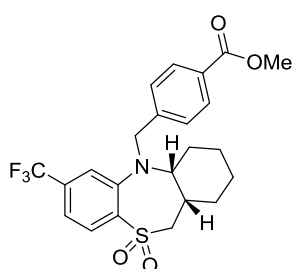
White powder. Recrystallization from EtOH. Mp = 174 °C. ^{1}H NMR (400 MHz, CDCl$_3$): δ 0.84-0.95, 1.02-1.13, 1.19-1.29, 1.40-1.50, 1.58-1.62 and 1.73-1.77 (1H, 1H, 1H, 3H, 1H and 1H, 6 × m, (CH$_2$)$_4$); 2.66-2.70 (1H, m, C<u>H</u>CH$_2$S); 3.12-3.18 (2H, m, (<u>H</u>CH)S and CHN); 3.40-3.47 (1H, m, (HC<u>H</u>)S); 3.92 (3H, s, CH$_3$O); 4.43 and 4.61 (2 × 1H, 2 × d, J = 13.9 Hz, (HCH)N); 7.39 (1H, s, CH$_{arom}$); 7.41 (1H, d, J = 8.2 Hz, CH$_{arom}$); 7.67 (2H, d, J = 8.2 Hz, CH$_{arom}$); 8.05 (2H, d, J = 8.2 Hz, CH$_{arom}$); 8.16 (1H, d, J = 8.2 Hz, CH$_{arom}$). ^{13}C NMR (100.6 MHz, CDCl$_3$): δ 19.8, 23.9, 26.2 and 31.2 ((CH$_2$)$_4$), 34.9 (<u>C</u>HCH$_2$S), 52.1 (CH$_3$O), 52.7 (CH$_2$S), 58.9 (CH$_2$N), 62.3 (CHN), 119.4 (q, J = 3.5 Hz, CH$_{arom}$), 120.4 (q, J = 3.5 Hz, CH$_{arom}$), 123.2 (q, J = 273.3 Hz, F$_3$C$_{quat}$), 128.6 and 129.2 (3 × CH$_{arom}$), 129.7 (C$_{arom,quat}$), 130.0 (2 × CH$_{arom}$), 136.0 (q, J = 32.8 Hz, F$_3$CC$_{arom,quat}$), 138.1, 143.2 and 148.3 (3 × C$_{arom,quat}$), 166.9 (C=O). ^{19}F NMR (376.5 MHz, CDCl$_3$): δ (-63.2) (s). IR (ATR, cm^{-1}): $v_{C=O}$ = 1728; v_{max} = 2941, 1428, 1312, 1279, 1172, 1156, 1134, 1086, 1068, 1057, 892, 835, 795. MS (70eV): m/z (%) 468 (M$^+$+1, 100). HRMS (ESI) Anal. Calcd. for C$_{23}$H$_{25}$F$_3$NO$_4$S 468.1451 [M+H]$^+$, Found 468.1470.

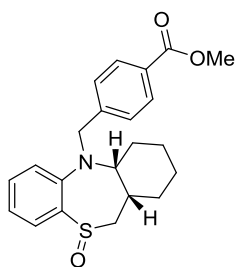### *cis-N-*(4-Methoxycarbonylbenzyl)-1,2,3,4,4a,5,11,11a-octahydrodibenzo[*b,e*][1,4]-thiazepine-10-oxide 22d (26%)

White powder. Recrystallization from EtOH. Mp = 182 °C. ^{1}H NMR (400 MHz, CDCl$_3$): δ 0.61-0.72, 1.01-1.22, 1.32-1.35, 1.41-1.50 and 1.60-1.70 (1H, 2H, 1H, 2H and 2H, 5 × m, (CH$_2$)$_4$); 2.52-2.56 (1H, m, CHCH$_2$S); 2.85-2.90 (2H, m, (HCH)S and CHN); 3.30 (1H, t, *J* = 13.0 Hz, (HCH)S); 3.92 (3H, s, CH$_3$O); 4.34 and 4.47 (2 × 1H, 2 × d, *J* = 14.0 Hz, (HCH)N); 7.13 (1H, d, *J* = 7.5 Hz, CH$_{arom}$); 7.32 (1H, t, *J* = 7.5 Hz, CH$_{arom}$); 7.38 (1H, t × d, *J* = 7.5, 1.5 Hz, CH$_{arom}$); 7.51 (2H, d, *J* = 8.2 Hz, CH$_{arom}$); 7.79 (1H, d × d, *J* = 7.5, 1.5 Hz, CH$_{arom}$); 8.01 (2H, d, *J* = 8.2 Hz, CH$_{arom}$). ^{13}C NMR (100.6 MHz, CDCl$_3$): δ 20.1, 24.3, 26.3 and 32.2 ((CH$_2$)$_4$), 36.7 (CHCH$_2$S), 52.1 (CH$_3$O), 53.1 (CH$_2$S), 58.7 (CH$_2$N), 60.3 (CHN), 122.6, 124.0, 124.8 and 128.4 (5 × CH$_{arom}$), 129.4 (C$_{arom,quat}$), 129.8 and 130.3 (3 × CH$_{arom}$), 140.5, 144.1 and 144.8 (3 × C$_{arom,quat}$), 166.9 (C=O). IR (ATR, cm^{-1}): ν$_{C=O}$ = 1713; ν$_{max}$ = 2927, 1279, 1110, 1070, 1036, 1024, 948, 860, 774, 761, 747, 702. MS (70eV): m/z (%) 384 (M$^+$+1, 100). HRMS (ESI) Anal. Calcd. for C$_{22}$H$_{26}$NO$_3$S 384.1628 [M+H]$^+$, Found 384.1639.

5.4.6.5. Synthesis of esters 20 and 23

General procedure: A flask (25 mL) was charged with **19a1** (219 mg, 1 mmol), potassium carbonate (415 mg, 3 mmol, 3 equiv), and methyl 4-(bromomethyl)benzoate (687 mg, 3 mmol, 3 equiv). The reaction mixture (neat) was placed under nitrogen atmosphere and stirred for 3 h at 120 °C, after which it was cooled to room temperature and dissolved in ethyl acetate (20 mL). After extraction with water (20 mL) and saturated brine (15 mL), the organic fraction was dried with magnesium sulfate, filtered, and evaporated. The excess of methyl 4-(bromomethyl)benzoate was removed by vacuum distillation (0.5 mbar, 120 °C), and further purification was done by means of column chromatography, which afforded pure *cis-N-*(4-methoxycarbonylbenzyl)-1,2,3,4,4a,5,11,11a-octahydrodibenzo[*b,e*][1,4]-thiazepine **20a** (235 mg, 0.64 mmol, 64%). When reversed-phase column chromatography was used, no initial high-vacuum distillation had to be performed. Different reaction temperatures were necessary to synthesize the different compounds to obtain a liquefied melt (120-150 °C).

cis-N-(4-Methoxycarbonylbenzyl)-1,2,3,4,4a,5,11,11a-octahydrodibenzo[*b,e*][1,4]-thiazepine 20a (64%)
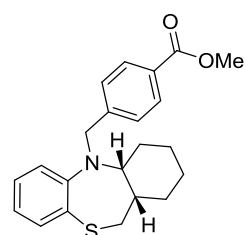
Very viscous colorless liquid. Purification by column chromatography (EtOAc/PE 3/97, Rf = 0.04). ^{1}H NMR (400 MHz, CDCl$_3$): δ 0.86-0.97, 1.07-1.32, 1.36-1.45, 1.49-1.53, 1.57-1.63 and 1.67-1.72 (1H, 3H, 1H, 1H, 1H and 1H, 6 × m, CH$_2$CH$_2$CH$_2$CH$_2$); 2.29-2.36 (1H, m, CHCH$_2$S); 2.42 (1H, d × d, *J* = 14.1, 3.2 Hz, (HCH)S); 2.93 (1H, d × d, *J* = 14.1, 12.8 Hz, (HCH)S); 3.02 (1H, d × t, *J* = 12.6, 3.9 Hz, CHN); 3.93 (3H, s, CH$_3$O); 4.42 and 4.56 (2 × 1H, 2 × d, *J* = 14.4 Hz, CH$_2$N); 6.95 (1H, t × d, *J* = 7.7, 1.3 Hz, CH$_{arom}$); 7.08 (1H, d × d, *J* = 7.7, 1.3 Hz, CH$_{arom}$); 7.22 (1H, t × d, *J* = 7.7, 1.6 Hz, CH$_{arom}$); 7.59 (1H, d × d, *J* = 7.7, 1.6 Hz, CH$_{arom}$); 7.65 and 8.02 (2 × 2H, 2 × d, *J* = 8.3 Hz, 4 × CH$_{arom}$). ^{13}C NMR (100.6 MHz, CDCl$_3$): δ 20.3, 24.2 and 26.6 (CH$_2$CH$_2$CH$_2$CH$_2$), 30.6 (CH$_2$S), 32.7 (CH$_2$CH$_2$CH$_2$CH$_2$), 42.5 (CHCH$_2$S), 52.0 (CH$_3$O), 59.3 (CH$_2$N), 61.3 (CHN),

122.8, 123.6, 128.2 and 128.3 (5 × CH_{arom}), 128.9 ($C_{arom,quat}$), 129.6 (2 × CH_{arom}), 132.1 ($C_{arom,quat}$), 133.3 (CH_{arom}), 145.7 and 152.0 (2 × $C_{arom,quat}$), 167.1 (C=O). IR (ATR, cm⁻¹): $v_{C=O}$ = 1717; v_{max} = 1610, 1474, 1433, 1414, 1314, 1274, 1218, 1192, 1173, 1139, 1099, 1019, 878, 857, 767, 754, 739, 700. MS (70eV): m/z (%) 368 (M⁺+1, 100). HRMS (ESI) Anal. Calcd. for $C_{22}H_{26}NO_2S$ 368.1679 [M+H]⁺, Found 368.1680.

cis-7-Chloro-N-(4-methoxycarbonylbenzyl)-1,2,3,4,4a,5,11,11a-octahydrodibenzo[b,e]-[1,4]thiazepine 20b (58%)

Light brwon oil. Purification by column chromatography (EtOAc/PE 3/97, Rf = 0.19). ¹H NMR (400 MHz, CDCl₃): δ 0.88-0.95, 1.08-1.23, 1.29-1.40, 1.46-1.57 and 1.67-1.70 (1H, 2H, 2H, 2H and 1H, 5 × m, $(CH_2)_4$); 2.25-2.28 (1H, m, $CHCH_2S$); 2.37 (1H, d × d, J = 14.2, 3.2 Hz, (HCH)S); 2.84-2.90 (1H, m, (HCH)S); 2.99 (1H, d × t, J = 12.5, 3.6 Hz, CHN); 3.90 (3H, s, CH₃O); 4.36 and 4.48 (2 × 1H, 2 × d, J = 14.3 Hz, (HCH)N); 6.90 (1H, d × d, J = 8.2, 2.0 Hz, CH_{arom}); 7.03 (1H, d, J = 2.0 Hz, CH_{arom}); 7.47 (1H, d, J = 8.2 Hz, CH_{arom}); 7.61 (2H, d, J = 8.1 Hz CH_{arom}); 8.01 (2H, d, J = 8.1 Hz, CH_{arom}). ¹³C NMR (100.6 MHz, CDCl₃): δ 20.2, 24.2 and 26.5 ($(CH_2)_3$), 30.3 (CH₂S), 32.7 (CH₂), 42.5 (CHCH₂S), 52.0 (CH₃O), 59.3 (CH₂N), 61.4 (CHN), 122.8, 123.5 and 128.2 (4 × CH_{arom}), 129.1 ($C_{arom,quat}$), 129.7 (2 × CH_{arom}), 130.3 and 133.9 (2 × $C_{arom,quat}$), 134.0 (CH_{arom}), 145.0 and 153.3 (2 × $C_{arom,quat}$), 167.0 (C=O). IR (ATR, cm⁻¹): $v_{C=O}$ = 1718; v_{max} = 2923, 1570, 1470, 1434, 1275, 1098, 898, 886, 807, 759, 731. MS (70eV): m/z (%) 402/4 (M⁺+1, 100). HRMS (ESI) Anal. Calcd. for $C_{22}H_{25}ClNO_2S$ 402.1289 [M+H]⁺, Found 402.1297.

cis-N-(4-Methoxycarbonylbenzyl)-7-trifluoromethyl-1,2,3,4,4a,5,11,11a-octahydro-dibenzo[b,e][1,4]thiazepine 20c (66%)
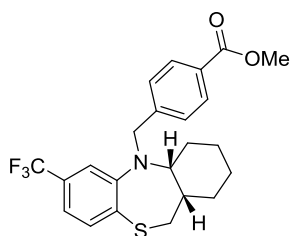
Light brown oil. Purification by column chromatography (EtOAc/PE 3/97, Rf = 0.10). ¹H NMR (400 MHz, CDCl₃): δ 0.87-0.94, 1.08-1.21, 1.30-1.43, 1.46-1.52, 1.56-1.61 and 1.68-1.72 (1H, 2H, 2H, 1H, 1H and 1H, 6 × m, $(CH_2)_4$); 2.27-2.30 (1H, m, $CHCH_2S$); 2.43 (1H, d × d, J = 14.2, 3.4 Hz, (HCH)S); 2.92 (1H, d × d, J = 14.2, 12.9 Hz, (HCH)S); 3.04 (1H, d × t, J = 12.5, 3.9 Hz, CHN); 3.91 (3H, s, CH₃O); 4.43 and 4.53 (2 × 1H, 2 × d, J = 14.2 Hz, (HCH)N); 7.15-7.17 (1H, m, CH_{arom}); 7.24-7.25 (1H, m, CH_{arom}); 7.61 (2H, d, J = 8.2 Hz, CH_{arom}); 7.66 (1H, d, J = 7.8 Hz, CH_{arom}); 8.01 (2H, d, J = 8.2 Hz, CH_{arom}). ¹⁹F NMR (376.5 MHz, D₆-DMSO): δ (-62.5) (s). ¹³C NMR (100.6 MHz, CDCl₃): δ 20.2, 24.3 and 26.5 ($(CH_2)_3$), 30.2 (CH₂S), 32.6 (CH₂), 42.2 (CHCH₂S), 52.1 (CH₃O), 59.4 (CH₂N), 61.2 (CHN), 119.2 (q, J = 3.7 Hz, CH_{arom}), 119.8 (q, J = 3.7 Hz, CH_{arom}), 124.0 (q, J = 272.4 Hz, F_3C_{quat}), 128.2 (2 × CH_{arom}), 129.2 ($C_{arom,quat}$), 129.7 (2 × CH_{arom}), 129.9 (q, J = 35.0 Hz, $F_3CC_{arom,quat}$), 133.5 (CH_{arom}), 136.2, 144.8 and 152.5 (3 × $C_{arom,quat}$), 167.1 (C=O). IR (ATR, cm⁻¹): $v_{C=O}$ = 1719; v_{max} = 2926, 1322, 1276, 1164, 1118, 1089, 900, 890, 824, 761, 735. MS (70eV): m/z (%) 436 (M⁺+1, 100).

cis-*N*-(4-Methoxycarbonylbenzyl)-6,6a,7,8,9,10,11,11a-octahydro-12*H*-benzo[*b*]-cyclohepta[*e*][1,4]thiazepine 20d (56%)
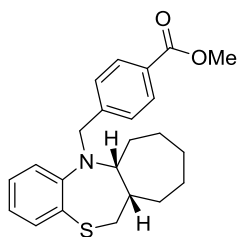
Very viscous yellow oil. Purification by column chromatography (EtOAc/PE 3/97, Rf = 0.21). ^{1}H NMR (400 MHz, CDCl$_3$): δ 1.14-1.38 and 1.50-1.75 (5H and 5H, 2 × m, CH$_2$CH$_2$CH$_2$CH$_2$CH$_2$); 2.29-2.37 (1H, m, C*H*CH$_2$S); 2.57 (1H, d × d, *J* = 13.9, 10.0 Hz, (*H*CH)S); 2.86 (1H, d × d, *J* = 13.9, 2.9 Hz, (HC*H*)S); 3.12-3.16 (1H, m, CHN); 3.91 (3H, s, CH$_3$O); 4.37 and 4.50 (2 × 1H, 2 × d, *J* = 14.6 Hz, CH$_2$N); 6.88 (1H, t × d, *J* = 7.6, 1.4 Hz, CH$_{arom}$); 6.98 (1H, d × d, *J* = 7.6, 1.4 Hz, CH$_{arom}$); 7.13 (1H, t × d, *J* = 7.6, 1.4 Hz, CH$_{arom}$); 7.41 (1H, d × d, *J* = 7.6, 1.4 Hz, CH$_{arom}$); 7.56 and 8.00 (2 × 2H, 2 × d, *J* = 8.2 Hz, 4 × CH$_{arom}$). ^{13}C NMR (100.6 MHz, CDCl$_3$): δ 24.4, 26.7, 28.0, 29.2 and 31.8 (CH$_2$CH$_2$CH$_2$CH$_2$CH$_2$), 33.2 (CH$_2$S), 44.1 (*C*HCH$_2$S), 52.0 (CH$_3$O), 59.1 (CH$_2$N), 63.9 (CHN), 122.4, 123.2, 127.4 and 128.2 (5 × CH$_{arom}$), 129.0 (C$_{arom,quat}$), 129.7 (2 × CH$_{arom}$), 131.1 (C$_{arom,quat}$), 131.9 (CH$_{arom}$), 145.5 and 150.7 (2 × C$_{arom,quat}$), 167.1 (C=O). IR (ATR, cm^{-1}): ν$_{C=O}$ = 1717; ν$_{max}$ = 1474, 1454, 1431, 1412, 1271, 1098, 1016, 964, 851, 752, 735, 700, 457. MS (70eV): m/z (%) 382 (M$^+$+1, 100).

trans-7-Chloro-*N*-(4-methoxycarbonylbenzyl)-1,2,3,4,4a,5,11,11a-octahydrodibenzo-[*b*,*e*][1,4]thiazepine 23a (47%)
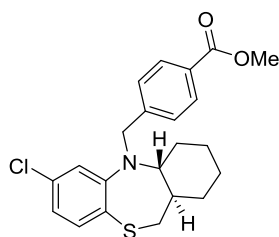
White powder. Purification by automated reverse-phase column chromatography (CH$_3$CN/H$_2$O 30-100%). Mp = 134 °C. ^{1}H NMR (400 MHz, CDCl$_3$): δ 1.04-1.25, 1.58-1.70, 1.75-1.78 and 2.00-2.05 (4H, 3H, 1H and 1H, 4 × m, (CH$_2$)$_4$CH); 2.82 and 2.96 (2H and 1H, 2 × s(br), CH$_2$S and CHN); 3.90 (3H, s, CH$_3$O); 4.40 (2H, s, CH$_2$N); 6.85-6.90 (2H, m, CH$_{arom}$); 7.19 (1H, d, *J* = 8.2 Hz, CH$_{arom}$); 7.54 and 7.99 (2 × 2H, 2 × d, *J* = 8.1 Hz, CH$_{arom}$). ^{13}C NMR (100.6 MHz, CDCl$_3$): δ 25.5, 25.8, 26.5 and 33.0 ((CH$_2$)$_4$, 1 × s(br)), 34.8 (CH$_2$S, s(br)), 41.1 (*C*HCH$_2$S, s(br)), 52.0 (CH$_3$O), 54.3 (CH$_2$N, s(br)), 65.6 (CHN, s(br)), 123.3 (2 × CH$_{arom}$, s(br)), 127.9 (2 × CH$_{arom}$, s(br)), 129.0 (C$_{arom,quat}$), 129.8 (2 × CH$_{arom}$ and C$_{arom,quat}$), 131.7 (CH$_{arom}$), 132.3, 144.9 and 148.7 (3 × C$_{arom,quat}$, 2 × s(br)), 167.0 (C=O). IR (cm^{-1}): ν$_{C=O}$ = 1717; ν$_{max}$ = 1431, 1273, 1173, 1096, 1018, 860, 750, 702, 592. MS (70eV): m/z (%) 402/4 (M$^+$+1, 100).

trans-*N*-(4-Methoxycarbonylbenzyl)-6,6a,7,8,9,10,11,11a-octahydro-12*H*-benzo[*b*]-cyclohepta[*e*][1,4]thiazepine 23b (37%)
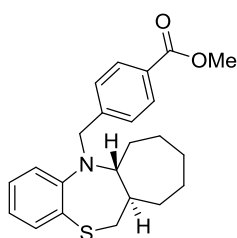
Very viscous yellow oil. Purification by automated reverse-phase column chromatography (CH$_3$CN/H$_2$O 30-100%). ^{1}H NMR (400 MHz, CDCl$_3$): δ 1.18-1.28, 1.34-1.57, 1.61-1.75, 1.81-1.88 and 2.08-2.14 (2H, 5H, 2H, 1H and 1H, 5 × m, CH$_2$CH$_2$CH$_2$CH$_2$CH$_2$CH); 2.66 (1H, d, *J* = 11.4 Hz, (*H*CH)S); 2.84 (1H, t, *J* = 9.1 Hz, CHN); 3.17 (1H, d × d, *J* = 11.4, 8.8 Hz, (HC*H*)S); 3.88 (3H, s, CH$_3$O); 4.28 and 4.37 (2 × 1H, 2 × d, *J* = 14.8 Hz, CH$_2$N); 6.88 (1H, t × d, *J* = 7.6, 1.3 Hz, CH$_{arom}$); 6.94 (1H, d × d, *J* = 7.6, 1.3 Hz, CH$_{arom}$); 7.01 (1H, t × d, *J* = 7.6, 1.3 Hz, CH$_{arom}$); 7.21 (1H, d × d, *J* = 7.6, 1.3 Hz, CH$_{arom}$); 7.55 and 7.98 (2 × 2H, 2 × d, *J* = 8.2 Hz, 4 × CH$_{arom}$). ^{13}C NMR (100.6 MHz, CDCl$_3$): δ 24.6, 25.5, 26.0, 28.6 and 34.9 (CH$_2$CH$_2$CH$_2$CH$_2$CH$_2$), 36.7 (CH$_2$S), 44.8 (*C*HCH$_2$S), 52.0 (CH$_3$O), 55.9 (CH$_2$N), 67.0 (CHN), 123.8, 123.9, 126.1 and 128.5 (5 × CH$_{arom}$), 128.9 (C$_{arom,quat}$), 129.6 and 129.7 (3 × CH$_{arom}$), 132.4 (C$_{arom,quat}$), 145.2 and 147.3 (2 × C$_{arom,quat}$), 167.1 (C=O). IR (ATR, cm^{-1}): ν$_{C=O}$ = 1715; ν$_{max}$ = 1472, 1431, 1269, 1098, 1016, 951, 853, 748, 731, 700, 459. MS (70eV): m/z (%) 382 (M$^+$+1, 100).

5.4.6.6. Synthesis of hydroxamic acids 24-26

General procedure: Compound **20a** (0.367 g, 1 mmol) was dissolved in THF (10 mL), and to this solution was added hydroxylamine (50% in water, 6.1 mL, 100 mmol, 100 equiv) followed by potassium hydroxide in methanol (4M, 12.5 mL, 50 mmol). The resulting mixture was stirred for 10 min at room temperature before it was poured into a saturated aqueous solution of NaHCO$_3$ (10 mL). This aqueous solution was extracted twice with ethyl acetate, after which the combined organic fractions were washed with water (10 mL) and a saturated brine solution (10 mL), dried (MgSO$_4$), filtered, and evaporated. Purification by crystallization from EtOH yielded *cis-N*-(4-hydroxycarbamoylbenzyl)-1,2,3,4,4a,5,11,11a-octahydrodibenzo[*b,e*][1,4]-thiazepine **24a** (0.287 g, 0.78 mmol, 78%) as a white powder.

cis-*N*-(4-Hydroxycarbamoylbenzyl)-1,2,3,4,4a,5,11,11a-octahydrodibenzo[*b,e*][1,4]-thiazepine 24a (78%)
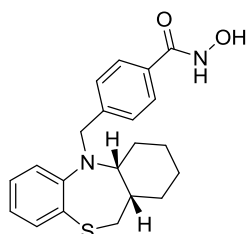
White powder. Recrystallization from EtOH. Mp = 116.5 °C. ^{1}H NMR (400 MHz, D$_6$-DMSO): δ 0.73-0.83, 1.11-1.21, 1.30-1.38, 1.44-1.47 and 1.59-1.62 (1H, 3H, 1H, 1H and 2H, 5 × m, CH$_2$CH$_2$CH$_2$CH$_2$); 2.19-2.23 (1H, m, CHCH$_2$S); 2.47 (1H, d × d, *J* = 13.8, 3.4 Hz, (HCH)S); 2.83 (1H, t, *J* = 13.8 Hz, (HCH)S); 3.04 (1H, d × t, *J* = 12.5, 3.6 Hz, CHN); 4.43 and 4.53 (2 × 1H, 2 × d, *J* = 14.8 Hz, CH$_2$N); 6.90 (1H, t × d, *J* = 7.6, 1.3 Hz, CH$_{arom}$); 7.15 (1H, d × d, *J* = 7.6, 1.3 Hz, CH$_{arom}$); 7.22 (1H, t × d, *J* = 7.6, 1.3 Hz, CH$_{arom}$); 7.47 (1H, d × d, *J* = 7.6, 1.3 Hz, CH$_{arom}$); 7.54 and 7.68 (2 × 2H, 2 × d, *J* = 8.1 Hz, 4 × CH$_{arom}$); 9.03 (1H, s(br), OH); 11.13 (1H, s(br), NH). ^{13}C NMR (100.6 MHz, D$_6$-DMSO): δ 20.2, 24.4 and 26.5 (CH$_2$CH$_2$CH$_2$CH$_2$), 29.9 (CH$_2$S), 32.6 (CH$_2$CH$_2$CH$_2$CH$_2$), 42.6 (CHCH$_2$S), 58.8 (CH$_2$N), 61.6 (CHN), 122.9, 124.0, 127.2, 128.2 and 128.8 (7 × CH$_{arom}$), 131.5 and 131.9 (2 × C$_{arom,quat}$), 133.3 (CH$_{arom}$), 143.8 and 152.0 (2 × C$_{arom,quat}$), 164.4 (C=O). IR (ATR, cm^{-1}): ν$_{NH/OH}$ = 3206; ν$_{C=O}$ = 1614; ν$_{max}$ = 1568, 1472, 1448, 1314, 1218, 1140, 1122, 1096, 1030, 1015, 897, 878, 844, 764, 738. MS (70eV): m/z (%) 369 (M$^+$+1, 100). HRMS (ESI) Anal. Calcd. for C$_{21}$H$_{25}$N$_2$O$_2$S 369.1631 [M+H]$^+$, Found 369.1638.

cis-7-Chloro-*N*-(4-hydroxycarbamoylbenzyl)-1,2,3,4,4a,5,11,11a-octahydrodibenzo[*b,e*]-[1,4]thiazepine 24b (73%)
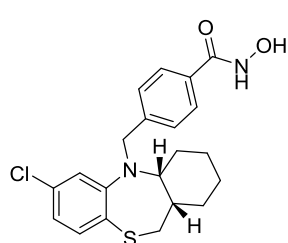
White powder. Recrystallization from EtOH. Mp = 111 °C. ^{1}H NMR (400 MHz, D$_6$-DMSO): δ 0.77-0.86, 1.14-1.24, 1.30-1.36, 1.48-1.51 and 1.57-1.61 (1H, 3H, 1H, 1H and 2H, 5 × m, (CH$_2$)$_4$); 2.18-2.21 (1H, m, CHCH$_2$S); 2.46-2.51 (1H, m, (HCH)S); 2.80-2.87 (1H, m, (HCH)S); 3.05-3.10 (1H, m, CHN); 4.44 and 4.53 (2 × 1H, 2 × d, *J* = 14.7 Hz, (HCH)N); 6.95 (1H, d × d, *J* = 8.1, 2.1 Hz, CH$_{arom}$); 7.18 (1H, d, *J* = 2.1 Hz, CH$_{arom}$); 7.46-7.51 (3H, m, CH$_{arom}$); 7.69 (2H, d, *J* = 8.1 Hz, CH$_{arom}$); 8.99 (1H, s(br), OH); 11.16 (1H, s(br), NH). ^{13}C NMR (100.6 MHz, D$_6$-DMSO): δ 20.2, 24.3 and 26.5 ((CH$_2$)$_3$), 29.5 (CH$_2$S), 32.5 (CH$_2$), 42.6 (CHCH$_2$S), 58.8 (CH$_2$N), 61.9 (CHN), 122.7, 123.7, 127.1 and 128.1 (5 × CH$_{arom}$), 130.1, 132.0 and 133.2 (3 × C$_{arom,quat,}$), 134.4 (2 × CH$_{arom}$), 143.2 and 153.5 (2 × C$_{arom,quat}$), 164.2 (C=O). IR (ATR, cm^{-1}): ν$_{NH/OH}$ = 3204; ν$_{C=O}$ = 1613; ν$_{max}$ = 2923, 2853, 1613, 1568, 1550, 1470, 1449, 1378, 1097, 899, 886, 806, 729 . MS (70eV): m/z (%) 403/5 (M$^+$+1, 100). HRMS (ESI) Anal. Calcd. for C$_{21}$H$_{24}$ClN$_2$O$_2$S 403.1242 [M+H]$^+$, Found 403.1247.

cis-*N*-(4-Hydroxycarbamoylbenzyl)-7-trifluoromethyl-1,2,3,4,4a,5,11,11a-octahydro-dibenzo[*b,e*][1,4]thiazepine 24c (91%)
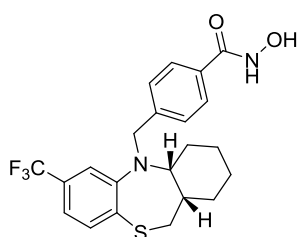
White powder. Recrystallization from EtOH. Mp = 92 °C. ^{1}H NMR (400 MHz, D$_6$-DMSO): δ 0.77-0.83, 1.16-1.22, 1.32-1.38, 1.48-1.51 and 1.58-1.61 (1H, 3H, 1H, 1H and 2H, 5 × m, (CH$_2$)$_4$); 2.20-2.23 (1H, m, CHCH$_2$S); 2.53-2.56 (1H, m, (HCH)S); 2.84-2.91 (1H, m, (HCH)S); 3.10-3.13 (1H, m, CHN); 4.51 and 4.58 (2 × 1H, 2 × d, *J* = 14.7 Hz, (HCH)N); 7.21 (1H, d, *J* = 7.8 Hz, CH$_{arom}$); 7.39 (1H, s, CH$_{arom}$); 7.52 (2H, d, *J* = 8.0 Hz, CH$_{arom}$); 7.66-7.68 (3H, m, CH$_{arom}$); 9.08 (1H, s(br), OH); 11.18 (1H, s(br), NH). ^{13}C NMR (100.6 MHz, D$_6$-DMSO): δ 20.1, 24.4 and 26.4 ((CH$_2$)$_3$), 29.3 (CH$_2$S), 32.4 (CH$_2$), 42.3 (CHCH$_2$S), 58.8 (CH$_2$N), 61.8 (CHN), 119.2 (q, *J* = 3.8 Hz, CH$_{arom}$), 120.1 (q, *J* = 3.8 Hz, CH$_{arom}$), 124.5 (q, *J* = 272.2 Hz, F$_3$C$_{quat}$), 127.2 and 128.3 (4 × CH$_{arom}$), 129.2 (q, *J* = 31.6 Hz, F$_3$CC$_{arom,quat}$), 131.8 (C$_{arom,quat}$), 133.9 (CH$_{arom}$), 136.4, 143.3 and 152.5 (3 × C$_{arom,quat}$), 164.5 (C=O). ^{19}F NMR (376.5 MHz, D$_6$-DMSO): δ (-60.9) (s). IR (ATR, cm^{-1}): v$_{NH/OH}$ = 3208; v$_{C=O}$ = 1614; v$_{max}$ = 2925, 1422, 1322, 1164, 1120, 1090, 1039, 1016, 899, 824, 733. MS (70eV): m/z (%) 437 (M$^+$+1, 100). HRMS (ESI) Anal. Calcd. for C$_{22}$H$_{24}$F$_3$N$_2$O$_2$S 437.1505 [M+H]$^+$, Found 437.1514.

cis-*N*-(4-Hydroxycarbamoylbenzyl)-6,6a,7,8,9,10,11,11a-octahydro-12*H*-benzo[*b*]cyclohepta[*e*][1,4]thiazepine 24d (95%)
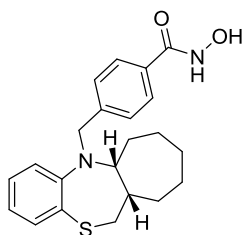
White powder. Recrystallization from ethanol. Mp = 95 °C. ^{1}H NMR (400 MHz, D$_6$-DMSO): δ 1.12-1.26, 1.28-1.35 and 1.48-1.71 (4H, 1H and 5H, 3 × m, (CH$_2$)$_5$); 2.27-2.33 (1H, m, CHCH$_2$S); 2.51-2.57 (1H, m, (HCH)S); 2.91-2.95 (1H, m, (HCH)S); 3.18-3.23 (1H, m, CHN); 4.39 and 4.50 (2 × 1H, 2 × d, *J* = 14.8 Hz, CH$_2$N); 6.85 (1H, t, *J* = 7.4 Hz, CH$_{arom}$); 7.06 (1H, d, *J* = 7.4 Hz, CH$_{arom}$); 7.12 (1H, t, *J* = 7.4 Hz, CH$_{arom}$); 7.31 (1H, d, *J* = 7.4 Hz, CH$_{arom}$); 7.50 and 7.69 (2 × 2H, 2 × d, *J* = 8.1 Hz, 4 × CH$_{arom}$); 8.98 (1H, s(br), OH); 11.14 (1H, s(br), NH). ^{13}C NMR (100.6 MHz, D$_6$-DMSO): δ 24.7, 26.3, 28.0, 29.2 and 31.5 ((CH$_2$)$_5$), 32.7 (CH$_2$S), 44.1 (CHCH$_2$S), 58.4 (CH$_2$N), 64.3 (CHN), 122.6, 123.7, 127.3, 127.8 and 128.3 (7 × CH$_{arom}$), 130.7 (C$_{arom,quat}$), 131.7 (CH$_{arom}$), 131.8 (C$_{arom,quat}$), 143.7 and 150.5 (2 × C$_{arom,quat}$), 164.6 (C=O). IR (ATR, cm^{-1}): v$_{NH/OH}$ = 3179; v$_{C=O}$ = 1611; v$_{max}$ = 1566, 1474, 1454, 1300, 1275, 1215, 1101, 1013, 895, 847, 733, 457. MS (70eV): m/z (%) 383 (M$^+$+1, 100). HRMS (ESI) Anal. Calcd. for C$_{22}$H$_{27}$N$_2$O$_2$S 383.1788 [M+H]$^+$, Found 383.1789.

cis-*N*-(4-Hydroxycarbamoylbenzyl)-1,2,3,4,4a,5,11,11a-octahydrodibenzo[*b,e*][1,4]-thiazepine-10,10-dioxide 25a (25%)
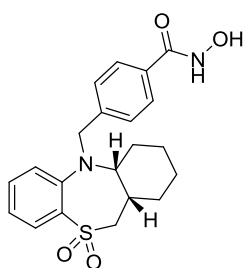
White powder. Recrystallization from EtOH. Mp = 242 °C. ^{1}H NMR (400 MHz, D$_6$-DMSO): δ 0.82-0.91, 1.15-1.24, 1.38-1.40 and 1.61-1.64 (1H, 3H, 2H and 2H, 4 × m, (CH$_2$)$_4$); 2.55-2.58 (1H, m, CHCH$_2$S); 3.13-3.16 (1H, m, CHN); 3.27-3.30 (1H, m, (HCH)S); 3.57-3.64 (1H, m, (HCH)S); 4.46 and 4.62 (2 × 1H, 2 × d, *J* = 14.8 Hz, (HCH)N); 7.16-7.20 (1H, m, CH$_{arom}$); 7.28-7.30 (1H, m, CH$_{arom}$); 7.52-7.56 (1H, m, CH$_{arom}$), 7.62-7.69 (4H, m, 4 × CH$_{arom}$); 7.83-7.86 (1H, m, CH$_{arom}$); 9.00 (1H, s(br), OH); 11.13 (1H, s(br), NH). ^{13}C NMR (100.6 MHz, D$_6$-DMSO): δ 19.7, 23.7, 26.4 and 31.0 ((CH$_2$)$_4$), 35.6 (CHCH$_2$S), 52.3 (CH$_2$S), 58.3 (CH$_2$N), 63.0 (CHN), 122.8, 124.5, 127.2, 127.7 and 128.5 (7 x CH$_{arom}$), 131.9 (C$_{arom,quat}$), 134.5 (CH$_{arom}$), 135.4, 143.2 and 147.6 (3 × C$_{arom,quat}$), 164.5 (C=O). IR (ATR, cm^{-1}): v$_{NH/OH}$ = 3298; v$_{C=O}$ = 1644; v$_{max}$ = 2926, 2854, 1478, 1464, 1446, 1307, 1273, 1243, 1150, 1126, 1092, 1070, 1015, 876, 768,

745. MS (70eV): m/z (%) 401 (M$^+$+1, 100). HRMS (ESI) Anal. Calcd. for C$_{21}$H$_{25}$N$_2$O$_4$S 401.1530 [M+H]$^+$, Found 401.1540.

cis-7-Chloro-*N*-(4-hydroxycarbamoylbenzyl)-1,2,3,4,4a,5,11,11a-octahydrodibenzo[*b*,*e*]-[1,4]thiazepine-10,10-dioxide 25b (79%)
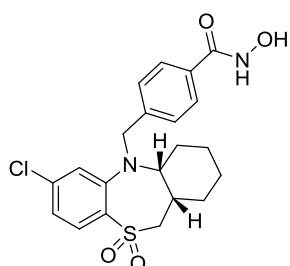
White powder. Recrystallization from EtOH. Mp = 222 °C. ^{1}H NMR (400 MHz, D$_6$-DMSO): δ 0.92-0.98, 1.15-1.23, 1.34-1.44 and 1.61-1.64 (1H, 3H, 2H and 2H, 4 × m, (CH$_2$)$_4$); 2.52-2.54 (1H, m, CHCH$_2$S); 3.16-3.19 (1H, m, CHN); 3.32-3.37 (1H, m, (HCH)S); 3.63-3.70 (1H, m, (HCH)S); 4.47 and 4.65 (2 × 1H, 2 × d, *J* = 14.8 Hz, (HCH)N); 7.24 (1H, d, *J* = 8.4 Hz, CH$_{arom}$); 7.35 (1H, s, CH$_{arom}$); 7.60 (2H, d, *J* = 7.9 Hz, CH$_{arom}$); 7.70 (2H, d, *J* = 7.9 Hz, CH$_{arom}$); 7.83 (1H, d, *J* = 8.4 Hz, CH$_{arom}$); 9.08 (1H, s(br), OH); 11.20 (1H, s(br), NH). ^{13}C NMR (100.6 MHz, D$_6$-DMSO): δ 19.6, 23.7, 26.4 and 31.0 ((CH$_2$)$_4$), 35.4 (CHCH$_2$S),
52.0 (CH$_2$S), 58.2 (CH$_2$N), 63.4 (CHN), 122.7, 124.3, 127.3, 128.4 and 129.5 (7 x CH$_{arom}$), 132.1, 134.1, 139.2, 142.6 and 149.0 (5 × C$_{arom,quat}$), 164.3 (C=O). IR (ATR, cm^{-1}): ν$_{NH/OH}$ = 3271; ν$_{C=O}$ = 1641; ν$_{max}$ = 2927, 2856, 1579, 1555, 1450, 1382, 1307, 1287, 1150, 1130, 1093, 885, 793, 728. MS (70eV): m/z (%) 435/7 (M$^+$+1, 100). HRMS (ESI) Anal. Calcd. for C$_{21}$H$_{24}$ClN$_2$O$_4$S 435.1140 [M+H]$^+$, Found 435.1123.

### *cis*-*N*-(4-Hydroxycarbamoylbenzyl)-7-trifluoromethyl-1,2,3,4,4a,5,11,11a-octahydro-dibenzo[*b*,*e*][1,4]thiazepine-10,10-dioxide 25c (69%)
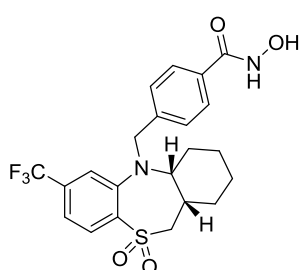
White powder. Recrystallization from EtOH. Mp = 228 °C. ^{1}H NMR (400 MHz, D$_6$-DMSO): δ 0.88-0.97, 1.16-1.24, 1.36-1.44 and 1.60-1.67 (1H, 3H, 2H and 2H, 4 × m, (CH$_2$)$_4$); 2.54-2.57 (1H, m, CHCH$_2$S); 3.20-3.25 (1H, m, CHN); 3.42 (1H, d × d, *J* = 15.2, 3.2 Hz, (HCH)S); 3.71-3.78 (1H, m, (HCH)S); 4.56 and 4.72 (2 × 1H, 2 × d, *J* = 14.7 Hz, (HCH)N); 7.53 (1H, d, *J* = 8.2 Hz, CH$_{arom}$); 7.57 (1H, s, CH$_{arom}$); 7.61 (2H, d, *J* = 8.2 Hz, CH$_{arom}$); 7.69 (2H, d, *J* = 8.2 Hz, CH$_{arom}$); 8.04 (1H, d, *J* = 8.2 Hz, CH$_{arom}$); 9.02 (1H, s(br), OH); 11.17 (1H, s(br), NH). ^{13}C NMR (100.6 MHz, D$_6$-DMSO): δ 19.5, 23.8, 26.4 and 30.9
((CH$_2$)$_4$), 35.4 (CHCH$_2$S), 51.8 (CH$_2$S), 58.2 (CH$_2$N), 63.4 (CHN), 119.2 (q, *J* = 3.6 Hz, CH$_{arom}$), 121.2 (q, *J* = 3.6 Hz, CH$_{arom}$), 123.8 (q, *J* = 273.5 Hz, F$_3$C$_{quat}$), 127.3, 128.5 and 129.2 (5 × CH$_{arom}$), 132.0 (C$_{arom,quat}$), 134.2 (q, *J* = 32.0 Hz, F$_3$CC$_{arom,quat}$), 138.6, 142.6 and 148.3 (3 × C$_{arom,quat}$), 164.4 (C=O). ^{19}F NMR (376.5 MHz, D$_6$-DMSO): δ (-61.7) (s). IR (ATR, cm^{-1}): ν$_{NH/OH}$ = 3300; ν$_{C=O}$ = 1644; ν$_{max}$ = 2928, 1432, 1393, 1324, 1291, 1172, 1155, 1130, 1085, 1068, 1016, 894, 827, 794. MS (70eV): m/z (%) 469 (M$^+$+1, 100). HRMS (ESI) Anal. Calcd. for C$_{22}$H$_{24}$F$_3$N$_2$O$_4$S 469.1403 [M+H]$^+$, Found 469.1414.

cis-N-(4-Hydroxycarbamoylbenzyl)-1,2,3,4,4a,5,11,11a-octahydrodibenzo[*b,e*][1,4]-thiazepine-10-oxide 25d (96%)
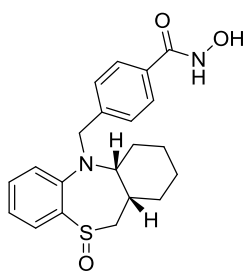
White powder. Recrystallization from EtOH. Mp = 202 °C. ^{1}H NMR (400 MHz, D$_6$-DMSO): δ 0.49-0.60, 1.06-1.22, 1.40-1.47 and 1.58-1.66 (1H, 3H, 2H and 2H, 4 × m, (CH$_2$)$_4$); 2.54-2.57 (1H, m, C$\underline{H}$CH$_2$S); 2.91-3.01 (2H, m, ($\underline{H}$CH)S and CHN); 3.15-3.22 (1H, m, (HC$\underline{H}$)S); 4.39 and 4.56 (2 × 1H, 2 × d, *J* = 14.5 Hz, (HCH)N); 7.27-7.30 (2H, m, CH$_{arom}$); 7.36-7.40 (1H, m, CH$_{arom}$); 7.46 (2H, d, *J* = 8.1 Hz, CH$_{arom}$), 7.55-7.57 (1H, m, CH$_{arom}$); 7.68 (2H, d, *J* = 8.1 Hz, CH$_{arom}$); 8.98 (1H, s(br), OH); 11.13 (1H, s(br), NH). ^{13}C NMR (100.6 MHz, D$_6$-DMSO): δ 24.8, 29.3, 31.1 and 36.7 ((CH$_2$)$_4$), 41.4 ($\underline{C}$HCH$_2$S), 57.1 (CH$_2$S), 62.7 (CH$_2$N), 65.6 (CHN), 128.2, 128.3, 129.4, 132.1, 133.2 and 135.3 (8 x CH$_{arom}$), 136.8, 145.8, 147.6 and 149.5 (4 × C$_{arom,quat}$), 169.4 (C=O). IR (ATR, cm^{-1}): v$_{NH/OH}$ = 3213; v$_{C=O}$ = 1641; v$_{max}$ = 2925, 2850, 1571, 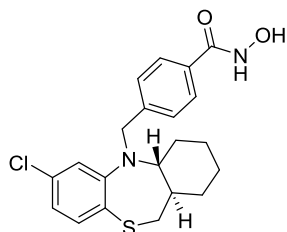1474, 1445, 1410, 1373, 1280, 1155, 1013, 898, 862, 769, 742. MS (70eV): m/z (%) 385 (M$^+$+1, 40). HRMS (ESI) Anal. Calcd. for C$_{21}$H$_{25}$N$_2$O$_3$S 385.1580 [M+H]$^+$, Found 385.1569.

trans-7-Chloro-N-(4-hydroxycarbamoylbenzyl)-1,2,3,4,4a,5,11,11a-octahydrodibenzo-[*b,e*][1,4]thiazepine 26a (77%)

White powder. Crystallization from acetonitrile. Mp = 111 °C. ^{1}H NMR (400 MHz, CDCl$_3$): δ 0.98-1.22, 1.56-1.67, 1.72-1.75 and 1.98-2.01 (4H, 3H, 1H and 1H, 4 × m, (CH$_2$)$_4$CH); 2.79 and 2.92 (2H and 1H, 2 × s(br), CH$_2$S and CHN); 4.33 (2H, s, CH$_2$N); 6.84-6.87 (2H, m, CH$_{arom}$); 7.18 (1H, d, *J* = 8.1 Hz, CH$_{arom}$); 7.47-7.48 (2H, m, CH$_{arom}$); 7.64 (2H, d, *J* = 7.5 Hz CH$_{arom}$); 9,19 (1H, s(br), OH). ^{13}C NMR (100.6 MHz, CDCl$_3$): δ 25.4, 25.8, 26.3 and 33.0 ((CH$_2$)$_4$, 1 × s(br)), 34.6 (CH$_2$S, s(br)), 41.0 ($\underline{C}$HCH$_2$S, s(br)), 54.2 (CH$_2$N, s(br)), 65.5 (CHN, s(br)), 123.4 (2 × CH$_{arom}$, s(br)), 127.1 (2 × CH$_{arom}$), 128.2 (2 × CH$_{arom}$ and C$_{arom,quat}$), 129.6 (C$_{arom,quat}$), 131.7 (CH$_{arom}$), 132.3, 144.1 and 148.6 (3 × C$_{arom,quat}$, 2 × s(br)), 166.9 (C=O). IR (ATR, cm^{-1}): v$_{NH/OH}$ = 3179; v$_{C=O}$ = 1611; v$_{max}$ = 1568, 1470, 1098, 1013, 895, 843, 729, 457. MS (70eV): m/z (%) 403/5 (M$^+$+1, 100). HRMS (ESI) Anal. Calcd. for C$_{21}$H$_{24}$ClN$_2$O$_2$S 403.1242 [M+H]$^+$, Found 403.1259.

trans-N-(4-Hydroxycarbamoylbenzyl)-6,6a,7,8,9,10,11,11a-octahydro-12*H*-benzo[*b*]cyclohepta[*e*][1,4]thiazepine 26b (78%)
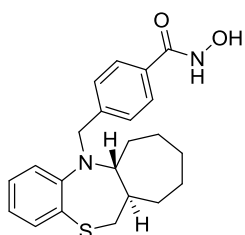
White powder. Recrystallization from acetonitrile. Mp = 90 °C. ^{1}H NMR (400 MHz, D$_6$-DMSO): δ 1.12-1.21, 1.23-1.29, 1.36-1.46, 1.50-1.55, 1.57-1.63, 1.74-1.80 and 2.10-2.14 (1H, 1H, 4H, 1H, 1H, 2H and 1H, 7 × m, (CH$_2$)$_5$CH); 2.73 (1H, d, *J* = 11.4 Hz, ($\underline{H}$CH)S); 2.96 (1H, t, *J* = 9.1 Hz, CHN); 3.21 (1H, d × d, *J* = 11.4, 8.6 Hz, (HC$\underline{H}$)S); 4.29 and 4.44 (2 × 1H, 2 × d, *J* = 15.1 Hz, CH$_2$N); 6.84 (1H, t × d, *J* = 7.6, 1.2 Hz, CH$_{arom}$); 7.01 (1H, t × d, *J* = 7.6, 1.2 Hz, CH$_{arom}$); 7.07 (1H, t × d, *J* = 7.6, 1.2 Hz, CH$_{arom}$); 7.11 (1H, d × d, *J* = 7.6, 1.2 Hz, CH$_{arom}$); 7.51 and 7.65 (2 × 2H, 2 × d, *J* = 8.1 Hz, 4 × CH$_{arom}$); 8.99 (1H, s(br), OH); 11.13 (1H, s(br), NH). ^{13}C NMR (100.6 MHz, D$_6$-DMSO): δ 24.5, 25.5, 26.1, 28.8 and 34.7 ((CH$_2$)$_5$), 36.2 (CH$_2$S), 45.0 ($\underline{C}$HCH$_2$S), 55.1 (CH$_2$N), 68.1 (CHN), 124.0, 124.2, 126.4, 127.2, 128.5 and 129.5 (8 × CH$_{arom}$), 131.7, 132.0, 143.5 and 147.0 (4 × C$_{arom,quat}$), 164.5 (C=O). IR (ATR, cm^{-1}): v$_{NH/OH}$ = 3200; v$_{C=O}$ = 1624; v$_{max}$ = 1566, 1472, 1306, 1152, 1113, 1015, 899, 851, 748, 611, 463. MS (70eV): m/z (%) 383 (M$^+$+1, 100). HRMS (ESI) Anal. Calcd. for C$_{22}$H$_{27}$N$_2$O$_2$S 383.1788 [M+H]$^+$, Found 383.1797.

6. Exploration of thiaheterocyclic *h*HDAC6 inhibitors as potential antiplasmodial agents

Abstract: The recurring resistance of the malaria parasite to many antimalarial drugs compels the discovery of innovative chemical entities with new modes of action. Pan-HDAC inhibitors have recently been presented as powerful novel antimalarials, although their application is hampered due to possible toxic side effects. This drawback might be neutralized by the deployment of isoform-selective HDAC inhibitors. In this chapter, 42 thiaheterocyclic benzohydroxamic acids, 17 of them being potent and selective hHDAC6 inhibitors, were tested to investigate a possible correlation between hHDAC6 inhibition and antiplasmodial activity. Four HDAC6 inhibitors showed submicromolar potency against a chloroquine-sensitive and a chloroquine-resistant strain of Plasmodium falciparum with high Selectivity Indices, pointing to the importance and relevance of exploring hHDAC6 inhibitors as potential antiplasmodial drugs.

6.1. Introduction

Malaria is a devastating parasitic disease, exemplified by the fact that roughly 3.2 billion people are at risk of contracting malaria and that this disease caused roughly 438 000 deaths in 2015, with an estimated 306 000 casualties in the group of children under the age of five (WHO).[150] The main culprit causing this infection is the protozoan species *Plasmodium falciparum*, transmitted by mosquitoes of the genus *Anopheles*.[151] In the past fifteen years (2000-2015), considerable progress has been made toward revoking this infection, as illustrated by a declining the number of malaria cases and deaths (18 and 48%, respectively).[150] However, there still is a pressing need to reduce the number of victims even further and to find solutions to address all challenges associated with this disease. A pertinent challenge relates to the expanding resistance of the Plasmodium parasite toward several treatment regimes. Indeed, resistance has emerged with respect to the standard antimalarials chloroquine, sulfadoxine, pyrimethamine and, more recently, artemisinin.[152] The acquired artemisinin resistance is particularly alarming, since artemisinin combination therapies represent the first-in-line treatment option for malaria nowadays.

A consequence of this recurring resistance is the urgent need to develop new medicines with alternative mechanisms of action, in order to impede or deter the parasite from developing resistance by applying combination therapies. In that regard, histone deacetylase inhibitors (HDACi's) might offer new treatment opportunities, as several known HDAC inhibitors have recently been shown to demonstrate a promising activity against *Plasmodium falciparum* and other malarial strains.[14,153-155] HDACs (histone deacetylases) and HATs (histone acetyl transferases) function as regulators of lysine acetylation, an important posttranslational modification responsible for the neutralization of the positive charges on lysine residues, and as such adjusting the exact mode of action of the targeted protein.[124] HDAC's were first been discovered as histone lysine modifying enzymes but are now generally accepted to be lysine deacetylases (KDACs), also deacetylating several non-histone proteins.[121] In humans, this group of enzymes comprises four classes, with class I (HDAC1, 2, 3 and 8), IIa (HDAC4, 5, 7 and 9), IIb (HDAC6 and 10) and IV (HDAC11) employing zinc as an essential cofactor, while class III (sirtuins1-7) uses NAD^+ for its deacetylase activity.[6] On the other hand, five HDAC isoforms are known for *Plasmodium falciparum*: *Pf*HDAC1, with homology to human class I, *Pf*HDAC2 and 3, with homology to human class II, and *Pf*Sir2A and *Pf*Sir2B, with homology to human class III.[156] So far, mainly broad-spectrum HDAC inhibitors (pan-HDACi's) have been tested for their activity against *P. falciparum*, revealing high toxicities in the (low) nanomolar range toward the malaria parasite.[11, 113] A major drawback associated with these broad-spectrum HDAC inhibitors involves the interaction with all human Zn^{2+}-dependent HDACs, culminating in a higher risk to elicit toxic side effects upon administration. Therefore, the

selective inhibition of *pf*HDACs over *h*HDAC isoforms represents a relevant challenge in antimalarial drug discovery and has led to the assessment of many *h*HDAC inhibitors as potential antiplasmodial agents. In that respect, a library screen of 2000 compounds has revealed (*E*)-7-[2-(2-bromobenzylidene)hydrazinyl]-*N*-hydroxy-7-oxoheptanamide to be such a selective compound and, in another report, a specific class of methylamides has been shown to be *pf*HDAC selective.[157,158]

An alternative strategy could imply the examination of selective *h*HDAC inhibitors (instead of pan-*h*HDAC inhibitors) as novel antimalarial compounds. This approach lowers the risk of host toxicity without potentially compromising a pronounced antiplasmodial activity.[159] Selective human HDAC6 inhibitors could possibly serve this goal as it is known that mice lacking HDAC6 develop rather normally,[11] so minor to no side effects are expected upon deployment of these agents. Bearing this rationale in mind, we decided to test all benzohydroxamic acids (described in previous parts II-V) for their antiplasmodial activity, with several representatives being highly potent and selective *h*HDAC6 inhibitors. Indeed, a systematic exploration of the possible correlation between *h*HDAC6 inhibitors and antiplasmodial activity has not been performed so far and could reveal new opportunities in antimalarial drug development.

6.2. Antimalarial evaluation of thiaheterocyclic benzohydroxamic acids

This brief chapter focusses on the antiplasmodial evaluation of three innovative classes of benzohydroxamic acids **1-3**, all featuring a different thiahetero(bi- or tri-)cyclic 'cap group' (Figure 1). Class **1** consists of molecules containing a saturated thiaheterocyclic ring annulated onto an indole core (designated as Tubathians), class **2** comprises benzothiophenes embodying a nitrogen atom in the linker region, and class **3** includes cycloalkane-annulated 1,5-benzothiazepine scaffolds. Because of small structural modifications with respect to the 'mother structure' within each class (Figure 1, Table 1), a broad set of 42 compounds with divergent decoration patterns is synthetically available. The preparation of these compounds **1-3** has been described in previous parts II-V, together with a detailed account on their HDAC6 selectivity, cellular activity (α-tubulin acetylation, a known substrate of HDAC6) and mutagenicity. These different classes include a number of highly potent and selective *h*HDAC6 inhibitors (Table 2), which have in common a *para*-substituted benzohydroxamic acid fragment, no substituents in the *meta*-position with respect to the hydroxamic acid group, and superior HDAC6 inhibitory activity for sulfoxides and sulfones over the corresponding sulfides.
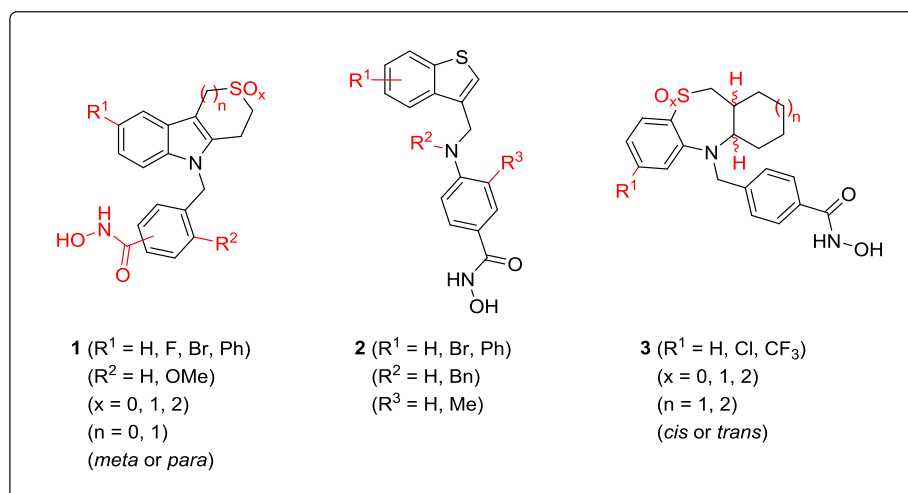
Figure 1. Available thiaheterocyclic benzohydroxamic acids **1-3**.

Table 1. Substitution pattern of thiaheterocyclic benzohydroxamic acids **1-3**

cmpd	R^1	R^2	R^3	x	n	config.^{a}	cmpd	R^1	R^2	R^3	x	n	config.^{a}
1a	H	H	-	0	1	*para*	**2a**	H	H	H	-	-	-
1b	H	OMe	-	0	1	*para*	**2b**	H	Bn	H	-	-	-
1c	F	H	-	0	1	*para*	**2c**	5-Br	H	H	-	-	-
1d	F	OMe	-	0	1	*para*	**2d**	5-Br	Bn	H	-	-	-
1e	H	H	-	2	1	*para*	**2e**	5-Ph	H	H	-	-	-
1f	H	OMe	-	2	1	*para*	**2f**	5-Ph	Bn	H	-	-	-
1g	F	H	-	2	1	*para*	**2g**	6-Br	H	H	-	-	-
1h	F	OMe	-	2	1	*para*	**2h**	6-Br	Bn	H	-	-	-
1i	Br	H	-	2	1	*para*	**2i**	6-Ph	H	H	-	-	-
1j	H	H	-	1	1	*para*	**2j**	6-Ph	Bn	H	-	-	-
1k	F	H	-	1	1	*para*	**2k**	H	H	Me	-	-	-
1l	H	H	-	2	0	*para*	**3a**	H	-	-	0	1	*cis*
1m	F	H	-	2	0	*para*	**3b**	Cl	-	-	0	1	*cis*
1n	H	H	-	0	1	*meta*	**3c**	CF$_3$	-	-	0	1	*cis*
1o	F	H	-	0	1	*meta*	**3d**	H	-	-	2	1	*cis*
1p	H	H	-	2	1	*meta*	**3e**	Cl	-	-	2	1	*cis*
1q	F	H	-	2	1	*meta*	**3f**	CF$_3$	-	-	2	1	*cis*
1r	Ph	H	-	2	1	*meta*	**3g**	H	-	-	1	1	*cis*
1s	H	H	-	2	0	*meta*	**3h**	H	-	-	0	2	*cis*
1t	F	H	-	2	0	*meta*	**3i**	Cl	-	-	0	1	*trans*
1u	Br	H	-	1	0	*meta*	**3j**	H	-	-	0	2	*trans*

^{a} The *para-* and *meta*-configuration for compounds **1** refers to the position of the hydroxamic acid group on the aromatic ring with respect to the aminomethyl substituent.

The antiplasmodial activity of this set of structures was first determined through a modified parasite lactate dehydrogenase assay against a chloroquine-sensitive (CQS) strain of *P. falciparum* (NF54).[160,161] When the molecules proved to be reasonably active against this strain (IC$_{50}$ < 5 µM), a second assay was performed against a chloroquine-resistant (CQR) strain of *P. falciparum* (Dd2), as well as an MTT-assay (3-(4,5-dimethylthiazol-2-yl)-2,5-diphenyltetrazolium bromide) on CHO cells (Chinese Hamster Ovarian) to assess their mammalian cytotoxicity (Table 2).[162] Finally, a selectivity index (SI = IC$_{50}$ CHO/IC$_{50}$ NF54) and a resistance index (RI = IC$_{50}$ Dd2/IC$_{50}$ NF54) was calculated to be able to easily compare the therapeutic window (active concentration vs. toxic concentration) and sensitivity toward resistance developing. Table 2 shows that all 42 benzohydroxamic acids **1-3** display interesting antiplasmodial activities (IC$_{50}$ values against the CQS strain between 0.11 and 37.5 µM). The potent HDAC6 inhibitors **1i**, **1k**, **1l**, **3d**, **3e** and **3f** were also found to be highly active against both CQS and CQR parasitic strains (dark blue tinted, IC$_{50}$ CQS and CQR < 1 µM, IC$_{50}$ HDAC6 < 0.07 µM). However, other active HDAC6 inhibitors did not demonstrate a distinct submicromolar parasitic toxicity (for example **1a**, **1e** and **1g**). Thus, no consistent correlation can be drawn between *h*HDAC6 inhibition and antiplasmodial activity, which could be expected considering the inevitable differences between human and parasite HDAC isoforms.[156] On the other hand, it is remarkable to note that the most effective antiplasmodial compounds all are powerful *h*HDAC6 inhibitors, and none of the less active *h*HDAC6 inhibitors showed submicromolar antiplasmodial potency. Based on these observations, it can be suggested that strong *h*HDAC6 inhibitory activity is a necessary but not a sufficient condition for thiaheterocyclic benzohydroxamic acids to exert submicromolar antiplasmodial activity as well. From the six compounds showing the most promising antiplasmodial activity, four molecules have excellent selectivity indices higher than 300 (**1i**, **1k**, **1l** and **3d**), which means that the concentration at which they kill the parasite is at least 300 times lower than their toxic concentration for CHO cells. Comparison of the resistance indices (RI) suggests that the tested molecules have comparable activity (RI = 0.3 - 3.9) against both strains (CQS and CQR). This is in marked contrast to the control drug chloroquine, which is 17 times less active against the CQR strain (RI = 17.5).

Table 2. IC$_{50}$ values (µM) of compounds **1-3** determined for a normal (NF54) and chloroquine-resistant (Dd2) *Plasmodium falciparum* strain, CHO cells and HDAC6[a]

cmpd	NF54	Dd2	CHO	SI[b]	RI[c]	HDAC6	cmpd	NF54	Dd2	CHO	SI[b]	RI[c]	HDAC6
1a	37.5	-	-	-	-	0.015	2a	1.60	2.13	12.7	8	1.3	0.014
1b	14.0	-	-	-	-	-	2b	32.4	-	-	-	-	-
1c	2.2	3.1	105.2	48	1.4	0.022	2c	1.02	2.4	31.0	30	2.4	0.037
1d	23.2	-	-	-	-	-	2d	17.8	-	-	-	-	-
1e	10.8	-	-	-	-	0.002	2e	5.07	-	-	-	-	-
1f	21.0	-	-	-	-	2.0	2f	5.75	-	-	-	-	-
1g	15.8	-	-	-	-	0.004	2g	1.30	1.58	46.1	35	1.2	0.064
1h	32.7	-	-	-	-	1.3	2h	8.45	-	-	-	-	-
1i	0.11	0.43	109.0	991	3.9	0.003	2i	3.34	1.14	31.2	9	0.3	-
1j	1.28	1.3	>282	>217	1.0	0.014	2j	5.02	-	-	-	-	-
1k	0.40	0.80	>269	>673	2.0	0.009	2k	36.8	-	-	-	-	-
1l	0.92	0.66	>281	>305	0.7	0.008	3a	1.59	>2.7	103.9	65	-	0.036
1m	1.07	1.55	>267	>250	1.7	0.016	3b	>2.48	>2.48	41.4	-	-	0.650
1n	1.48	2.18	>295	>199	1.5	-	3c	1.53	>2.29	61.5	40	-	0.200
1o	1.32	1.44	48.1	36	1.1	-	3d	0.36	0.94	107.6	303	2.6	0.008
1p	5.45	-	-	-	-	-	3e	0.47	0.44	35.4	75	0.9	0.068
1q	7.84	-	-	-	-	-	3f	0.87	0.70	56.8	65	0.8	0.011
1r	8.13	-	-	-	-	-	3g	1.25	>2.60	172.9	138	-	0.006
1s	12.2	-	-	-	-	-	3h	>2.61	>2.61	87.0	-	-	0.033
1t	9.80	-	-	-	-	-	3i	>2.48	1.57	50.9	-	-	0.160
1u	11.9	-	-	-	-	-	3j	>2.61	>2.61	61.7	-	-	0.092

[a] Dark blue: IC$_{50}$ value of the hydroxamic acid lower than 1 µM against both *P. falciparum* strains. -: not determined. References: Chloroquine IC$_{50}$-NF54 = 0.01 µM, IC$_{50}$-Dd2 = 0.175 µM; Artesunate IC$_{50}$-NF54 < 0.01 µM, IC$_{50}$-Dd2 = 0.016 µM; Emetine IC$_{50}$-CHO = 0.112 µM. [b] SI (Selectivity Index) = IC$_{50}$ (CHO)/IC$_{50}$ (NF54). [c] RI (Resistance Index) = IC$_{50}$ (Dd2)/IC$_{50}$ (NF54).

6.3. Conclusions

42 Thiaheterocyclic benzohydroxamic acids **1-3**, 17 of them previously being identified as highly potent and selective *h*HDAC6 inhibitors, were assessed in terms of their antiplasmodial profile. This study revealed six selective HDAC6 inhibitors to demonstrate submicromolar antiplasmodial potency against both a chloroquine-sensitive and a chloroquine-resistant strain, and four of these structures (**1i**, **1k**, **1l** and **3d**) also proved to have an excellent therapeutic window (SI > 300). On the other hand, hydroxamic acids which do not strongly inhibit *h*HDAC6, appear to possess only moderate antiplasmodial effects. Thus, potent and selective *h*HDAC6 inhibitory activity of thiaheterocyclic benzohydroxamic acids seems to be a necessary but not a sufficient condition to elicit pronounced antiplasmodial activity as well. Moreover, selective *h*HDAC6 inhibitors can induce powerful *P. falciparum* toxicity without being toxic for CHO cells (as a model for mammalian cytotoxicity). In conclusion, *h*HDAC6 inhibitory activity and antiplasmodial activity are somehow interconnected, and these HDAC6i new chemical entities can certainly be considered a valuable starting point for further medicinal chemistry investigation *en route* to novel types of antiplasmodial drugs.

6.4. Experimental details

6.4.1. Antiplasmodial assays

The antiplasmodial assays were performed by the Department of Medicine, University of Cape Town and the Department of Chemistry and Institute of Infectious Disease and Molecular Medicine, University of Cape Town (Prof. K. Chibale). Continuous *in vitro* cultures of asexual erythrocyte stages of *P. falciparum* were maintained using a modified method of Trager and Jensen.[160] Quantitative assessment of antiplasmodial activity *in vitro* was determined via the parasite lactate dehydrogenase assay using a modified method described by Makler.[161] The test samples were prepared to a 20 mg/mL stock solution in 100% DMSO. Stock solutions were stored at -20 °C. Further dilutions were prepared in complete medium on the day of the experiment. Chloroquine (CQ) and artesunate were used as the reference drugs. A full dose-response was performed to determine the concentration inhibiting 50% of parasite growth (IC_{50} value). Test samples were tested at a starting concentration of 100 µg/mL, which was then serially diluted twofold in complete medium to give 10 concentrations; with the lowest concentration being 0.2 µg/mL. The same dilution technique was used for all samples. References were tested at a starting concentration of 1 µg/mL. The highest concentration of solvent to which the parasites were exposed to had no measurable effect on the parasite viability (data not shown).

6.4.2. MTT assays

The MTT assays were performed by the Department of Medicine, University of Cape Town and the Department of Chemistry and Institute of Infectious Disease and Molecular Medicine, University of Cape Town (Prof. K. Chibale). Test samples were screened for *in vitro* cytotoxicity against a mammalian cell-line, Chinese Hamster Ovarian (CHO), using the 3-(4,5-dimethylthiazol-2-yl)-2,5-diphenyltetrazolium bromide (MTT)-assay. The MTT-assay is used as a colorimetric assay for cellular growth and survival, and compares well with other available assays.[162,163] The tetrazolium salt MTT was used to measure all growth and chemosensitivity. The test samples were tested in triplicate on one occasion. The same stock solutions prepared for antiplasmodial evaluation were used for cytotoxicity testing. Test compounds were stored at -20 °C until use. Dilutions were prepared on the day of the experiment. Emetine was used as the reference drug in all experiments. The starting concentration was 100 µg/mL, which was serially diluted in complete medium with 10-fold dilutions to give 6 concentrations, the lowest being 0.001 µg/mL. The highest concentration of solvent to which the cells were exposed to had no measurable effect on the cell viability (data not shown). The 50% inhibitory

concentration (IC_{50}) values were obtained from full dose-response curves, using a non-linear dose-response curve fitting analysis via GraphPad Prism v.4 software.

PERSPECTIVES

This PhD thesis was devoted to the target-based early-phased drug discovery of novel selective HDAC6 inhibitors. Following up on Tubastatin A, one of the most selective HDAC6 inhibitors discovered to date, analogues structures bearing a thiaheterocyclic benzohydroxamic acid structure were proposed and synthesized. In attempts to completely fill the tubular space of HDAC6, structures **1** and **2** were synthesized carrying extra substituents (methoxy and methyl groups) on the aromatic linker (Figure 1). However, the tubular space to the catalytic site of HDAC6 appeared to be too small, and thus these kinds of transformations were not tolerated. On the other hand, bicyclic-capped HDAC6 inhibitor **3** substituted with a fluorine atom in the linker has been developed in a recent publication and appeared to be the most potent HDAC6 inhibitor with excellent selectivity over the other HDAC isoforms in a series of similar compounds.[36] Therefore, in future research it would be interesting to synthesize derivatives of the most potent compounds described in this PhD thesis substituted with a fluorine atom on the aromatic linker, e.g. structures **4** and **5** (Figure 1).
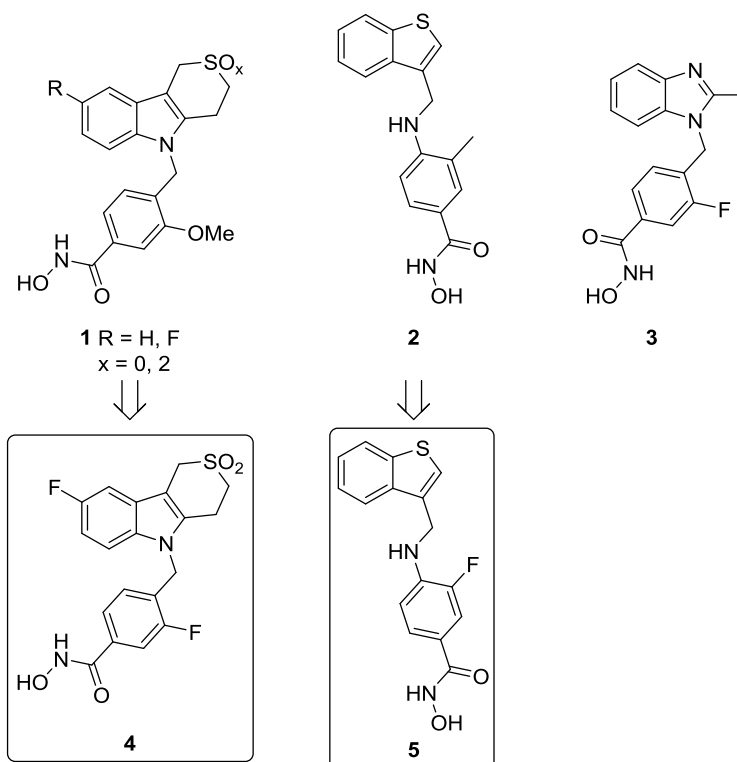
Figure 1. Rational design of fluoro-substituted HDAC6 inhibitors **4-5** to exploit the tubular channel of HDAC6.

Another problem regarding the development of hydroxamic acid-based HDAC inhibitors for therapeutic uses outside the field of oncology, is their potential mutagenicity.[147] The most logical strategy to circumvent this issue, is to develop alternatives with other zinc-binding groups. More precisely, the replacement of the hydroxamic acid functionality in **6** with a trifluoromethylketone in **7**, a silanediol in **8**, and a mercaptoacetamide in **9** (Figure 2) would

represent reasonable strategies for the development of potent and selective HDAC6 inhibitors.[164,165] Undoubtedly, also the combination of the first and second approach (Figure 1 and 2) would result in interesting molecules for evaluation as potent and selective HDAC6 inhibitors.
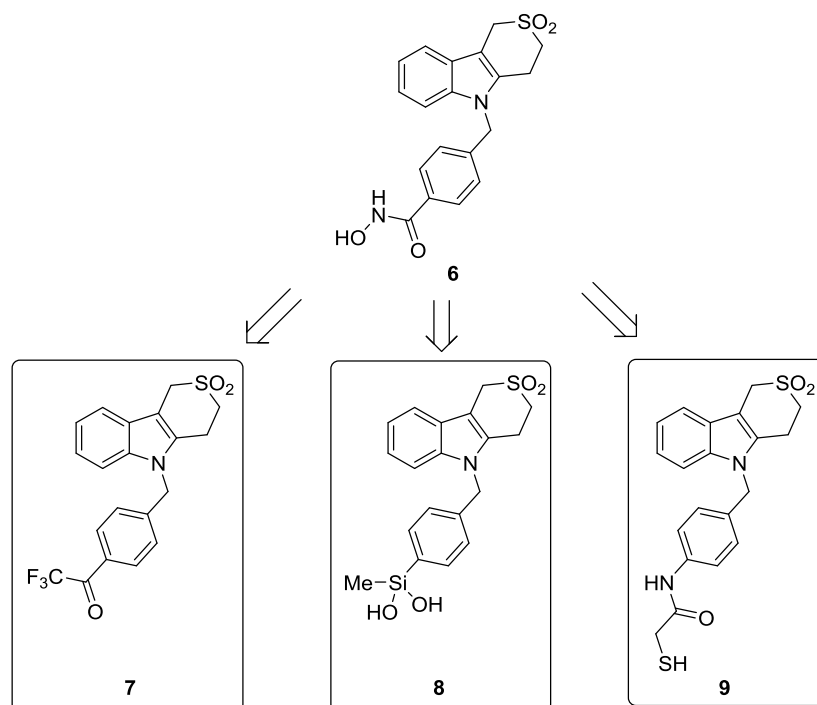
Figure 2. Rational-design of potential HDAC6 inhibitors holding alternative zinc-binding groups.

As this PhD thesis started from a target-based drug discovery approach, it would certainly be valuable to merge this with phenotypic assays discovered in the HDAC6 field. As such, the high biological complexity of a disease state would be integrated in the drug discovery program. A first start was already presented regarding the antiplasmodial activity of the benzohydroxamic acids synthesized during this PhD, which indeed resulted in novel structure-activity relationships specific for this parasitic infection. Currently, also other phenotypic assays are evaluated in the oncology field by our group at the Laboratory Experimental Cancer Research (UZGent, Prof. De Wever), and it would be interesting to see this expanded to the field of immunology and neurology. As such, the three main medicinal areas concerning HDAC6 would be covered.[10]

In parallel with the discovery of an adequate phenotypic assay for HDAC6 inhibition, the most promising structures presented in this manuscript should be further evaluated for their ADME/Tox properties (CYP inhibition, hERG channel inhibition, microsomal stability, plasma protein binding, CACO-2 permeability, micronucleus test, growth inhibition, metalloproteinase screen) as a selection tool to determine which compounds should be further evaluated for their *in vivo* pharmacokinetic properties. When a compound is obtained with favourable properties,

this drug should be further tested in an animal model which is selected from the most promising phenotypic assay.

SUMMARY

The non-selective inhibition profile of marketed HDAC inhibitors is associated with undesired toxicities, and therefore the design and development of isozyme-selective inhibitors has emerged as an important challenge. In that regard, HDAC6 (belonging to HDAC class IIb) has arisen as an interesting target since its activity is associated with biological pathways in neurodegenerative diseases, cancer and immunology. One of the first druglike and selective HDAC6 inhibitors reported is Tubastatin A (**i**, Figure 1), a benzohydroxamic acid moiety linked to a γ-tetrahydrocarboline heterocycle. The benzohydroxamic acid skeleton is wider than the alkyl chain typically observed in pan-HDAC inhibitors and ensures selectivity toward HDAC6. Therefore, it was chosen to keep this benzohydroxamic acid scaffold intact while exploring variation at the cap-region. In that mind-set, the evaluation of thiaheterocyclic benzohydroxamic acids was identified as an unexplored field within HDAC6 inhibitor design. Therefore, during this PhD thesis three novel classes of thiaheterocyclic benzohydroxamic acids were synthesized (**ii**, **iii** and **iv**, Figure 1) and evaluated for their potential to act as selective HDAC6 inhibitors.
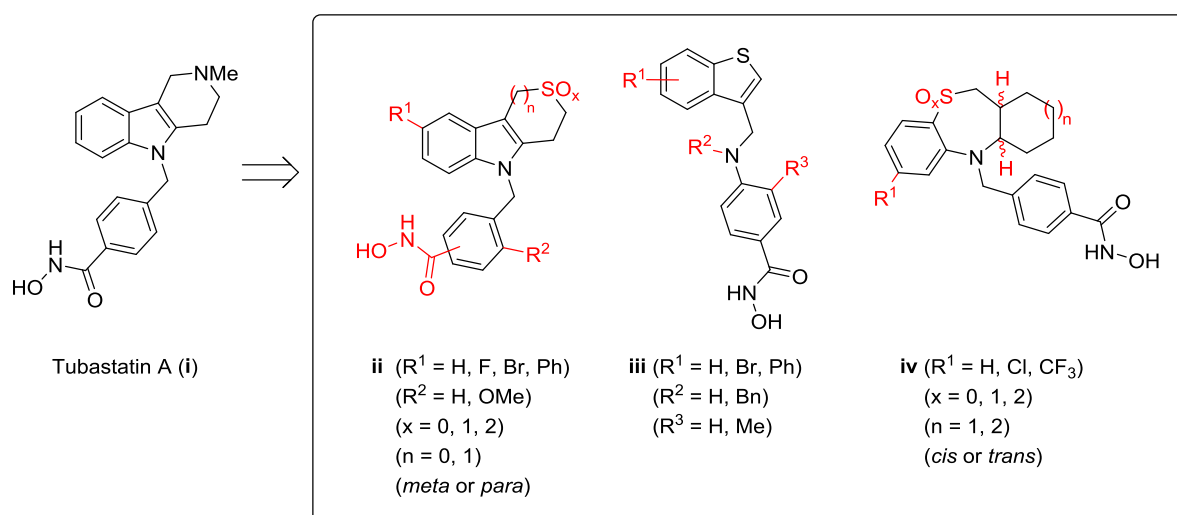
Figure 1. Synthesized thiaheterocyclic benzohydroxamic acids **ii**, **iii** and **iv**.

In the first chapter of this dissertation, a literature overview was presented concerning the synthesis and biological activity of the most representative benzohydroxamic acid-based histone deacetylase inhibitors published to date. Based on this information we discovered that careful optimization of the part following the benzohydroxamic acid, i.e., the linker region and the cap-group, can lead to inhibitors which are HDAC6 selective, non-selective, HDAC8 selective or dual HDAC6/8 selective. Moreover, the importance of the benzohydroxamic acid building block in the chemical architecture of HDAC inhibitors is demonstrated.

In the second and third chapter, the synthesis and biological evaluation of structures **ii** was discussed (Scheme 1). The synthetic pathway started with the formation of heterocycles **vii** via a bismuth nitrate-catalyzed Fisher indole synthesis employing hydrazines **v** and cyclic ketones **vi**. The sulfur atom present in these heterocycles was then selectively oxidized toward sulfoxides **viii** or sulfones **ix**. In one case, a Suzuki-Miyaura coupling was successfully performed to obtain a phenyl-substituted heterocyclic cap-group **ix** (R^1 = Ph, n = 1, 60%). These indole-containing heterocycles **vii-ix** were then *N*-deprotonated by sodium hydride and subsequently reacted with benzyl bromides **x**. This route produced 21 esters **xi** which, in a final step, were converted toward a set of 21 novel thiaheterocyclic benzohydroxamic acids **ii**.
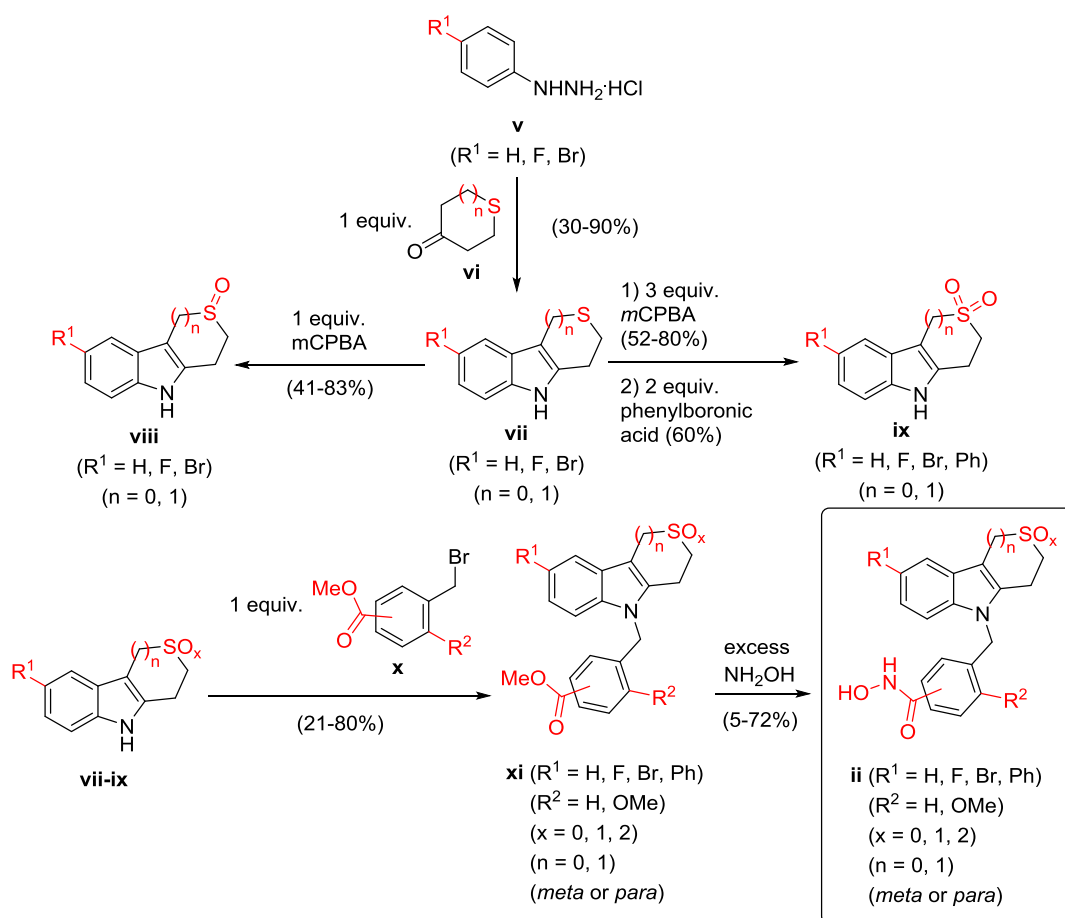
Scheme 1. Synthetic pathway presented in chapters II and III.

From these 21 potential HDAC6 inhibitors **ii**, 11 compounds demonstrated more than 70% inhibition of HDAC6 at a concentration of 10 µM and nine of them had an IC_{50} value lower than 0.1 µM. These nine inhibitors all bear a *para*-substituted hydroxamic acid moiety with respect to the heterocyclic cap-group and do not hold an extra methoxy group on the aromatic linker. Moreover, the oxidized sulfur analogs (x = 1 or 2) demonstrated an improved HDAC6 inhibition potency, which was explained *in silico* by the extra hydrogen bond potential of the oxygen

atoms on the sulfur atom with neighbouring amino acid residues. Through enzyme and cellular assays, the selectivity for HDAC6 was determined, and all nine inhibitors proved to be potent and selective inhibitors. ADME/Tox evaluation of these nine potent HDAC6 inhibitors revealed that the sulfur oxidized analogs had an improved profile over the non-oxidized derivatives, which directs future lead optimization toward *para*-substituted sulfoxides ans sulfones **ii**.

In chapter IV, the synthesis and biological activity of benzohydroxamic acids **iii** was evaluated (Scheme 2). From commercially available benzothiophene-3-carbaldehyde **xii**, 6-bromo-benzothiophene-3-carbaldehyde **xiii** was formed applying five equiv of bromine. Then, commercially available 5-bromobenzothiophene-3-carbaldehyde **xiv** and the synthesized carbaldehyde **xiii** were subjected to a Suzuki-Miyaura coupling yielding phenyl-substituted compounds **xv** and **xvi**. These precursors **xii-xvi** were subjected to a reductive amination employing consequtively methyl 4-aminobenzoate **xvii** and sodium cyanoborohydride. The secondary amino group present in esters **xviii** was further derivatized with benzyl bromide and gave tertiairy amines **xix** in good yields. Final conversion of the 11 available esters **xviii-xix** with hydroxylamine resulted in the formation of the premised benzohydroxamic acids **iii**.
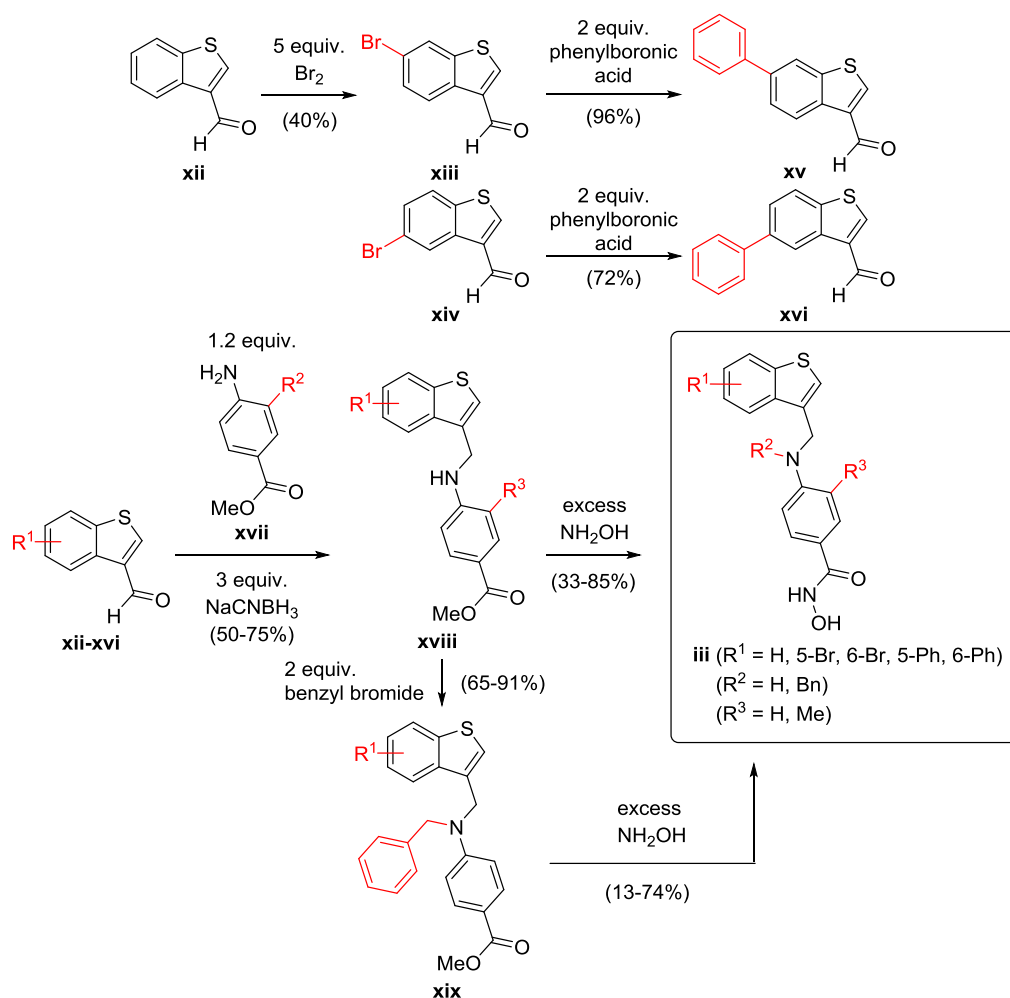
Scheme 2. Synthetic pathway presented in chapter IV.

In total 11 benzothiophene benzohydroxamic acids **iii** were evaluated for their potential to selectively inhibit HDAC6. Nine of these compounds showed more than 70% inhibition of the HDAC6 activity at 10 µM, and three of them had an IC_{50} value lower than 0.1 µM. These highly potent structures **iii** (R^1 = H, 5-Br, 6-Br, R^2 = H, R^3 = H) contained a secondary amino group and were substituted with a bromine or hydrogen atom on the cap-group. Furthermore, these structures showed a selectivity profile comparable with that of Tubastatin A, and it was demonstrated that HDAC6 inhibition can be uncoupled from transcriptional inhibition at the level of activated NF-κB, AP-1, and GR.

In Chapter V, a detailed description of the synthesis and biological evaluation of benzohydroxamic acids **iv** was presented (Scheme 3). Via an aldol condensation, β-hydroxyketones **xxi** were prepared from ketones **xx** employing paraformaldehyde. In the next step, a tosylation, a reaction with 2-aminothiophenol **xxii** and a reduction using sodium cyanoborohydride were performed in one pot, and this resulted in the formation of *cis*- and *trans*-annulated benzothiazepines **xxiii** which were obtained in a diastereomerically pure form via column chromatography. This concerned the first report on the detailed synthesis and isolation of both diastereomers of tricyclic cyclohexane- and cycloheptane-fused tetrahydrobenzothiazepines **xxiii**, and the correct structure was secured by X-ray crystallography. These heterocyclic structures **xxiii** were treated with methyl 4-(bromomethyl)benzoate **xxiv** (neat) which gave esters **xxv** in acceptable yields. The sulfur atom present in the heterocyclic cap-group of sulfides **xxv** was selectively oxidized to a sulfoxide or a sulfone and yielded compounds **xxvi.** Finally, esters **xxv-xxvi** were transformed to hydroxamic acids **iv** employing an excess of hydroxylamine.
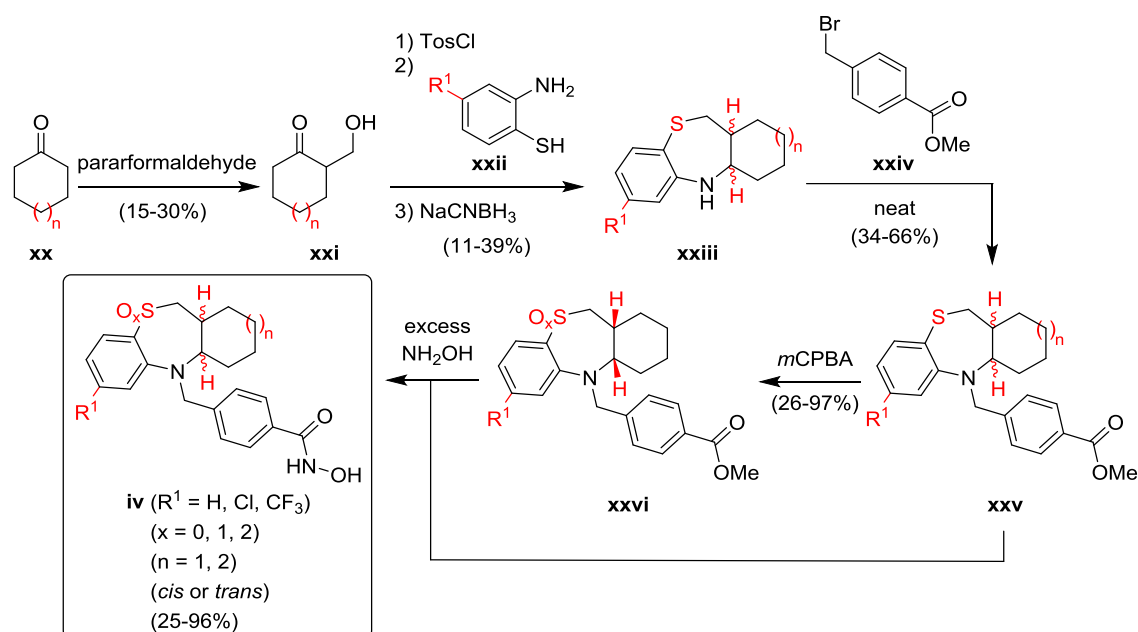
Scheme 3. Synthetic pathway presented in chapter V.

In total, ten benzohydroxamic acids **iv** were efficiently synthesized and tested for their ability to inhibit HDAC6. All these inhibitors were shown to be highly active HDAC6 inhibitors at a concentration of 10 µM (96-100% inhibition). Therefore, for all ten hydroxamic acids **iv** the IC_{50} values toward HDAC6 were determined, and all inhibitors showed nanomolar potential (6.3-650 nM). In accordance with previous observations regarding the effect of *S*-oxidation, oxidized sulfur analogs **iv** (x = 1, 2) were again demonstrated to be more potent HDAC6 inhibitors than their non-oxidized counterparts. This superior HDAC6 inhibitory activity was supported by a molecular dynamics simulation, which again revealed the possibility of additional hydrogen bonding between a sulfur-bound oxygen atom and an amino acid residue. Five compounds showed an IC_{50} value lower then 50 nM, and their selectivity toward the other HDAC isoforms was determined via enzyme and cellular assays. These assays revealed that this class of molecules can be regarded as highly potent and selective HDAC6 inhibitors suitable for further assessment.

In the final chapter (chapter VI), all 42 thiaheterocyclic benzohydroxamic acids synthesized during this PhD thesis were evaluated as potential antiplasmodial agents. Several pan-HDAC inhibitors are known to exert powerful antimalarial activity, but their possible toxicity delays further development. A problem which might be circumvented by the deployment of isoform-selective HDAC inhibitors, such as several of the inhibitors described in this dissertation. Six selective HDAC6 inhibitors were demonstrated to exhibit submicromolar antiplasmodial potency against both a chloroquine-sensitive and a chloroquine-resistant *Plasmodium falciparum* strain, and four of these structures **xxvii-xxx** also proved to have an excellent therapeutic window (SI > 300, Figure 2). On the other hand, hydroxamic acids which do not strongly inhibit *h*HDAC6, appear to possess only moderate antiplasmodial effects. Thus, potent and selective *h*HDAC6 inhibitory activity of thiaheterocyclic benzohydroxamic acids seems to be a necessary but not a sufficient condition to elicit pronounced antiplasmodial activity as well.

xxvii	**xxviii**	**xxix**	**xxx**
IC_{50} NF54 = 0.11 µM	IC_{50} NF54 = 0.40 µM	IC_{50} NF54 = 0.92 µM	IC_{50} NF54 = 0.36 µM
IC_{50} Dd2 = 0.43 µM	IC_{50} Dd2 = 0.80 µM	IC_{50} Dd2 = 0.66 µM	IC_{50} Dd2 = 0.94 µM
IC_{50} CHO = 109.0 µM	IC_{50} CHO > 269 µM	IC_{50} CHO > 281 µM	IC_{50} CHO = 107.6 µM
SI = 991	SI > 673	SI > 305	SI = 303
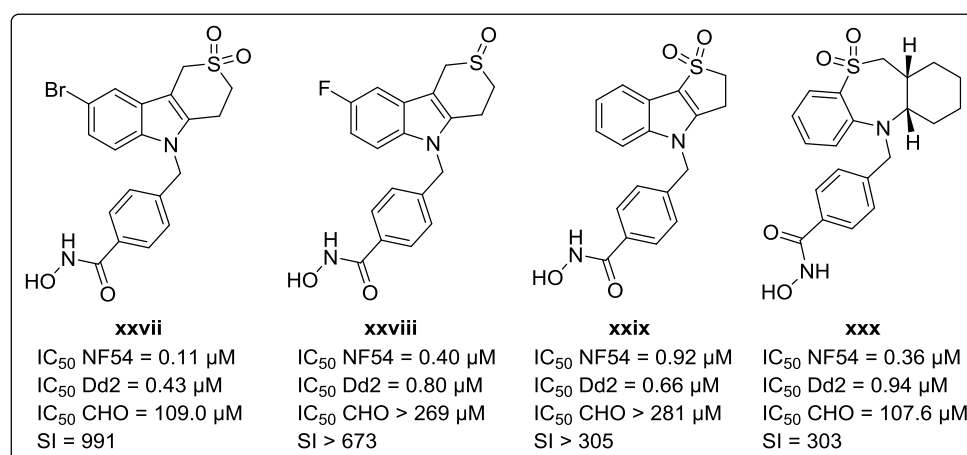
Figure 2. Most potent antiplasmodial benzohydroxamic acids described in chapter VI.

In conclusion, from each class (**ii**, **iii** and **iv**) several lead structures were discovered demonstrating excellent HDAC6 inhibitory activity and selectivity (Figure 3). This clearly demonstrates the potential of thiaheterocyclic benzohydroxamic acids in the discovery of selective HDAC6 inhibitors.
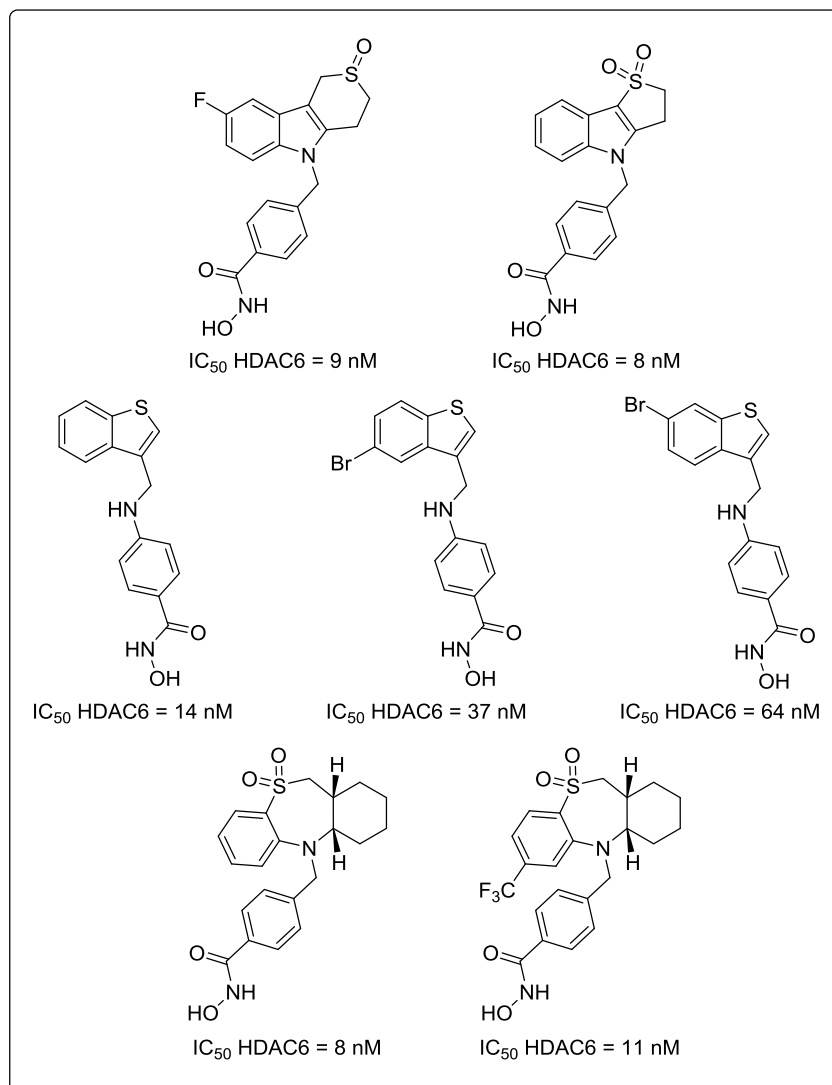
Figure 3. Most potent representatives from each class **ii**, **iii** and **iv**.

SAMENVATTING

Het gebrek aan selectiviteit van gecommercialiseerde HDAC-inhibitoren wordt geassocieerd met ongewenste toxiciteit; en daarom is het onderzoek naar het ontwerp en de ontwikkeling van isozym-selectieve inhibitoren een 'hot topic' binnen de medicinale chemie. In dat verband is HDAC6 een interessant doelwit binnen de HDAC-familie. HDAC6 behoort tot HDAC-klasse IIb, en zijn activiteit wordt gerelateerd aan verschillende aandoening zoals neurodegeneratieve ziekten, kanker en immuunziekten. Eén van de eerst gerapporteerde selectieve HDAC6 inhibitoren die bovendien vele karakteristieken heeft van een klassiek medicijn is Tubastatin A (**i**, Figuur 1). Deze inhibitor bestaat uit een benzohydroxamzure eenheid die gekoppeld is aan een γ-tetrahydrocarboline heterocyclishe structuur. Het benzohydroxamzure skelet is breder dan de typische alkylketen van niet-selectieve HDAC-inhibitoren, en dit geeft aanleiding tot een verbeterde selectiviteit voor HDAC6. Daarom werd gekozen om deze benzohydroxamzure functionaliteit intact te houden en werden enkel structuren ontworpen met variaties in de heterocyclische regio. In dat opzicht vormt de ontwikkeling van thiaheterocyclische benzohydroxamzuren een ononderzocht domein binnen het ontwerp van nieuwe selectieve HDAC6-inhibitoren en werden tijdens dit doctoraat drie nieuwe klassen thiaheterocyclische benzohydroxamzuren gesynthetiseerd **ii**, **iii** en **iv** (Figuur 1).
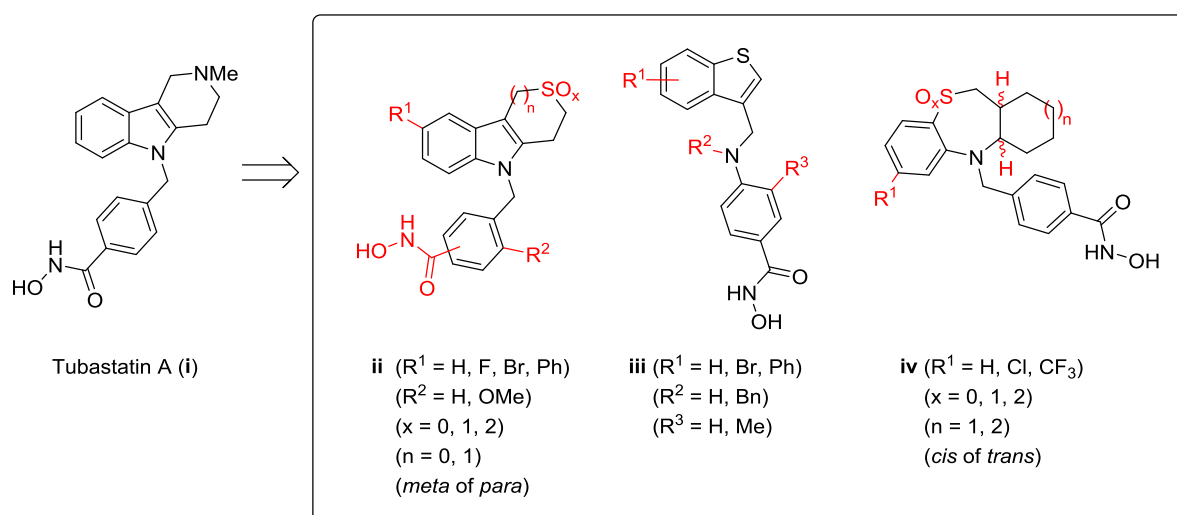
Figuur 1. Gesynthetiseerde thiaheterocyclische benzohydroxamzuren **ii**, **iii** en **iv**.

In het eerste hoofdstuk van dit onderzoek werd een literatuuroverzicht gegeven over de synthese en biologische activiteit van de meest veelbelovende benzohydroxamzuur-gebaseerde histondeacetylase inhibitoren tot op heden gepubliceerd. Via dit overzicht werd ontdekt dat door optimalizatie van het deel volgend op de benzohydroxamzure eenheid inhibitoren kunnen worden ontworpen die HDAC6-selectief, niet selectief, HDAC8-selectief of HDAC6- en 8-selectief zijn. Bovendien werd het belang van de benzohydroxamzure structuur tijdens het ontwerpen van HDAC-inhibitoren aangetoond.

In het tweede en derde hoofdstuk werd de synthese en biologische evaluatie van structuren **ii** beschreven (Schema 1). De syntheseroute startte met de vorming van heterocyclische ringen **vii** via een bismuthnitraat-gekataliseerde Fisher-indoolsynthese gebruik makende van hydrazinen **v** en cyclische ketonen **vi**. Het zwavelatoom aanwezig in deze ringen werd selectief geoxideerd tot sulfoxiden **viii** of sulfonen **ix**. In één geval werd succesvol een Suzuki-Miyaura-koppeling uitgevoerd om zo toegang te krijgen tot fenylgesubstitueerd derivaat **ix** (R^1 = Ph, n = 1, 60%). Deze indoolbevattende structuren **vii-ix** werden *N*-gedeprotoneerd door natriumhydride en daaropvolgend gereageerd met benzylbromide **x**. Zo werden 21 esters **xi** geproduceerd die in een laatste stap werden omgezet tot nieuwe thiaheterocyclische benzohydroxamzuren **ii**.
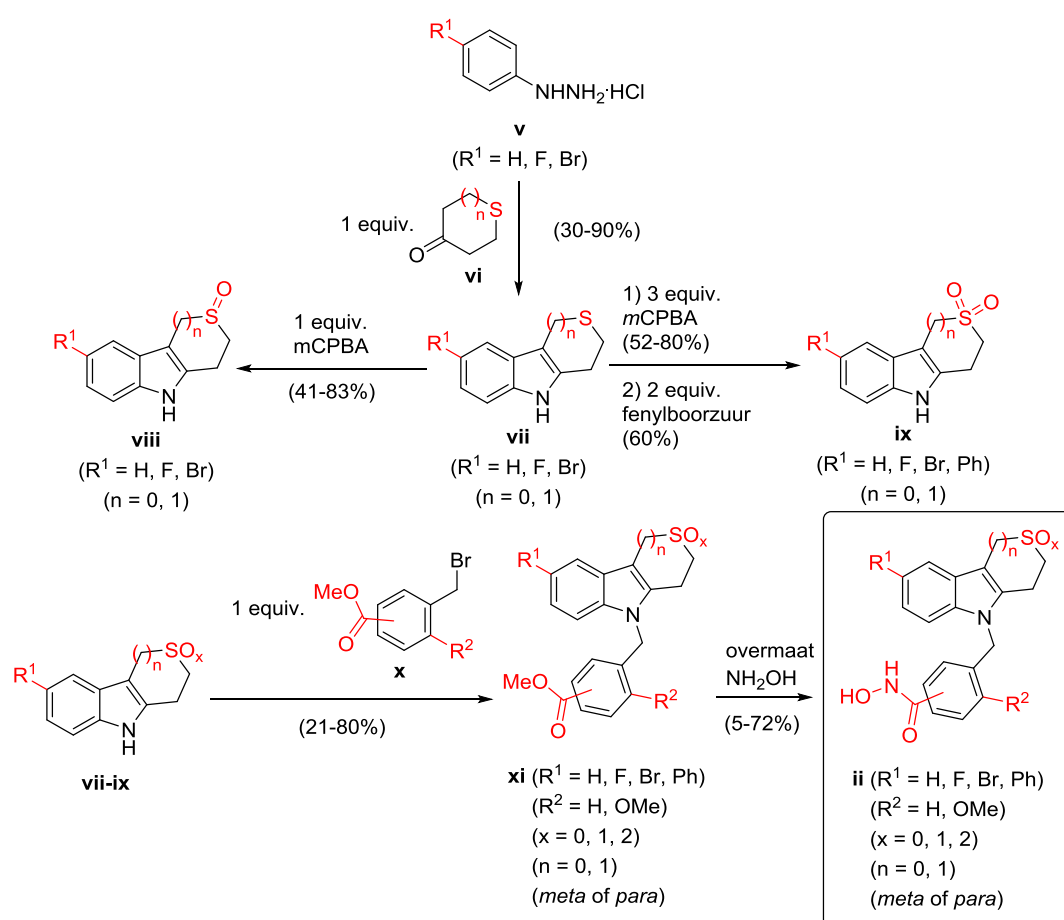
Schema 1. Syntheseroute beschreven in hoofdstukken II en III.

Van alle 21 gesynthetiseerde HDAC6 inhibitoren **ii** vertoonden 11 verbindingen meer dan 70% inhibitie van HDAC6 bij een concentratie van 10 µM, en van deze 11 structuren bezaten negen inhibitoren een IC_{50}-waarde lager dan 0.1 µM. Deze negen moleculen zijn allemaal *para*-gesubstitueerd en dragen geen extra methoxygroep op de aromatische linker. Verder bezaten de geoxideerde zwavelanalogen (x = 1 of 2) een beter HDAC6-inhibitieprofiel, wat kan worden

verklaard door de mogelijkheid tot extra waterstofbrugvorming van de zuurstofatomen op het zwavelatoom met naburige aminozuurzijketens. De selectiviteit ten opzichte van HDAC1-11 werd bepaald via enzym- en celtesten, waarbij werd aangetoond dat alle negen inhibitoren selectief blijken te zijn voor HDAC6. ADME/Tox-evaluatie van deze negen actieve HDAC6-inhibitoren onthulde dat de geoxideerde zwavelanalogen een beter profiel vertoonden dan de niet-geoxideerde derivaten, waardoor de *para*-gesubstitueerde sulfoxiden en sulfonen kunnen dienen als 'lead'-structuren voor verdere optimalisatie.

In hoofdstuk IV werd de synthese en biologische activiteit van benzohydroxamzuren **iii** besproken (Schema 2). Vertrekkende vanuit commercieel beschikbaar benzothiofeen-3-carbaldehyde **xii** werd 6-broombenzothiofeen-3-carbaldehyde **xiii** gevormd gebruik makende van vijf equiv broom. Vervolgens werden het commercieel beschikbaar 5-broombenzothiofeen-3-carbaldehyde **xiv** en het aangemaakte carbaldehyde **xiii** onderworpen aan een Suzuki-Miyaura-koppeling, hetgeen aanleiding gaf tot de vorming van fenyl-gederivatiseerde aldehyden **xv** en **xvi**. Deze precursoren **xii-xvi** werden verder reductief geamineerd m.b.v. methyl-4-aminobenzoaat **xvii** en natriumcyaanboorhydride. Het stikstofatoom aanwezig in esters **xviii** werd dan gederivatiseerd met benzylbromide en vormde tertiaire aminen **xix** in goede opbrengsten. Finale omzetting van de 11 beschikbare esters **xviii-xix** met hydroxylamine resulteerde in de vorming van benzohydroxamzuren **iii**.
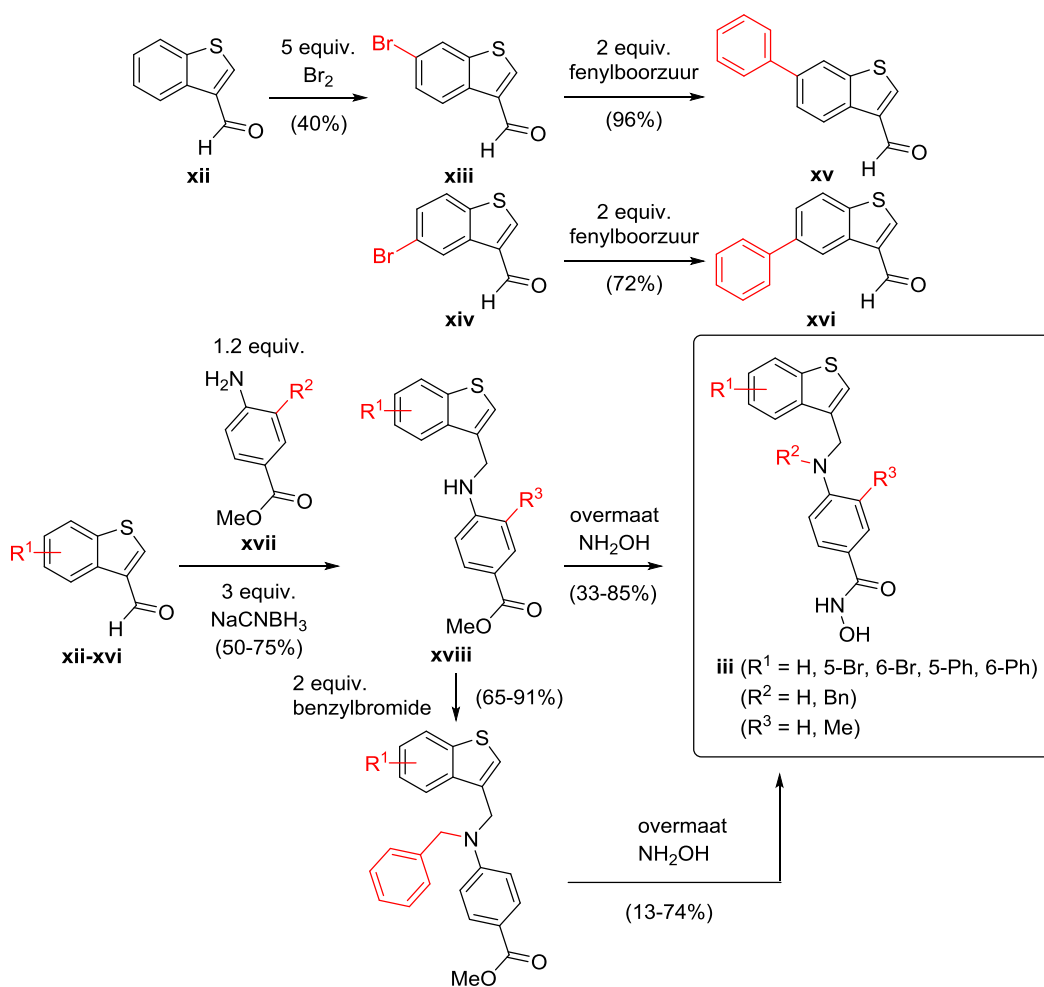
Schema 2. Syntheseroute beschreven in hoofdstuk IV.

In totaal werden 11 benzothiofeen-benzohydroxamzuren **iii** geëvalueerd m.b.t. hun potentieel om HDAC6 selectief te inhiberen. Negen van deze verbindingen vertoonden meer dan 70% inhibitie van HDAC6 bij een concentratie van 10 µM, en drie structuren hadden een IC_{50}-waarde lager dan 0.1 µM. Deze hoogactieve structuren **iii** (R^1 = H, 5-Br, 6-Br, R^2 = H, R^3 = H) bevatten een secundair amine en zijn gesubstitueerd met een broom- of waterstofatoom op de 'cap'-groep. Bovendien bezitten deze structuren een selectiviteitsprofiel vergelijkbaar met het profiel van Tubastatin A en werd aangetoond dat HDAC6-inhibitie ontkoppeld kan worden van transcriptionele inhibitie op het niveau van geactiveerd NF-κB, AP-1 en GR.

In hoofdstuk V werd een gedetailleerd overzicht gegeven van de synthese en biologische evaluatie van benzohydroxamzuren **iv** (Schema 3). Via een aldolcondensatie werden β-hydroxyketonen **xxi** gemaakt uit ketonen **xx** met behulp van paraformaldehyde. In de volgende stap werden tegelijk een tosylering, een reactie met 2-aminothiophenol **xxii** en een reductie door middel van natriumcyaanboorhydride uitgevoerd met als resultaat de vorming van zowel *cis*- en *trans*- benzothiazepinen **xxiii** die diastereomeer zuiver werden bekomen via

kolomchromtografie. Dit is de eerste maal dat de gedetailleerde synthese en isolatie van beide diastereomeren van tricyclische cyclohexaan- en cycloheptaan-gefuseerde tetrahydrobenzothiazepinen **xxiii** werd beschreven, waarbij de correcte structuur werd bevestigd via X-stralendiffractie. Deze heterocyclische structuren **xxiii** werden onder solventvrije reactiecondities gemengd met methyl-4-(broommethyl)benzoaat **xxiv**, hetgeen aanleiding gaf tot de vorming van esters **xxv**. Het zwavelatoom aanwezig in de heterocyclische 'cap'-groep van sulfiden **xxv** werd selectief geoxideerd tot sulfoxide en sulfonen **xxvi**. In de laatste stap werden esters **xxv-xxvi** getransformeerd tot hydroxamzuren **iv** door gebruik te maken van een overmaat hydroxylamine.
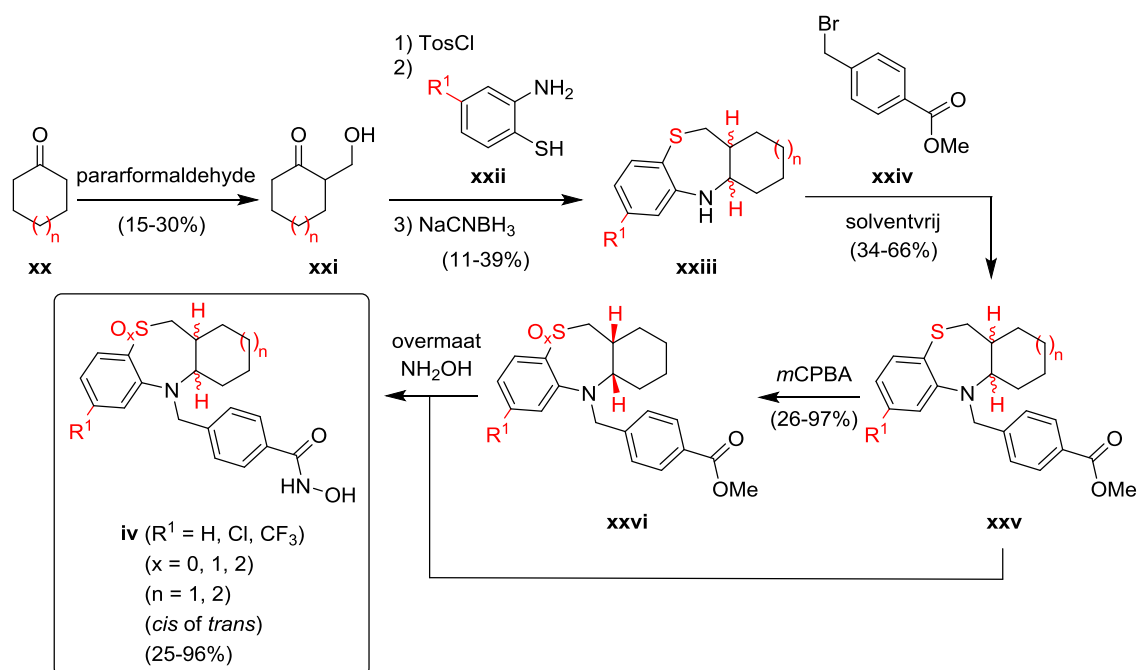
Schema 3. Syntheseroute beschreven in hoofdstuk V.

In totaal werden tien benzohydroxamzuren **iv** efficient gesynthetiseerd en getest m.b.t. hun vermogen om HDAC6 te inhiberen. Al deze inhibitoren vertoonden zeer krachtige HDAC6-inhibitie bij een concentratie van 10 µM (96-100% inhibitie). Daarom werden van alle tien de hydroxamzuren **iv** de IC_{50}-waarden voor HDAC6 bepaald en werd gevonden dat alle inhibitoren nanomolaire activiteit (6,3-650 nM) bezitten. In overeenstemming met vorige observaties omtrent het effect van *S*-oxidatie vertoonden de geoxideerde zwavelderivaten **iv** (x = 1, 2) wederom een lager IC_{50}-waarde dan de niet-geoxideerde tegenhangers. Dit superieur HDAC6-profiel werd ondersteund door moleculair dynamische simulaties *in silico*, die de mogelijkheid tot additionele waterstofbrugvorming van het zwavelgebonden zuurstofatoom met een aminozuurzijketen onthulden. Vijf benzothiazepinen beschikten over een IC_{50}-waarde lager dan 50 nM en hun selectiviteit ten opzichte van de andere HDAC-isozymen werd bepaald

via enzym- en celassays. Uit deze testen bleek dat deze klasse verbindingen kan worden beschouwd als zeer krachtige en selectieve HDAC6-inhibitoren geschikt voor verdere evaluatie.

In het laatste hoofdstuk (hoofdstuk VI) werden alle 42 aangemaakte thiaheterocyclische benzohydroxamzuren geëvalueerd als potentiële antimalariamedicijnen. Verschillende 'pan'-HDAC-inhibitoren zijn gekend een impressionante antimalaria-activiteit te bezitten, maar hun mogelijke toxiciteit vertraagt de verdere ontwikkeling tot antimalariamiddel. Dit probleem kan mogelijk worden omzeild door de ontwikkeling van isoform-selectieve HDAC-inhibitoren, zoals verschillende inhibitoren beschreven in dit werk. Tijdens deze studie werden zes selectieve HDAC6-inhibitoren gevonden die submicromolaire antiplasmodiale activiteit vertonen tegen zowel een chloroquine-gevoelige als een chloroquine-resistente *Plasmodium falciparum* stam, en vier structuren **xxvii-xxx** vertoonden daarenboven een excellente therapeutische index (SI > 300, Figuur 2). Daarnaast bezaten de hydroxamzuren die *h*HDAC6 niet goed inhiberen, lage antiplasmodiale effecten. Er kan dus besloten worden dat krachtige en selectieve *h*HDAC6-inhibitie een noodzakelijke maar niet voldoende voorwaarde is voor thiaheterocyclische benzohydroxamzuren om goede antimalaria-activiteit te vertonen.
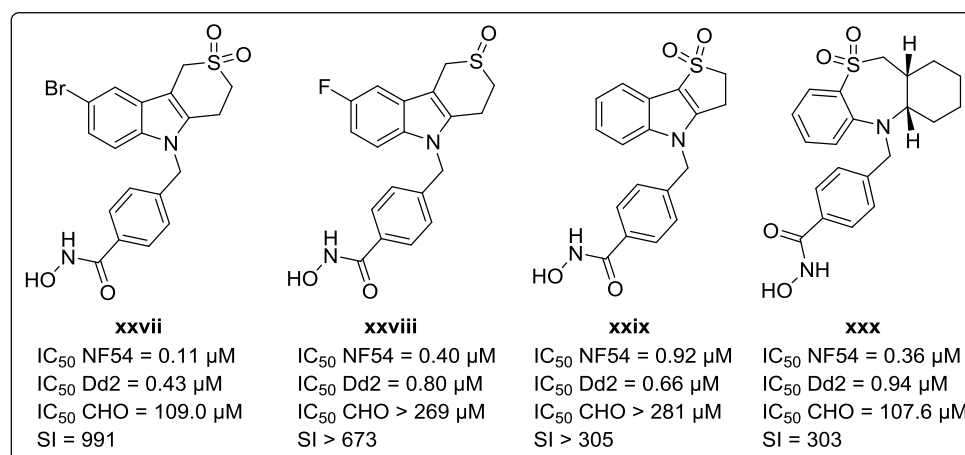
Figuur 2. Meest krachtige antiplasmodiale benzohydroxamzuren beschreven in hoofdstuk VI.

Als overkoepelende conclusie kan worden gesteld dat van iedere klasse **ii**, **iii** en **iv** verschillende 'lead'-structuren werden ontdekt die krachtige HDAC6-inhibitie en selectiviteit vertonen (Figuur 3). Dit toont duidelijk het potentieel aan van thiaheterocyclische benzohydroxamzuren voor het ontdekken van selectieve HDAC6-inhibitoren.
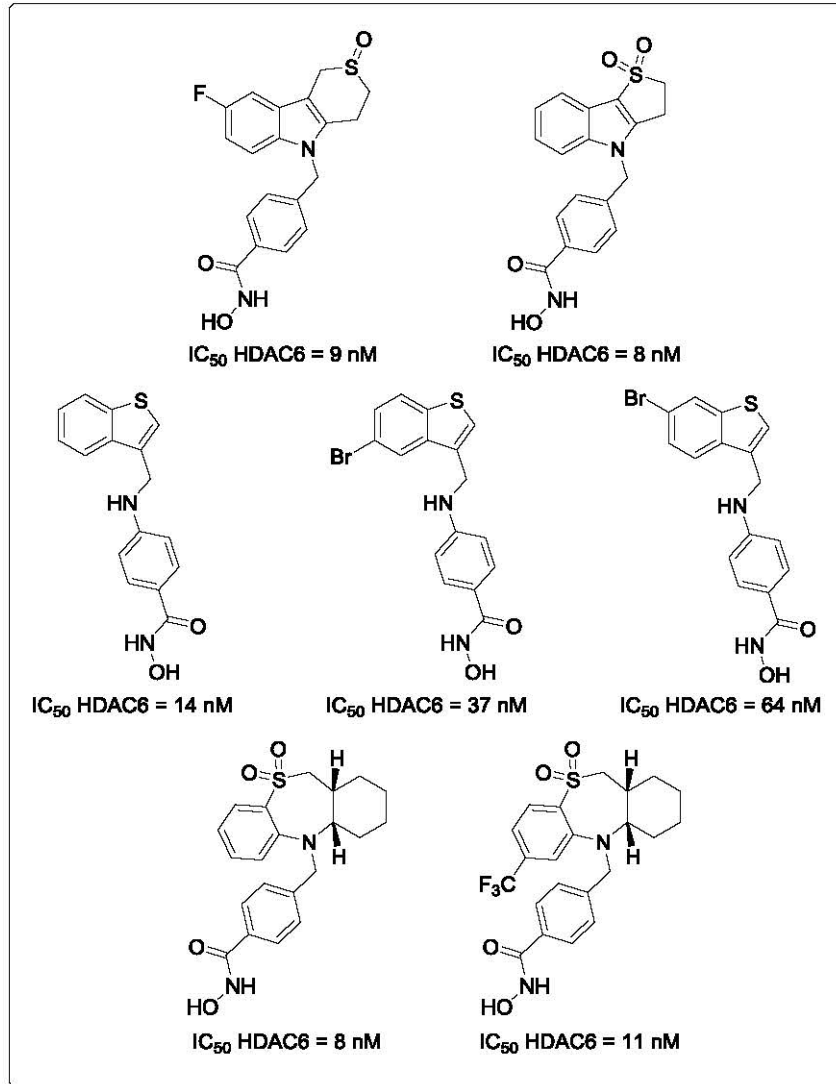
Figuur 3. Meest interessante derivaten van elke klasse **ii**, **iii** en **iv**.

REFERENCES

1. Swinney, D. C.; Anthony, J. *Nat. Rev. Drug Discov.* **2011**, *10*, 507.
2. Swinney, D. C. *Clin. Pharmacol. Ther.* **2013**, *93*, 299.
3. Dokmanovic, M.; Clarke, C.; Marks, P. A. *Mol. Cancer Res.* **2007**, *5*, 981.
4. Marks, P. A. *Biochim. Biophys. Acta* **2010**, *1799*, 717.
5. Allis, C. D.; Berger, S. L.; Cote, J.; Dent, S.; Jenuwien, T.; Kouzarides, T.; Pillus, L.; Reinberg, D.; Shi, Y.; Shiekhattar, R.; Shilatifard, A.; Workman, J.; Zhang, Y. *Cell* **2007**, *131*, 633.
6. De Ruijter, A. J. M.; Van Gennip, A. H.; Caron, H. N.; Kemp, S.; Van Kuilenburg, A. B. P. *Biochem. J.* **2003**, *370*, 737.
7. Miyake, Y.; Keusch, J. J.; Wang, L.; Saito, M.; Hess, D.; Wang, X.; Melancon, B. J.; Helquist, P.; Gut, H.; Matthias, P. *Nat. Chem. Biol.* **2016**, *12*, 748.
8. Li, Y.; Shin, D.; Kwon, S. H. *FEBS J.* **2013**, *280*, 775.
9. Hai, Y.; Christianson, D. W. *Nat. Chem. Biol.* **2016**, *12*, 741.
10. Kalin, J. H.; Bergman, J. A. *J. Med. Chem.* **2013**, *56*, 6297.
11. Zhang, Y.; Kwon, S.; Yamaguchi, T.; Cubizolles, F.; Rousseaux, S.; Kneissel, M.; Cao, C.; Li, N.; Cheng, H. L.; Chua, K.; Lombard, D.; Mizeracki, A.; Matthias, G.; Alt, F. W.; Khochbin, S.; Matthias, P. *Mol. Cell Biol.* **2008**, *28*, 1688.
12. Haggarty, S. J.; Koeller, K. M.; Wong, J. C.; Grozinger, C. M.; Schreiber, S. L. *Proc. Natl. Acad. Sci. USA* **2003**, *100*, 4389.
13. Butler, K. V.; Kalin, J.; Brochier, C.; Vistoli, G.; Langley, B.; Kozikowski, A. P. *J. Am. Chem. Soc.* **2010**, *132*, 10842.
14. Andrews, K. T.; Tran, T. N.; Wheatley, N. C.; Fairlie, D. P. *Curr. Top. Med. Chem.* **2009**, *9*, 292.
15. Codd, R. *Coord. Chem. Rev.* **2008**, *252*, 1387.
16. Arrowsmith, C. H.; Bountra, C.; Fish, P. V.; Lee, K.; Schapira, M. *Nat. Rev. Drug. Discov.* **2012**, *11*, 384.
17. Scholz, C.; Weinert, B. T.; Wagner, S. A.; Beli, P.; Miyake, Y.; Qi, J.; Jensen, L. J.; Streicher, W.; McCarthy, A. R.; Westwood, N. J.; Lain, S.; Cox, J.; Matthias, P.; Mann, M.; Bradner, J. E.; Choudhary, C. *Nat. Biotechnol.* **2015**, *33*, 415.
18. Dinarello, C. A.; Fossati, G.; Mascagni, P. *Mol. Med.* **2011**, *17*, 333.
19. Bolden, J. E.; Peart, M. J.; Johnstone, R. W. *Nat. Rev. Drug Discov.* **2006**, *5*, 769.
20. Marks, P. A. *Oncogene* **2007**, *26*, 1351.
21. Mann, B. S.; Johnson, J. R.; Cohen, M. H.; Justice, R.; Pazdur, R. *The oncologist* **2007**, *12*, 1247.
22. Bantscheff, M.; Hopf, C.; Savitski, M. M.; Dittmann, A.; Grandi, P.; Michon, A. M.; Schlegl, J.; Abraham, Y.; Becher, I.; Bergamini, G.; Boesche, M.; Delling, M.; Dumpelfeld, B.; Eberhard, D.; Huthmacher, C.; Mathieson, T.; Poeckel, D.; Reader, V.; Strunk, K.; Sweetman, G.; Kruse, U.; Neubauer, G.; Ramsden, N. G.; Drewes, G. *Nat. Biotechnol.* **2011**, *29*, 255.
23. Wagner, F. F.; Olson, D. E.; Gale, J. P.; Kaya, T.; Weiwer, M.; Aidoud, N.; Thomas, M.; Davoine, E. L.; Lemercier, B. C.; Zhang, Y. L.; Holson, E. B. *J. Med. Chem.* **2013**, *56*, 1772.
24. Lee, J. H.; Mahendran, A.; Yao, Y.; Ngo, L.; Venta-Perez, G.; Choy, M. L.; Kim, N.; Ham, W. S.; Breslow, R.; Marks, P. A. *Proc. Natl. Acad. Sci. USA* **2013**, *110*, 15704.
25. Breslow, R.; Marks, P. A. **2013**, *WO2013052110*.
26. Lee, J. H.; Yao, Y.; Mahendran, A.; Ngo, L.; Venta-Perez, G.; Choy, M. L.; Breslow, R.; Marks, P. A. *Proc. Natl. Acad. Sci. USA* **2015**, *112*, 12005.
27. Breslow, R.; Marks, P. A.; Mahendran, A.; Yao, Y. **2015**, *WO2015100363*.
28. Sodji, Q. H.; Kornacki, J. R.; McDonald, J. F.; Mrksich, M.; Oyelere, A. K. *Eur. J. Med. Chem.* **2015**, *96*, 340.
29. Tang, G.; Wong, J. C.; Zhang, W.; Wang, Z.; Zhang, N.; Peng, Z.; Zhang, Z.; Rong, Y.; Li, S.; Zhang, M.; Yu, L.; Feng, T.; Zhang, X.; Wu, X.; Wu, J. Z.; Chen, L. *J. Med. Chem.* **2014**, *57*, 8026.

30. Lin, X.; Chen, W.; Qiu, Z.; Guo, L.; Zhu, W.; Li, W.; Wang, Z.; Zhang, W.; Zhang, Z.; Rong, Y.; Zhang, M.; Yu, L.; Zhong, S.; Zhao, R.; Wu, X.; Wong, J. C.; Tang, G. *J. Med. Chem.* **2015**, *58*, 2809.

31. Yu, C. W.; Chang, P. T.; Hsin, L. W.; Chern, J. W. *J. Med. Chem.* **2013**, *56*, 6775.

32. Smil, D. V.; Manku, S.; Chantigny, Y. A.; Leit, S.; Wahhab, A.; Yan, T. P.; Fournel, M.; Maroun, C.; Li, Z.; Lemieux, A. M.; Nicolescu, A.; Rahil, J.; Lefebvre, S.; Panetta, A.; Besterman, J. M.; Deziel, R. *Bioorg. Med. Chem. Lett.* **2009**, *19*, 688.

33. Leit, S.; Wahhab, A.; Allan, M.; Smil, D.; Tessier, P.; Deziel, R.; Chantigny, Y. A. **2007**, *US20070155730*.

34. Kalin, J. H.; Butler, K. V.; Akimova, T.; Hancock, W. W.; Kozikowski, A. P. *J. Med. Chem.* **2012**, *55*, 639.

35. Mahboobi, S.; Sellmer, A.; Pongratz, H.; Leon-Hardt, M.; Krämer, O.; Böhmer, F.-D.; Kelter, G. **2016**, *WO2016020369*.

36. Shen, S.; Benoy, V.; Bergman, J. A.; Kalin, J. H.; Frojuello, M.; Vistoli, G.; Haeck, W.; Van Den Bosch, L.; Kozikowski, A. P. *ACS Chem. Neurosci.* **2016**, *7*, 240.

37. d'Ydewalle, C.; Krishnan, J.; Chiheb, D. M.; Van Damme, P.; Irobi, J.; Kozikowski, A. P.; Vanden Berghe, P.; Timmerman, V.; Robberecht, W.; Van Den Bosch, L. *Nat. Med.* **2011**, *17*, 968.

38. Blackburn, C.; Barrett, C.; Chin, J.; Garcia, K.; Gigstad, K.; Gould, A.; Gutierrez, J.; Harrison, S.; Hoar, K.; Lynch, C.; Rowland, R. S.; Tsu, C.; Ringeling, J.; Xu, H. *J. Med. Chem.* **2013**, *56*, 7201.

39. Bergman, J. A.; Woan, K.; Perez-Villarroel, P.; Villagra, A.; Sotomayor, E. M.; Kozikowski, A. P. *J. Med. Chem.* **2012**, *55*, 9891.

40. Shuttleworth, S. J.; Cecil, A. R. L.; Maccormick, S.; Nodes, W. J.; Tomassi, C. D.; Silva, F. A. **2016**, *WO2016067038*.

41. Cossío Mora, F. P.; Zubia Olascoaga, A.; Vara Salazar, Y. I.; San Sebastián Larzabal, E.; Otaegui Ansa, D.; Masdeu Margalef, M. d. C.; Aldaba Arévalo, E. **2011**, *WO2011039353*.

42. Zhang, C.; Chou, C. J. *Org. Lett.* **2016**, *18*, 5512.

43. Buggy, J. J.; Cao, Z. A.; Bass, K. E.; Verner, E.; Balasubramanian, S.; Liu, L.; Schultz, B. E.; Young, P. R.; Dalrymple, S. A. *Mol. Cancer Ther.* **2006**, *5*, 1309.

44. Verner, E. J.; Sendzik, M.; Baskaran, C.; Buggy, J. J.; Robinson, J. **2004**, *WO2004092115*.

45. Leoni, F.; Fossati, G.; Lewis, E. C.; Lee, J. K.; Porro, G.; Pagani, P.; Modena, D.; Moras, M. L.; Pozzi, P.; Reznikov, L. L.; Siegmund, B.; Fantuzzi, G.; Dinarello, C. A.; Mascagni, P. *Mol. Med.* **2005**, *11*, 1.

46. Tan, J.; Cang, S.; Ma, Y.; Petrillo, R. L.; Liu, D. *J. Hematol. Oncol.* **2010**, *3*, 1.

47. Bertolini, G.; Biffi, M.; Leoni, F.; Mizrahi, J.; Pavich, G.; Mascagni, P. **1997**, *US6034096*.

48. Lu, Q.; Yang, Y.-T.; Chen, C.-S.; Davis, M.; Byrd, J. C.; Ertherton, M. R.; Umar, A.; Chen, C.-S. *J. Med. Chem.* **2004**, *47*, 467.

49. Lu, Q.; Wang, D.-S.; Chen, C.-S.; Hu, Y.-D.; Chen, C.-S. *J. Med. Chem.* **2005**, *48*, 5530.

50. Cheng, H.; Xie, Z.; Jones, W. P.; Wei, X. T.; Liu, Z.; Wang, D.; Kulp, S. K.; Wang, J.; Coss, C. C.; Chen, C. S.; Marcucci, G.; Garzon, R.; Covey, J. M.; Phelps, M. A.; Chan, K. K. *AAPS J.* **2016**, *18*, 737.

51. Burns, S. S.; Akhmametyeva, E. M.; Oblinger, J. L.; Bush, M. L.; Huang, J.; Senner, V.; Chen, C. S.; Jacob, A.; Welling, D. B.; Chang, L. S. *Cancer Res.* **2013**, *73*, 792.

52. Lin, T. Y.; Fenger, J.; Murahari, S.; Bear, M. D.; Kulp, S. K.; Wang, D.; Chen, C. S.; Kisseberth, W. C.; London, C. A. *Blood* **2010**, *115*, 4217.

53. Guzman, M. L.; Yang, N.; Sharma, K. K.; Balys, M.; Corbett, C. A.; Jordan, C. T.; Becker, M. W.; Steidl, U.; Abdel-Wahab, O.; Levine, R. L.; Marcucci, G.; Roboz, G. J.; Hassane, D. C. *Mol. Cancer Ther.* **2014**, *13*, 1979.

54. Xu, W.; Xu, B.; Yao, Y.; Yu, X.; Shen, J. *Biochem. Biophys. Res. Commun.* **2015**, *463*, 545.

55. Li, D. R.; Zhang, H.; Peek, E.; Wang, S.; Du, L.; Li, G.; Chin, A. I. *J. Urol.* **2015**, *194*, 547.

56. Richon, V. M.; Emiliani, S.; Verdin, E.; Webb, Y.; Breslow, R.; Rifkind, R. A.; Marks, P. A. *Proc. Natl. Acad. Sci. USA* **1998**, *95*, 3003.
57. Breslow, R.; Marks, P. A.; Fifkind, R. **1995**, *WO9531977*.
58. Hiriyan, J.; Shivarudraiah, P.; Gavara, G.; Annamalai, P.; Natesan, S.; Sambasivam, G.; Sukumaran, S. K. *Anticancer Res.* **2015**, *35*, 229.
59. Cao, Z. A.; Bass, K. E.; Balasubramanian, S.; Liu, L.; Schultz, B.; Verner, E.; Dai, Y.; Molina, R. A.; Davis, J. R.; Misialek, S.; Sendzik, M.; Orr, C. J.; Leung, L.; Callan, O.; Young, P.; Dalrymple, S. A.; Buggy, J. J. *Mol. Cancer Ther.* **2006**, *5*, 1693.
60. Sendzik, M. **2005**, *WO2005019174*.
61. Tang, W.; Luo, T.; Greenberg, E. F.; Bradner, J. E.; Schreiber, S. L. *Bioorg. Med. Chem. Lett.* **2011**, *21*, 2601.
62. Heimburg, T.; Chakrabarti, A.; Lancelot, J.; Marek, M.; Melesina, J.; Hauser, A. T.; Shaik, T. B.; Duclaud, S.; Robaa, D.; Erdmann, F.; Schmidt, M.; Romier, C.; Pierce, R. J.; Jung, M.; Sippl, W. *J. Med. Chem.* **2016**, *59*, 2423.
63. Balasubramanian, S.; Ramos, J.; Luo, W.; Sirisawad, M.; Verner, E.; Buggy, J. J. *Leukemia* **2008**, *22*, 1026.
64. Buggy, J. J.; Balasubramanian, S.; Verner, E.; Tai, V. W.-F.; Lee, C.-S. **2007**, *WO2007109178*.
65. Kulandaivelu, U.; Chilakamari, L. M.; Jadav, S. S.; Rao, T. R.; Jayaveera, K. N.; Shireesha, B.; Hauser, A. T.; Senger, J.; Marek, M.; Romier, C.; Jung, M.; Jayaprakash, V. *Bioorg. Chem.* **2014**, *57*, 116.
66. Krennhrubec, K.; Marshall, B. L.; Hedglin, M.; Verdin, E.; Ulrich, S. M. *Bioorg. Med. Chem. Lett.* **2007**, *17*, 2874.
67. Suzuki, T.; Ota, Y.; Ri, M.; Bando, M.; Gotoh, A.; Itoh, Y.; Tsumoto, H.; Tatum, P. R.; Mizukami, T.; Nakagawa, H.; Iida, S.; Ueda, R.; Shirahige, K.; Miyata, N. *J. Med. Chem.* **2012**, *55*, 9562.
68. Suzuki, T.; Muto, N.; Bando, M.; Itoh, Y.; Masaki, A.; Ri, M.; Ota, Y.; Nakagawa, H.; Iida, S.; Shirahige, K.; Miyata, N. *ChemMedChem* **2014**, *9*, 657.
69. Olson, D. E.; Wagner, F. F.; Kaya, T.; Gale, J. P.; Aidoud, N.; Davoine, E. L.; Lazzaro, F.; Weiwer, M.; Zhang, Y. L.; Holson, E. B. *J. Med. Chem.* **2013**, *56*, 4816.
70. Rodrigues, D. A.; Ferreira-Silva, G. A.; Ferreira, A. C.; Fernandes, R. A.; Kwee, J. K.; Sant'Anna, C. M.; Ionta, M.; Fraga, C. A. *J. Med. Chem.* **2016**, *59*, 655.
71. Kim, H.-J.; Bae, S.-C. *Am. J. Transl. Res.* **2011**, *3*, 166.
72. Di Marcotullio, L.; Canettieri, G.; Infante, P.; Greco, A.; Gulino, A. *Biochim. Biophys. Acta* **2011**, *1815*, 241.
73. Shein, N. A.; Shohami, E. *Mol. Med.* **2011**, *17*, 448.
74. Kazantsev, A. G.; Thompson, L. M. *Nat. Rev. Drug Discov.* **2008**, *7*, 854.
75. Karagiannis, T. C.; El-Osta, A. *Leukemia* **2007**, *21*, 61.
76. Thaler, F.; Minucci, S. *Exp. Op. Drug Disc.* **2011**, *6*, 393.
77. d'Ydewalle, C.; Bogaert, E.; Van Den Bosch, L. *Traffic* **2012**, *13*, 771.
78. Li, G.; Jiang, H.; Chang, M.; Xie, H.; Hu, L. *J. Neurol. Sci.* **2011**, *304*, 1.
79. Aldana-Masangkay, G. I.; Sakamoto, K. M. *J. Biomed. Biotechnol.* **2011**, *2011*, 1.
80. Valenzuela-Fernandez, A.; Cabrero, J. R.; Serrador, J. M.; Sanchez-Madrid, F. *Trends Cell Biol.* **2008**, *18*, 291.
81. Boyault, C.; Sadoul, K.; Pabion, M.; Khochbin, S. *Oncogene* **2007**, *26*, 5468.
82. Kalin, J. H.; Zhang, H.; Gaudrel-Grosay, S.; Vistoli, G.; Kozikowski, A. P. *ChemMedChem* **2012**, *7*, 425.
83. Suzuki, T.; Kouketsu, A.; Itoh, Y.; Hisakawa, S.; Maeda, S.; Yoshida, M.; Nakagawa, H.; Miyata, N. *J. Med. Chem.* **2006**, *49*, 4809.
84. Ontoria, J. M.; Altamura, S.; Di Marco, A.; Ferrigno, F.; Laufer, R.; Muraglia, E.; Palumbi, M. C.; Rowley, M.; Scarpelli, R.; Schultz-Fademrecht, C.; Serafini, S.; Steinkuhler, C.; Jones, P. *J. Med. Chem.* **2009**, *52*, 6782.
85. Schäfer, S.; Saunders, L.; Eliseeva, E.; Velena, A.; Jung, M.; Schwienhorst, A.; Strasser, A.; Dickmanns, A.; Ficner, R.; Schlimme, S.; Sippl, W.; Verdin, E.; Jung, M. *Bioorg. Med. Chem.* **2008**, *16*, 2011.

86. Olsen, C. A.; Ghadiri, M. R. *J. Med. Chem.* **2009**, *52*, 7836.
87. Schäfer, S.; Saunders, S.; Schlimme, S.; Valkov, V.; Wagner, J. M.; Kratz, F.; Sippl, W.; Verdin, E.; Jung, M. *ChemMedChem* **2009**, *4*, 283.
88. Gupta, P. K.; Reid, R. C.; Liu, L.; Lucke, A. J.; Broomfield, S. A.; Andrews, M. R.; Sweet, M. J.; Fairlie, D. P. *Bioorg. Med. Chem. Lett.* **2010**, *20*, 7067.
89. Rivieccio, M. A.; Brochier, C.; Willis, D. E.; Walker, B. A.; D'Annibale, M. A.; McLaughlin, K.; Siddiq, A.; Kozikowski, A. P.; Jaffrey, S. R.; Twiss, J. L.; Ratan, R. R.; Langley, B. *Proc. Natl. Acad. Sci. USA* **2009**, *106*, 19599.
90. Wong, J. C.; Hong, R.; Schreiber, S. L. *J. Am. Chem. Soc.* **2003**, *125*, 5586.
91. Dossetter, A. G. *Med. Chem. Commun.* **2012**, *3*, 1518.
92. Sudhakara, A.; Jayadevappa, H.; Kumar, H. N. H.; Mahadevan, K. M. *Lett. Org. Chem.* **2009**, *6*, 159.
93. Krieger, E.; Koraimann, G.; Vriend, G. *Proteins* **2002**, *47*, 393.
94. Vriend, G. *J. Mol. Graph.* **1990**, *8*, 52.
95. Duan, Y.; Wu, C.; Chowdhury, S.; Lee, M. C.; Xiong, G. M.; Zhang, W.; Yang, R.; Cieplak, P.; Luo, R.; Lee, T.; Caldwell, J.; Wang, J. M.; Kollman, P. *J. Comput. Chem.* **2003**, *24*, 1999.
96. Morris, G. M.; Goodsell, D. S.; Halliday, R. S.; Huey, R.; Hart, W. E.; Belew, R. K.; Olson, A. J. *J. Comput. Chem.* **1998**, *19*, 1639.
97. Schrodinger, L. **2010**.
98. Strahl, B. D.; Allis, C. D. *Nature* **2000**, *403*, 41.
99. Xu, D.-Q.; Wu, J.; Luo, S.-P.; Zhang, J.-X.; Wu, J.-Y.; Du, X.-H.; Xu, Z.-Y. *Green Chem.* **2009**, *11*, 1239.
100. Gregoretti, I. V.; Lee, Y. M.; Goodson, H. V. *J. Mol. Biol.* **2004**, *338*, 17.
101. Van Helleputte, L.; Benoy, V.; Van Den Bosch, L. *Res. Rep. Biol.* **2014**, *5*, 1.
102. Shakespear, M. R.; Halili, M. A.; Irvine, K. M.; Fairlie, D. P.; Sweet, M. J. *Trends Immunol.* **2011**, *32*, 335.
103. Woan, K. V.; Lienlaf, M.; Perez-Villaroel, P.; Lee, C.; Cheng, F.; Knox, T.; Woods, D. M.; Barrios, K.; Powers, J.; Sahakian, E.; Wang, H. W.; Canales, J.; Marante, D.; Smalley, K. S.; Bergman, J.; Seto, E.; Kozikowski, A.; Pinilla-Ibarz, J.; Sarnaik, A.; Celis, E.; Weber, J.; Sotomayor, E. M.; Villagra, A. *Mol. Oncol.* **2015**, *9*, 1447.
104. De Vreese, R.; Verhaeghe, T.; Desmet, T.; D'hooghe, M. *Chem. Commun.* **2013**, *49*, 3775.
105. Thaler, F.; Mercurio, C. *ChemMedChem* **2014**, *9*, 523.
106. Kozlov, M. V.; Kleymenova, A. A.; Konduktorov, K. A.; Kochetkov, S. N. *Russ. J. Bioorg. Chem.* **2013**, *39*, 102.
107. Wang, C. Y. *Mutat. Res.* **1977**, *56*, 7.
108. Skipper, P. L.; Tannenbaum, S. R.; Thilly, W. G.; Furth, E. E.; Bishop, W. W. *Cancer Res.* **1980**, *40*, 4704.
109. Trott, O.; Olson, A. J. *J. Comput. Chem.* **2010**, *31*, 455.
110. Taunton, J.; Hassig, C. A.; Schreiber, S. L. *Science* **1996**, *272*, 408.
111. Xu, W. S.; Parmigiani, R. B.; Marks, P. A. *Oncogene* **2007**, *26*, 5541.
112. Thomas, E. A. *Mol. Neurobiol.* **2009**, *40*, 33.
113. Hubbert, C.; Guardiola, A.; Shao, R.; Kawaguchi, Y.; Ito, A.; Nixon, A.; Yoshida, M.; Wang, X. F.; Yao, T. P. *Nature* **2002**, *417*, 455.
114. Valente, S.; Tardugno, M.; Conte, M.; Cirilli, R.; Perrone, A.; Ragno, R.; Simeoni, S.; Tramontano, A.; Massa, S.; Nebbioso, A.; Miceli, M.; Franci, G.; Brosch, G.; Altucci, L.; Mai, A. *ChemMedChem* **2011**, *6*, 698.
115. Liger, F.; Pellet-Rostaing, S.; Popowycz, F.; Lemaire, M. *Tetrahedron Lett.* **2011**, *52*, 3736.
116. Kovacs, J. J.; Murphy, P. J.; Gaillard, S.; Zhao, X.; Wu, J. T.; Nicchitta, C. V.; Yoshida, M.; Toft, D. O.; Pratt, W. B.; Yao, T. P. *Mol. Cell* **2005**, *18*, 601.
117. De Bosscher, K.; Vanden Berghe, W.; Beck, I. M.; Van Molle, W.; Hennuyer, N.; Hapgood, J.; Libert, C.; Staels, B.; Louw, A.; Haegeman, G. *Proc. Natl. Acad. Sci. U. S. A.* **2005**, *102*, 15827.

118. Vishwakarma, S.; Iyer, L. R.; Muley, M.; Singh, P. K.; Shastry, A.; Saxena, A.; Kulathingal, J.; Vijaykanth, G.; Raghul, J.; Rajesh, N.; Rathinasamy, S.; Kachhadia, V.; Kilambi, N.; Rajgopal, S.; Balasubramanian, G.; Narayanan, S. *Int. Immunopharmacol.* **2013**, *16*, 72.

119. Vanden Berghe, W.; Vermeulen, L.; De Wilde, G.; De Bosscher, K.; Boone, E.; Haegeman, G. *Biochem. Pharmacol.* **2000**, *60*, 1185.

120. Plaisance, S.; Vanden Berghe, W.; Boone, E.; Fiers, W.; Haegeman, G. *Mol. Cell. Biol.* **1997**, *17*, 3733.

121. Choudhary, C.; Kumar, C.; Gnad, F.; Nielsen, M. L.; Rehman, M.; Walther, T. C.; Olsen, J. V.; Mann, M. *Science* **2009**, *325*, 834.

122. Yang, X. J.; Seto, E. *Mol. Cell* **2008**, *31*, 449.

123. Glozak, M. A.; Sengupta, N.; Zhang, X.; Seto, E. *Gene* **2005**, *363*, 15.

124. Haberland, M.; Montgomery, R. L.; Olson, E. N. *Nat. Rev. Genet.* **2009**, *10*, 32.

125. Chuang, D. M.; Leng, Y.; Marinova, Z.; Kim, H. J.; Chiu, C. T. *Trends Neurosci.* **2009**, *32*, 591.

126. Covington, H. E., 3rd; Maze, I.; LaPlant, Q. C.; Vialou, V. F.; Ohnishi, Y. N.; Berton, O.; Fass, D. M.; Renthal, W.; Rush, A. J., 3rd; Wu, E. Y.; Ghose, S.; Krishnan, V.; Russo, S. J.; Tamminga, C.; Haggarty, S. J.; Nestler, E. J. *J. Neurosci.* **2009**, *29*, 11451.

127. Blanchard, F.; Chipoy, C. *Drug Discov. Today* **2005**, *10*, 197.

128. Halili, M. A.; Andrews, M. R.; Sweet, M. J.; Fairlie, D. P. *Curr. Top. Med. Chem.* **2009**, *9*, 309.

129. Subramanian, S.; Bates, S. E.; Wright, J. J.; Espinoza-Delgado, I.; Piekarz, R. L. *Pharmaceuticals* **2010**, *3*, 2751.

130. Bruserud, Ø.; Stapnes, C.; Ersvær, E.; Gjertsen, B. T.; Ryningen, A. *Curr. Pharm. Biotechnol.*, *8*, 388.

131. Batchu, S. N.; Brijmohan, A. S.; Advani, A. *Clin. Sci.* **2016**, *130*, 987.

132. Yang, Z.; Wang, T.; Wang, F.; Niu, T.; Liu, Z.; Chen, X.; Long, C.; Tang, M.; Cao, D.; Wang, X.; Xiang, W.; Yi, Y.; Ma, L.; You, J.; Chen, L. *J. Med. Chem.* **2016**, *59*, 1455.

133. De Vreese, R.; Van Steen, N.; Verhaeghe, T.; Desmet, T.; Bougarne, N.; De Bosscher, K.; Benoy, V.; Haeck, W.; Van Den Bosch, L.; D'hooghe, M. *Chem. Commun.* **2015**, *51*, 9868.

134. Senger, J.; Melesina, J.; Marek, M.; Romier, C.; Oehme, I.; Witt, O.; Sippl, W.; Jung, M. *J. Med. Chem.* **2016**, *59*, 1545.

135. Sodji, Q. H.; Patil, V.; Kornacki, J. R.; Mrksich, M.; Oyelere, A. K. *J. Med. Chem.* **2013**, *56*, 9969.

136. Wang, L.; Kofler, M.; Brosch, G.; Melesina, J.; Sippl, W.; Martinez, E. D.; Easmon, J. *PloS one* **2015**, *10*, 1.

137. Diedrich, D.; Hamacher, A.; Gertzen, C. G.; Alves Avelar, L. A.; Reiss, G. J.; Kurz, T.; Gohlke, H.; Kassack, M. U.; Hansen, F. K. *Chem. Commun.* **2016**, *52*, 3219.

138. Gaisina, I. N.; Tueckmantel, W.; Ugolkov, A.; Shen, S.; Hoffen, J.; Dubrovskyi, O.; Mazar, A.; Schoon, R. A.; Billadeau, D.; Kozikowski, A. P. *ChemMedChem* **2016**, *11*, 81.

139. Jochems, J.; Boulden, J.; Lee, B. G.; Blendy, J. A.; Jarpe, M.; Mazitschek, R.; Van Duzer, J. H.; Jones, S.; Berton, O. *Neuropsychopharmacol.* **2014**, *39*, 389.

140. Yoo, J.; Kim, S. J.; Son, D.; Seo, H.; Baek, S. Y.; Maeng, C. Y.; Lee, C.; Kim, I. S.; Jung, Y. H.; Lee, S. M.; Park, H. J. *Eur. J. Med. Chem.* **2016**, *116*, 126.

141. De Vreese, R.; Depetter, Y.; Verhaeghe, T.; Desmet, T.; Benoy, V.; Haeck, W.; Van Den Bosch, L.; D'hooghe, M. *Org. Biomol. Chem.* **2016**, *14*, 2537.

142. Bariwal, J. B.; Upadhyay, K. D.; Manvar, A. T.; Trivedi, J. C.; Singh, J. S.; Jain, K. S.; Shah, A. K. *Eur. J. Med. Chem.* **2008**, *43*, 2279.

143. Gill, R. K.; Aggarwal, N.; Kumari, J.; Kumari, M.; Kaur, P.; Kaur, M.; Rani, A.; Bansal, A.; Shah, A.; Bariwal, J. *Chem. Biol. Interface* **2013**, *3*, 146.

144. El-Bayouki, K. A. M. *Org. Chem. Int.* **2013**, *2013*, 1.

145. Hideg, K.; Hankovszky, H. O. *Acta Chim. Hung.* **1968**, *56*, 405.

146. Wipf, P.; Aslan, D. C. *J. Org. Chem.* **2001**, *66*, 337.

147. Shen, S.; Kozikowski, A. P. *ChemMedChem* **2016**, *11*, 15.

148. Dolomanov, O. V.; Bourhis, L. J.; Gildea, R. J.; Howard, J. A. K.; Puschmann, H. *J. Appl. Crystallogr.* **2009**, *42*, 339.
149. Sheldrick, G. M. *Acta Crystallogr. Sect. A* **2008**, *64*, 112.
150. *World Health Organization* **2015**, 1.
151. White, N. J.; Pukrittayakamee, S.; Hien, T. T.; Faiz, M. A.; Mokuolu, O. A.; Dondorp, A. M. *Lancet* **2014**, *383*, 723.
152. Miller, L. H.; Ackerman, H. C.; Su, X. Z.; Wellems, T. E. *Nat. Med.* **2013**, *19*, 156.
153. Andrews, K. T.; Haque, A.; Jones, M. K. *Immunol. Cell Biol.* **2012**, *90*, 66.
154. Aneja, B.; Kumar, B.; Jairajpuri, M. A.; Abid, M. *RSC Adv.* **2016**, *6*, 18364.
155. Wang, Q.; Rosa, B. A.; Nare, B.; Powell, K.; Valente, S.; Rotili, D.; Mai, A.; Marshall, G. R.; Mitreva, M. *PLoS Negl. Trop. Dis.* **2015**, *9*, e0004026.
156. Engel, J. A.; Jones, A. J.; Avery, V. M.; Sumanadasa, S. D.; Ng, S. S.; Fairlie, D. P.; Adams, T. S.; Andrews, K. T. *Int. J. Parasitol. Drugs Drug Resist.* **2015**, *5*, 117.
157. Patel, V.; Mazitschek, R.; Coleman, B.; Nguyen, C.; Urgaonkar, S.; Cortese, J.; Barker, R. H.; Greenberg, E.; Tang, W.; Bradner, J. E.; Schreiber, S. L.; Duraisingh, M. T.; Wirth, D. F.; Clardy, J. *J. Med. Chem.* **2009**, *52*, 2185.
158. Ontoria, J. M.; Paonessa, G.; Ponzi, S.; Ferrigno, F.; Nizi, E.; Biancofiore, I.; Malancona, S.; Graziani, R.; Roberts, D.; Willis, P.; Bresciani, A.; Gennari, N.; Cecchetti, O.; Monteagudo, E.; Orsale, M. V.; Veneziano, M.; Di Marco, A.; Cellucci, A.; Laufer, R.; Altamura, S.; Summa, V.; Harper, S. *ACS Med. Chem. Lett.* **2016**, *7*, 454.
159. Hansen, F. K.; Sumanadasa, S. D.; Stenzel, K.; Duffy, S.; Meister, S.; Marek, L.; Schmetter, R.; Kuna, K.; Hamacher, A.; Mordmuller, B.; Kassack, M. U.; Winzeler, E. A.; Avery, V. M.; Andrews, K. T.; Kurz, T. *Eur. J. Med. Chem.* **2014**, *82*, 204.
160. Trager, W.; Jensen, J. B. *Science* **1976**, *193*, 673.
161. Makler, M. T.; Ries, J. M.; Williams, J. A.; Bancroft, J. E.; Piper, R. C.; Gibbins, B. L.; Hinrichs, D. J. *Am. J. Trop. Med. Hyg.* **1993**, *48*, 739.
162. Mosmann, T. *J. Immunol. Methods* **1983**, *65*, 55.
163. Rubinstein, L. V.; Shoemaker, R. H.; Paull, K. D.; Simon, R. M.; Tosini, S.; Skehan, P.; Scudiero, D. A.; Monks, A.; Boyd, M. R. *J. Natl. Cancer Inst.* **1990**, *82*, 1113.
164. Madsen, A. S.; Kristensen, H. M.; Lanz, G.; Olsen, C. A. *ChemMedChem* **2014**, *9*, 614.
165. Sung, Y. M.; Lee, T.; Yoon, H.; DiBattista, A. M.; Song, J. M.; Sohn, Y.; Moffat, E. I.; Turner, R. S.; Jung, M.; Kim, J.; Hoe, H. S. *Exp. Neurol.* **2013**, *239*, 192.

CURRICULUM VITAE

Personalia

Name:	Rob De Vreese
Title:	ir.
Address:	Roeselarestraat 395, 8560 Wevelgem
Date of birth:	20/09/1988
Place of birth:	Brugge
GSM:	+32476574260
Email:	rdvreese@hotmail.be

Education

2000-2006: High school, Sciences and Mathematics, Sint-Lodewijkscollege, Sint-Andries

2006-2009: Bachelor of Science in Bioscience Engineering: Chemistry and Food Technology, Ghent University, Degree: **Distinction**

2009-2011: Master of Science in Bioscience Engineering: Chemistry and Bioprocess Technology, Ghent University, Degree: **Distinction**

2011-present: Doctor of Applied Biological Sciences: Chemistry and Bioprocess Technology, Ghent University, Assisting Academic Staff (50% research, 50% education)

International experience

September 2009 - January 2010: Erasmus Spain, Universidad Politécnica de Valencia

Work experience

Summer worker july 2006: employee, Dupont Jan Kaas Import nv.

Summer worker july 2007, july 2008 and july 2009: employee, building of exhibitions, municipality of Knokke-Heist

2011-present: Assisting Academic Staff, Ghent University

Research experience

2008-2009: Bachelor thesis: "*Increasing the thermoresistance of plastics for the packaging of foods: a state-of-the-art*"
Department of Food Safety and Food Quality
Faculty of Bioscience Engineering, Ghent University
Promoters: Prof. Dr. ir. F. Devlieghere and Ing. G. Dohogne

2010-2011: Master thesis: *"Synthesis of novel purine-β-lactam hybrids and conversion to N9-functionalized purines"*
Department of Sustainable Organic Chemistry and Technology
Faculty of Bioscience Engineering, Ghent University
Promoters: Prof. Dr. ir. N. De Kimpe and Prof. Dr. ir. M. D'hooghe

2011-present: PhD thesis: *"Synthesis of thiaheterocyclic benzohydroxamic acids and evaluation of their HDAC6 inhibitory activity"*
Department of Sustainable Organic Chemistry and Technology
Faculty of Bioscience Engineering, Ghent University
Promoter: Prof. Dr. ir. M. D'hooghe

List of publications

Scientific publications in international journals with peer review (A1-papers):

1) D'hooghe, M.; Mollet, K.; **De Vreese, R.**; Jonckers, T. H. M.; Dams, G.; De Kimpe, N. "Design, synthesis, and antiviral evaluation of purine-β-lactam and purine-aminopropanol hybrids" *J. Med. Chem.* **2012**, 55, 5637-5641. (I.F. 5.61)

2) **De Vreese, R.**; D'hooghe, M. "*N*-Heterocyclic carbene/Bronsted acid cooperative catalysis as a powerful tool in organic synthesis" *Beilstein J. Org. Chem.* **2012**, 8, 398-402. (I.F. 2.80)

3) **De Vreese, R.**; Verhaeghe, T.; Desmet, T.; D'hooghe, M. "Potent and selective HDAC6 inhibitory activity of *N*-(4-hydroxycarbamoylbenzyl)-1,2,4,9-tetrahydro-3-thia-9-azafluorenes as novel sulfur analogues of Tubastatin A" *Chem. Commun.* **2013**, 49, 3775-3777. (I.F. 6.72)

4) Piens, N.; **De Vreese, R.;** De Neve, N.; Van Hecke, K.; Balzarini, J.; De Kimpe, N.; D'hooghe, M. "Synthesis of novel thymine-β-lactam hybrids and evaluation of their antitumor activity" *Synthesis* **2014**, 46, 2436-2444. (I.F. 2.69)

5) Chen, C.; Van der Borght, J.; **De Vreese, R.**; D'hooghe, M.; Soetaert, W.; Desmet, T. "Engineering the specificity of trehalose phosphorylase as a general strategy for the production of glycosyl phosphates" *Chem. Commun.* **2014**, 50, 7834-7836. (I.F. 6.83)

6) **De Vreese, R.**; Van Steen, N.; Verhaeghe, T.; Desmet, T.; Bougarne, N.; De Bosscher, K.; Benoy, V.; Haeck, W.; Van Den Bosch, L.; D'hooghe, M. "Synthesis of benzothiophene-based hydroxamic acids as potent and selective HDAC6 inhibitors" *Chem. Commun.* **2015**, 51, 9868-9871. (I.F. 6.57)

7) **De Vreese, R.**; Depetter, Y.; Verhaeghe, T.; Desmet, T.; Benoy, V.; Haeck, W.; Van Den Bosch, L.; D'hooghe, M. "Synthesis and SAR assessment of novel Tubathian analogs in the pursuit of potent and selective HDAC6 inhibitors" *Org. Biomol. Chem.* **2016**, 14, 2537-2549. (I.F. 3.56)

8) **De Vreese, R.**; Grootaert, C.; D'Hoore, Sander; Theppawong, A.; Van Damme, S.; Van Bogaert, M.; Van Camp, J.; D'hooghe, M. "Synthesis of novel curcuminoids accommodating a central β-enaminone motif and their impact on cell growth and oxidative stress" *Eur. J. Med. Chem.* **2016**, 123, 727-736. (I.F. 3.90)

9) Verhaeghe T.; De Winter, K.; Berland, M.; **De Vreese, R.**; D'hooghe, M.; Offman, B.; Desmet, T. "Converting bulk sugars into prebiotics: semi-rational design of a transglucosylase with controlled selectivity" *Chem. Commun.* **2016**, 52, 3687-3689. (I.F. 6.57)

10) Theppawong, A.; **De Vreese, R.**; Vannecke, L.; Grootaert, C.; Van Camp, J.; D'hooghe, M. "Synthesis and biological assessment of novel N-(hydroxy/methoxy)alkyl β-enaminone curcuminoids" *Bioorg. Med. Chem. Lett.* **2016**, 26, 5650-5656. (I.F. 2.49)

11) **De Vreese, R.**; Galle, L.; Depetter, Y.; Franceus, J.; Desmet, T.; Van Hecke, K.; Benoy, V.; Van Den Bosch, L.; D'hooghe, M. "Synthesis of potent and selective HDAC6 inhibitors bearing a cyclohexane- or cycloheptane-annulated 1,5-benzothiazepine scaffold" *Chem. Eur. J.* **2017**, 23, 128-136. (I.F. 5.77)

12) **De Vreese, R.**; de Kock, C.; Smith, P. J.; Chibale, K.; D'hooghe, M. "Exploration of thiaheterocyclic *h*HDAC6 inhibitors as potential antiplasmodial agents"*, Future Med. Chem.* **2017**, 9, 357-364. (I.F. 3.35)

13) **De Vreese, R.**; D'hooghe, M. "Synthesis and applications of benzohydroxamic acid-based histone deacetylase inhibitors", *Eur. J. Med. Chem.* **2017**, accepted. (I.F. 3.90)

Patents:

1) Bracke, M.; D'hooghe, M.; **De Vreese, R.** "HDAC6 inhibitors and uses thereof" WO2014147178.
2) **De Vreese, R.**; D'hooghe, M. "Selective HDAC6 inhibitors and uses thererof" WO2016110541.
3) **De Vreese, R.**; D'hooghe, M. "Novel HDAC6 inhibitors and their uses" *patent under review*.

Active participation at conferences

1) **De Vreese, R.**; D'hooghe M. "Potent and selective HDAC6 inhibitory activity of *N*-(4-hydroxycarbamoylbenzyl)-1,2,4,9-tetrahydro-3-thia-9-azafluorenes as novel sulfur analogues of Tubastatin A" (poster P-15). *17th Sigma-Aldrich Organic Synthesis Meeting.* (December 5 - 6, **2013**, Blankenberge, Belgium).
2) **De Vreese, R.**; D'hooghe M. "Potent and selective HDAC6 inhibitory activity of *N*-(4-hydroxycarbamoylbenzyl)-1,2,4,9-tetrahydro-3-thia-9-azafluorenes as novel sulfur analogues of Tubastatin A" (poster OMC-10-T). *Chemistry Conference for Young Scientists 2014 (ChemCYS 2014).* (February 27 - 28, **2014**, Blankenberge, Belgium).
3) **De Vreese, R.**; D'hooghe M. "Synthesis and Biological evaluation of novel sulfur analogues of Tubastatin A with pronounced and selective HDAC6 inhibitory activity" (poster EM05). *50th International Conference on Medicinal Chemistry (RICT 2014).* (July 2 - 4, **2014**, Rouen, France).
4) **De Vreese, R.**; D'hooghe M. "Synthesis and Biological evaluation of novel sulfur analogues of Tubastatin A with pronounced and selective HDAC6 inhibitory activity" (poster P-19). *18th Sigma-Aldrich Organic Synthesis Meeting.* (December 4 - 5, **2014**, Blankenberge, Belgium).
5) **De Vreese, R.**; D'hooghe M. "Synthesis and SAR assessment of novel selective HDAC6 inhibitors" (oral presentation CS&M1). *1st Chemical Research in Flanders Symposium (CRF1).* (October 24 - 26, **2016**, Blankenberge, Belgium).

Tutoring of Master thesis students

1) Dereu, L. "Synthese van bis-8-hydroxychinolinen uitgaande van 5-halogeen- en 5-amino-8-hydroxychinoline" (2011-2012).
2) De Neve, N. "Synthese van nieuwe guanine-β-lactamhybriden en thymine-β-lactamhybriden" (2011-2012).
3) Taillieu, F. "Aanwending van 5-broom-8-hydroxychinoline en 8-hydroxychinoline-2-carboxaldehyde voor de synthese van bis-8-hydroxychinolinen" (2012-2013).
4) Van Bogaert, M. "Synthese van 5-amino-1,7-diarylhepta-1,4,6-trieen-3-onen als nieuwe stikstofanaloga van curcumine" (2012-2013).
5) Van Steen, N. "Synthese van 3-[(4-hydroxycarbamoylfenyl)-aminomethyl]benzothiofenen als potentiële HDAC6-inhibitoren" (2012-2013).
6) Harth, T. "Synthese van bis-8-hydroxychinolinen via palladiumgekatalyseerde koppeling van 5-broom-8-hydroxychinoline met areendiboorzuren" (2013-2014).
7) Van Damme, S. "Bereiding van 5-amino-1,7-diarylhepta-1,4,6-triëen-3-onen als nieuwe curcumine-analoga" (2013-2014).
8) Depetter, Y. "Synthese van *N*-(hydroxycarbamoylbenzyl)-gesubstitueerdetetrahydro-3-thia-9-azafluorenen en dihydrothiëno[3,2-b]indolen als potentiële HDAC6-inhibitoren" (2013-2014).
9) Goethals, S. "Evaluatie van de antikankeractiviteit van nieuwe HDAC6-inhibitoren met een *N*-(4-hydroxycarbamoylbenzyl)-1,2,4,9-tetrahydro-3-thia-9-azafluoreenskelet" (2014-2015).

10) Galle, L. "Synthese van *N*-(4-hydroxycarbamoylbenzyl)-gesubstitueerde octahydrodibenzo[*b*,*e*][1,4]thiazepinen als potentiële HDAC6-inhibitoren" (2014-2015).

11) Vannecke, L. "Synthese van 5-hydroxyalkylamino- en 5-methoxyalkylamino-1,7-diarylhepta-1,4,6-triëen-3-onen als nieuwe stikstofanaloga van curcumine" (2015-2016).

12) Van de Walle, T. "Synthese van azaheteroaromatische analoga van curcumine met potentiële antikankeractiviteit" (2015-2016).

13) Vanden Bussche, F. "Synthese van *N*-{2-[(4-(hydroxycarbamoyl)benzyl)-amino]ethyl}indolinen als potentiële HDAC6-inhibitoren" (2015-2016).

14) Geurs, S. In progress (2016-2017).